2025-2026 CALIFORNIA CURRENT ECOSYSTEM STATUS REPORT

A report of the NOAA California Current Integrated Ecosystem Assessment Team (CCIEA) to the Pacific Fishery Management Council

Edited by: Mary Hunsicker, Andrew Leising, Amanda Phillips, Nick Tolimieri, Isaac Schroeder, Lynn DeWitt, & Gregory Williams

Northwest and Southwest Fisheries Science Centers

2026-02-09

With contributions from:

Anna Abelman, Kelly Andrews, Toby Auth, Tracie Barry, John (Jack) Barth, Kirby Bartlett, Anna Bolm, Jerry Borchert, Noelle Bowlin, Brian Burke, Shallin Busch, Sherri Charter, Megan Cimino, Jason Cope, Kelly Corbett, Jeff Cowen, Elizabeth Daly, Russel (Rusty) Dame, Meredith Elliott, Blake Feist, Jerome Fiechter, John Field, Jennifer Fisher, Zachary Forster, Christopher Free, Ryan Gasbarro, Matthew George, Abigail Golden, Thomas Good, Christina Grant, Correigh Greene, Ana Sofia Guerra, Chris Harvey, Elliott Hazen, Daniel Holland, Brian Hoover, Ali Hossain, Matthew Hunter, Jennifer (Lilah) Isé, Kym Jacobson, Michael Jacox, Jaime Jahncke, Mike Johns, Christy Juhasz, Isaac Kaplan, William Kennerley, Su Kim, Dan Lawson, Connor Lewis-Smith, Nerea Lezama-Ochoa, Kirsten Lindquist, Owen Liu, Nate Mantua, Jace Marquardt, Sharon Melin, Monique Messié, Rebecca Miller, Stephanie Moore, Cheryl Morgan, Barbara Muhling, Stuart Munsch, Shannon Murphy, Karma Norman, Rachael Orben, Julia Parrish, Scott Pearson, Elizabeth Phillips, Stephen Pierce, Antonella Preti, Leif Rasmuson, Josiah Renfree, Travis Richards, Tanya Rogers, Jan Roletto, Daniel Rudnick, Lauren Saez, Keith Sakuma, Jameal Samhouri, Jarrod Santora, Will Satterthwaite, Kayleigh Somers, Beckye Stanton, Kevin Stierhoff, Florence Sullivan, Rasmus Swalethorp, William Sydeman, Andrew Thompson, Sarah Ann Thompson, Duy Truong, Brian VerWey, Cathleen Vestfals, Amanda Warlick, Pete Warzybok, William Watson, Curt Whitmire, Jeannette Zamon, Samantha Zeman, Vanessa Zubkousky-White, Juan Zwolinski

Table of Contents

1. INTRODUCTION 6
1.1 SAMPLING LOCATIONS 8
2. CLIMATE AND OCEAN DRIVERS 10
Key Message 10
2.1 Basin-Scale Indicators 10
2.2 Upwelling and Habitat Compression 13
2.3 Hypoxia and Ocean Acidification 15
2.4 Snowpack and Hydrology 17
3. FOCAL COMPONENTS OF ECOLOGICAL INTEGRITY 19
Key Message 19
3.1 Copepods and Krill 19
3.2 CPS and Regional Forage Availability 21
3.2.1 Coastwide Coastal Pelagic Species (CPS) 21
3.2.2 Regional forage composition 21
3.3 Salmon Indicators 24
3.3.1 Stoplight tables 25
3.4 Groundfish 29
3.4.1 Status of groundfish biomass and fishing pressure 29
3.5 Highly Migratory Species (HMS) 30
3.5.1 HMS diet 30
3.6 Seabird Indicators 32
3.6.1 Fledgling production 32
3.6.2 Mortality 33
3.7 Marine Mammals 33
3.7.1 Whale entanglements 33
3.7.2 Sea lions 34
3.8 Harmful Algal Blooms (HABs) 34
4. HUMAN WELLBEING 37
Key Message 37
4.1 Social Vulnerability 37
4.2 Diversification of Fishery Revenues 40
4.3 Fisheries Participation Networks 41
5. Fishing and Non-fishing Human Activities 44

Key Message 44
5.1 Coastwide Landings by Major Fisheries 44
5.2 Ecosystem Interactions with New Ocean-use Sectors 46
6. Synthesis 46
7. LITERATURE CITED 49
Appendix A — CONTRIBUTORS TO THIS REPORT 57
Appendix B — SUMMARY INFOGRAPHICS for the 2025-2026 ESR 59
Appendix C — LIST OF FIGURES AND DATA SOURCES 62
Appendix D — NEAR TERM CLIMATE AND ECOSYSTEM FORECASTS 65
D.1 Forecasts for 2026 65
D.1.1 ENSO 65
D.1.2 Marine Heatwaves 66
D.1.3 Temperature observations to avoid loggerheads (TOTAL) 68
D.2 Uncertainty in climate and ecosystem predictions 69
D.3 Revisiting forecasts from 2025 69
Appendix E — DEVELOPING INDICATORS OF CLIMATE CHANGE 71
E.1 Contextualizing climate variability and change 71
E.1.1 The Pacific Decadal Oscillation in a changing climate 71
E.1.2 Time-dependent climate and ecosystem relationships 74
E.2 New Synthesis Tools 78
E.2.1 Measuring and communicating projected shifts in species distributions 78
E.2.2 Community-wide projected shift direction 79
E.3 Implications for Fisheries and State Jurisdictions 80
E.3.1 Species-specific spatial trends 83
E.4 Fishing fleets as ecosystem sentinels 85
E.5 State of knowledge on future changes in the CCE 86
E.5.1 Ocean and biogeochemical change 86
E.5.2 Distribution and abundance of groundfish and CPS 87
E.5.3 Vulnerability and risk for groundfish and CPS fleets 87
Appendix F — CLIMATE AND OCEAN INDICATORS 88
F.1 Basin-scale Climate/Ocean Indicators at Seasonal Time Scales 88
F.2 Assessing Marine Heatwaves in 2025 93
F.3 Habitat Compression Index 95
F.4 Seasonal Dissolved Oxygen and Ocean Acidification Indicators 96

Appendix G — SNOWPACK, STREAMFLOW, AND STREAM TEMPERATURE 102
Appendix H — COASTAL PELAGIC SPECIES DATA FROM SUMMER 2025 107
Appendix I — REGIONAL FORAGE AVAILABILITY 111
I.1 Northern California Current Forage 111
I.2 Central California Current Forage 112
I.3 Southern California Current Forage 114
I.4 Coastwide krill abundance 117
I.5 Dungeness crab megalopae 118
Appendix J — SALMON 119
J.1 Salmon Stoplight Table Format 119
J.2 Ecosystem Indicator-based Outlooks for Chinook Salmon Escapement in the Columbia River Basin 119
J.3 Ecosystem Conditions for Chinook Salmon in California 122
Appendix K — GROUNDFISH 127
K.1 Status of groundfish biomass and fishing pressure 127
K.1.1 *Pacific Survey Explorer* 128
K.2 Recruitment of rockfishes along the Washington Coast 128
K.3 Pelagic juvenile groundfishes: abundance and diversity through time 130
K.4 Abundance trends in Ecosystems Components species 132
Appendix L — HIGHLY MIGRATORY SPECIES (HMS) 134
L.1 HMS Stock Assessment Information 134
L.2 HMS Diet Information 136
Appendix M — SEABIRD PRODUCTIVITY, DIET, AT-SEA DENSITY, AND MORTALITY 141
M.1 Seabird Productivity 141
M.2 Seabird Diets 144
M.3 Seabird At-Sea Density 147
M.4 Seabird Mortality 150
Appendix N — MARINE MAMMALS 154
N.1 Whale Entanglements 154
Appendix O — HARMFUL ALGAL BLOOMS 156
O.1 Domoic Acid, Paralytic Shellfish Toxins, and Diarrhetic Shellfish Toxins in Washington 158
O.2 Domoic Acid and Paralytic Shellfish Toxin in Oregon 159
O.3 Domoic Acid and Paralytic Shellfish Toxins in California 159

Appendix P — PORT-LEVEL REVENUE CONCENTRATION....162
Appendix Q — SOCIAL VULNERABILITY OF COMMERCIAL and RECREATIONAL FISHING-DEPENDENT COMMUNITIES....164
Appendix R — FLEET DIVERSIFICATION INDICATORS FOR MAJOR WEST COAST PORTS....167
Appendix S — FISHERIES PARTICIPATION NETWORKS....169
Appendix T — STATE-BY-STATE FISHERY LANDINGS AND REVENUES....180
T.1 State-by-State Landings....180
T.2 Commercial Fisheries Revenue....183
Appendix U — IDENTIFYING INTERACTIONS AMONG ECOSYSTEM INDICATORS & NEW OCEAN-USE SECTORS....188
U.1 IEA Approach to Understanding Interactions with New Ocean-use Sectors....188
U.2 Ecological and Fisheries Indicators relevant to Offshore Wind Planning and Development....189
U.2.1 Ecological Components....190
U.2.2 Fisheries Components....193
Appendix V — Methodological Overviews....195
Appendix W — Changes In This Year's Report....195

1. INTRODUCTION

Link to report synthesis: Report Synthesis

The Fishery Ecosystem Plan (FEP) establishes a reporting process wherein NOAA provides the Pacific Fishery Management Council with a yearly update on the status of the California Current Ecosystem (CCE), as derived from environmental, biological, economic and social indicators. NOAA's California Current Integrated Ecosystem Assessment (CCIEA) team is responsible for this report. This report has been produced annually since 2013.

This report summarizes CCE status based on data and analyses that generally run through 2025 and some that extend into 2026. Highlights are summarized in Box 1.1, and Chapter 6 features a report synthesis and summary.

Appendices provide additional information or clarification on recent indicators. Additionally, Appendix D features short-term forecasts of environmental conditions for the CCE in 2026, which are derived from indicator data and models. Appendix E features long-term projections of climate variability and potential responses of many target and protected species, including new synthesis tools for assessing climate impacts in the CCE.

We have removed some of the static methodological descriptions from the main section of the report to an online Ecosystem Status Report (ESR) Technical Documentation appendix (Appendix V, online version). Due to the temporary government furlough and changes in staffing and funding, this year's report has notable changes relative to past reports (detailed in Appendix W).

Box 1.1. 2025-26 California Current Ecosystem Status Report Highlights

KEY TAKEAWAYS FROM 2025

- Strong upwelling coastwide led to productive coastal conditions, held marine heatwave offshore.
- Diverse and abundant forage coastwide, including anchovy, YOY rockfish, juvenile salmon.
- Record HAB events in southern CA.
- Rapid spring melt-out, high temperatures, below-normal snowpack, & looming drought in the north.
- High precipitation alleviated drought in CA, but snowpack remains exceptionally low.



Unfavorable Conditions and Risk factors

- Largest marine heatwave on record (dating to 1982); record offshore sea surface temperatures.
- HAB toxins impacted marine life, human health, and fisheries, with unusual dinoflagellate blooms increasing.
- Confirmed whale entanglements remain at 2024 levels.
- Coastwide total landings remain well below (>1 SD) the long-term average; CA salmon fisheries remained closed.
- Four port groups closed major processor facilities, and groundfish port-level revenue concentration increased.

Mixed to Positive Ecological Signals

- Early, strong, and consistent upwelling, but possibly a shorter than normal season with an early fall transition.
- Krill abundant coastwide and increased in the north relative to recent years.
- Near average returns predicted for adult Chinook salmon returning to the Columbia Basin in 2026 and 2027.
- Fledgling production at all seabird colonies rebound from 2024.
- Total revenue increased from 2024 mainly due to increased landings of Pacific whiting, HMS, and market squid, while crab landings decreased.

NOAA FISHERIES

An extended graphical summary is provided in Appendix B

1.1 SAMPLING LOCATIONS

We refer to areas north of Cape Mendocino as the "Northern CCE," Cape Mendocino to Point Conception as the "Central CCE", and south of Point Conception as the "Southern CCE." Figure 1.1 shows sampling areas for most regional oceanographic data. Key oceanographic transects are the Newport Line off Oregon, the Trinidad Head Line off northern California, and CalCOFI lines further south. Sampling is complemented by basin-scale oceanographic observations and outputs from various models. Figure 1.1 also shows sampling areas for most biological indicators in the shaded marine regions. The shaded terrestrial areas in Figure 1.1 represent freshwater ecoregions in the CCE, and are the basis for indicators for snowpack, flows, and stream temperatures.

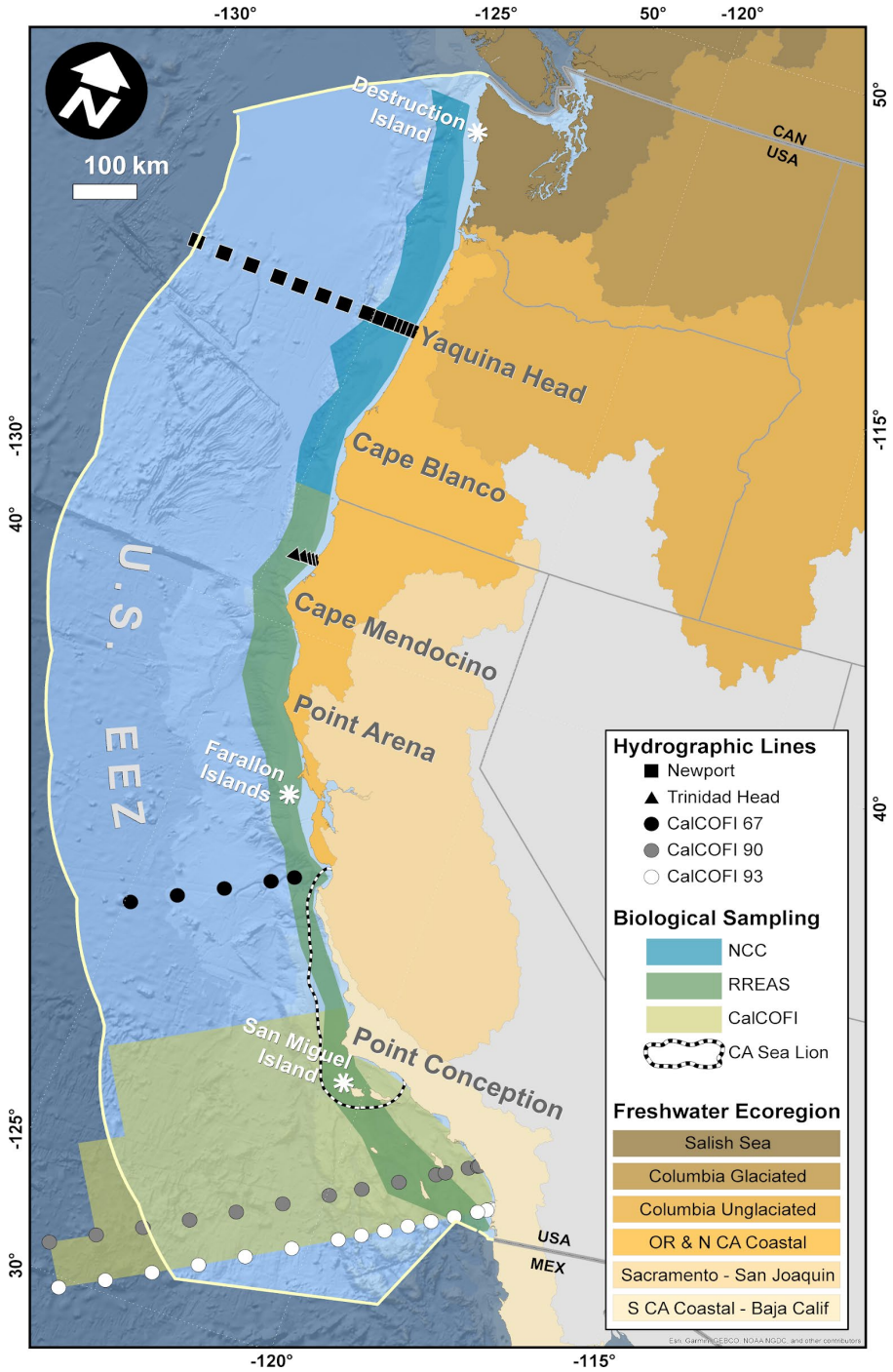


Figure 1.1: Map of most sampling efforts in the California Current Ecosystem (CCE) and U.S. West Coast Exclusive Economic Zone (EEZ). Symbols indicate hydrographic line sampling stations for oceanographic data. Shaded ocean regions represent biological sampling areas for the Northern California Current (NCC), which includes the Juvenile Salmon and Ocean Ecology Survey (JSOES) and the NCC Ecosystem Survey; the Rockfish Recruitment and Ecosystem Assessment Survey (RREAS); and the CalCOFI sampling region. The NCC and RREAS shaded areas, combined, also approximate the survey footprints for NOAA's Integrated West Coast Pelagics Survey and the West Coast Groundfish Bottom Trawl Survey. Dashed line approximates foraging area for adult female California sea lions from the San Miguel colony. Shaded terrestrial areas represent the six freshwater ecoregions in the CCE.

2. CLIMATE AND OCEAN DRIVERS

Key Message

The California Current during 2025 experienced a strong marine heatwave (MHW) which contributed to record breaking surface temperatures offshore during the summer, compression of cold water habitat towards the coast, and coastal warming during the late summer through mid winter. However, because upwelling was persistent and strong during the summer, nearshore waters remained cool, promoting favorable productive conditions coastally during this key period. Additionally, there were several unusual pulses of strong upwelling nearly coastwide in January and February, which may have contributed to harmful algal blooms. Bottom oxygen levels were mostly favorable. Snowpack was above normal at the start of the year in most western regions, however, warmer-than-normal spring storms and then continued warm weather led to early melt and reduced snowpack. Reduced snowpack and precipitation then contributed to some areas of drought during the summer. Streams were warmer than normal and flows were low during late summer, similar to past years.

2.1 Basin-Scale Indicators

We use three indices to characterize large-scale physical ecosystem states in the North Pacific:

(1) The Oceanic Niño Index (ONI) describes the equatorial El Niño Southern Oscillation (ENSO). An ONI above 0.5 °C indicates El Niño conditions, which often lead to lower primary production, weaker upwelling, poleward transport of equatorial waters and species, and more southerly storm tracks in the CCE. An ONI below -0.5 °C means La Niña conditions, which influence atmospheric pressure conditions that lead to upwelling-favorable winds that drive productivity in the CCE.

(2) The Pacific Decadal Oscillation (PDO) describes North Pacific sea surface temperature (SST) anomalies that may persist for many years. Positive PDOs are associated with warmer SST and lower productivity in the CCE, while negative PDOs indicate cooler SST and are associated with higher productivity.

(3) The North Pacific Gyre Oscillation (NPGO), an index of sea surface height, indicates changes in circulation that affect source waters for the CCE. Positive NPGOs are associated with strong equatorward flow and higher salinity, nutrients, and chlorophyll-a. Negative NPGOs are associated with decreased subarctic source water and lower CCE productivity.

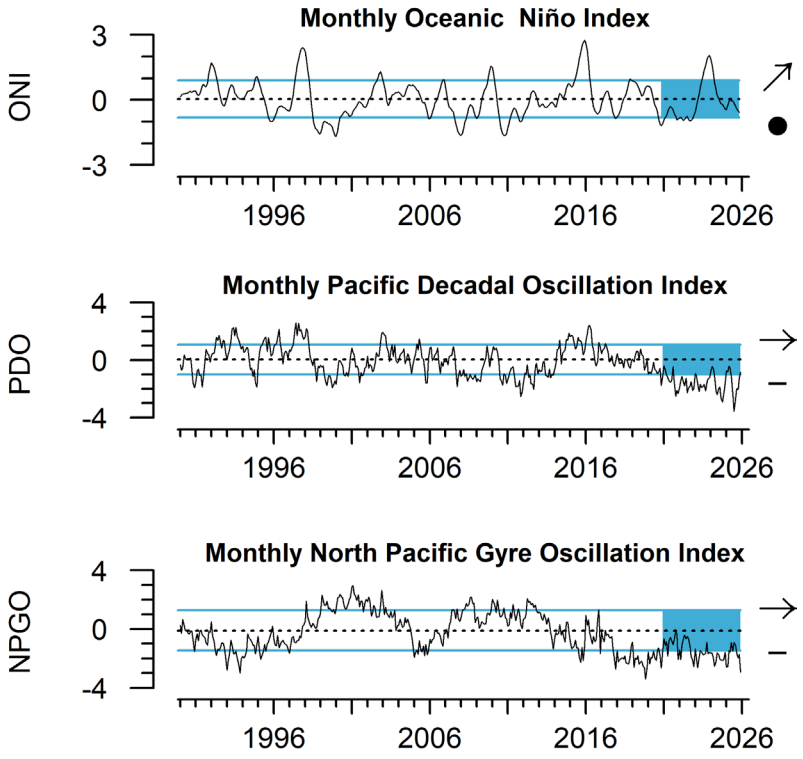


Figure 2.1: Monthly values of the Oceanic Niño Index (ONI), Pacific Decadal Oscillation (PDO), and North Pacific Gyre Oscillation (NPGO) from 1990-2025 relative to the mean (dashed line) ± s.d. (blue lines) from 1991-2020. The blue shaded area is the most recent five years of data. Arrows indicate if the recent five-year trend is positive (↗), neutral (→), or negative (↘). Symbols indicate if the recent five-year mean is above the upper blue line (+), within the blue lines (•), or below the lower blue line (-).

Basin-scale indices suggest average to above average conditions for productivity in 2025: the ONI was negative to neutral during the year, whereas the PDO and NPGO were negative during the entire year (Fig. 2.1). The ONI remained neutral or negative, reflective of the mild La Niña conditions during the remainder of the year. The PDO remained negative for a 7th consecutive year (Fig. 2.1), reflecting that sea surface temperatures offshore were generally warmer than onshore, even with the overall warmer than normal conditions both offshore and at times onshore (for a further discussion, see Appendix E). After reaching relatively low values in 2019 and early 2020, the NPGO has remained neutral to low (Fig. 2.1). This indicates that the general circulation in the CCE is weaker than average. Seasonal values for all indices are in Appendix F.

The northeast Pacific continues to experience large marine heatwaves (MHW) in surface waters, with 2025 seeing the largest (by area) MHW observed since satellite monitoring began in 1982 (Fig. 2.2). At the beginning of the year, coastal SST was average, but with a large lingering MHW farther offshore to the southwest. Between February and April, this far offshore MHW mostly dissipated, only to re-emerge in mid to late May in the same

region, and was fully formed by July (Fig. 2.2), during which time coastal waters were cooler than normal due to strong upwelling. During August, the offshore MHW grew dramatically in size, reaching its maximum areal extent of ~10 million km^2 on Sept. 10th, 2025 (Fig. 2.2). In early September, the overall average SST of this NEP region (shown in Fig. 2.2) set a new record approximately 0.6 °C higher than the previous record set in 2019. This timing coincides with record air temperatures over land throughout areas of the Pacific Northwest. After September, as is typical for these recent MHWs, this MHW decreased in size and receded from some of the coast, however, during December, large portions of the coast remained much warmer than normal, to a similar extent only seen during past large El Niños such as the 1997-1998 event, and the "warm blob" of 2014-2015 (Fig. 2.2). Additional information on the 2025 marine heatwave is in Section F.2.

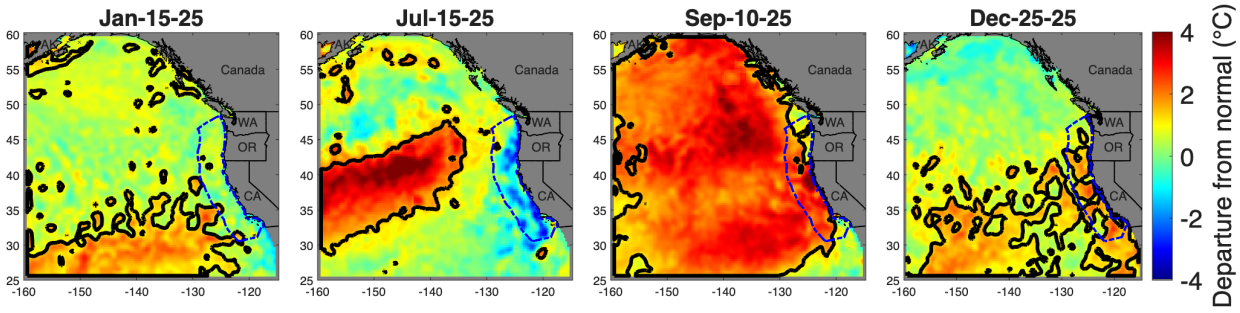


Figure 2.2: Progression of the 2025 marine heatwave in the northeast Pacific Ocean. Colors represent standardized SST anomalies. Heavy black lines denote regions that meet the criteria for a marine heatwave (see Appendix F.2). Blue dashed line outlines the US exclusive economic zone (EEZ).

Subsurface temperatures (>50m depth) in the coastal CCE were cooler than normal to average for the winter through mid-summer of 2025, with a switch to warmer-than-normal temperatures during the late summer and fall in the upper 50m, reflective of the presence of the large marine heatwave (Fig. 2.3, see also Appendix F). It is important to note that unlike the El Niño of 1997-1998, and the 2014-2015 and 2019 MHWs, this MHW only appears to have extended to <50 m deep in coastal regions, as evidenced by subsurface sampling both off Oregon and Southern California (Fig. 2.3).

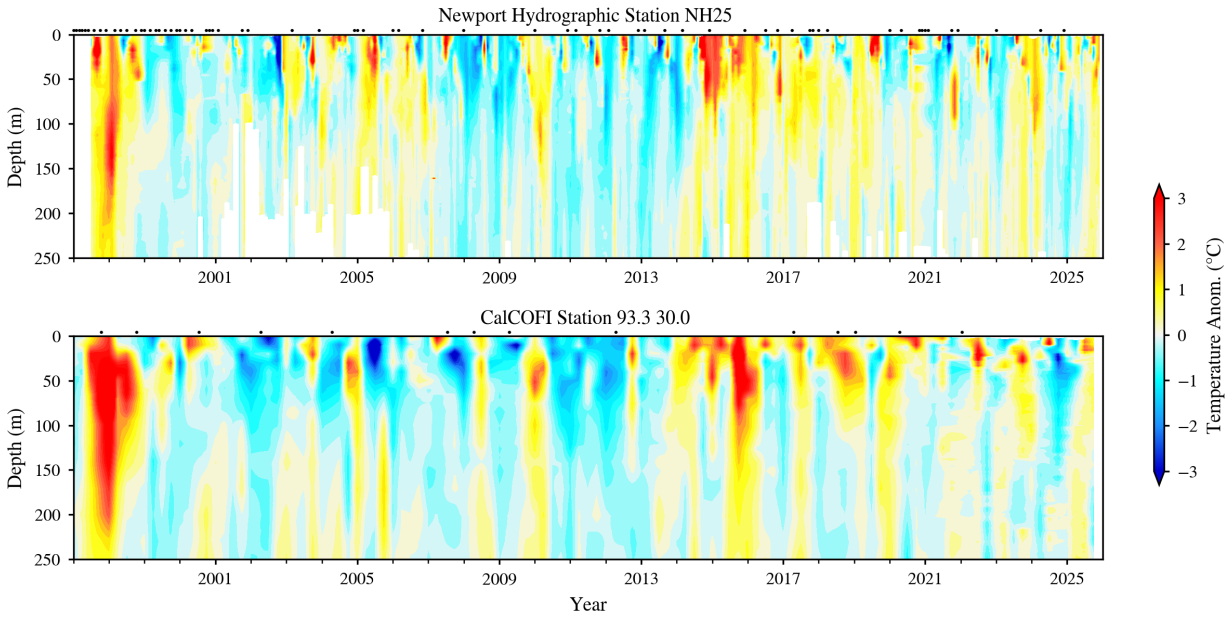


Figure 2.3: Time-depth temperature anomalies at Newport station NH25 and CalCOFI station 93.30, from 1997 through 2025. Transect locations are in Fig. 1.1. Note: small circles at top of plots represent missing observations which have been filled via interpolation. NHL sampling is bi-monthly, while CalCOFI sampling is quarterly.

2.2 Upwelling and Habitat Compression

Upwelling is a major driver of coastal productivity in the CCE. It occurs when equator-ward coastal winds force deep, cold, nutrient-rich water to the surface. The greatest upwelling in the CCE occurs off central California and typically peaks in June. Here, we present the Bakun upwelling index (Bakun 1973) as an estimate of the vertical flux of water and nutrients (the Bakun index was used in lieu of the CUTI and BEUTI indices, which were not available this year due to downtime of the UCSC-ROMS ocean model used for those calculations).

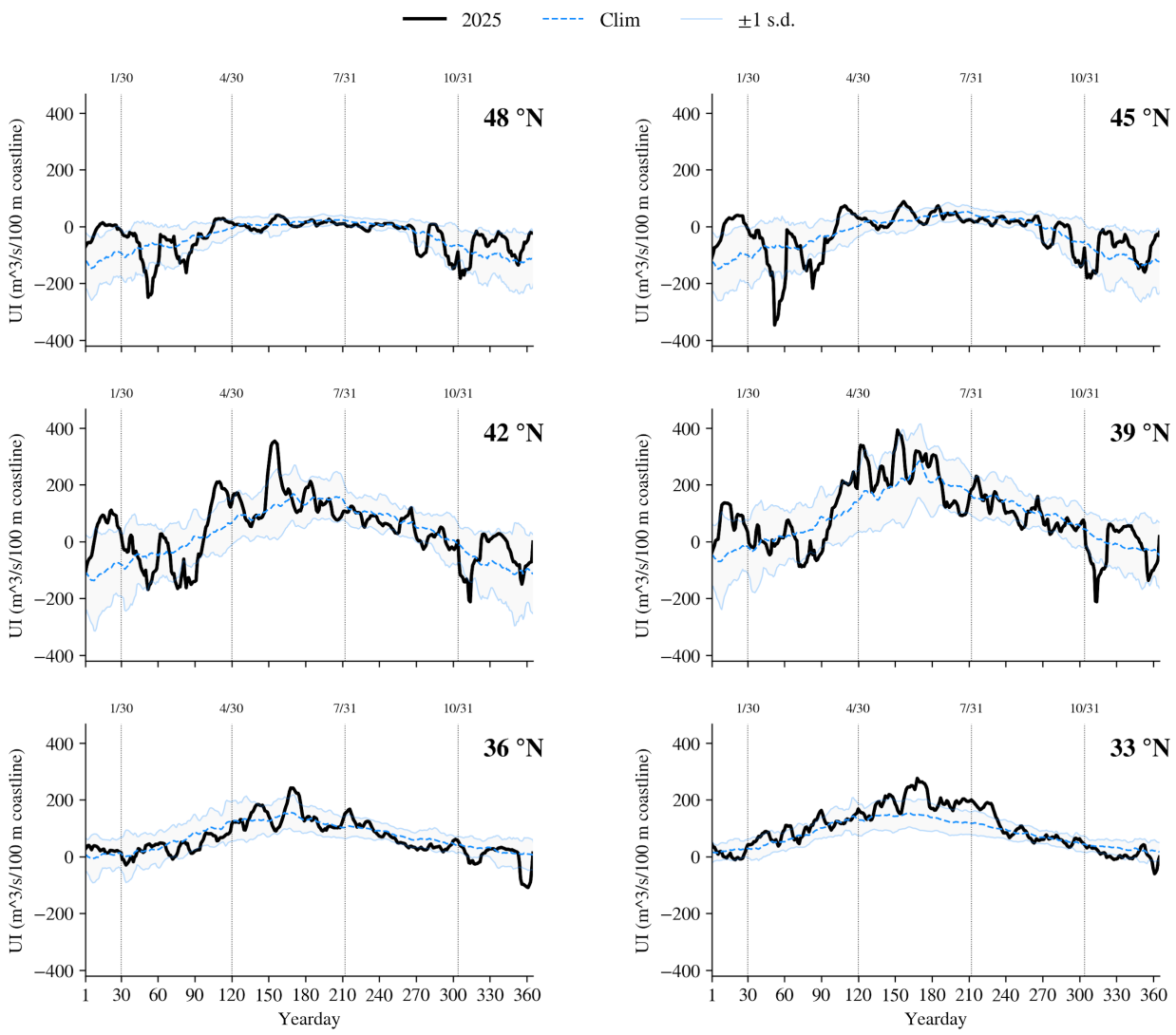


Figure 2.4: Daily estimates (1-day moving average) of offshore Ekman transport of water (Bakun Upwelling index) in 2025, relative to the 1967-2025 climatological average (blue dashed line) ± 1.0 s.d..(shaded area), at latitudes 33°N to 48°N.

Overall, 2025 saw average to above average total integrated upwelling compared to past years for most of the coastline (Fig. F.6). Unusual this year were several pulses of upwelling nearly coastwide during January and February (Fig. 2.4), which may have contributed to the large harmful algal bloom event that occurred just after those upwelling pulses (Appendix O). However, early winter pulses of upwelling have also been known to lead to higher seabird reproductive success and greater rockfish growth (Black et al. 2010, 2011b; Schroeder et al. 2019). There was a rapid transition from downwelling to upwelling in early April (~day 90 in Fig. 2.4). After this transition, upwelling remained fairly average or above average for most of the summer, except for a few occasional relaxation events, particularly at mid-latitudes from 36-42 °N (Fig. 2.4). The fall transition to a mostly

downwelling state occurred in late August/early September, at which point the large offshore MHW extended into the coastal region, especially impacting northern California (Fig. 2.2), and with warmer than normal ocean temperatures observed the entire region (Fig. 2.3). Taken together, the upwelling pattern for 2025 suggests average to above average productivity throughout the CCE.

Santora et al. (2020) developed the habitat compression index (HCI) to describe how much cool, productive water is available adjacent to the coast. HCI ranges from 0 (= complete absence of cool surface water in the region) to 1 (= cool water fully extending 150 km from the coast). During 2025, compression off of central California was average during winter and spring, with a shift to lower values (higher compression due to warmer offshore waters) during summer and fall, indicative of the intrusion of the large offshore marine heatwave (Fig. 2.5, Section F.3).

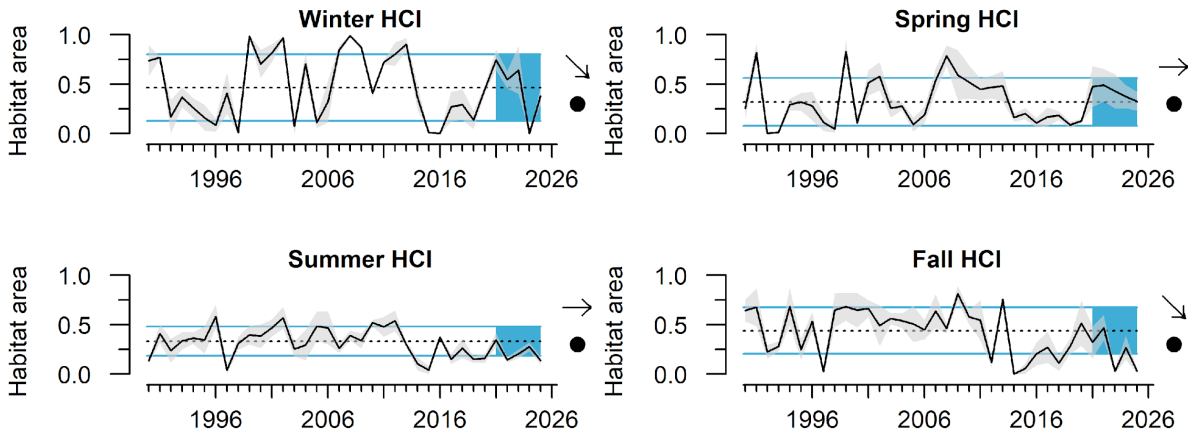


Figure 2.5: Mean habitat compression index (HCI) off central California in winter (Jan-Mar), spring (Apr-Jun), summer (Jul-Sep), and fall (Oct-Dec) for 1990-2025. Habitat area is the fraction of coastal habitat that is cooler than the threshold (higher values indicate less compression). Gray envelope indicates ± 1.0 s.e. Lines, colors, and symbols are as in Fig. 2.1.

2.3 Hypoxia and Ocean Acidification

Dissolved oxygen (DO) is influenced by processes such as currents, upwelling, air-sea exchange, primary production, and respiration. Low DO (including hypoxia when concentrations are < 1.4 ml DO/l) can compress habitat vertically and cause stress or die-offs in sensitive species (Chan et al. 2008). During 2025, the timing of the hypoxic period was similar to most other years (Fig. 2.6). DO concentrations were higher to the south, similar to 2024, as the nearshore station NH05 off Newport, Oregon only briefly experienced hypoxic conditions (Fig. 2.6), whereas the station off WA (CE07) experienced a longer period of hypoxia than Newport and compared to the previous year. The offshore station NH25 also did not experience as low oxygen levels this year as previous years (Section F.4). However, during the June JSOES survey, a larger than normal region of lower than normal bottom oxygen levels was noted off southern Washington and Oregon

(Section F.4). In southern California DO levels at 150 m were similar or slightly higher during the entire year compared to 2024, noting that this region typically is well above hypoxic values at these depths at all times.

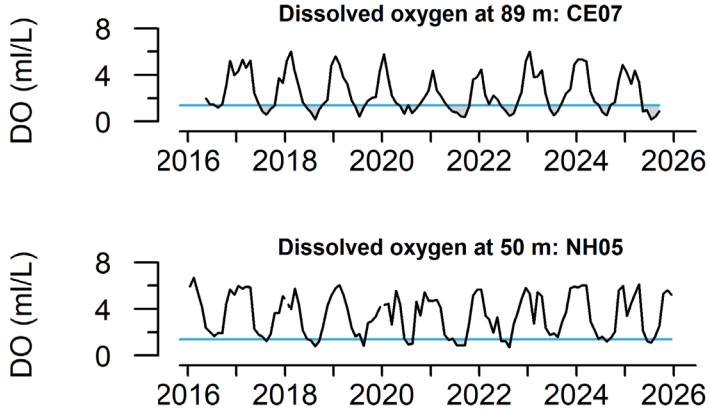


Figure 2.6: Near-bottom dissolved oxygen off Grays Harbor, WA (CE07) and Newport, OR from 1990-2025. Blue lines indicate the hypoxia threshold (1.4 ml DO/L).

Ocean acidification, caused by increased anthropogenic CO_2, reduces pH and carbonate ions in seawater and can create stressful conditions for many marine species (Feely et al. 2008; Busch and McElhany 2016). At station NH05 off Newport, the horizon depth of aragonite saturation state (a measure of the stability of a form of calcium carbonate in seawater) was above the reference threshold of 1.0 in winter, but decreased through spring and summer to < 1.0 (Fig. 2.7), a saturation state which can be corrosive for some shell-forming organisms. This seasonal pattern is typical at this station. Summer values were similar during 2025 to 2024, but with a shorter period of low values during the summer (see details in Section F.4).

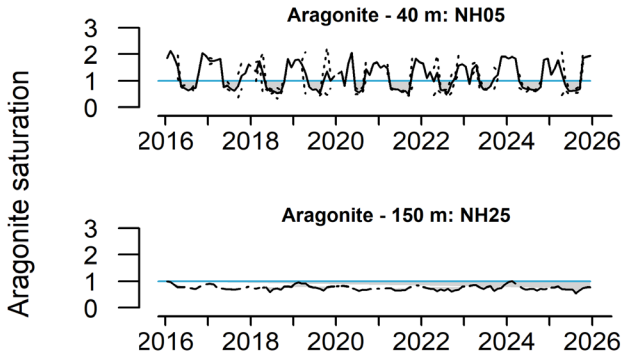


Figure 2.7: Aragonite saturation states off of Newport, OR from 2016-2025. Blue lines indicate the biological threshold for aragonite saturation state (1.0).

2.4 Snowpack and Hydrology

Snow-water equivalent (SWE) is the water content in snowpack. Snowmelt supplies cool freshwater to streams in spring, summer, and fall and is critical for salmon production (Section J, Appendix G). Winter storms created average to above average April 1 snowpack in 2025 (Fig. 2.8). With the exception of central California, April 1 snowpack was greater in 2025 than 2024. An early springtime snowmelt in 2025 and a dry summer led to moderate to severe drought conditions in the Pacific Northwest by early fall, while central and northern California had no or only mild dry conditions. Southern California also experienced moderate to severe drought.

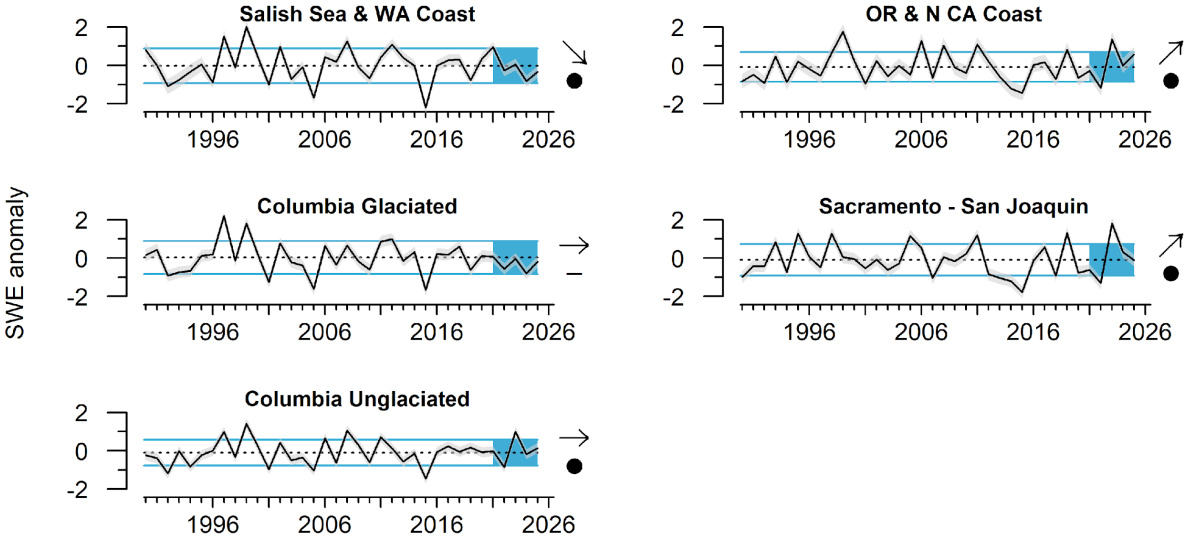


Figure 2.8: Anomalies of April 1st snow-water equivalent (SWE) in freshwater ecoregions of the CCE, 1990-2025. Error envelopes represent 95% credible intervals. Lines, colors and symbols are as in Fig. 2.1. Ecoregions are mapped in Fig. 1.1.

As of January 26th, 2026, fall and early winter storms led to high precipitation levels throughout most of the western U.S., with California being drought-free for the first time in 25 years (https://droughtmonitor.unl.edu/). However, the storms delivering high precipitation occurred during warmer than normal atmospheric temperatures, which generated a high fraction of rain rather than snow, as well as rain on snow, events that reduced snowpack. As a result, 2026 snowpack levels (as of February 5) are exceptionally low throughout most of the west, except for northern Washington, central California, and central Idaho (Fig. G.1). Thus, even though the majority of the west is currently not experiencing drought, if the presently low snowpack persists it could lead to a challenging year for outmigrating juvenile salmon in snow-fed watersheds as spring transitions to summer in 2026. Looking forward, winter precipitation outlooks for February-April suggest slightly lower than normal precipitation in the south, and average or slightly higher than normal precipitation in the Pacific Northwest. Precipitation outlooks for 2026 and longer suggest average conditions throughout the west (https://droughtmonitor.unl.edu)

In 2025, streamflows were generally near average conditions and August stream temperatures were warm (Figs. G.3, G.4). Values of 7-day minimum flows were slightly lower in 2025 than 2024 across all ecoregions, while patterns in 1-day maximum flows relative to 2024 were comparatively mixed. August mean maximum temperatures increased relative to 2024 in all ecoregions. Outside of central and southern California, these 2025 temperatures were above average (Fig. G.2, Appendix G).

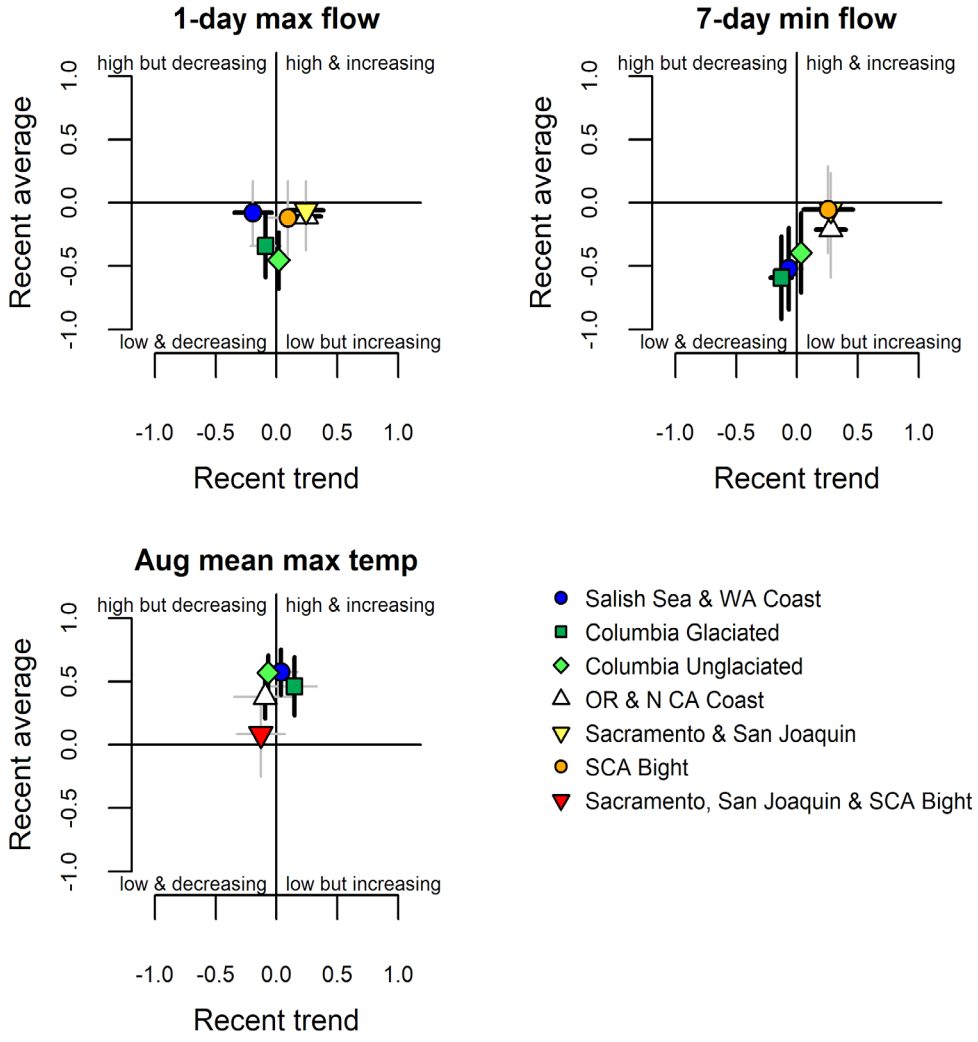


Figure 2.9: Recent (2021-2025) averages and trends in maximum and minimum flow in streams within six freshwater ecoregions. Symbols for each ecoregion fall into quadrants based on recent average (high or low) and recent trend (increasing or decreasing) relative to long-term data (1980-present). Error bars represent 95% credible intervals. Heavy black error bars represent significant differences from zero. Ecoregions correspond to freshwater ecoregions (Fig. 1.1).

Five-year status and trends for regional hydrology are shown in quadrant plots (Fig. 2.9), which indicate if conditions over the last five years were above or below average (y-axis), and had increasing or decreasing trends (x-axis). Overall, both maximum and minimum flows have shown evidence of widespread lows in their recent status, while trends have been mixed (Fig. 2.9). For both indicators, the five-year average was below or near the long-term average for all ecoregions. Five-year trends suggested a latitudinal cline, with both flow indicators trending negative in the north and more positive in the south. Concomitant with patterns of summer low flows, recent average maximum August temperatures were above-average for all ecoregions. Five-year trends in water temperature showed an inverted pattern compared to low flows, with northern ecoregions trending upward but southern ecoregions trending downward.

High August stream temperatures in recent years suggest challenging conditions for adult upstream migrants and juvenile life history types that inhabit watersheds during summer, particularly in seasonally warmer basins. Low 7-day minimum flows in recent years generally suggest poor juvenile rearing conditions, while outcomes of low 1-day maximum flows are more complex and context-dependent.

3. FOCAL COMPONENTS OF ECOLOGICAL INTEGRITY

Key Message

In 2025, ecological indicators reflected both mixed and favorable marine conditions throughout most of the year. The forage community continued to be diverse and productive. Anchovy and juvenile groundfishes remained abundant in the Central and Southern CCE and were an important prey source for top predators. Juvenile stages of groundfish and salmon and krill were abundant in the Northern CCE. Recent ocean conditions for adult Chinook salmon returning to the Columbia River Basin were consistent with near-average returns in 2026, and returns of Sacramento River Fall Chinook and Central Valley Spring Chinook in 2026 will reflect a mix of favorable and unfavorable habitat conditions. Most seabird colonies recovered from lower productivity in the previous year. Pyrosomes reached their highest abundance in Central CCE. Harmful algal blooms continued to impact marine life, shellfish fisheries, and human health. Several ocean and ecological indicators supported the development of risk tables for 2025 groundfish stock assessments.

3.1 Copepods and Krill

Copepod biomass anomalies represent variation in northern copepods (cold-water crustacean zooplankton species rich in wax esters and fatty acids) and southern copepods (smaller species with lower fat content and nutritional quality). Northern copepods usually dominate the summer zooplankton community along the Newport Line off central Oregon (Fig. 1.1), while southern copepods dominate in winter. Positive northern copepod anomalies generally correlate with stronger returns of Chinook salmon to Bonneville Dam and coho salmon to coastal Oregon (Peterson et al. 2014).

Copepod indicators suggest moderate feeding conditions for pelagic fishes off central Oregon in 2025. Lipid-rich northern copepods were above average along the Newport Line during winter and spring. Northern copepod anomalies declined in late summer to near average through the remainder of the year (Fig. 3.1, top). Historically, high northern copepod biomass anomalies have been a common pattern under La Niña and negative PDO conditions (Keister et al. 2011; Fisher et al. 2015). Southern copepod biomass was below average during most of 2025, increasing to well above average by early 2026 (Fig. 3.1, bottom).

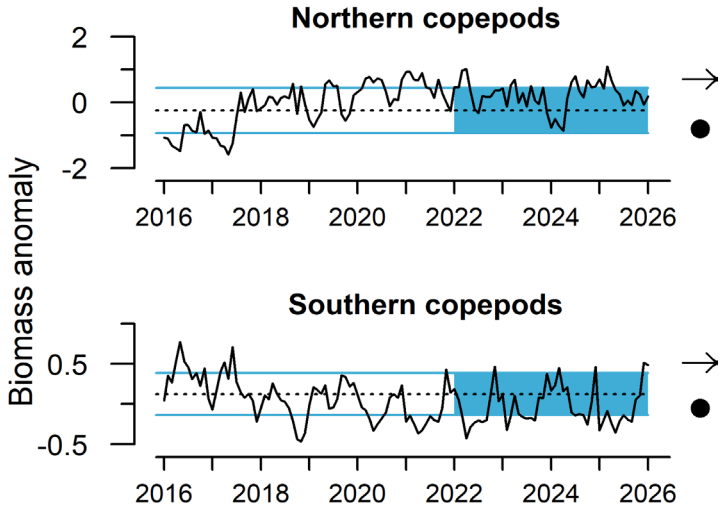


Figure 3.1: Monthly northern and southern copepod biomass anomalies from station NH05 off Newport, OR from 2016-2026. Positive values indicate above-average biomass, and negative values indicate below-average biomass. Lines, colors, and symbols are as in Fig. 2.1.

Krill are among the most important prey groups in the CCE, and information on krill abundance is collected during regional and coastwide surveys. In spring 2025, catches of krill were close to average off central California (see Figs. 3.4, I.2), and moderate catches of krill were observed in the northern region of the CCE (see Fig. 3.3). Krill were also quantified using acoustic backscatter data (see Phillips et al. 2022) during the inaugural Integrated West Coast Pelagics Survey and the Canadian Ecosystem and Pacific Hake Trawl Survey, conducted June-September 2025 from Point Conception to northern British Columbia. The nautical area scattering coefficient (NASC), which represents relative krill abundance between 50-300 m depth, indicated that krill abundance increased in 2025 compared with the past two survey years (2021 and 2023), particularly in the Northern CCE, though krill abundance was not anomalously high. Most krill were located near the 200-m shelf break off Oregon, Washington, and British Columbia (Columbia, Vancouver and Charlotte regions), with less krill observed off California (Fig. 3.2, Section I.4).

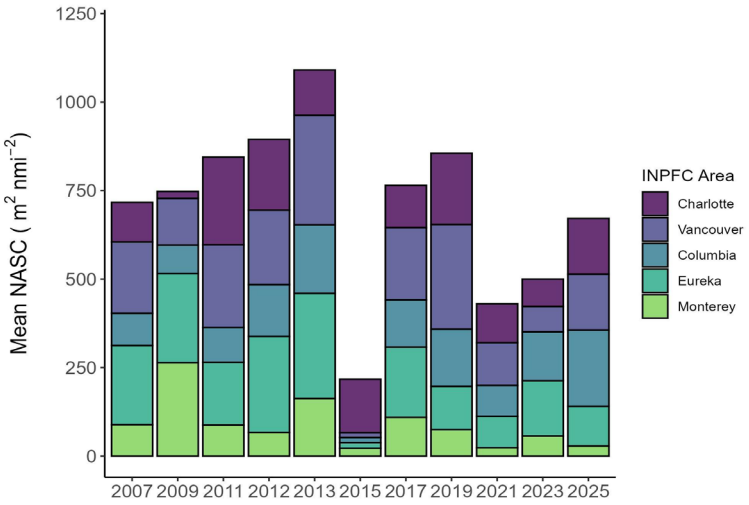


Figure 3.2: Regional abundance of krill in the California Current, based on biannual hydroacoustic sampling. Relative krill abundance is represented as the mean nautical area scattering coefficient (NASC) plotted by five historic International North Pacific Fishery Council management areas. Note: abundance data is available every odd year from 2007-2025 and 2012

3.2 CPS and Regional Forage Availability

3.2.1 Coastwide Coastal Pelagic Species (CPS)

The NOAA Southwest Fisheries Science Center has conducted CPS surveys in most years since 2006, typically spanning the continental shelf from San Diego to Cape Flattery. In summer 2025, the CPS survey was conducted as part of the Integrated West Coast Pelagics Survey. The central stock of northern anchovy remained highly abundant in 2025, after peaking at ~2.75 million tons in 2021 Stierhoff et al. (in press). Jack mackerel dominated CPS biomass offshore of Washington and Oregon, while northern anchovy prevailed south of Fort Bragg (Fig. H.1). In the nearshore region, northern anchovy were prevalent south of Bodega Bay, Pacific sardine were most abundant south of Monterey Bay and around Fort Bragg, and jack mackerel and Pacific herring were dominant north of Fort Bragg (Fig. H.2). The 2025 biomass estimates are preliminary and therefore not presented in this report (Stierhoff et al. in press). More information on the survey and CPS data is in Appendix H.

3.2.2 Regional forage composition

The regional surveys that produce CCE forage data use different gears and survey designs, which makes regional comparisons difficult. Here we present results of cluster analysis methods that are used to identify regional shifts in forage composition (Thompson et al. 2019). See the caption of Figure 3.3 for how to interpret the plots.

Northern CCE: The JSOES survey off Washington and Oregon (Fig. 1.1) targets juvenile salmon in surface waters, and also samples surface-oriented fishes, squid, and jellies. The 2025 forage assemblage was similar to the previous two years (Fig. 3.3). Juvenile salmon

abundances were generally high in 2025, as juvenile chum and yearling coho catches were the highest on record since 1998, subyearling Chinook the fourth highest, and juvenile sockeye and yearling Chinook were slightly above average. Catches of three of four gelatinous invertebrates (water jelly, sea nettle and egg yolk jelly) were above average, and 'young-of-year' (YOY) sablefish, market squid, and moon jelly were near average abundances. Pompano, which had been rare in the region prior to 2014, were at their highest level since 2017. Juvenile salmon time series are discussed further in Section 3.3, and data for the remaining species are in Appendix I.1.

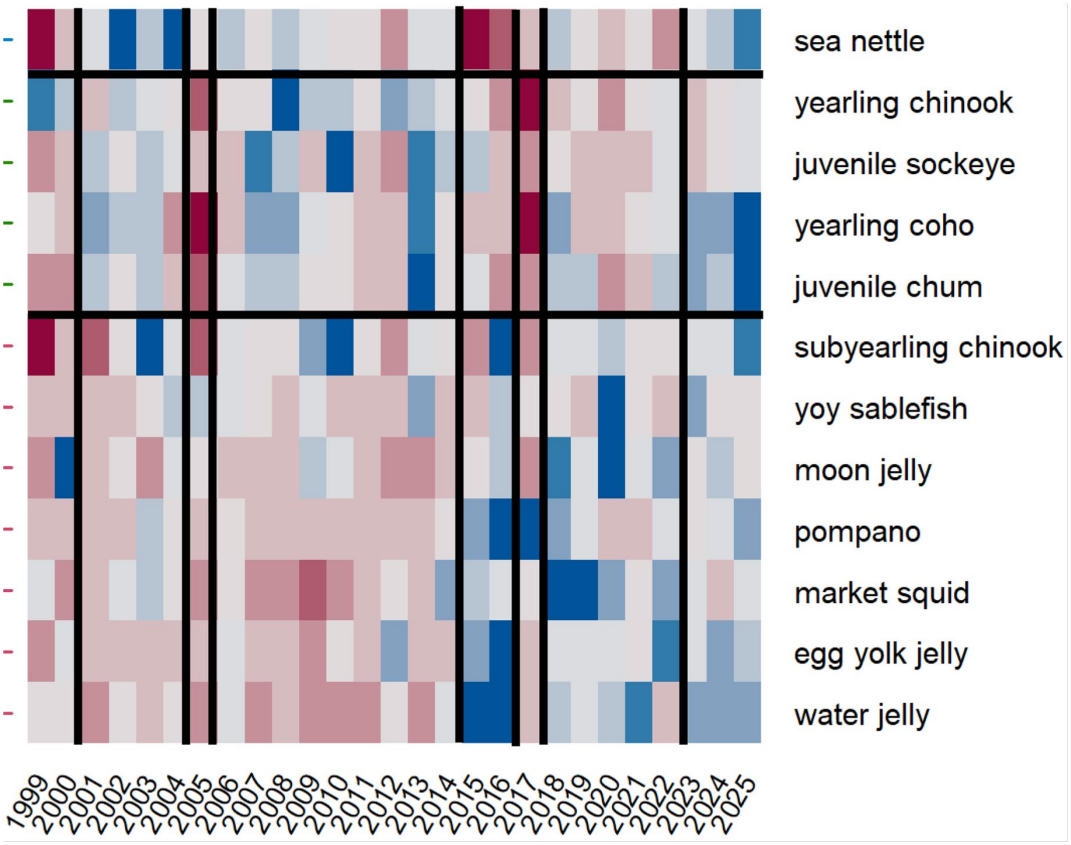


Figure 3.3: Cluster analysis of pelagic community indicators in the Northern CCE, 1999-2025. Colors indicate relative catch per unit effort (blue = high, white = average, red = low). Horizontal bars separate clusters of typically co-occurring species. Vertical bars demarcate breaks in assemblage structure between years.

Central CCE: Data presented in Figure 3.4 are from the RREAS survey (Fig. 1.1) that targets pelagic YOY rockfishes, and samples other pelagic species off central California. In 2025, species abundances in the area centered off Monterey Bay were similar to 2021-2024 (Fig. 3.4). YOY rockfishes were highly abundant for a third consecutive year, while YOY anchovy, YOY Pacific hake, and myctophids declined from high abundances in 2024 to slightly below average in 2025. Adult anchovy abundance continued a downward trend, though was still above the long-term average, and adult sardine was low. Notably, catches of pyrosomes significantly increased and were at their highest level on record, and octopus

was at the highest level compared to the past several years. Market squid and krill were near-average in 2025. Overall, combined forage was above average off the central coast of California. Time series of these catch data are in Appendix I.2.

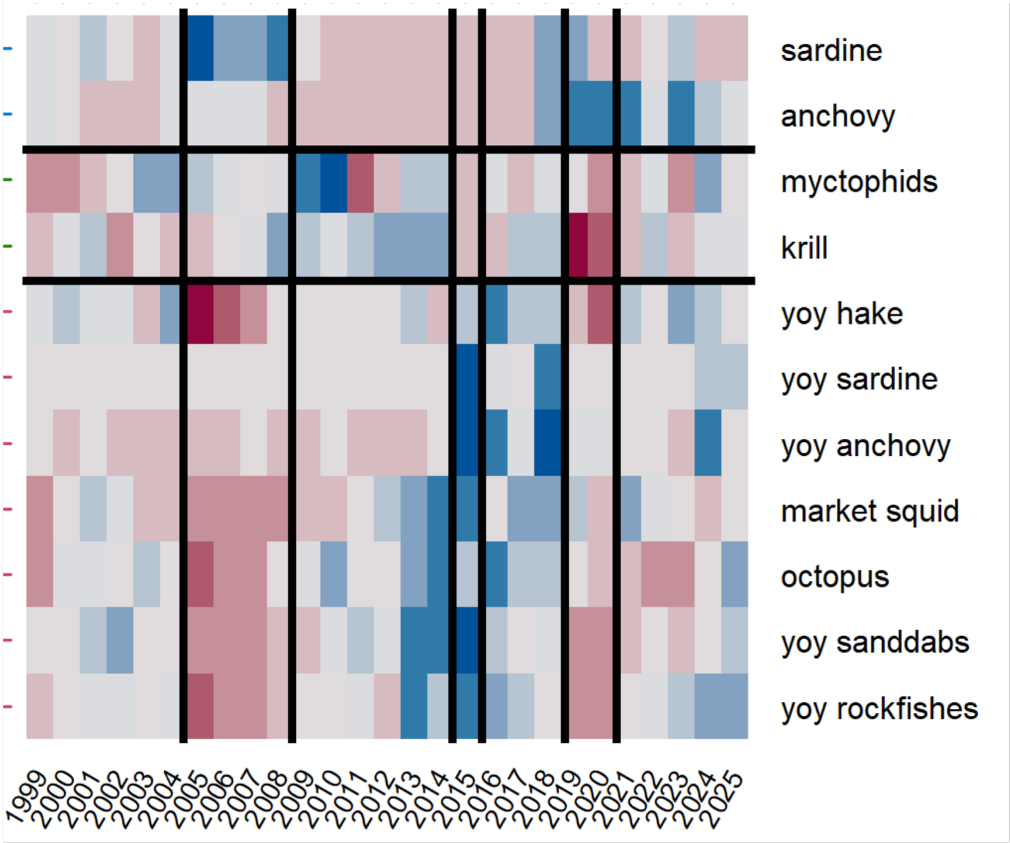


Figure 3.4: Cluster analysis of forage indicators in the Central CCE, 1999-2025. See Fig. 3.3 for how to interpret the plot.

Southern CCE: Forage data for the Southern CCE come from spring CalCOFI line 90 larval fish surveys (Fig. 1.1). In most years, CalCOFI contributes larval fish data from lines 80 and 90; however, due to staff losses and the federal government furlough in 2025, data was limited to line 90. The impact of not including line 80 data in this analysis is not yet clear at this point; line 80 is a more northern line extending off the typically more productive region slightly north of Pt. Conception. The larval fish assemblage in 2025 was very similar to the past eight years (Fig. 3.5). Anchovy, southern mesopelagics, and California smoothtongue increased rapidly in 2017 and have remained high through 2025. Among flatfishes, sanddabs and English sole increased toward historically high values and slender sole was above average. Rockfishes declined from high abundances over the past several years to below average in 2025 while croakers remained high. Pacific hake and jack mackerel were close to average and sardine and Pacific mackerel were absent. Time series of catches are available in Section I.3.

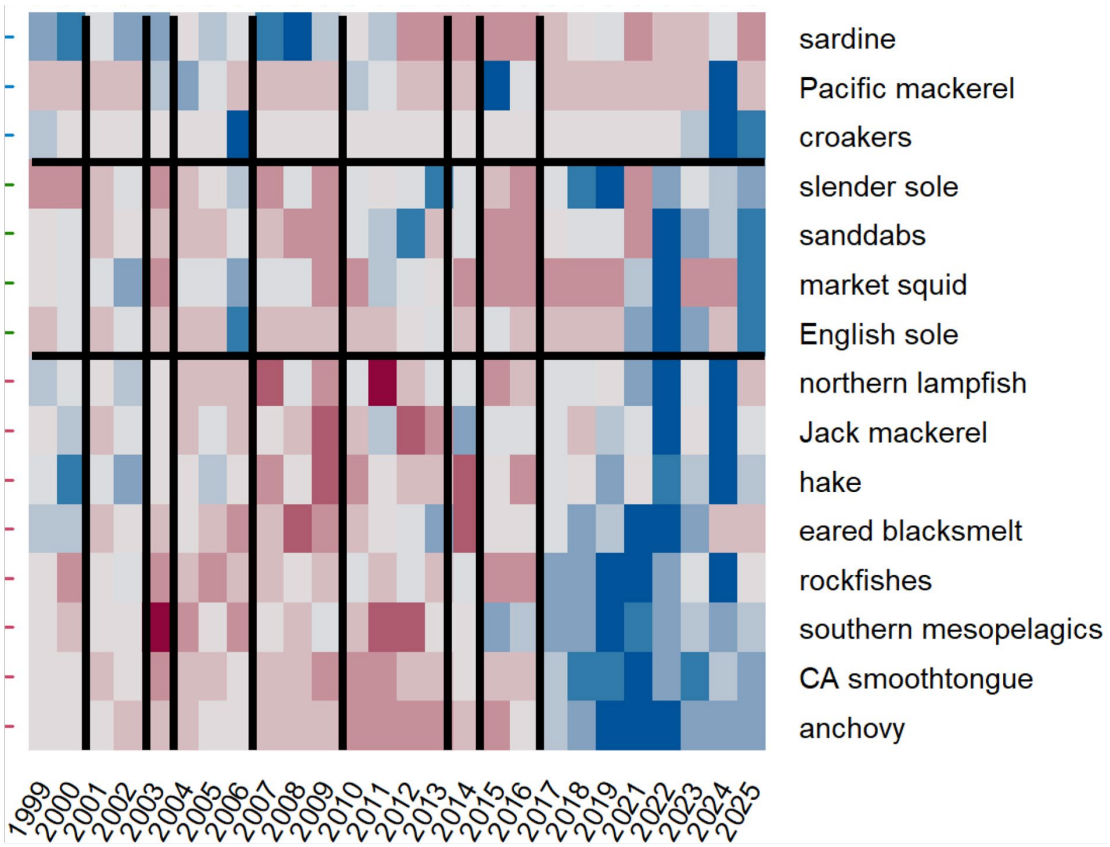


Figure 3.5: Cluster analysis of forage indicators in the Southern CCE, 1999-2025. See Fig. 3.3 for how to interpret the plot.

3.3 Salmon Indicators

Juvenile salmon abundance: Catches of juvenile coho and Chinook salmon from June surveys in the Northern CCE (Fig. 1.1) are indicators of salmon survival during their first few weeks at sea. Catch-per-unit-effort of yearling Chinook salmon in 2025 was once again close to the time series average. Catches of yearling coho salmon were the highest in the 28-year time series and suggest an increasing five-year trend in their early marine survival (Fig. 3.6). Juvenile rockfish are a key prey item of juvenile coho (Daly et al. 2013) and their abundance has also increased in the Northern CCE in recent years.

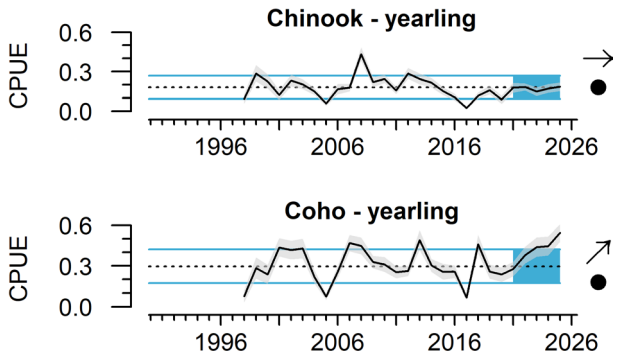


Figure 3.6: Catch per unit effort of yearling Chinook salmon (top) and yearling coho salmon (bottom) off Oregon and Washington in June, 1998-2025. Gray envelope indicates ±1 s.e. Lines, colors, and symbols are as in Fig. 2.1.

3.3.1 Stoplight tables

Long-term associations between oceanographic conditions, food web structure, and salmon productivity support qualitative outlooks of Chinook salmon returns to the Bonneville Dam and smolt-to-adult survival of Oregon Coast coho salmon (Burke et al. 2013; Peterson et al. 2014). The "stoplight table" (Fig. 3.7) summarizes many indicators shown elsewhere in this report (PDO, ONI, SST, deep temperature, copepods, juvenile salmon catch) relevant to salmon returns.

The 2025 ocean ecosystem indicators suggest juvenile salmon from Columbia River stocks experienced moderate conditions during their spring outmigration to the ocean. Indices of winter larval fish biomass were lower than average, despite cool coastal SST in January and February, suggesting less favorable feeding conditions for salmon. However, most of the basin and local scale indicators are consistent with fair ocean conditions that are somewhat favorable for Northern CCE stocks of salmon (Fig. 3.7).

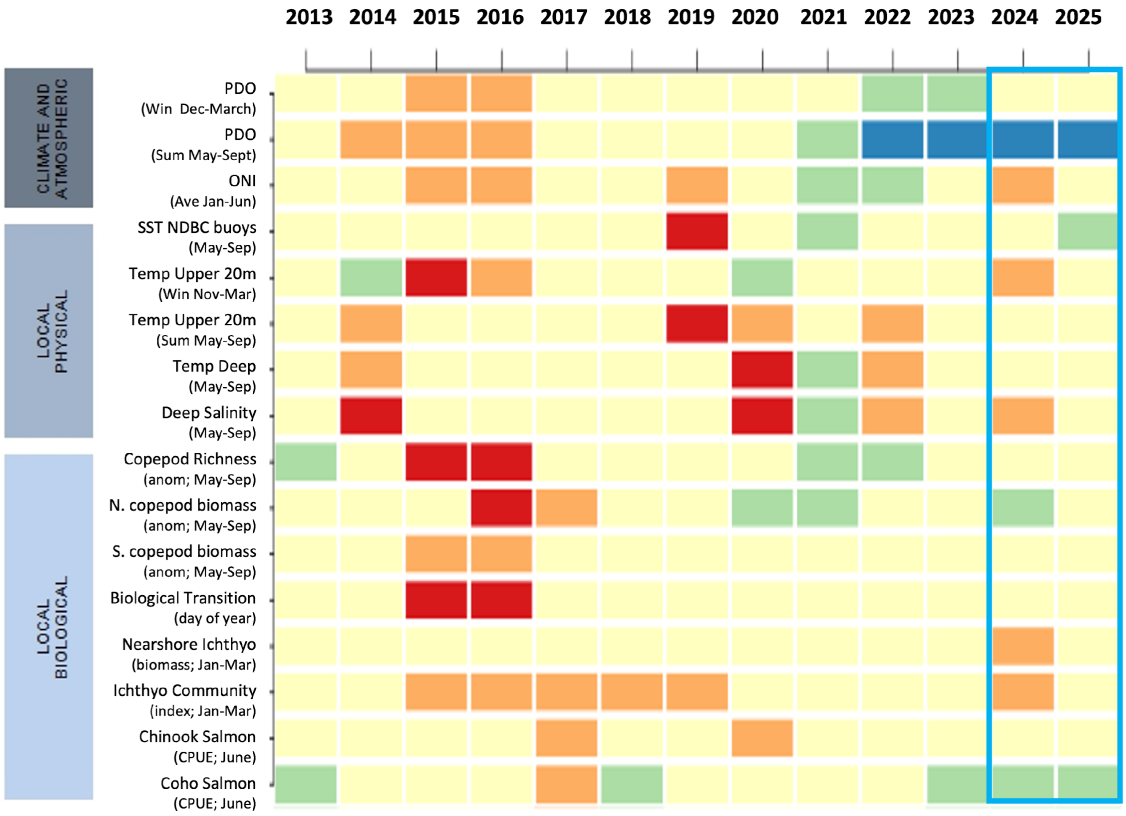


Figure 3.7: Stoplight table of conditions for smolt years 2013-2025 for coho salmon originating in coastal Oregon and Chinook salmon from the Columbia Basin. Colors represent a given year's indicator relative to the reference period (1998-2020). Blue: >2 s.d. above the mean; green: >1 s.d. above the mean; yellow: ±1 s.d. of the mean; orange: >1 s.d. below the mean; red: >2 s.d. below the mean. Chinook salmon from smolt year 2024 and coho salmon from smolt year 2025 (outlined in blue box) represent the dominant adult age classes returning in 2026. See https://connect.fisheries.noaa.gov for the full stoplight table with years 1998-2025.

Marine conditions in 2025 were consistent with average survival for coho salmon returning to this area in 2026. Chinook salmon spend two years or more in the ocean, therefore for their return to the Columbia Basin in 2026, we look to conditions in 2024, which reflect a mix of poor and intermediate conditions. We also use quantitative models based on stoplight indicators in Figure 3.7 and spatial patterns of SST to generate outlooks for Chinook salmon returns in 2026 and 2027 (see Appendix J.2). The models suggest predicted counts of Chinook salmon returning to the Snake and Upper Columbia rivers in 2026 will be lower than the 2025 returns, but close to the 10-year average (Fig. 3.8). These models also suggest lower adult returns for smolts that went to sea in 2024 (most of which will return in 2026) than for salmon that went to sea in 2025 (returning in 2027). The

mean rank of ecosystem indicators in the stoplight table suggests poorer ocean conditions in 2024 compared to 2025, though not by much (Fig. 3.7). Outlooks based on SST, as well as outlooks for steelhead returns, are presented in Appendix J.

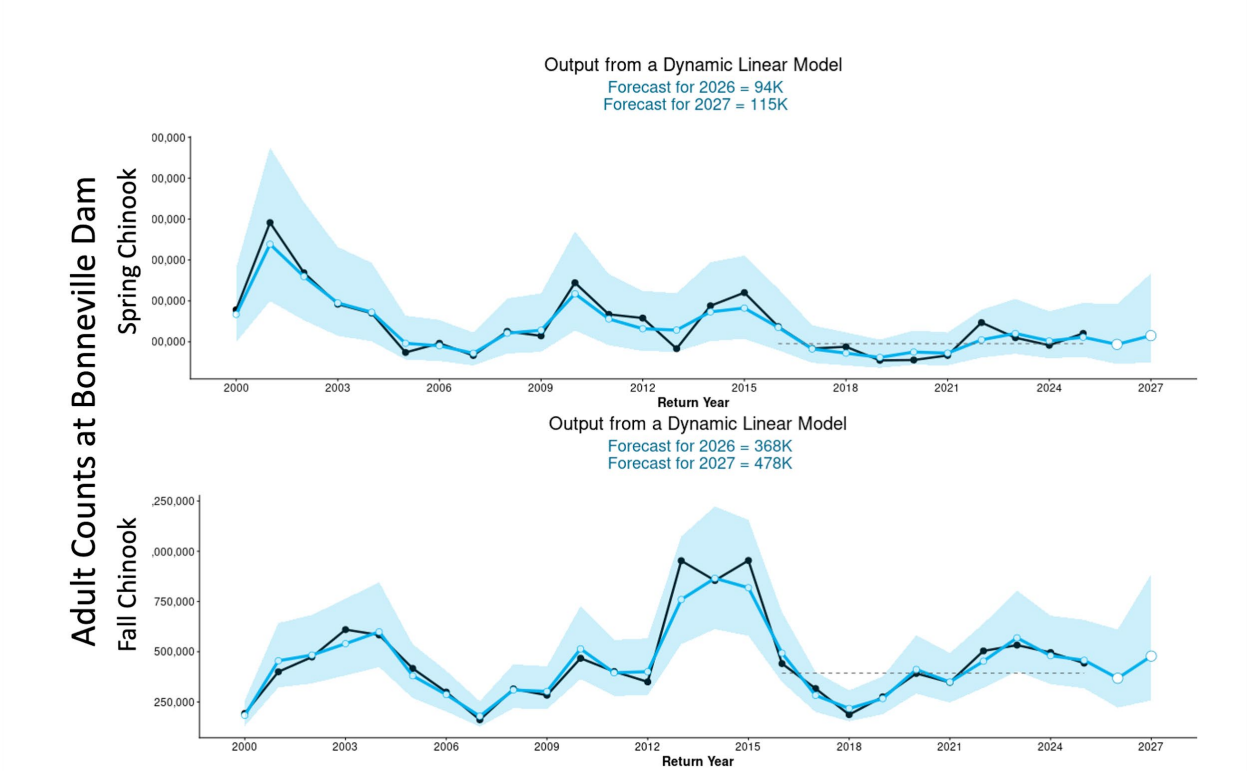


Figure 3.8: Observed and modeled adult salmon counts at Bonneville Dam (black lines) for spring Chinook salmon (top row) and fall Chinook salmon (bottom row). Predictions are based on salmon stoplight indicators lagged by two years. Years on the x-axes are adult return years. Blue lines are model fits; shaded areas are 95% confidence intervals (or prediction intervals for 2026 and 2027). Gray dashed lines are the recent 10-year average. Outlooks based on SST lagged two years are shown in Section J.2.

The Council's Habitat Committee, Salmon Technical Team, and others including CCIEA scientists have developed a comprehensive stoplight table for Central Valley Spring Chinook salmon, Sacramento River Fall Chinook salmon, and Klamath River Fall Chinook salmon (Fig. 3.9). This table features indicators from throughout the stocks' life histories, spanning the 1983-2024 brood years, which were recently refined based on their utility to generate recruitment outlooks see Section J.3.

Overall, habitat conditions for the three salmon stocks have improved marginally in recent years. However, these recent improvements have happened within an overarching, multi-decadal decline in conditions. Indicators for the most recent brood years suggest outmigration flows were improved for Central Valley Spring Chinook and Sacramento River

Fall Chinook, and early marine predation pressure may have been relatively low, but recent outmigration temperatures were unfavorably warm. These contrasting patterns of highly favorable outmigration flows and highly unfavorable outmigration temperatures were unusual for Central Valley Spring and Sacramento River Fall Chinook. The counts of natural area spawners for these stocks were also poor for much of the past decade, limiting the stocks' ability to take advantage of the recent high stream flows. For Klamath River Fall Chinook, both outmigration temperatures and sea surface temperatures were unfavorable during recent brood years.

Indicators summarizing spawning, incubation, and outmigration conditions lead adult returns by two to three years, and therefore indicator-based outlooks can be made two years in advance. The recent habitat conditions suggest returns of Sacramento River Fall and Central Valley Spring Chinook in 2026 and 2027 will reflect a mix of favorable and unfavorable conditions including some novel combinations whose effects are difficult to predict. Klamath River Fall Chinook salmon indicator-based outlooks are consistent with low returns in 2026 and 2027. More information about the indicators, as well as egg thiamine concentrations, can be found in Section J.3.

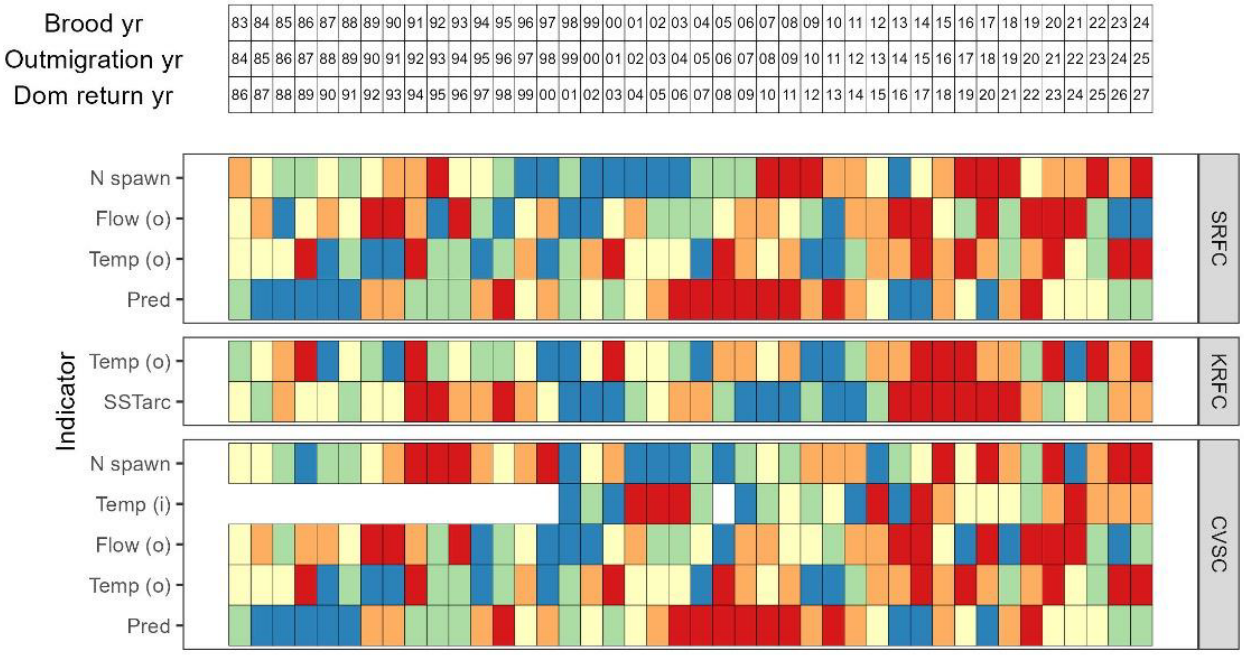


Figure 3.9: Stoplight charts of indicators key to the recruitment of Sacramento River Fall Chinook, Central Valley Spring Chinook and Klamath River Fall Chinook stocks. Rows are ordered by basin of origin, then life stage. Cooler colors for each cell represent hypothesized better habitat conditions. Colors for each cell represent quintiles of hypothesized conditions, which range from poor (red) to favorable (blue).

3.4 Groundfish

3.4.1 Status of groundfish biomass and fishing pressure

The CCIEA Team regularly presents the status of groundfish biomass and fishing pressure based on the most recent stock assessments. This year's report includes updated information for five stocks and one stock complex from the 2025 assessments, including Chilipepper rockfish, the California stock for Quillback rockfish, sablefish, yelloweye rockfish, yellowtail rockfish north of 40° 10' N , and Rougheye/Blackspotted rockfishes.

Most groundfish stock biomasses are above biomass limit reference points (LRPs; Fig. 3.10, x-axis), with only one since 2021, copper rockfish in southern California, estimated to be below the LRP. The full assessment of quillback rockfish in California has updated the previously overfished stock status to being a stock above the biomass target. For management purposes, the southern California substock of copper rockfish was combined with the northern California substock, and the California substock is not considered overfished. The other new stock assessments do not indicate any new overfished or overfishing designations. See Appendix K for more information on groundfish stock status, including a new interactive tool for exploring groundfish data.

CCIEA oceanographic and ecosystem indicators were used to develop risk tables for 2025 groundfish assessments, including yellowtail rockfish north of 40° 10' N, Chilipepper rockfish, sablefish, and Pacific whiting. Together, the risk tables generally indicated neutral to favorable ecosystem conditions for those stocks (2025 West Coast Groundfish Stock Assessments at-a-glance).

In previous ESRs, we have included trends in juvenile groundfish biomass indices. However, U.S. West Coast Groundfish Bottom Trawl Survey data from 2025 were not available in time for us to generate those indices for this year's report. In Appendix K, we present new analyses relevant to groundfish recruitment, diversity, and ecosystem component species to generate discussion around new groundfish indicators to potentially include in future ESRs. In Appendix E, we also present long-term projections of the spatial distribution of groundfish under climate change and the potential implications of these projections to fisheries on the West Coast. Similar information is provided for CPS and Highly Migratory Species as well.

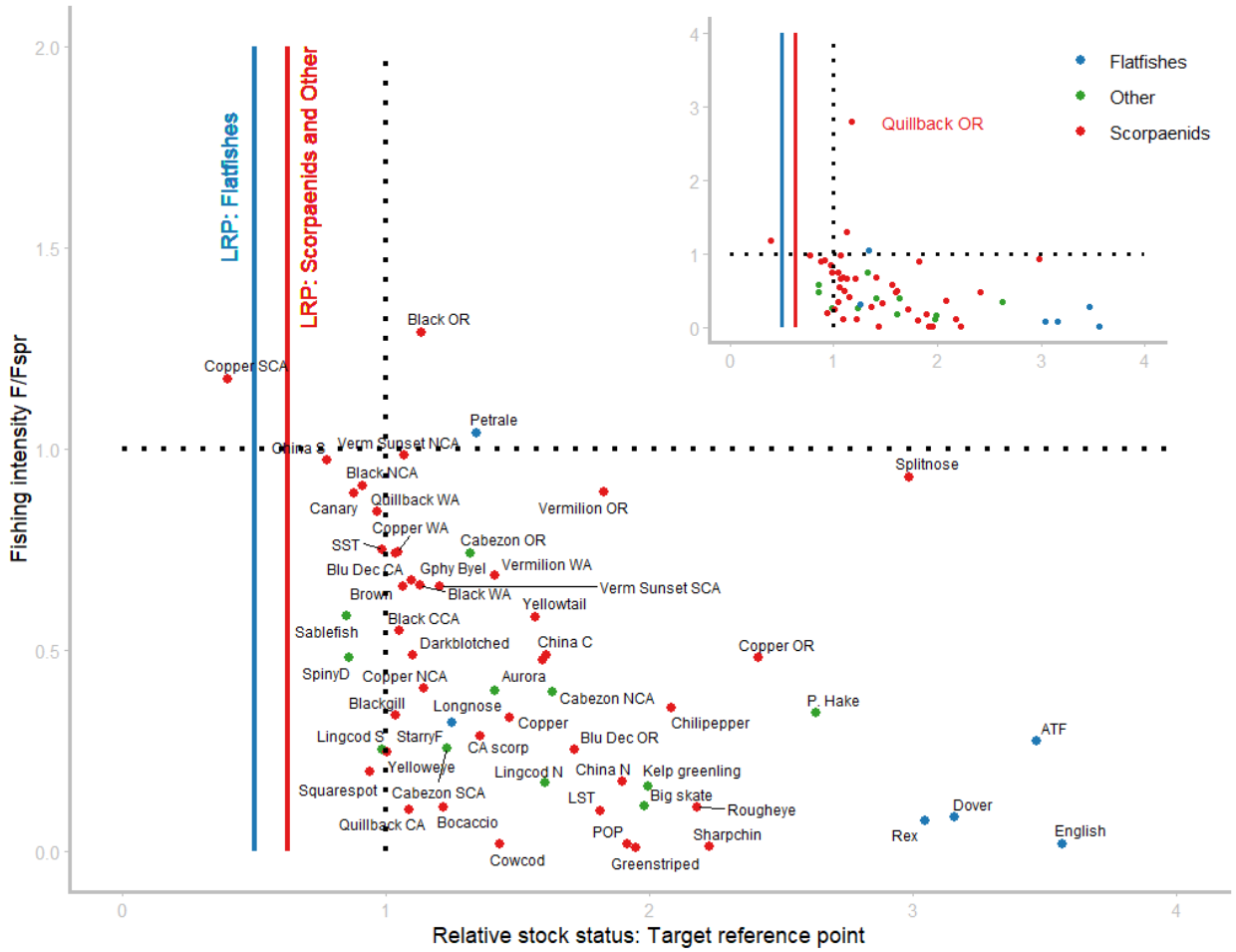


Figure 3.10: Stock status of CCE groundfish. Relative Stock Status is the ratio of the current year spawning biomass (in mt) or output (typically in billions of eggs) to unfished relative to the target reference point (as a percentage of unfished biomass; 0.4 for scopaenids and other fishes; 0.25 for flatfishes). Fishing Intensity uses the fishing rate to achieve a specific spawner potential ratio (SPR), defined as F/FSPR, where SPR is the maximum sustainable yield (MSY) proxy. The horizontal line is the fishing intensity rate reference; above the line is above the reference level and indicates overfishing. Vertical lines are the biomass target reference points (TRP=1; dashed line) and limit reference points (LRPs; red lines); left of the LRP indicates an overfished status. Symbols indicate taxonomic groups. All points represent values from the most recent PFMC-adopted full stock assessments.

3.5 Highly Migratory Species (HMS)

3.5.1 HMS diet

HMS are opportunistic predators and information on their diets complements forage surveys, offers insight into how forage varies in space and time, and provides direct

measures of forage use by these predators. Analyses of stomach contents from Pacific bluefin tuna, albacore tuna, and swordfish collected by commercial and recreational fishers in central and southern California indicate that anchovy and Pacific hake continue to be important prey items for HMS (Fig. 3.11). Consumption of anchovy by Pacific bluefin tuna and swordfish was lower in 2024 relative to the previous year. In contrast, the consumption of hake by these two predators was higher in 2024. The proportion of hake in swordfish diets has been above the long-term average since 2021 and increased to 44% in 2024, surpassing anchovy as the dominant prey item for this species. Consumption of Pacific sardine by albacore tuna decreased from record high levels in the northern region of the CCE. Rockfish consumption increased for all three predators and was near to above average for swordfish and albacore in 2024. Observations of rockfish and sardine abundances in the ecosystem surveys suggest this trend will continue for 2025.

These findings highlight the dynamic nature of HMS feeding behavior, which is influenced by factors such as prey availability and environmental conditions. See Appendix L for more information on HMS diets and updates to the yellowfin tuna stock assessment. We note that near-real time HMS diet data will not be available for the foreseeable future due to staffing changes. New information on the spatial movements of albacore and Pacific bluefin tuna and the HMS fishing fleet in relation to ocean conditions during fishing seasons from 2010 to the 2025 is also included in Appendix E.

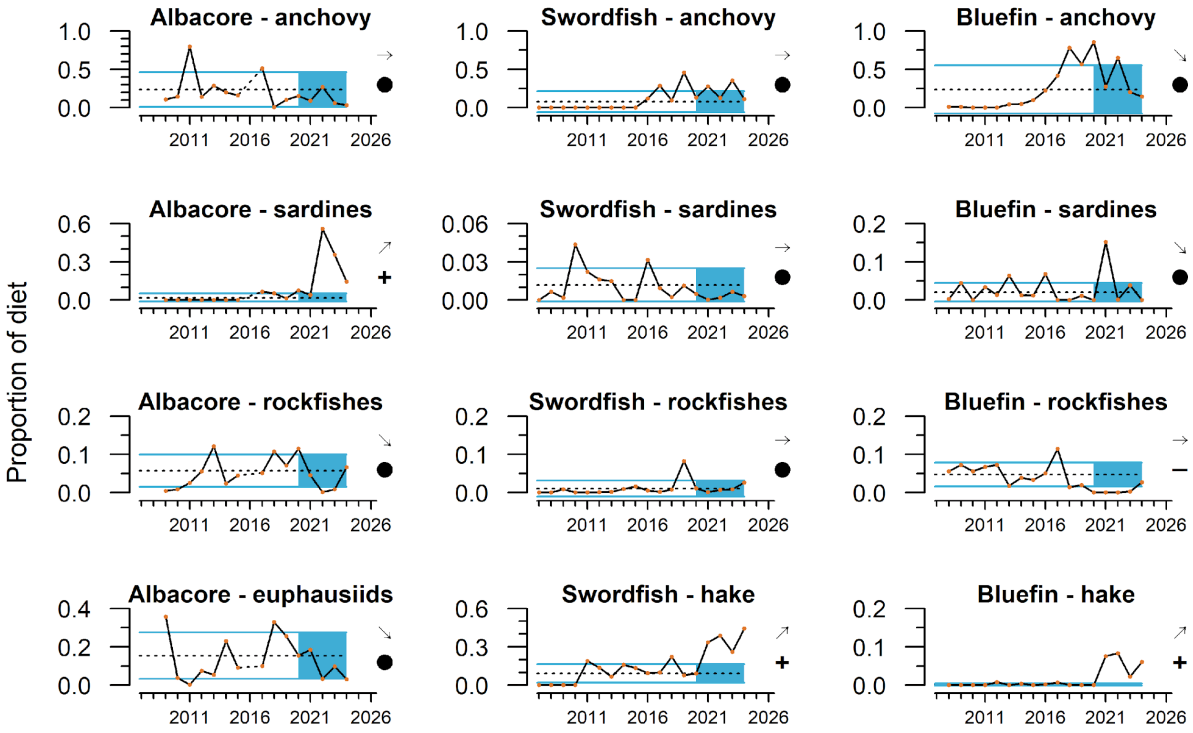


Figure 3.11: Diets of albacore tuna, swordfish, and Pacific bluefin tuna sampled from commercial and recreational fisheries in the Northern and Central CCE, 2008-2024. Data represent the mean proportional abundance of four key prey classes in predator diets. Lines, colors, and symbols are as in Fig. 2.1.

3.6 Seabird Indicators

Seabird indicators (productivity, density, diet, and mortality) reflect population health and condition of seabirds, as well as links to lower trophic levels and other conditions in the CCE. The species we report on here and in Appendix M represent a breadth of foraging strategies, life histories, and spatial ranges.

3.6.1 Fledgling production

In 2025, fledgling production at seabird colonies on Yaquina Head, Oregon and Destruction Island, Washington increased relative to the previous year. Productivity of rhinoceros auklets, common murres, and Brandt's and pelagic cormorants were near or above average (Appendix M). These improvements in seabird reproductive success may be a reflection of the anomalous late-winter upwelling, which can improve parental condition (Schroeder et al. 2009; Black et al. 2011a). Smelts and Pacific sand lance dominated the diets of rhinoceros auklet chicks in the Northern CCE and consumption of herring by auklet chicks was about average. Smelts also dominated the diets of common murre while consumption of juvenile rockfishes declined compared to the past two years to near average (Appendix M). The significant increase in Brandt's cormorant productivity in the Northern and Central CCE is likely related to the increase in anchovies in their diets (Appendices M and I).

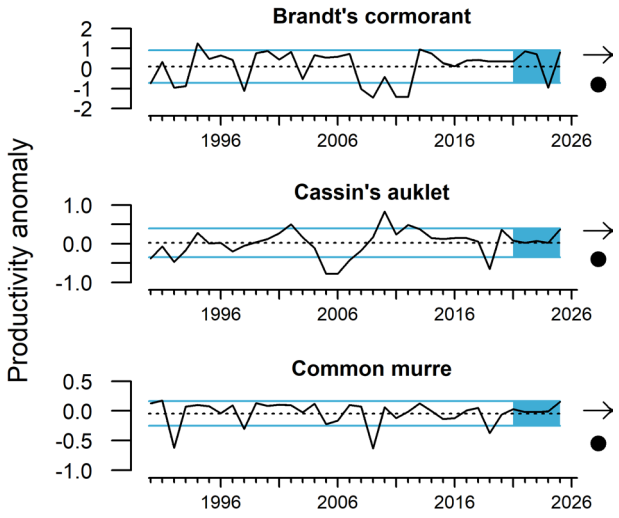


Figure 3.12: Standardized productivity anomalies for three seabird species breeding at Southeast Farallon Island, CA through 2025. Lines, colors, and symbols are as in Fig. 2.1.

Seabird colonies on Southeast Farallon Island off central California also experienced near or above average fledgling production in 2025 (Fig. 3.12 and Appendix M). Brandt's cormorant productivity bounced back from a below average year in 2024. Cassin's auklet double-brooding levels were high; more than 80% of pairs that fledged a chick started a second brood, which is typical of years with good marine conditions (Johns et al. 2017) and again may be related to the late-winter upwelling. Consumption of anchovy by seabirds at Southeast Farallon Island increased in 2025 while consumption of juvenile rockfishes decreased. However, the proportion of juvenile rockfishes in the diets of most piscivorous seabirds was near or above average.

3.6.2 Mortality

Seabird mortalities reported on beaches in the northern and central regions of the CCE were near or below average for most species in 2025 (Appendix M). However, above average mortalities were reported for Brandt's cormorants and sooty shearwaters in those regions (Appendix M). There was also a die-off and strandings of brown pelicans on beaches of central and southern California in the spring and summer of 2025. Similar to 2024, pelican mortality is likely attributed to lower prey availability and greater intraspecific competition, although in 2025 there was evidence of domoic acid poisoning in brown pelicans.

3.7 Marine Mammals

3.7.1 Whale entanglements

Reports of whale entanglements along the West Coast increased beginning in 2014, and fluctuated over subsequent years. The dynamics of entanglement risk and reporting are complex, and are affected by shifts in ocean conditions and prey fields, changes in whale populations, changes in distribution and timing of fishing effort, and increased public awareness.

West Coast entanglement reports in 2025 remained below the peak years of 2015-2018 and were less than the number of confirmed reports in 2024 (Fig. 3.13). Humpback whales continued to be the most common species reported. Late-summer and early-fall increases in habitat compression (Fig. 2.5) and a nearshore increase in adult anchovy (a main prey of humpback whales) may have both contributed to increased entanglement risk and possibly the likelihood of detections overall. Most reports were in California, with an increase in reports in Washington compared to previous years. There were a few confirmed reports from Mexico involving U.S. gear. Confirmed entanglements involved gear from all three West Coast states, and two entanglements involved recreational gear from Canada. Multiple actions were taken in 2025 to reduce whale entanglement risk (see Appendix N.1, CDFW Whale Safe Fisheries). Also in 2025, NOAA Fisheries established the West Coast Take Reduction Team to address the incidental mortality and serious injury of two humpback whale stocks, including the endangered Central American/Southern Mexico-West Coast stock, in the sablefish pot fishery. See Appendix N.1 and for more information.

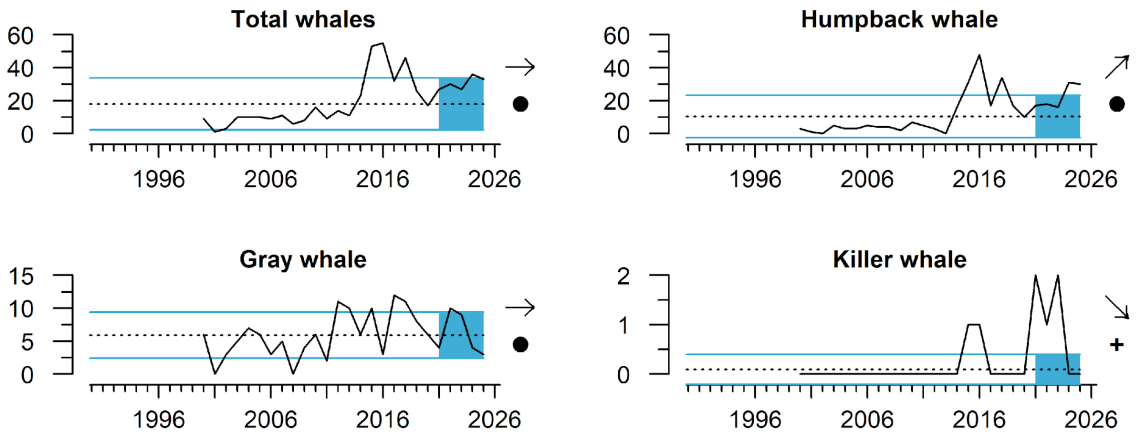


Figure 3.13: Numbers of whales for selected species confirmed as entangled in fishing gear along the West Coast from 2000-2025.

3.7.2 Sea lions

Due to a restructuring of research priorities, the Alaska Fisheries Science Center proposed the termination of the California Current Ecosystem Program that provides information on California sea lions for the ESR. This represents a significant loss for the ESR, as data on sea lion production and pup condition have traditionally been very useful in diagnosing early-year forage conditions within the southern California region. For 2025, these data were not available at the time of this writing, leaving us unclear as to the total impacts of a large harmful algal bloom within the southern California region that led to high numbers of marine mammal deaths and strandings (See Section 3.8 and Appendix O). Sea lion data will no longer be available after 2025.

3.8 Harmful Algal Blooms (HABs)

Blooms of the diatom genus *Pseudo-nitzschia* are common along the U.S. West Coast and can produce domoic acid, a toxin that can affect coastal food webs and lead to fishery closures. *Pseudo-nitzschia* HABs can cost tens of millions of dollars in lost revenue, particularly for the commercial Dungeness crab fishery, and cause a range of sociocultural impacts in fishing communities. In 2025, such blooms were again problematic for shellfish fisheries and marine life in California and southern Oregon (Fig. 3.14). A major domoic acid event in the Southern California Bight developed in early spring 2025 and lasted more than three months, leading to a large marine mammal stranding event. This is the fourth year in a row that a large marine mammal stranding event has been associated with a domoic acid event in southern California, with all events associated with upwelling. Bivalve shellfish harvests and the Pacific sardine fishery were also impacted by the 2025 Southern California Bight event (Appendix O). Recurrent toxic *Pseudo-nitzschia* blooms in southern Oregon resulted in the razor clam fishery being closed for all of 2025. Humboldt County in northern California also remained closed to razor clam harvesting throughout 2025, and the fishery in Del Norte County was closed for the first half of the year.

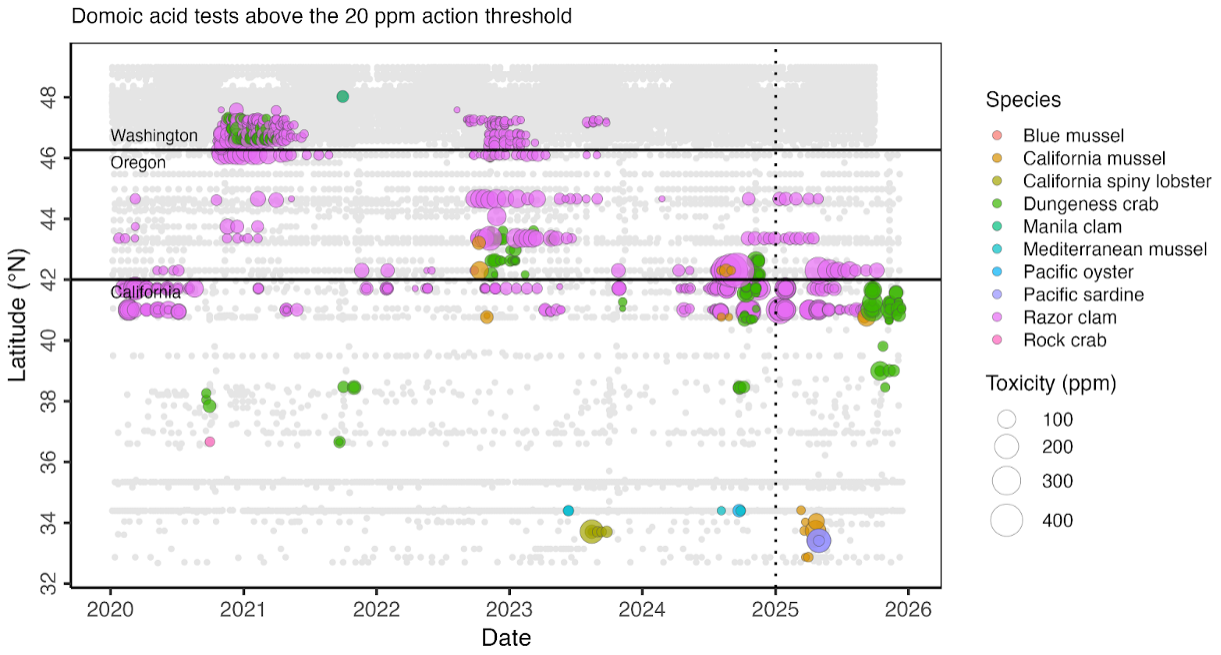


Figure 3.14: Domoic acid test results above the 20 ppm action threshold over the last six years. Grey points indicate a test result below the action threshold. Horizontal black lines indicate state boundaries and the vertical dotted line indicates the start of 2025.

A summary of management actions in the commercial Dungeness crab fishery in response to domoic acid and other issues, such as poor body condition and marine life entanglement risk, is shown in Figure 3.15. Dungeness crab tissues (viscera and meat) remained below regulatory thresholds in Oregon and Washington; however, the opening of the 2025-2026 commercial fishery was delayed in both States due to low meat recovery. Exceedances in the viscera and meat of Dungeness crab were detected in northern California in the fall of 2025, delaying the opening of the recreational Dungeness crab fishery. California's commercial Dungeness crab fishery was delayed due to marine life entanglement risk and meat quality testing, with meat quality tests unable to be completed due to the domoic acid event in northern California. This year marks the seventh consecutive year that the commercial Dungeness crab fishery has been delayed in California because of marine life entanglement risk concerns, and the first year that the fishery operated under some sort of restriction for the entire season.

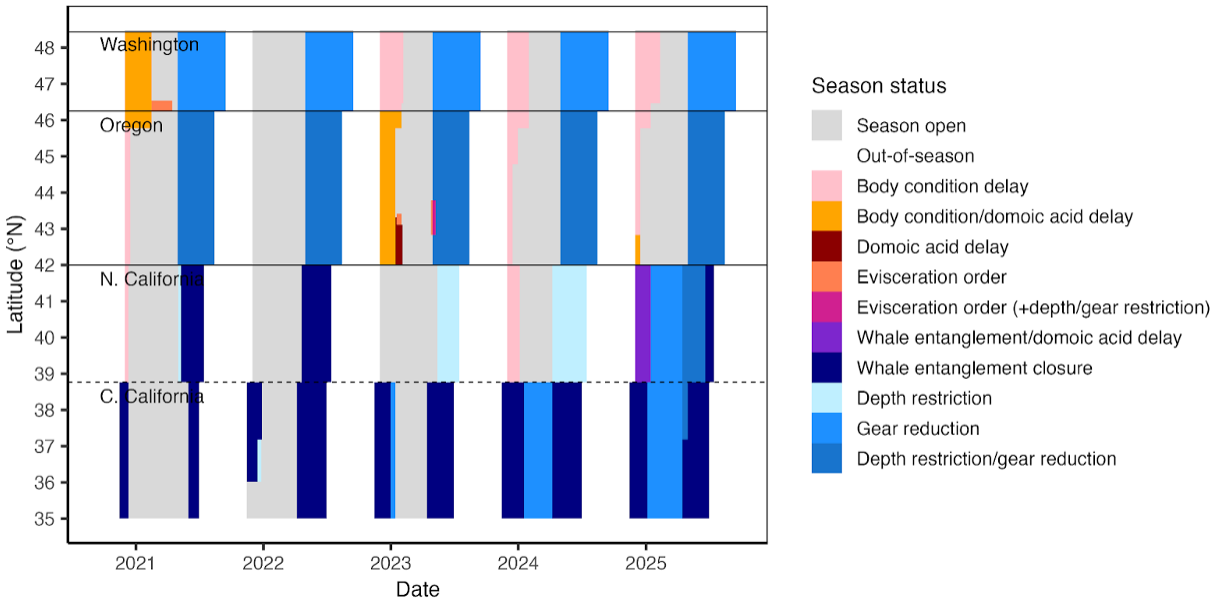


Figure 3.15: The spatial-temporal history of closures and management restrictions in the U.S. West Coast Dungeness crab fishery from 2021 to 2025, both HAB and non-HAB related. Solid black lines indicate state borders and the dashed line indicates the border between the northern and central California management zones. Gray shading indicates the commercial Dungeness crab fishing season in each region. Figure adapted from Free et al. (2022) using news releases from the California, Oregon, and Washington Departments of Fish and Wildlife.

Again in 2025, dinoflagellates (both harmful and nonharmful) comprise a larger portion of the phytoplankton community than previous years. Warmer temperatures and stratified water column conditions are generally favorable for dinoflagellates. Blooms of the toxic dinoflagellate *Alexandrium catenella* again closed or prompted consumption advisories for bivalve shellfish fisheries in 2025 (Fig. O.2) and sickened a person in Oregon with paralytic shellfish poisoning. This is the second year in a row that large-scale blooms of *Alexandrium catenella* occurred, which is unusual. In the Southern California Bight, a paralytic shellfish toxin (PST) event coincided with the domoic acid event in the spring, resulting in bivalve shellfish advisories issued for both domoic acid and PSTs. Multiple mussel harvesting closures occurred along much of the Oregon coast due to PSTs beginning in summer with the last closure lifted in December. In Washington, a PST event coincided with a Diarrhetic Shellfish Toxin (DST) event in late summer (Fig. O.2), but at a time when the regular seasonal mussel harvesting closure was already in effect. State level details of HAB dynamics and human health and fishery impacts are in Appendix O.

4. HUMAN WELLBEING

Key Message

Puget Sound, Newport, Crescent City and Eureka port groups closed major processor facilities in 2024. Concurrently, we saw an increase in the port-level revenue concentration for the groundfish-sector coastwide, and a loss of groundfish as a significant and connected fishery in affected Oregon and California ports. Port Orford and Crescent City displayed high commercial fishing engagement and social vulnerability in the year prior to processor closures, potentially increasing the impact of infrastructure changes on Oregon and Northern California fishing communities. Fishery revenue diversification continued to decrease across both vessels and ports, most notably among Californian vessels and in Newport and Northern California ports.

4.1 Social Vulnerability

Community vulnerability indices measure generalized socioeconomic vulnerability at the scale of census designated places (CDPs; towns and cities), allowing for fine-scale spatial comparisons among fishing-dependent communities across the California Current region. As in prior reports, we track the Community Social Vulnerability Index (CSVI), which summarizes multiple dimensions of social vulnerability derived from census-based indicators (e.g., demographics, personal disruption, poverty, housing characteristics and disruption, and labor force structure) for communities with commercial and recreational fishing activity (Lewis-Smith and Norman 2024). We also maintain indices of commercial and recreational fishing engagement on a census designated place scale, based on variables reflecting commercial fishing activity (e.g., landings, revenues, permits holder address, and processing), and recreational fishing activity (e.g., guide and charter permits, recreational retail shops, and marinas). Together, these indices provide a standardized framework for examining how social vulnerability intersects with commercial and recreational fishing engagement relative to other communities across regions.

In Figure 4.1, communities are positioned according to their relative social vulnerability (vertical axis) and fishing engagement (horizontal axis). Commercial and recreational engagement metrics are not directly comparable, however, engagement and social vulnerability can be compared across geographic regions for commercial and recreational fishing respectively. Communities located in the upper-right quadrant of each panel exhibit both higher social vulnerability and higher fishing engagement relative to other communities. Communities characterized by both high fishing engagement and higher social vulnerability may be particularly affected by downturns in fishing activity.

Due to data availability, the most recent social vulnerability and fishing engagement measures are from 2023. In 2023, the census designated places of Port Orford, Crescent City and Los Angeles had both high social vulnerability compared to other regions with moderate to high levels of commercial fishing engagement. In both Washington and California, the most highly engaged communities faced comparatively low social vulnerability, but also consisted of communities with large population sizes. Engagement reflects the absolute scale of fishing activity and infrastructure present in larger population

centers, whereas engagement per capita highlights small communities where fishing activity represents a relatively large share of local activity. To provide this complementary perspective, commercial and recreational fishing engagement standardized by population is presented in Appendix Q.

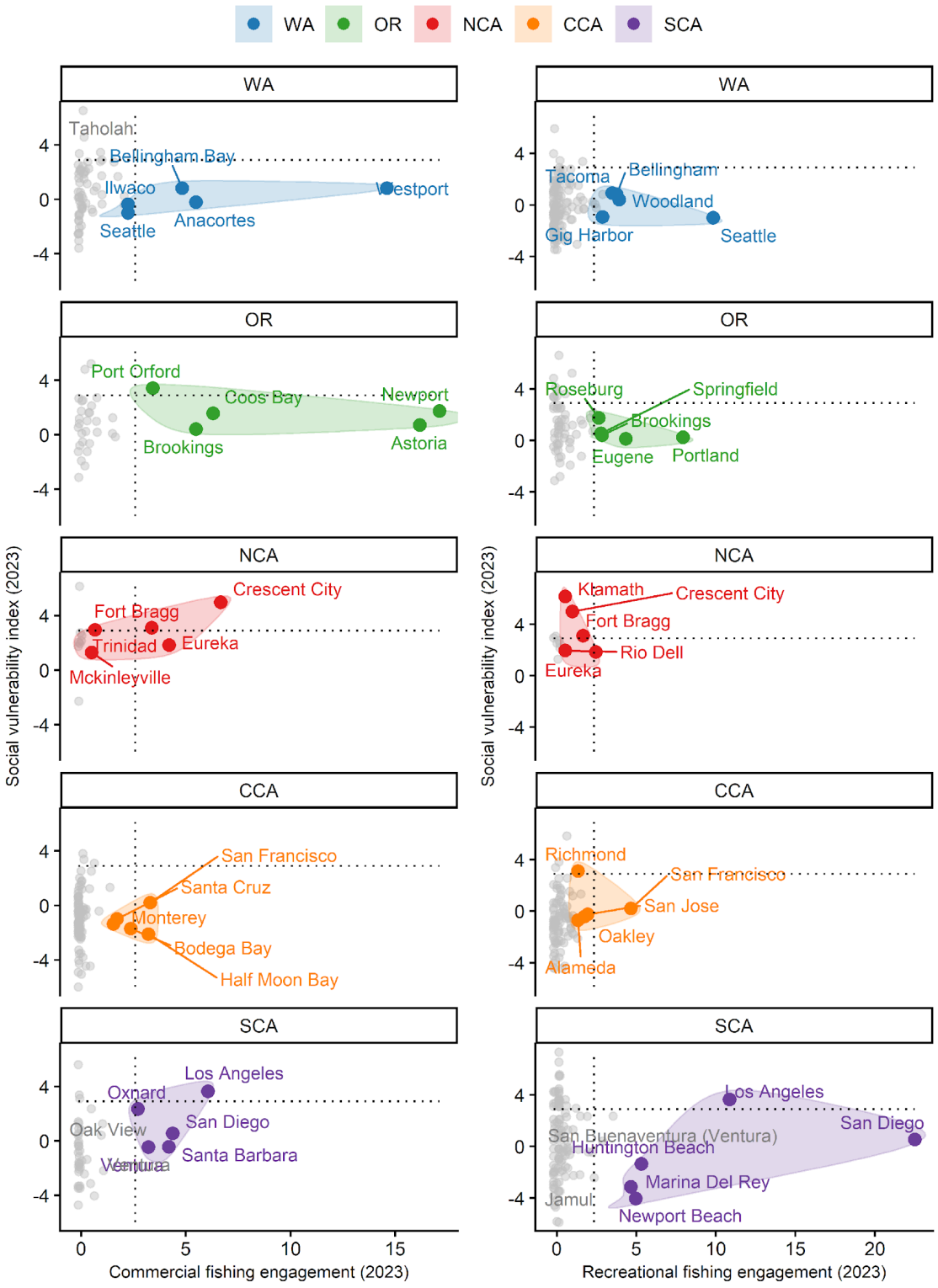


Figure 4.1: Commercial (left) and recreational (right) fishing engagement with social vulnerability scores in 2023 for communities in Washington, Oregon, and northern, central, and southern California. The five highest-scoring communities for fishing engagement are shown for each region. Dotted lines indicate 1 s.d. above the means for all communities.

4.2 Diversification of Fishery Revenues

Interannual variability in fishing revenue can be reduced by diversifying activities across multiple fisheries or regions, and more diversified fishers also tend to have higher total revenue (Kasperski and Holland 2013). In 2024, revenue diversification, which is measured by how revenue is spread across species groups, declined by 3% from the 2023 level for the current fleet of vessels fishing on the U.S. West Coast and in Alaska, falling to the lowest level observed since 1991 (Fig. 4.2 a-d). In 2024, vessels landing fish in California had a 2% decrease in average diversification relative to 2023, While those in Oregon and Washington fleets saw 4% and 2% increases in average diversification. Further information on port-level diversification and temporal diversification can be found in Appendix R.

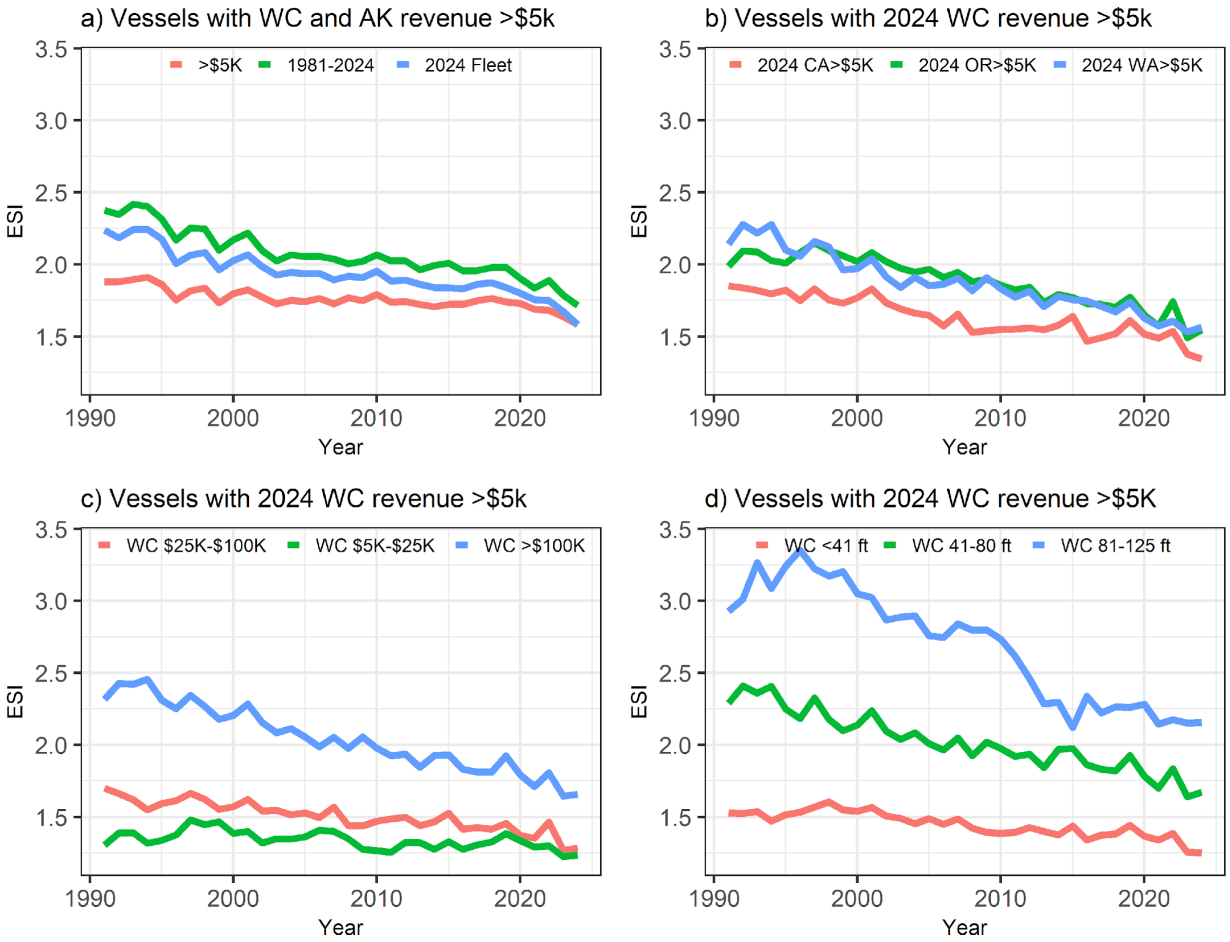


Figure 4.2: Average diversification for West Coast and Alaskan fishing vessels (top left) and for vessels in the 2024 West Coast Fleet, grouped by state (top right), average gross revenue class (bottom left) and vessel length class (bottom right).

NS-8 states that fisheries management measures should "provide for the sustained participation of (fishing) communities" and "minimize adverse economic impacts on such

communities; another indicator to track progress towards NS-8 is the Theil Index, an index used to assess the geographic concentration of fishing revenues compared to an ideal, perfectly equal state. Annually, the Theil Index is calculated for all fisheries and specific management groups, at the scale of the 21 port groups previously established for the economic Input-Output model for Pacific Coast fisheries (Leonard and Watson 2011). Across all fisheries, the Theil index for commercial fishing revenue remains relatively low and stable, while the groundfish sector showed an increase in concentration and HMS concentration continues a pattern of decreased concentration. See Appendix P for more details.

4.3 Fisheries Participation Networks

As fishers diversify their harvest portfolios, they create connections between fisheries, even when ecological links between the target species are weak or absent; we use fisheries participation networks (Fuller et al. 2017; Fisher et al. 2021) as a way to represent this information. In these networks, fisheries are depicted as nodes, and pairs of nodes are connected by lines called 'edges' that integrate information about vessels participating in both fisheries.

Fisheries participation networks representing IO-PAC port groups in the past year (November 2024 to November 2025, reflective of a Dungeness crab year) consisted of two to eleven fisheries nodes, with 1–33 links between the fisheries within each network (Fig. 4.3, see Appendix S); all IO-PAC port groups are illustrated in these figures except for Other Coastal WA and Unknown Ports. These snapshots in time depict the portfolios of fisheries that are economically important to individual vessels within a port group, based on a diversity of behaviors and choices at the level of individual vessels over the past year. For more details on the methods and interpretations of fisheries participation networks, reference Appendix S.

It is typical for the number of fisheries on which individual vessels and port groups are dependent to fluctuate (increase or decrease by one fishery) from year to year (Fig. S.1). However, in the last five years the number of fisheries in two Oregon port groups (Tillamook, Coos Bay) and three California port groups (Eureka, Fort Bragg, Morro Bay) has declined more substantially (Fig. S.1). Networks with fewer nodes are expected to have increased connectivity, yet edge density did not increase for any of these port groups (Fig. S.2), suggesting a reduced opportunity for participation across fisheries to buffer variability in income for individual vessels in these port groups. The Astoria and Bodega Bay port groups exhibited an increasing trend in the number of fisheries over the last five years, with Bodega Bay showing a corresponding and expected decline in connectivity (Fig. S.1, Fig. S.2). In Astoria, though the number of fisheries remains below the long-term average, the positive trend in the number of fisheries in its network over the last five years is accompanied by increasing connectivity and thereby realized potential for participation across multiple fisheries (Fig. S.1, Fig. S.2). While not showing a five-year trend, the average number of fisheries is below the long-term average for the Washington Coast and San Francisco port groups, and above the long-term average for San Diego (Fig. S.1). The connectivity between fisheries is below the long-term average for the Washington Coast and Fort Bragg port groups (Fig. S.2).

Future work to evaluate the causes and potential impacts of these patterns of fisheries participation could prove fruitful, especially in the context of historical or potential management actions and socioeconomic changes. Major processor facilities closed during 2024 in the Newport, Crescent City, and Eureka port groups, and those port groups either saw the elimination of Dover, thornyhead and sablefish (DTS) and all other groundfish (non-DTS) fisheries from their networks or a reduction in the contribution of DTS and non-DTS groundfish fisheries to annual vessel-level revenue (Fig. 4.3, Leising et al. 2025, Fig. S.1- S.3). However, a processor closed in 2024 in the Puget Sound port group, but somewhat counter intuitively more vessels were represented in the DTS groundfish fishery in 2025 than in 2024 (Fig. 4.3; see also Leising et al. 2025, Fig. S.3 - Fig. S.5). In a separate example, 2025 marked the third consecutive year in which California salmon fisheries were closed. Fisheries participation networks for port groups that were previously very economically-dependent on salmon fisheries (Harvey et al. 2023, fig. 5.4) have changed substantially since 2022, but in different ways. In Bodega Bay, there were more fisheries that were better connected in 2025 than in 2022, whereas in Monterey there were fewer fisheries and they were more poorly connected in 2025 than in 2022 (Fig. S.7).

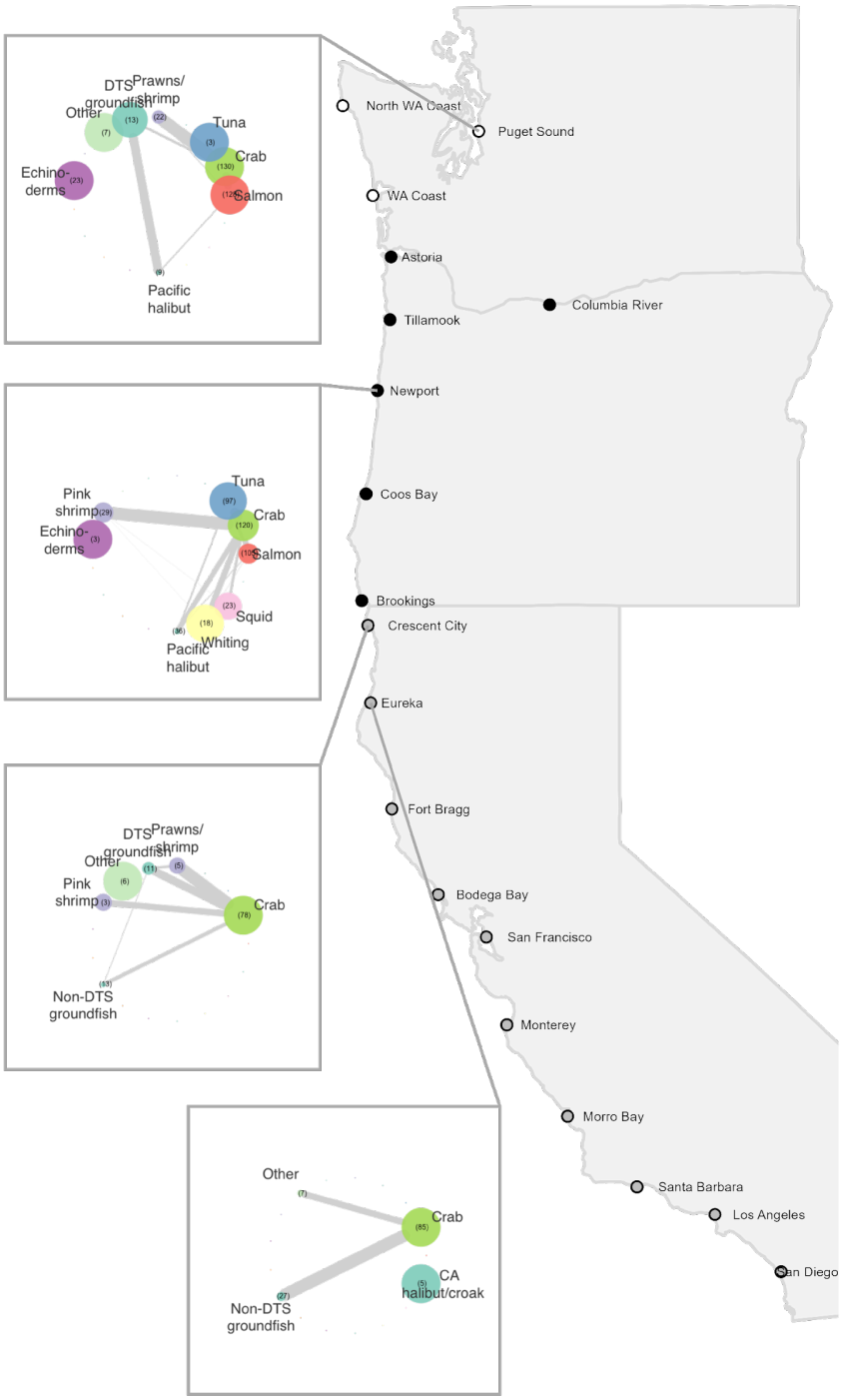


Figure 4.3: Fisheries participation networks for four IO-PAC port groups (Puget Sound, Newport, Crescent City, Eureka) that experienced processor closures in 2024. Networks are based on November 2024-November 2025 (the 2025 Dungeness crab year) landings receipts. Node size is proportional to the median contribution of a given fishery to annual vessel-level revenue; values in parentheses are the number of vessels participating in the fishery. Thickness of lines ("edges") is proportional to the number of vessels participating in both of the fisheries connected by the lines, and the evenness of revenue generated by each fishery in the pair.

5. Fishing and Non-fishing Human Activities

Key Message

In 2025, total coastwide commercial landings rebounded from 2024, which had the lowest total landings on the West Coast since the mid-1980's. Coastwide landings increased for several commercial fisheries, particularly Pacific whiting and market squid, while crab landings notably decreased. Total coastwide revenue also increased, albeit by a small margin. Recreational landings (excluding salmon) were among the lowest of the last 20 years. We also introduce a framework for developing ecosystem indicators to measure potential effects of new ocean-use sectors, using indicators identified for offshore wind energy suitability as a case study.

5.1 Coastwide Landings by Major Fisheries

Fishery landings are indicators of ecosystem services provided and also reflect removals from the CCE. In 2025, coastwide total landings increased 26% from 2024, although the most recent five-year average remained >1 s.d. below the long-term average (Fig. 5.1). This most recent year-to-year increase was largely driven by a 44% increase in Pacific whiting landings as the bulk of the species' spatial distribution returned to waters north of the CA/OR border. Landings from 5 of 9 commercial fisheries increased in 2025 compared to 2024: HMS (+89%), Pacific whiting (+44%), market squid (+38%), non-whiting groundfish (+17%), and shrimp (+15%). In contrast, landings from CPS finfish (-38%), crab (-33%), salmon (-32%), and Other species (-7%) fisheries decreased in 2025 from 2024. Over the past five years, shrimp landings were >1 s.d. above the long-term average, while salmon, CPS finfish, HMS and Other species landings were below long-term averages. Landings from Pacific whiting fisheries decreased from 2021 to 2025 while all other fisheries showed no recent trends. State-by-state landings and revenue are presented in Appendix T. There were no commercial landings of salmon in California in 2023-2025, as the fishery was closed.

Total revenue in commercial fisheries coastwide increased in 2025 by 6% from 2024, largely driven by increases in revenue from HMS, Pacific whiting, non-whiting groundfish, and market squid fisheries. State-by-state landings and revenue are presented in Appendix T.

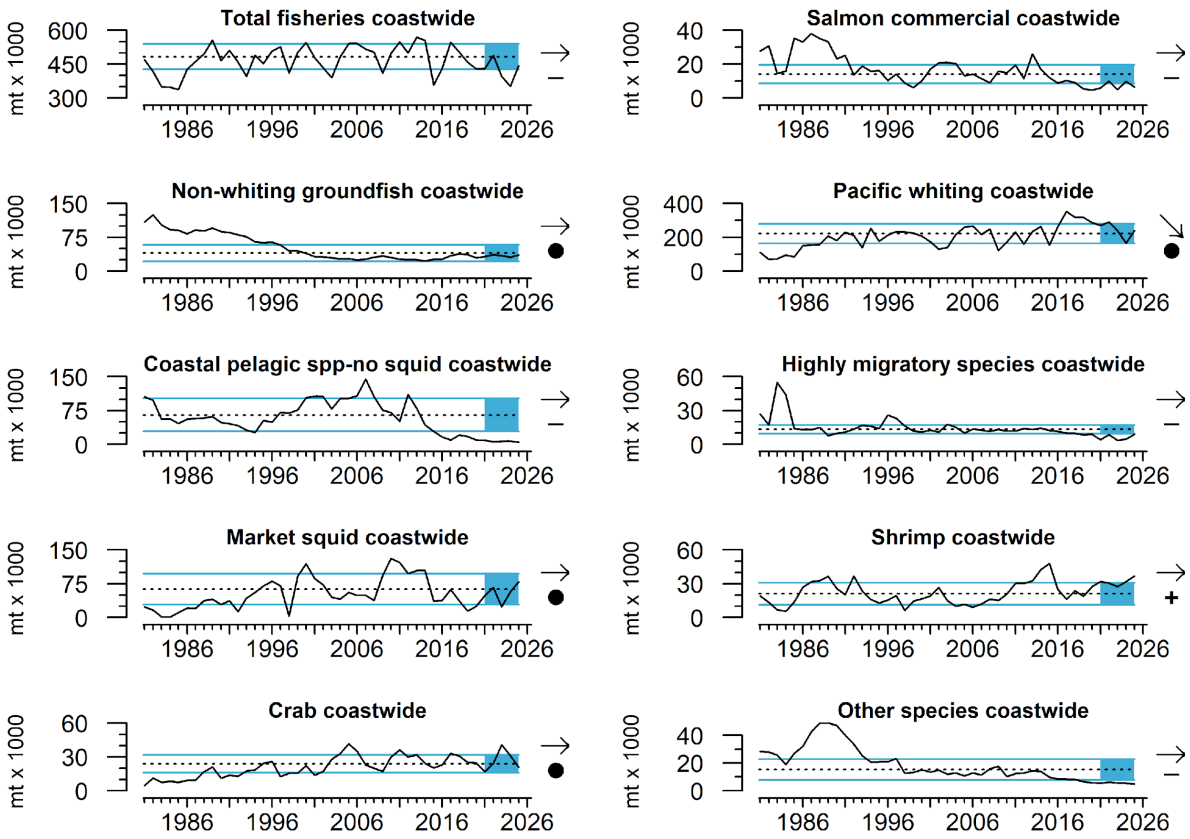


Figure 5.1: Annual landings from West Coast commercial fisheries (data from PacFIN and NORPAC), including total landings across all fisheries, from 1981-2025. Data were downloaded from PacFIN and NORPAC on January 1, 2026. Lines, colors, and symbols are as in Fig. 2.1.

Overall, recreational landings have declined from a peak in 2015 and were among the lowest of the 20-yr time series in 2025 (Fig. 5.1, left). The coastwide time series pattern generally follows landings across the top three targeted species: black rockfish, lingcod and albacore. Recreational salmon landings have varied within ~1 s.d. of long-term averages over the last five years (Fig. 5.2, right). Notably, the recreational salmon fishery in California was closed in 2023 and 2024, with very limited opportunities in 2025 (data from 2025 were not available at the time of this report). State-level recreational landings are in Appendix T.

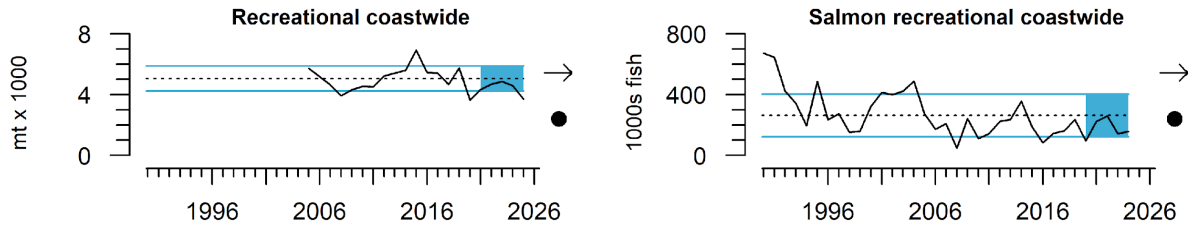


Figure 5.2: Annual landings from most West Coast recreational fisheries from 1981-2025 (data from RecFIN) and from recreational salmon fisheries from 1990-2024 (data from PFMC). Data from 2025 are complete through October. Lines, colors, and symbols are as in Fig. 2.1.

5.2 Ecosystem Interactions with New Ocean-use Sectors

Federal and state processes to pursue the development of new projects and completely new ocean-use sectors in the CCE have been underway in recent years. These new sectors include offshore aquaculture; oil, gas, and renewable energy extraction; and critical minerals mining. Development of these economic sectors in the CCE suggests the need for a portfolio of indicators specific to each sector that can inform planning, siting, monitoring, and mitigating for potential interactions with important ecosystem components. We illustrate the conceptual hierarchy of identifying indicators for key ecosystem components across the CCE's social ecological system (Fig. U.1). An inventory of ecosystem indicators could be developed through the first two steps of the IEA approach (i.e., the NOAA IEA Loop, Levin et al. 2009), which includes (i) developing conceptual models to identify key ecosystem components likely to respond to new ocean uses; and (ii) evaluating and selecting indicators capable of measuring baseline conditions and changes in status and trends of key ecosystem components. Appendix U includes a description of the full IEA approach relevant to understanding potential interactions with new ocean-use sectors, and presents an initial portfolio of ecosystem indicators relevant for offshore wind energy development.

6. Synthesis

Ocean conditions in the California Current Ecosystem (CCE) in 2025 were mainly favorable, with a rapid and strong physical transition in April to a productive upwelling state along the West Coast. Far offshore, there was a large marine heatwave which contributed to a record high average sea surface temperature across the Northeast Pacific. Coastal conditions remained favorable during the spring and summer, with consistent and strong upwelling acting to fertilize coastal waters and provide a cool buffer from the large offshore marine heatwave, until it penetrated to the coast in late summer. The enhanced spring and summer upwelling supported abundant and diverse prey sources for top predators throughout the ecosystem. Specifically, anchovy, juvenile groundfishes and krill remained abundant in the Central and Southern CCE, and juvenile rockfishes, juvenile salmon and

krill were abundant in the Northern CCE. Most seabird colonies recovered from lower productivity in the previous year, further indicating good prey availability. Late winter upwelling may have pre-conditioned the ecosystem to facilitate higher spring reproductive success for seabirds.

Early in 2025 the CCE experienced one of the largest harmful algal blooms on record, in terms of impacts to marine mammals in southern California due to domoic acid produced by the diatom *Pseudo-nitzschia*. The exact factors that led to this event are still unclear; however, it was noted that the bloom occurred within the context of the presence of warmer-than-normal waters offshore of Pt. Conception followed by brief yet strong upwelling events. This past year marked the second consecutive year of toxic dinoflagellate blooms off Oregon and southern California that are likely related to warmed and more stratified waters which favor this type of plankton, and may be an indicator of an ecosystem change. The multiple bloom events caused an array of fishery impacts, effects on top predators, and direct human health impacts.

Conditions on land showed an interesting pattern in 2025, as for the first time in a decade or longer, heavy rain during the fall led to California exiting drought status. Unfortunately, the same fall and early winter 2025-2026 rain events negatively impacted snow pack levels in the Pacific Northwest, as the rain and atmospheric conditions were warmer than normal, thus leading to snow melt rather than accumulation. The exceptionally low snowpack to date does not bode well for adequate streamflows later in the year to support good salmon habitat, with drought and precipitation forecasts suggesting lower rainfall in the south, and only slightly above average rainfall in the north.

Total coastwide commercial fishery landings increased relative to 2024, which had the lowest total landings on record since the 1980s. Pacific whiting and market squid fisheries largely contributed to the increased landings. While Pacific whiting is not managed by the PFMC, this fishery is highly connected to PFMC managed species in many ports (see Section 4.3). There was a notable decrease in Dungeness crab landings, and the California Dungeness crab fishery operated under restrictions (trap limits and depth restrictions) to reduce the potential for whale entanglements for the entire 2024-2025 fishing season. Furthermore, significant processor closures in Oregon and Northern California impacted commercial fishing communities including an overall reduction of groundfish fisheries participation in Newport. Ports with processor closures also saw an overall decline in participation across multiple fisheries, potentially reducing resilience to environmental or regulatory shocks.

The ongoing development of human wellbeing indicators supports Council efforts to better characterize the social and economic conditions of West Coast fishing communities. High social vulnerability in some northern Californian communities in 2023 combined with an increase in port-level concentration of groundfish revenue highlight risks for community wellbeing, and fishery engagement in 2025 and 2026, particularly for vessels and ports that target groundfish.

The suite of CCIEA indicators presented in the ESR, including ocean forecasts (Appendix D) and ecological outlooks and projections (Section 3.3, Appendices E and J), enable NOAA

scientists and their partners to effectively assess risk associated with ecosystem conditions in the coming months and years. In 2025, several CCIEA indicators were used by NOAA Fisheries to develop risk tables for West Coast groundfish and whiting fisheries. Looking forward to 2026, we note the ecosystem is transitioning back towards a neutral ENSO state, after being in a mild La Niña state during most of 2025 (Appendix D). There is a ~50/50 chance of neutral or El Niño conditions later in 2026 (NWS 2026), and similar to past years, marine heatwaves are forecast to continue in offshore regions. In 2025, the seasonal transition to downwelling occurred approximately one month earlier than typical, and nearshore coastal temperatures remained anomalously warm during December through February; both of which could have impacts during 2026. Air temperatures are forecast to be warmer than normal. Outlooks of adult salmon returns to the Columbia Basin in 2026 are near the 10-year average with slight improvements predicted for 2027. Returns of adult salmon stocks to the Central Valley in 2026 and 2027 will reflect a mix of favorable and unfavorable habitat conditions and are difficult to predict. Low adult returns are expected for Klamath River Fall Chinook salmon in the next two years based on recent conditions. With ongoing advances in ocean modeling, we expect to have more detailed short-term forecasts of ocean conditions starting later in 2026 which will support enhanced understanding of climate variability and change impacts on the CCE and West Coast fisheries and communities.

7. LITERATURE CITED

Abbott JK, Sakai Y, Holland DS (2023) Species, space and time: A quarter century of fishers' diversification strategies on the US West Coast. Fish and Fisheries 24:93–110

Abell R, Thieme ML, Revenga C, et al (2008) Freshwater ecoregions of the world: a new map of biogeographic units for freshwater biodiversity conservation. BioScience 58:403–414

Anderson DM, Fensin E, Gobler CJ, et al (2021) Marine harmful algal blooms (HABs) in the United States: History, current status and future trends. Harmful algae 102:101975

Ayache N, Bill BD, Brosnahan ML, et al (2023) A survey of *Dinophysis* spp. and their potential to cause diarrhetic shellfish poisoning in coastal waters of the United States. Journal of Phycology 59:658–680

Bakun A (1973) Coastal upwelling indices, west coast of North America, 1946-71. NOAA technical report NMFS-SSRF; 671.

Black BA, Schroeder ID, Sydeman WJ, et al (2010) Wintertime ocean conditions synchronize rockfish growth and seabird reproduction in the central California Current ecosystem. Canadian Journal of Fisheries and Aquatic Sciences 67:1149–1158

Black BA, Schroeder ID, Sydeman WJ, et al (2011a) Winter and summer upwelling modes and their biological importance in the California Current Ecosystem. Global Change Biology 17:2536–2545

Black BA, Schroeder ID, Sydeman WJ, Bograd SJ (2011b) Multidecadal growth-increment chronologies for North Pacific and North Atlantic rockfish species

Brodie S, Buil MP, Welch H, Bograd SJ, Hazen EL, Santora JA, Seary R, Schroeder ID, Jacox MG (2023) Ecological forecasts for marine resource management during climate extremes. Nature Communications 14

Burke BJ, Fullerton AH, Wells BK, Ohlberger J (2025) Improving salmon marine survival models with covariance map indices of sea surface temperature (CMISST) and sea surface height (CMISSH). Ecological Informatics 103575

Burke BJ, Peterson WT, Beckman BR, et al (2013) Multivariate models of adult Pacific salmon returns. PloS one 8:e54134

Busch DS, McElhany P (2016) Estimates of the direct effect of seawater pH on the survival rate of species groups in the California Current Ecosystem. PloS one 11:e0160669

Carlton J, Jossart J, Pendleton F, et al (2024) A wind energy area siting analysis for the Oregon call areas. OCS Study BOEM 15:

Chan F, Barth J, Lubchenco J, et al (2008) Emergence of anoxia in the California Current Large Marine Ecosystem. Science 319:920–920

Cimino MA, Santora JA, Schroeder I, et al (2020) Essential krill species habitat resolved by seasonal upwelling and ocean circulation models within the large marine ecosystem of the California Current System. Ecography 43:1536–1549

Cluett AA, Bograd SJ, Jacox MG, et al (2025) Pan-basin warming now overshadows robust Pacific Decadal Oscillation. Nature Climate Change 1–8

Cope JM, Lillier LK, Niles CB, et al (2024) Status of black rockfish (*Sebastes melanops*) in 2023 in state and federal waters off Washington state. Pacific Fishery Management Council, Portland OR

Daly EA, Auth TD, Brodeur RD, Peterson WT (2013) Winter ichthyoplankton biomass as a predictor of early summer prey fields and survival of juvenile salmon in the Northern California Current. Marine Ecology Progress Series 484:203–217

Demer DA, Zwolinski JP, Byers KA, et al (2012) Prediction and confirmation of seasonal migration of Pacific sardine (*Sardinops sagax*) in the California Current Ecosystem. Fishery Bulletin 110:52–70

Dick EJ, Field JC, Grunloh N, Rogers TL (2025) The Status of Chilipepper Rockfish in U.S. Waters off California, Oregon, and Washington in 2025. Pacific Fishery Management Council, Portland, OR.

Dyson K, Huppert DD (2010) Regional economic impacts of razor clam beach closures due to harmful algal blooms (HABs) on the Pacific coast of Washington. Harmful Algae 9:264–271

FDA (2011) Fish and Fishery Products Hazards and Controls Guidance, Appendix 5: FDA and EPA Safety Levels in Regulations and Guidance. Department of Health; Human Services, Public Health Service, Food; Drug Administration, Center for Food Safety; Applied Nutrition, Office of Food Safety

Feddern ML, Ward EJ, Litzow MA, et al (2025) Quantifying time-dependent climate and ecosystem relationships in the California Current System. Geophysical Research Letters 52:e2024GL113431

Feely RA, Sabine CL, Hernandez-Ayon JM, et al (2008) Evidence for upwelling of corrosive "acidified" water onto the continental shelf. Science 320:1490–1492

Fiechter J, Edwards CA, Moore AM (2018) Wind, circulation, and topographic effects on alongshore phytoplankton variability in the California Current. Geophysical Research Letters 45:3238–3245

Fiechter J, Santora JA, Chavez F, et al (2020) Krill hotspot formation and phenology in the California Current Ecosystem. Geophysical research letters 47:e2020GL088039

Field JC, Miller RR, Santora JA, et al (2021) Spatiotemporal patterns of variability in the abundance and distribution of winter-spawned pelagic juvenile rockfish in the California Current. PloS One 16:e0251638

Fisher JL, Peterson WT, Rykaczewski RR (2015) The impact of El Niño events on the pelagic food chain in the northern California Current. Global Change Biology 21:4401–4414

Fisher MC, Moore SK, Jardine SL, et al (2021) Climate shock effects and mediation in fisheries. Proceedings of the National Academy of Sciences 118:e2014379117

Ford MJ, Lindley ST, Barnas KA, et al (2025) Abundance trends of Pacific salmon during a quarter century of ESA protection. Fish and Fisheries 26:1087–1106

Fuller EC, Samhouri JF, Stoll JS, et al (2017) Characterizing fisheries connectivity in marine social–ecological systems. ICES Journal of Marine Science 74:2087–2096

Gasbarro R, Ainley DG, Andrews KS, et al (2025a) Projected changes to the extent and seasonality of seabird habitat in the California Current and implications for marine spatial planning. PLOS Climate 4:e0000687

Gasbarro R, Santora JA, Cimino M, et al (2025b) Composition and Functional Diversity of Juvenile Groundfish Assemblages in the California Current. Journal of Biogeography 52:e15108

Gladics AJ, Suryan RM, Parrish JK, et al (2015) Environmental drivers and reproductive consequences of variation in the diet of a marine predator. Journal of Marine Systems 146:72–81

Harvey CJ, Garfield NT, Williams GD, Tolimieri N (2023) California Current Integrated Ecosystem Assessment (CCIEA) California Current Ecosystem Status Report, 2023. Report to the Pacific Fishery Management Council. March 2023, Agenda Item I.1.a.

Harvey CJ, Garfield NT, Williams GD, Tolimieri N (2021) California Current Integrated Ecosystem Assessment (CCIEA) California Current Ecosystem Status Report, 2021. Report to the Pacific Fishery Management Council. March 2021, Agenda Item I.1.a.

Henson SA, Beaulieu C, Ilyina T, et al (2017) Rapid emergence of climate change in environmental drivers of marine ecosystems. Nature Communications 8:14682

Hobday AJ, Alexander LV, Perkins SE, et al (2016) A hierarchical approach to defining marine heatwaves. Progress in Oceanography 141:227–238

Holland DS, Leonard J (2020) Is a delay a disaster? Economic impacts of the delay of the California Dungeness crab fishery due to a harmful algal bloom. Harmful Algae 98:101904

Jacox MG, Bograd SJ, Fiechter J, et al (2024) Linking upwelling dynamics and subsurface nutrients to projected productivity changes in the California Current system. Geophysical Research Letters 51:e2023GL108096

Johns ME, Warzybok P, Bradley RW, et al (2017) Age, timing, and a variable environment affect double brooding of a long-lived seabird. Marine Ecology Progress Series 564:187–197

Jones T, Parrish JK, Lindsey J, et al (2024) Marine bird mass mortality events as an indicator of the impacts of ocean warming. Marine Ecology Progress Series 737:161–181

Kasperski S, Holland DS (2013) Income diversification and risk for fishermen. Proceedings of the National Academy of Sciences 110:2076–2081

Keister JE, Di Lorenzo E, Morgan C, et al (2011) Zooplankton species composition is linked to ocean transport in the Northern California Current. Global Change Biology 17:2498–2511

KL R, LC W, JA J, et al (2021) An Aquaculture Opportunity Area Atlas for the U.S. Gulf of Mexico. NOAA Technical Memorandum NOS NCCOS 299. 545 p. DOI:10.25923/8cb3-3r66

Lefebvre KA, Bargu S, Kieckhefer T, Silver MW (2002) From sanddabs to blue whales: the pervasiveness of domoic acid. Toxicon 40:971–977

Leising A, M. H, N. T, et al (2024) California Current Integrated Ecosystem Assessment (CCIEA) California Current Ecosystem Status Report, 2024. Report to the Pacific Fishery Management Council. March 2024, Agenda Item I.1.a.

Leising A, M. H, N. T, et al (2025) California Current Integrated Ecosystem Assessment (CCIEA) California Current Ecosystem Status Report, 2025. Report to the Pacific Fishery Management Council. March 2025, Agenda Item I.1.a.

Leising AW (in revision) Phenology of Northeast Pacific large marine heatwaves impacting the California Current Ecosystem. Frontiers in Marine Science

Leonard JL, Watson PS (2011) Description of the input-output model for Pacific coast fisheries. NOAA technical memorandum NMFS-NWFSC: 111. https://repository.library.noaa.gov/view/noaa/8718

Levin PS, Fogarty MJ, Murawski SA, Fluharty D (2009) Integrated ecosystem assessments: Developing the scientific basis for ecosystem-based management of the ocean. PLoS biology 7:e1000014

Lewis-Smith C, Norman K (2024) Developing US West Coast recreational fishing community measures: Applying an index approach in the context of COVID-19 and social vulnerability. Ocean & Coastal Management 255:107236

Lezama-Ochoa N, Brodie S, Welch H, et al (2024) Divergent responses of highly migratory species to climate change in the California Current. Diversity and Distributions 30:e13800

Lindgren F, Rue H (2015) Bayesian spatial modelling with R-INLA. Journal of Statistical Software 63:1–25

Litzow MA, Hunsicker ME, Ward EJ, et al (2020) Evaluating ecosystem change as Gulf of Alaska temperature exceeds the limits of preindustrial variability. Progress in Oceanography 186:102393

Liu OR, Kaplan IC, Hernvann P-Y, et al (2025) Climate change influences via species distribution shifts and century-scale warming in an end-to-end California Current Ecosystem model. Global Change Biology 31:e70021

Liu OR, Ward EJ, Anderson SC, et al (2023) Species redistribution creates unequal outcomes for multispecies fisheries under projected climate change. Science Advances 9:eadg5468

Lowry D, Wright S, Neuman M, et al (2022) Endangered Species Act Status Review Report: Sunflower Sea Star (*Pycnopodia helianthoides*). Final Report to the National Marine Fisheries Service, Office of Protected Resources. October 2022

Mantua NJ, Bell H, Todgham AE, et al (2025) Widespread thiamine deficiency in California salmon linked to an anchovy-dominated marine prey base. Proceedings of the National Academy of Sciences 122:e2426011122

Mantua NJ, Hare SR, Zhang Y, et al (1997) A Pacific interdecadal climate oscillation with impacts on salmon production. Bulletin of the American Meteorological Society 78:1069–1080

Marshall KN, Kaplan IC, Hodgson EE, et al (2017) Risks of ocean acidification in the California Current food web and fisheries: ecosystem model projections. Global Change Biology 23:1525–1539

McCabe RM, Hickey BM, Kudela RM, et al (2016) An unprecedented coastwide toxic algal bloom linked to anomalous ocean conditions. Geophysical Research Letters 43:10–366

McKibben SM, Peterson W, Wood AM, et al (2017) Climatic regulation of the neurotoxin domoic acid. Proceedings of the National Academy of Sciences 114:239–244

Messié M, Sancho-Gallegos DA, Fiechter J, et al (2022) Satellite-based Lagrangian model reveals how upwelling and oceanic circulation shape krill hotspots in the California Current System. Frontiers in Marine Science 9:835813

Moore SK, Cline MR, Blair K, et al (2019) An index of fisheries closures due to harmful algal blooms and a framework for identifying vulnerable fishing communities on the US West Coast. Marine Policy 110:103543

Moore SK, Dreyer SJ, Ekstrom JA, et al (2020) Harmful algal blooms and coastal communities: Socioeconomic impacts and actions taken to cope with the 2015 US West Coast domoic acid event. Harmful Algae 96:101799

Morgan CA, Beckman BR, Weitkamp LA, Fresh KL (2019) Recent ecosystem disturbance in the Northern California Current. Fisheries 44:465–474

Muhling B, Snyder S, Hazen EL, et al (2025) Climate change impacts to foraging seascapes for a highly migratory top predator. Movement Ecology 13:33

Munch S, Green C, Satterthwaite, WR (in review) Indicators of freshwater and marine ecosystem states provide two-year outlooks on California Chinook salmon recruitment, contextualize past dynamics, and document shifting baselines. Canadian Journal of Fisheries and Aquatic Sciences.

Neveu E, Moore AM, Edwards CA, et al (2016) An historical analysis of the California Current circulation using ROMS 4D-Var: System configuration and diagnostics. Ocean Modelling 99:133–151

Oken KL, Taylor IG, Feddern ML, et al (2025) Status of the yellowtail rockfish stock off the U.S. West Coast north of 40°10′ N in 2025. Pacific Fishery Management Council

Peterson WT, Fisher JL, Peterson JO, et al (2014) Applied fisheries oceanography: Ecosystem indicators of ocean conditions inform fisheries management in the California Current. Oceanography 27:80–89

PFMC (2015) Pacific Coast Groundfish Fishery Management Plan for the California, Oregon, and Washington Groundfish Fishery. Pacific Fishery Management Council, Portland, OR

Phillips EM, Chu D, Gauthier S, et al (2022) Spatiotemporal variability of euphausiids in the California Current Ecosystem: insights from a recently developed time series. ICES Journal of Marine Science 79:1312–1326

Pozo Buil M, Jacox MG, Fiechter J, et al (2021) A dynamically downscaled ensemble of future projections for the California Current System. Frontiers in Marine Science 8:612874

Quezada FJ, Tommasi D, Frawley TH, et al (2023) Catch as catch can: Markets, availability, and fishery closures drive distinct responses among the US West Coast coastal pelagic species fleet segments. Canadian Journal of Fisheries and Aquatic Sciences 81:1135–1153

Raghukumar K, Nelson T, Jacox M, et al (2023) Projected cross-shore changes in upwelling induced by offshore wind farm development along the California coast. Communications Earth & Environment 4:116

Ritzman J, Brodbeck A, Brostrom S, et al (2018) Economic and sociocultural impacts of fisheries closures in two fishing-dependent communities following the massive 2015 US West Coast harmful algal bloom. Harmful Algae 80:35–45

Samhouri JF, Feist BE, Jacox M, et al (2024) Stay or go? Geographic variation in risks due to climate change for fishing fleets that adapt in-place or adapt on-the-move. PLOS Climate 3:e0000285

Santora JA, Mantua NJ, Schroeder ID, et al (2020) Habitat compression and ecosystem shifts as potential links between marine heatwave and record whale entanglements. Nature Communications 11:1–12

Santora JA, Rogers TL, Cimino MA, et al (2021) Diverse integrated ecosystem approach overcomes pandemic-related fisheries monitoring challenges. Nature communications 12:1–10

Schroeder ID, Black BA, Sydeman WJ, et al (2013) The North Pacific High and wintertime pre-conditioning of California Current productivity. Geophysical Research Letters 40:541–546

Schroeder ID, Santora JA, Bograd SJ, et al (2019) Source water variability as a driver of rockfish recruitment in the California Current Ecosystem: implications for climate change and fisheries management. Canadian Journal of Fisheries and Aquatic Sciences 76:950–960

Schroeder ID, Sarkar N, Thompson SA, et al (2009) Winter pre-conditioning of seabird phenology in the California Current. Marine Ecology Progress Series 393:211–223

Schwing FB, Bond NA, Bograd SJ, et al (2006) Delayed coastal upwelling along the US West Coast in 2005: A historical perspective. Geophysical Research Letters 33:

Smith JA, Buil MP, Muhling B, et al (2023) Projecting climate change impacts from physics to fisheries: A view from three California Current fisheries. Progress in Oceanography 211:102973

Stierhoff KL, Renfree JS, Rojas-González RI, Vallarta-Zárate JP J. R. F.and Zwolinski (2023a) Distribution, biomass, and demography of coastal pelagic fishes in the California Current Ecosystem during summer 2021 based on acoustic-trawl sampling. U.S. Dep. Commer., NOAA Tech. Memo., NOAA-TM-NMFS-SWFSC-676: 85.

Stierhoff KL, Zwolinski JP, Demer DA (2020) Distribution, biomass, and demography of coastal pelagic fishes in the California Current Ecosystem during summer 2019 based on acoustic-trawl sampling

Stierhoff KL, Zwolinski JP, Refree JS, Demer DA (2023b) Distribution, biomass, and demography of coastal pelagic fishes in the California Current Ecosystem during summer 2022 based on acoustic-trawl sampling. U.S. Dep. Commer., NOAA Tech. Memo., NOAA-TM-NMFS-SWFSC-683:84.

Stierhoff KL, Zwolinski JP, Renfree JS, Demer DA (in press) Distribution, biomass, and demographics of coastal pelagic fishes in the California Current Ecosystem during summer 2025 based on acoustic-trawl sampling

Szoboszlai AI, Thayer JA, Wood SA, et al (2015) Forage species in predator diets: synthesis of data from the California Current. Ecological Informatics 29:45–56

Theil H (1967) Economics and Information Theory (Chicago and Amsterdam). Rand McNally andCo.; North-Holland Publishing Company

Thompson AR, Harvey CJ, Sydeman WJ, et al (2019) Indicators of pelagic forage community shifts in the California Current Large Marine Ecosystem, 1998–2016. Ecological Indicators 105:215–228

Thompson AR, Swalethorp R, Alksne M, et al (2024) State of the California Current Ecosystem report in 2022: A tale of two La Niñas. Frontiers in Marine Science 11:1294011

Tolimieri N, Shelton AO, Samhouri JF, et al (2023) Changes in kelp forest communities off Washington, USA, during and after the 2014-2016 marine heatwave and sea star wasting syndrome. Marine Ecology Progress Series 703:47–66

Tolimieri N, Wallace J, Haltuch M (2020) Spatio-temporal patterns in juvenile habitat for 13 groundfishes in the California Current Ecosystem. PloS one 15:e0237996

Trainer VL, Moore L, Bill BD, et al (2013) Diarrhetic shellfish toxins and other lipophilic toxins of human health concern in Washington State. Marine Drugs 11:1815–1835

Trainer VL, Moore SK, Hallegraeff G, et al (2020) Pelagic harmful algal blooms and climate change: Lessons from nature's experiments with extremes. Harmful algae 91:101591

Welch H, Hazen EL, Briscoe DK, et al (2019) Environmental indicators to reduce loggerhead turtle bycatch offshore of southern California. Ecological Indicators 98:657–664

Welch H, Holycross BM, Cluett AA, et al (2025) Fishing fleets as ecosystem sentinels. Proceedings of the National Academy of Sciences 122:e2516308122

Wildermuth RP, Tommasi D, Kuriyama P, et al (2023) Evaluating robustness of harvest control rules to climate-driven variability in pacific sardine recruitment. Canadian Journal of Fisheries and Aquatic Sciences 81:1029–1051

Zwolinski JP, Demer DA, Cutter Jr GR, et al (2014) Building on fisheries acoustics for marine ecosystem surveys. Oceanography 27:68–79

Appendix A — CONTRIBUTORS TO THIS REPORT

NWFSC, NOAA Fisheries Mr. Kelly Andrews, Dr. Brian Burke, Dr. Shallin Busch (Internal Reviewer), Dr. Jason Cope, Mr. Jeff Cowen, Dr. Blake Feist, Ms. Jennifer Fisher, Dr. Abigail Golden, Dr. Thomas Good, Dr. Ana Sofia Guerra, Dr. Chris Harvey, Dr. Daniel Holland, Dr. Mary Hunsicker (co-editor), Dr. Kym Jacobson, Dr. Isaac Kaplan, Ms. Su Kim, Mr. Connor Lewis-Smith, Dr. Stephanie Moore, Dr. Stuart Munsch, Dr. Karma Norman, Ms. Amanda Phillips (co-editor), Dr. Elizabeth Phillips, Dr. Jameal Samhouri, Dr. Kayleigh Somers, Dr. Nick Tolimieri (co-editor), Dr. Amanda Warlick, Mr. Curt Whitmire, Dr. Jen Zamon

AFSC, NOAA Fisheries Dr. Russell (Rusty) Dame, Dr. Sharon Melin

SWFSC, NOAA Fisheries Dr. Noelle Bowlin, Ms. Sherri Charter, Ms. Lynn deWitt (co-editor), Dr. John Field, Dr. Elliott Hazen, Dr. Michael Jacox, Dr. Andrew Leising (co-editor), Dr. Nate Mantua, Mr. Josiah Renfree, Dr. Tanya Rogers, Mr. Keith Sakuma, Dr. Jarrod Santora, Dr. Will Satterthwaite, Dr. Kevin Stierhoff, Dr. Andrew Thompson, Mr. William Watson

Oregon State University Dr. John (Jack) Barth, Ms. Anna Bolm, Ms. Elizabeth Daly, Mr. William Kennerley, Mr. Jace Marquardt, Ms. Cheryl Morgan, Dr. Rachael Orben, Mr. Brian VerWey, Ms. Samantha Zeman

NOAA Fisheries West Coast Region Mr. Dan Lawson, Ms. Lauren Saez

Pacific States Marine Fishery Commission Ms. Anna Abelman, Mr. Toby Auth, Mr. Gregory Williams (co-editor)

University of California-San Diego Dr. Dan Rudnick, Dr. Rasmus Swalethorp

University of California-Santa Barbara Dr. Chris Free

University of California-Santa Cruz Dr. Megan Cimino, Dr. Jerome Fiechter, Dr. Ryan Gasbarro, Dr. Nerea Lezama-Ochoa, Ms. Rebecca Miller, Dr. Barbara Muhling, Dr. Antonella Preti, Dr. Travis Richards, Dr. Isaac Schroeder (co-editor), Dr. Juan Zwolinski

University of Washington Dr. Owen Liu

California Department of Public Health Ms. Christina Grant, Ms. Ali Hossain, Mr. Duy Truong, Ms. Vanessa Zubkousky-White

California Department of Fish and Wildlife Ms. Christy Juhasz

CA Office of Environmental Health Hazard Assessment Dr. Shannon Murphy, Dr. Beckye Stanton

Oregon Department of Fish and Wildlife Ms. Kelly Corbett, Mr. Matthew Hunter, Dr. Leif Rasmuson, Ms. Cathleen Vestfals

Washington Department of Fish and Wildlife Mr. Zachary Forster, Dr. Matt George, Dr. Leif Rasmuson, Dr. Scott Pearson

Washington Department of Health Ms. Tracie Barry, Mr. Jerry Borchert

Beach Watch (Greater Farallones Association and Greater Farallones & Cordell Bank National Marine Sanctuaries) Ms. Kirsten Lindquist, Ms. Jan Roletto

BeachCOMBERS Ms. Kirby Bartlett

Coastal Observation and Seabird Survey Team Ms. Florence Sullivan, Dr. Julia Parrish

Farallon Institute Dr. Brian Hoover, Dr. William Sydeman, Ms. Sarah Ann Thompson

Monterey Bay Aquarium Research Institute Dr. Monique Messié

Point Blue Conservation Science Ms. Meredith Elliott, Dr. Jaime Jahncke, Dr. Mike Johns, Mr. Peter Warzybok

Skagit River System Cooperative Dr. Correigh Greene

West Coast Ocean Alliance Ms. Jennifer (Lilah) Isé

Appendix B — SUMMARY INFOGRAPHICS for the 2025-2026 ESR

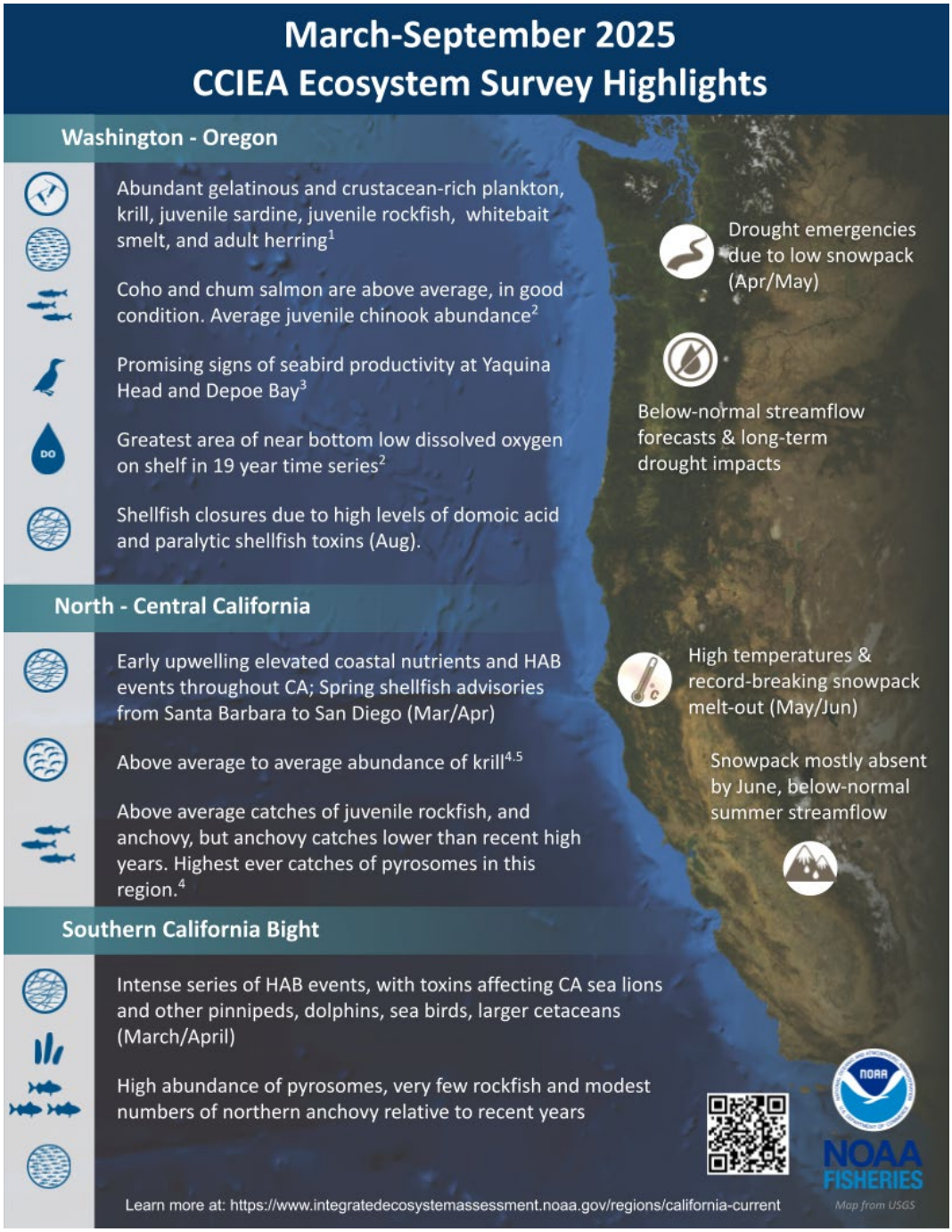


Figure B.1: Regional survey highlights assembled mid-year by IEA team. Survey data sources as follows: [1]Northern California Current Ecosystem survey (NCC), [2]Juvenile Salmon and Ocean Ecosystem Survey (JSOES), [3]Oregon State University / Yaquina Head , [4]Rockfish Recruitment and Ecosystem Assessment Survey (RREAS), [5]Integrated West Coast Pelagics Survey.

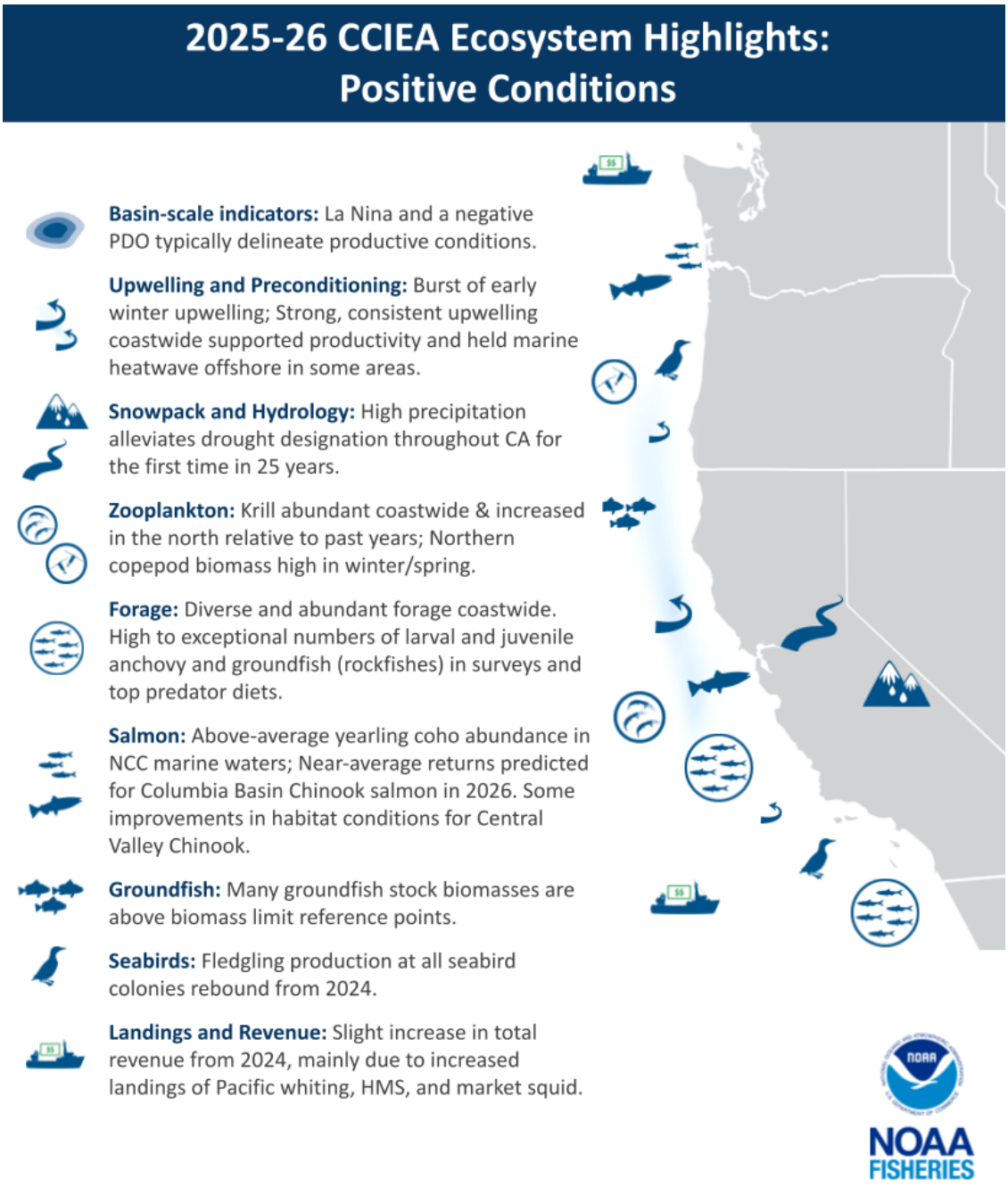


Figure B.2: Positive conditions in the California Current Ecosystem in 2025 and early 2026.



Figure B.3: Unfavorable conditions and risk factors in the California Current Ecosystem in 2025 and early 2026.

Appendix C — LIST OF FIGURES AND DATA SOURCES

Figure 1.1: Map of the California Current Ecosystem (CCE) and U.S. West Coast Exclusive Economic Zone (EEZ) created by B. Feist, NMFS/NWFSC. GIS layers of freshwater ecoregions derived from TNC & WWF (2008), based on Abell et al. (2008).

Figure 2.1: Oceanic Niño Index data are from the NOAA Climate Prediction Center (https://origin.cpc.ncep.noaa.gov/products/analysis_monitoring/ensostuff/ONI_v5.php). PDO index data are from ERSST V5 and served on the NCEI server (https://www.ncei.noaa.gov/pub/data/cmb/ersst/v5/index/ersst.v5.pdo.dat). North Pacific Gyre Oscillation data are from E. Di Lorenzo, Georgia Institute of Technology (http://www.o3d.org/npgo/).

Figure 2.2: Standardized sea surface temperature anomaly plots were created by A. Leising, NMFS/SWFSC, using SST data from NOAA's optimum interpolation sea surface temperature analysis (OISST; https://www.ncei.noaa.gov/products/optimum-interpolation-sst); SST anomaly calculated using climatology from NOAA's AVHRR-only OISST dataset. MHW conditions are delineated by values of the normalized SST + 1.29 s.d. from normal. Methods for tracking and classifying heatwaves are described in Thompson et al. 2019b and at the CCIEA blocktracker website project page.

Figure 2.3: Newport Hydrographic (NH) line temperature data are from the Newport Hydrographic Line Research Team, with data provided by A. Bolm, OSU/CIMERS, and J. Fisher, NMFS/NWFSC. Glider data along CalCOFI lines are from D. Rudnick and obtained from https://spraydata.ucsd.edu/projects/CUGN/.

Figure 2.4: Daily 2025 values of the Bakun Upwelling index are provided by M. Jacox, NMFS/SWFSC; detailed information about these indices can be found at https://go.usa.gov/xG6Jp.

Figure 2.5: Habitat Compression Index (HCI) estimates developed and provided by J. Santora, NMFS/SWFSC, and I. Schroeder, NMFS/SWFSC, UCSC.

Figure 2.6: Dissolved oxygen data from bottom mooring CE07 (https://oceanobservatories.org/site/ce07shsm/) obtained from NSF Ocean Observatories Initiative (2025). Newport Hydrographic (NH05) line dissolved oxygen data are from the Newport Hydrographic Line Research Team, with data provided by A. Bolm, OSU/CIMERS, and J. Fisher, NMFS/NWFSC.

Figure 2.7: Newport Hydrographic (NH) line aragonite saturation state data are from the Newport Hydrographic Line Research Team, with data provided by A. Bolm, OSU/CIMERS, and J. Fisher, NMFS/NWFSC.

Figure 2.8: Snow-water equivalent data were derived from the California Department of Water Resources snow survey (http://cdec.water.ca.gov/) and the Natural Resources Conservation Service's SNOTEL sites in WA, OR, CA and ID (http://www.wcc.nrcs.usda.gov/snow/). Data compilation and summary calculations by S. Munsch, NMFS/NWFSC.

Figure 2.9: Minimum and maximum streamflow data were provided by the US Geological Survey (http://waterdata.usgs.gov/nwis/sw). Data compilation and summary calculations by S. Munsch, NMFS/NWFSC.

Figure 3.1: Copepod biomass anomaly data are from the Newport Hydrographic Line Research Team, with data provided by A. Bolm, OSU/CIMERS, and J. Fisher, NMFS/NWFSC.

Figure 3.2. Krill abundance estimates derived from NOAA's 2025 Integrated West Coast Pelagics survey hydroacoustic data; provided by E. Phillips, NMFS/NWFSC.

Figure 3.3: Pelagic forage data from the Northern CCE from B. Burke, NMFS/NWFSC and C. Morgan, OSU/CIMRS. Data are derived from surface trawls taken during the NWFSC Juvenile Salmon & Ocean Ecosystem Survey (JSOES; https://www.fisheries.noaa.gov/west-coast/science-data/ocean-ecosystem-indicators-pacific-salmon-marine-survival-northern). Similarity analysis and cluster plot by A. Thompson, NMFS/SWFSC.

Figure 3.4: Pelagic forage data from the Central CCE were provided by J. Field, T. Rogers, K. Sakuma, and J. Santora, NMFS/SWFSC, from the SWFSC Rockfish Recruitment and Ecosystem Assessment Survey (https://go.usa.gov/xGMfR). Similarity analysis and cluster plot by A. Thompson, NMFS/SWFSC.

Figure 3.5: Pelagic forage larvae data from the Southern CCE were provided by A. Thompson, NMFS/SWFSC, from line 90 of spring CalCOFI surveys (https://calcofi.org/); data were not collected in 2020 due to survey cancellations associated with the COVID pandemic. Similarity analysis and cluster plot by A. Thompson, NMFS/SWFSC.

Figure 3.6: Data for at-sea juvenile salmon provided by B. Burke, NMFS/NWFSC and C. Morgan, OSU/CIMERS, from surface trawls taken during the NWFSC Juvenile Salmon and Ocean Ecosystem Survey (JSOES).

Figure 3.7: Stoplight table (statistical version) of indicators related to salmon in the northern CCE courtesy of B. Burke and K. Jacobson, NMFS/NWFSC, C. Morgan, J. Fisher, E. Daly, and S. Zeman, OSU/CIMERS, and T. Auth, PSMFC.(https://connect.fisheries.noaa.gov/Salmon_Indicators/).

Figure 3.8. Adult salmon returns are based on published model predictions in Burke et al. (2025), courtesy of B. Burke, NMFS/NWFSC.

Figure 3.9: Stoplight table of indicators and qualitative outlook for 2026/2027 Sacramento River Fall, Central Valley Spring, and Klamath River Fall Chinook salmon returns courtesy of S. Munsch and C. Greene, NMFS/NWFSC, and W. Satterthwaite, NMFS/SWFSC.

Figure 3.10: Groundfish stock status data, derived from NOAA Fisheries stock assessments, were compiled and provided by J. Cope, NMFS/NWFSC.

Figure 3.11: Albacore, swordfish, and bluefish tuna diet data provided by A. Preti and T. Richards, UCSC. Note these figures contain unpublished data.

Figure 3.12: Seabird fledgling production data from nesting colonies at Southeast Farallon Island, CA courtesy of J. Jahncke, Point Blue Conservation Science.

Figure 3.13: Whale entanglement data provided by D. Lawson and L. Saez, NMFS/WCR.

Figure 3.14: WA domoic acid data are provided by the Washington State Department of Health, OR data from the Oregon Department of Agriculture, and CA data from the California Department of Public Health. Figure created by C. Free, UCSB; adapted from Free et al. (2022).

Figure 3.15: Commercial Dungeness crab management restriction data are based on news releases from the California, Oregon, and Washington Departments of Fish and Wildlife, and reviewed by representatives from the Washington State Department of Health, Oregon Department of Agriculture, and the California Department of Public Health. Figure created by C. Free, UCSB; adapted from Free et al. (2022).

Figure 4.1: Community social vulnerability index (CSVI) and commercial and recreational fishery engagement data provided by C. Weng, NEFSC and C. Lewis-Smith, NMFS/NWFSC, PSMFC, based on data derived from the US Census Bureau's American Community Survey (ACS; https://www.census.gov/programs-surveys/acs/), PacFIN (http://pacfin.psmfc.org), ESRI business analyst, and guide and charter license data from CDFW, OSMB, and WDFW..

Figure 4.2: Fishery revenue diversification estimates were provided by D. Holland, NMFS/NWFSC, and R. Dame, NMFS/AFSC, utilizing data provided by PacFIN (http://pacfin.psmfc.org) and AKFIN (https://akfin.psmfc.org).

Figure 4.3: Fishery Participation Network data and analyses provided by J. Samhouri, NMFS/NWFSC, with data derived from PacFIN (http://pacfin.psmfc.org).

Figure 5.1: Data for commercial landings are from PacFIN (http://pacfin.psmfc.org) and NORPAC (North Pacific Groundfish Observer Program). Data acquired and plotted by K. Andrews, NMFS/NWFSC.

Figure 5.2: Data for recreational landings are from RecFIN (http://www.recfin.org/) and the CDFW Pelagic Fisheries and Ecosystem Data Sharing index). Data acquired and plotted by K. Andrews, NMFS/NWFSC.

Appendix D — NEAR TERM CLIMATE AND ECOSYSTEM FORECASTS

Based on feedback from the PFMC and its associated subcommittees (Agenda Item H.1.b Supplemental EAS Report, March 2023; Agenda Item H.1.b Supplemental EWG Report 1, March 2024), we present short-term ecosystem predictions in this standalone appendix. A separate appendix is provided for indicators of climate variability and change (Appendix E). Outlooks for adult Chinook salmon returns to the Columbia basin and California river basins are presented in the salmon appendix (Appendix J).

D.1 Forecasts for 2026

D.1.1 ENSO

The El Niño - Southern Oscillation (ENSO) is the best source of predictability for marine ecosystem conditions in the CCE. El Niño events tend to produce warm ocean conditions and lower productivity, while La Niña tends to produce the opposite. Thus, in considering how conditions are likely to evolve in 2026, we start with forecasts of ENSO.

As of January 2026, conditions in the equatorial Pacific are weakly La Niña and transitioning to ENSO-neutral. ENSO neutral is favored to persist through spring and into summer, with elevated chances of El Niño emerging in late summer / fall 2026 (Fig. D.1). Given the current and predicted ENSO conditions, we do not expect strong ENSO impacts on the CCE through summer 2026. If El Niño develops thereafter, it could impact the CCE in winter 2026/2027 and further into 2027.

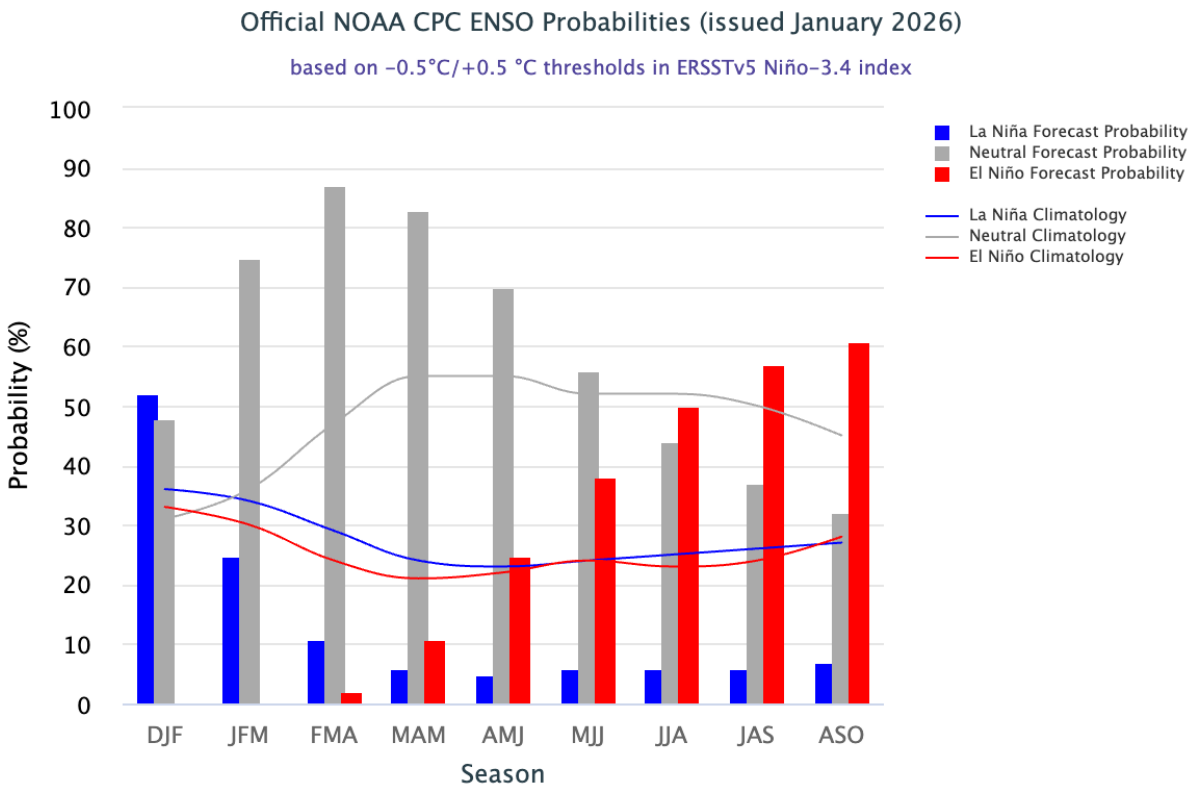


Figure D.1: CPC ENSO forecast, indicating the chances of El Niño, La Niña, or ENSO-neutral conditions for 3-month periods based on an ensemble of climate model forecasts. Accessed Jan. 28, 2026 at https://iri.columbia.edu/our-expertise/climate/forecasts/enso/current/.

D.1.2 Marine Heatwaves

Since 2022, NOAA has provided marine heatwave (MHW) forecasts, updated monthly. The latest forecasts for the Northeast Pacific indicate slightly elevated probabilities of MHWs in the U.S. EEZ through spring of 2026 (Fig. D.2), persisting from existing MHWs along the coast in December-Jananuary 2025-26. Widespread warm anomalies offshore of the EEZ are predicted to intensify in summer, and MHW likelihoods increase for parts of the coast in fall, reaching ~50% off Southern California. Note that under normal historical conditions, the likelihood of a MHW is 10%, so a forecast of 50% indicates greatly elevated MHW risk.

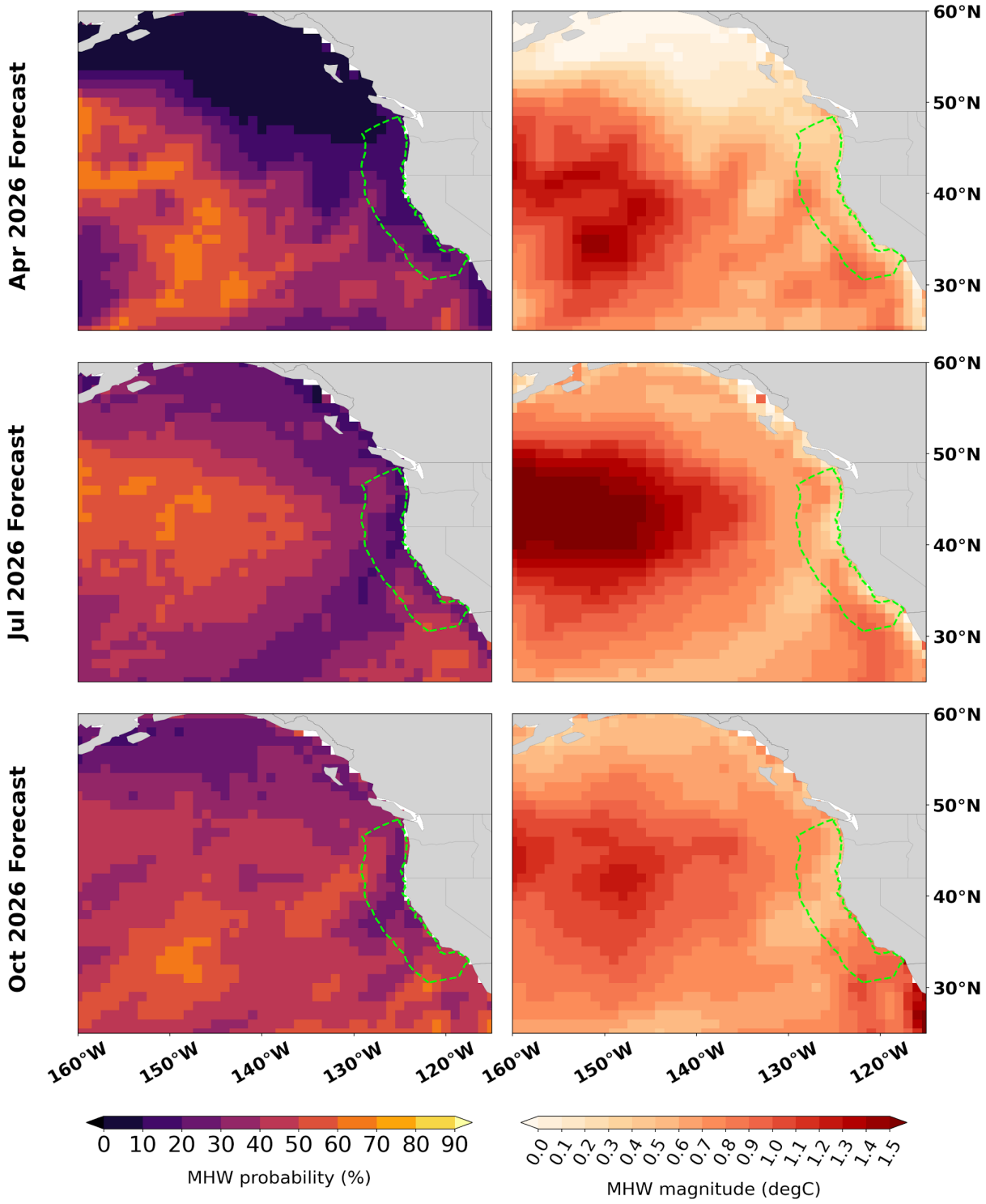


Figure D.2: Forecast likelihood of marine heatwaves in the Northeast Pacific Ocean through fall 2026. (Left) Forecast MHW probability and (right) forecast SST anomaly for three months (top-bottom; April, July, October). The U.S. EEZ is outlined in green. Forecasts are updated each month and are available from psl.noaa.gov/marine-heatwaves.

D.1.3 Temperature observations to avoid loggerheads (TOTAL)

As an example of how we could expand model-based forecasts in years to come, we present an experimental forecast of the Temperature Observations To Avoid Loggerheads (TOTAL) tool. The TOTAL tool tracks anomalies of SST in the Southern California Bight with an alert indicating that 6-month average SST anomalies have exceeded a threshold of ~0.8°C and there is an increased likelihood of Loggerhead turtle presence (and potential interaction risk) in the area based on historical data (Welch et al. 2019). A retrospective analysis found that using climate model forecasts, TOTAL could be predicted months in advance, potentially providing advance warning of risks (Brodie et al 2023).

The latest experimental TOTAL forecast (as of writing in January 2025) shows low risk of a TOTAL alert throughout 2025 (Fig. D.3). Since spring of 2024, the TOTAL index has steadily declined to its current state, near zero. Neutral to slightly cool values in the SCB are expected to continue through spring, with TOTAL alert likelihoods under 5%. Thereafter, warming is predicted, though the forecast chance of an alert remains under 10% through August.

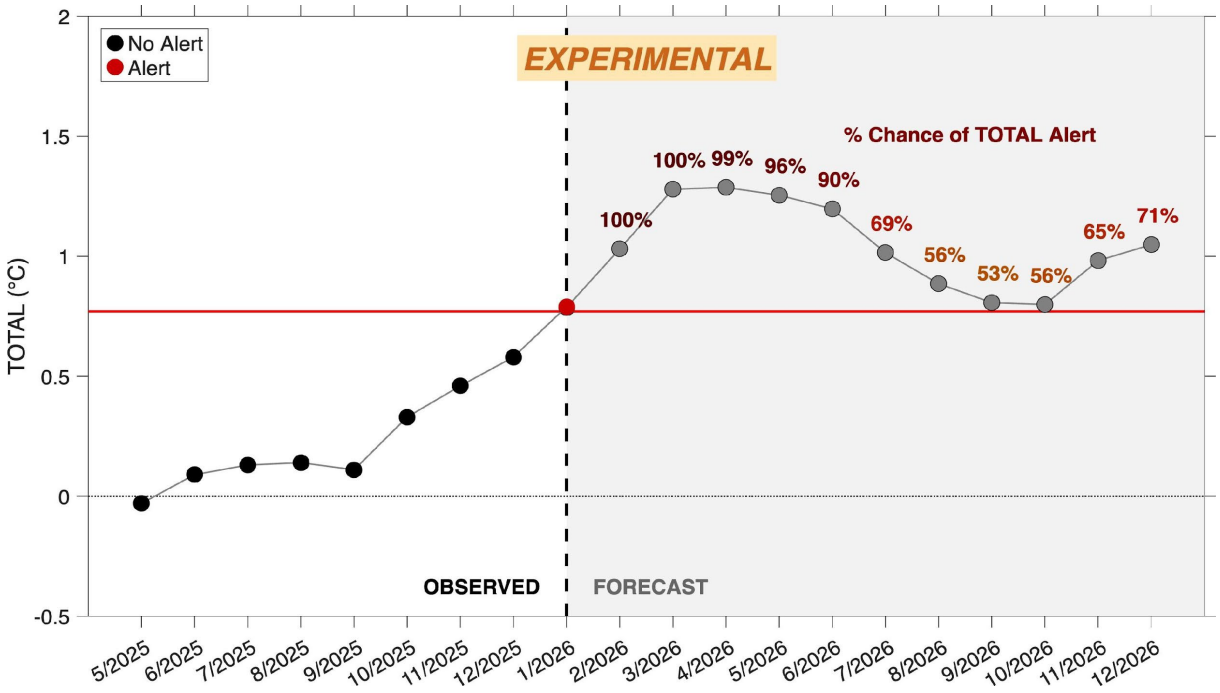


Figure D.3: Forecast likelihood of a Temperature Observations To Avoid Loggerheads (TOTAL) alert in 2026. TOTAL was designed to indicate increased risk of Loggerhead turtle interactions; an alert occurs when the 6-month average sea surface temperature anomaly in the Southern California Bight exceeds 0.77°C. Predicted TOTAL values are indicated on the y-axis for recent observations (black dots) and forecasts (gray dots). Numbers above forecast dots indicate the predicted chance of a TOTAL alert occurring each month. Forecasts developed and provided in collaboration with NOAA's Physical Sciences Laboratory.

D.2 Uncertainty in climate and ecosystem predictions

To contextualize the use of forecast information in decision making, we offer a brief discussion of forecast uncertainty. In this context, one must recognize that decisions made based on forecasts will not be perfect, but should be better than what is possible with no forecasts. As an analogy, if someone could win 60% of blackjack hands, they would become rich over time, despite losses along the way. For ecosystem forecasts, there are three key sources of uncertainty: (1) uncertainty in how the climate itself will evolve, (2) noise in environmental and ecological relationships, and (3) changes over time in environmental and ecological relationships (also known as "nonstationarity"). We briefly describe each source of uncertainty and how it can be accounted for in physical and biological models. For more detailed discussion, please see the 2023-2024 Climate Change Appendix.

1. When predicting what will happen in coming weeks and months, the greatest source of uncertainty is internal variability – unpredictable change that occurs due to the naturally chaotic nature of the climate (the "butterfly effect"). In order to account for this uncertainty, climate forecasts (like weather forecasts) are actually made up of many forecasts from which one can obtain the likelihood of an outcome given uncertainty.

2. Often, our understanding of responses between environmental variables, or between species and their environments, is based on empirical correlations. These relationships are imperfect. For example, El Niño increases the likelihood of a warm CCE, but cold CCE conditions are still possible during El Niño. Thus, individual years may deviate from the "expected" outcome, but the relationship still provides useful information, enabling predictions that are better than if climate were ignored altogether.

3. Non-stationarity refers to when a relationship between variables has changed such that past correlations no longer apply. Concerns of nonstationarity can be mitigated by (1) relying on environmental-biological relationships that are more mechanistic (e.g., modeling species responses to proximate ocean conditions rather than large-scale climate indices), and (2) using ensembles of ecological models with different formulations to capture uncertainty and identify robust responses.

D.3 Revisiting forecasts from 2025

- In last year's ESR, we presented predictions for ENSO, marine heatwaves, and TOTAL in 2025. Here, we briefly evaluate those predictions (Table D.1) as a means to weigh the merits of similar predictions in the future. As detailed below, all three predictions proved highly accurate (Appendix D from the 2024-25 Ecosystem Status Report, Leising et al. 2025).

Table D.1: Assessment of forecasts from the 2024-25 Ecosystem Status Report

Index	Forecast	Outcome
ENSO	Shift from La Niña early in the year to ENSO-neutral around April, with neutral persisting through fall 2025	La Niña conditions faded after January and ENSO-neutral persisted until September. After September, weak La Niña conditions returned.
MHW	Low probabilities of MHWs in the US EEZ through spring of 2025, then increasing through summer into fall, particularly north of Cape Mendocino, with forecast probabilities exceeding 50%. Farther offshore, elevated chances of MHWs are present and increasing throughout 2025	Along the coast, no appreciable MHW activity occurred through spring and early summer, though MHWs were present farther offshore. MHW conditions expanded to cover much of the U.S. west coast in August/September, remained off California for October/November, and then again covered much of the coast in December
TOTAL	Low risk of a TOTAL alert throughout 2025. Likelihoods under 5% through spring before increasing through spring and summer but remaining low (~5-20%)	As predicted, the TOTAL indicator decreased through spring before increasing in summer and fall but remaining well below the alert threshold

Appendix E — DEVELOPING INDICATORS OF CLIMATE CHANGE

Climate change shapes risk to meeting fisheries management objectives by affecting the distribution, seasonal timing, productivity, abundance, and physiological response of marine species, as well as influencing fishing practices. For instance, changes in productivity can influence projections of rebuilding timelines and estimated reference points used in harvest setting processes. Shifts in distribution can affect the regional availability of target species or the risk of bycatch of non-target species. These and other connections between climate change, ecology, socioeconomic dynamics, and management procedures provide essential context for navigating ecosystem change.

There is a continually growing body of research on climate variability, future change, and their impacts in the California Current. Here, we (1) contextualize climate variability and change by discussing our latest understanding of their interactions and influences on the ecosystem, (2) highlight several additional insights that are new for this year – a synthesis of projected species distribution changes and an example of how fishing fleets can serve as sentinels of ecosystem variability, and (3) summarize past research on projected future change, with a focus on the physical environment, groundfish, and CPS.

E.1 Contextualizing climate variability and change

In the North Pacific, long-term warming trends are overshadowing interannual variability, further complicating long-standing efforts to understand relationships between large-scale climate and regional ecosystem responses. Recent research, described below, has shed new light on the relationship between long-term trends and variability, as well as the stability of observed climate and ecosystem relationships.

E.1.1 The Pacific Decadal Oscillation in a changing climate

The Pacific Decadal Oscillation (PDO) has served as a key index linking basin-scale climate variability to marine ecosystem changes in the California Current System since its definition in 1997 (Mantua et al. 1997). In recent years, however, apparent departures from previously documented PDO–ecosystem correlations have raised concerns about the stability of the mode and its continued relevance as an ecosystem indicator in a warming climate Thompson et al. (2024). A recent study shows that PDO-related sea surface temperature (SST) variability is now increasingly overprinted by basin-wide warming of the North Pacific, helping to explain the apparent changes in PDO impacts in the California Current System (Cluett et al. 2025).

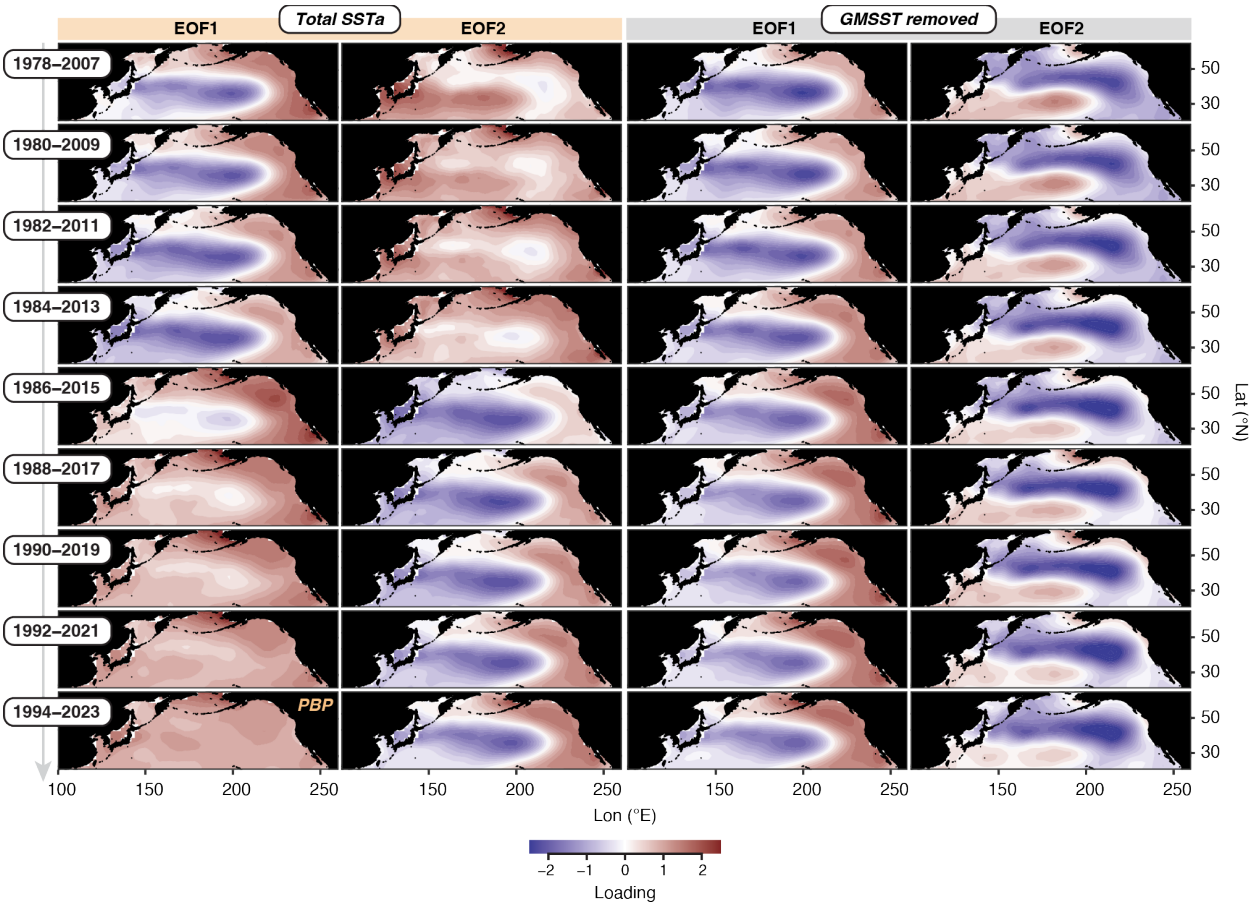


Figure E.1: Leading patterns of North Pacific SST variability during sliding retrospective 30-year windows. In the left two columns, empirical orthogonal functions (EOFs) were calculated without removal of the global mean SST anomalies (i.e., based on the total SST anomalies). In the right two columns, EOFs were calculated following the removal of global mean SST anomalies (GMSST).

The PDO is defined as the leading empirical orthogonal function (EOF) of North Pacific SST anomalies after removal of the global mean SST anomaly (Mantua et al. 1997). By construction, it represents the dominant pattern of North Pacific SST variability independent of global-scale warming. In its positive phase, the canonical PDO pattern features relatively warm SSTs throughout the California Current System and cooler SSTs in the central and western Pacific (Fig. E.1; GMSST-removed EOF 1). Prior to 2014, this pattern remained dominant even when the global mean SST anomaly was not removed prior to calculation. Over the past decade, however, the leading EOF of North Pacific SSTs calculated without removing the global mean anomaly has shifted to a unidirectional, basin-wide warming pattern (Fig. E.1; total SST anomaly EOF 1). This emergent pattern, termed the Pan-Basin Pattern (PBP), provides a new index for describing secular basin-wide warming (Fig. E.2).

Despite the growing prominence of the PBP, neither the spatial structure nor the strength of the PDO has changed significantly. The PDO remains clearly identifiable, appearing as the second dominant pattern when the global mean SST anomaly is retained and as the leading pattern when it is removed. Its continued presence and contribution to overall variability indicate that PDO-related dynamics remain robust. In the California Current System, SSTs increasingly reflect the combined influence of the PDO and the PBP, representing climate variability superimposed on a warming baseline. Interactions between the two patterns help explain recent novel ocean conditions, including prolonged coastal warming along North America from 2014 to 2020 when both patterns were in positive phases, as well as the unexpected lack of cooling during the subsequent negative PDO phase beginning in 2021.

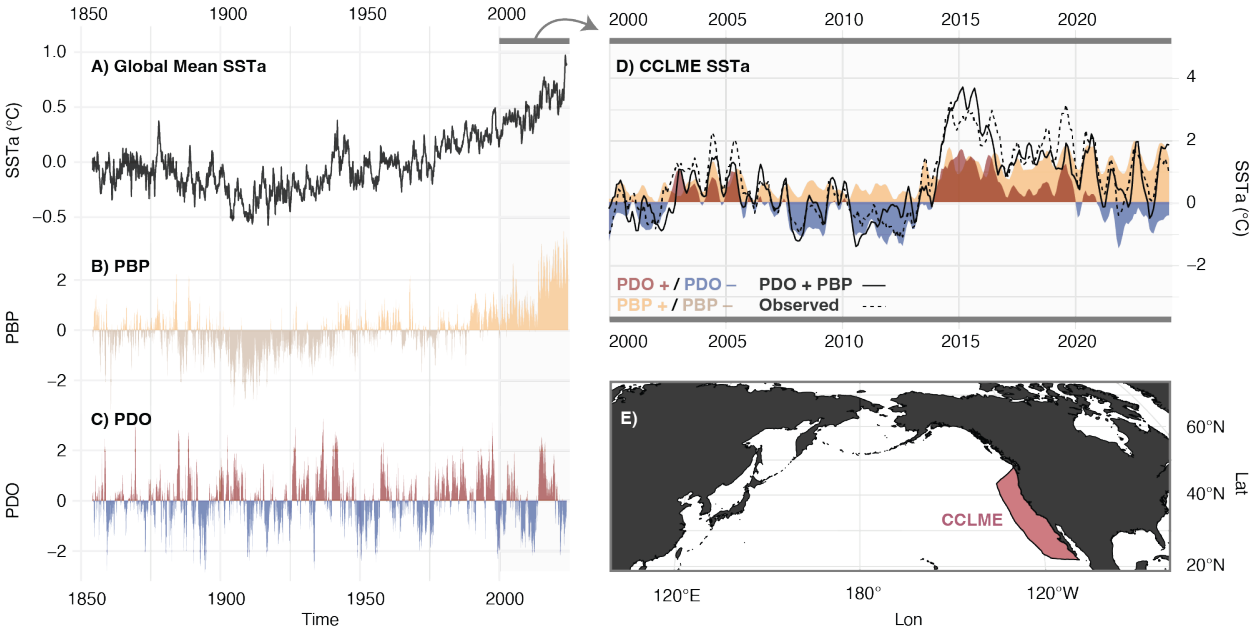


Figure E.2: Time series of basin-wide patterns and their regional expressions in the California Current. A) The global mean SST (GMSST) anomaly, B) PBP index, C) PDO index, D) Decomposed SST anomalies in the California Current Large Marine Ecosystem (CCLME) associated with the PBP (yellow) and PDO (red and blue) compared with the total SST anomalies (solid black lines) and PBP + PDO SST anomalies (dashed black lines). E) Map of the California Current Large Marine Ecosystem (CCLME).

Historically, the PDO has served as a reliable proxy for SST across much of the North Pacific, including the California Current Ecosystem. As regional SSTs increasingly diverge from those historically expected based on PDO signals, there is a growing need to distinguish impacts driven directly by temperature anomalies from those associated with PDO-related dynamical processes, such as changes in upwelling or transport. Given the continued stability of the PDO pattern, the PDO index is likely to remain a useful indicator of North Pacific climate variability. However, its ecological relevance may increasingly lie in

what it reveals about changing ocean dynamics rather than regional SST anomalies alone. Approaches that jointly consider PDO and PBP signals may help recover lost ecological inference.

E.1.2 Time-dependent climate and ecosystem relationships

The PDO and other climate indices (i.e., Oceanic Niño Index, North Pacific High, North Pacific Gyre Oscillation) summarize variability in sea surface temperature, sea surface height, and sea level pressure across the northeast Pacific. These basin-scale indices correlate with local physical conditions that influence food webs and species abundances. The correlations between climate indices and local ecological conditions provide critical insight for how food webs respond to climate. In the Gulf of Alaska, the Aleutian Low is a dominant pattern in atmospheric forcing and a decrease in variability in the Aleutian Low starting in 1989 altered the relationship between PDO and important, local, environmental conditions (i.e., SSH, ice cover, wind). This subsequently altered the ecological meaning of the PDO across the region (Litzow et al. 2020) by changing the relationship between the PDO and associated species abundances, including Pacific salmon. In the CCS, changes in the relationships between biological conditions and the PDO were also observed but were not apparently driven by weakening relationships between climate and local environmental conditions, as the relationships between PDO and SST, SSH, upwelling, oxygen, and salinity, were consistent before and after 1988/1989 (Litzow et al. 2020).

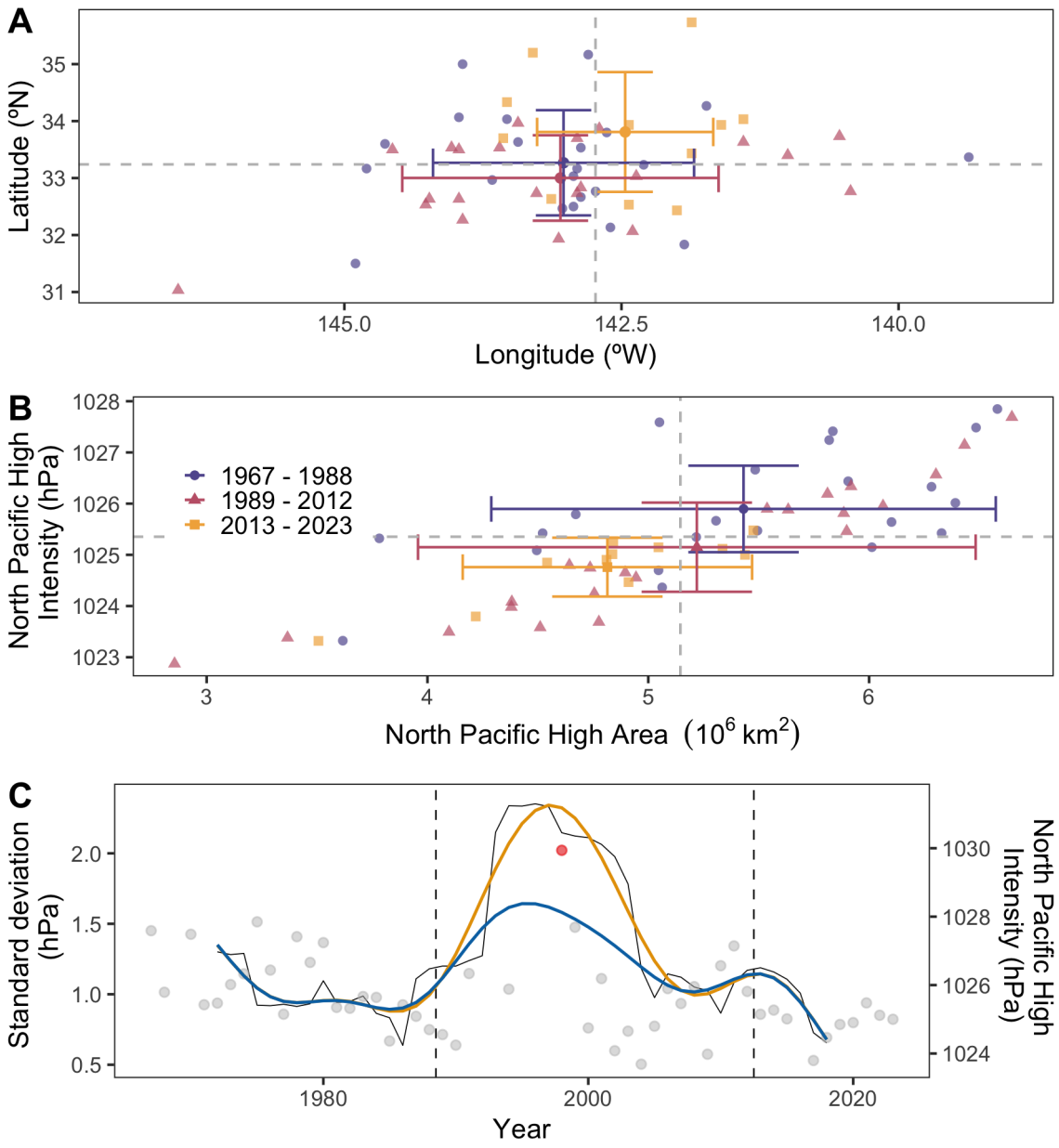


Figure E.3: (a) Location, (b) intensity (hPa) and area (106 km2), and (c) temporal variance (s.d. over 11-year rolling windows) of mean springtime (April–June) conditions of the North Pacific High-pressure system (black line) with trend lines (nonparametric linear regressions) illustrating the inclusion of an outlier in 1998 (orange) and exclusion of 1998 (blue). Points are annual observations and period-specific means (1967–1988, purple; 1989–2012, red; 2013–2023, yellow) with tails denoting 1 s.d.. Dashed lines show (a) the 1967–2023 mean location, (b) 1967–2023 mean intensity and area, and (c) the breaks between 1988/1989 and 2012/2013 periods.

A recent study investigated time-varying relationships between climate indices and biological responses in the CCE, with a specific focus on how climate relationships force food webs via the regional physical conditions that link climate forcing to ecological responses (Feddern et al. 2025). In the CCE, regional atmospheric forcing is characterized by the strength, position, and timing of the North Pacific High which is associated with springtime upwelling (Schwing et al. 2006; Schroeder et al. 2013). Unlike the Aleutian Low, patterns in variability, strength, location, and extent of the North Pacific High since 1989 have remained consistent with historical observations (Fig. E.3), although the pressure system has been smaller, weaker, and located further north since 2013 compared to the long-term (1967 - 2023) average. Four climate indices (PDO, NPGO, NPH, and ONI) typically used to interpret food web-climate interactions in the CCE all had consistent relationships through time with regional upwelling phenology across the CCE (Fig. E.4). More specifically, the relationships between each of the four climate indices and the timing of the spring transition, total magnitude of the upwelling season, and the length of upwelling season were consistent through time when comparing three time periods with documented climatic shifts: pre-1989 when Aleutian Low variability was high (Litzow et al. 2020), 1989 - 2012 when Aleutian Low variability was low (Litzow et al. 2020), and post-2013 when the Pan Basin warming was the dominant pattern in sea surface temperatures (Cluett et al. 2025).

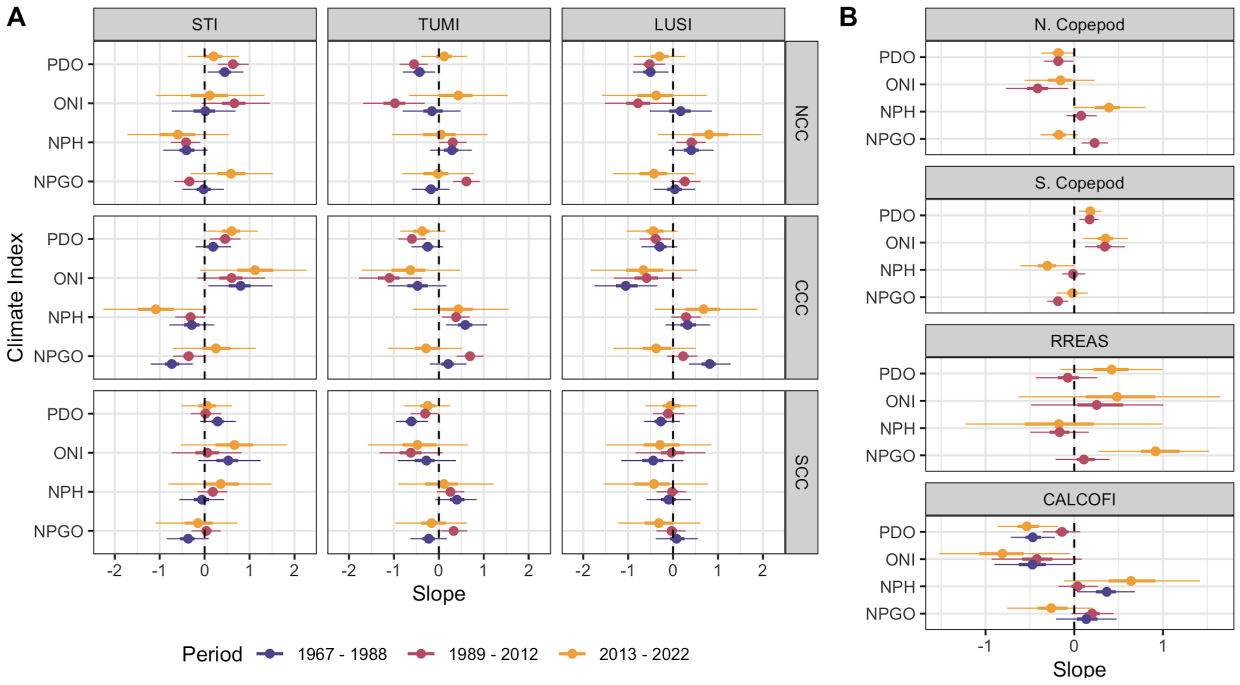


Figure E.4: Posterior summaries of the intercepts from Bayesian linear regression models between (a) climate indices and proximate physical conditions described by upwelling indices and (b) climate indices and biological conditions. RREAS and copepod data were not available for the first period, and thus are not shown on (b). For all plots points denote the posterior median, thick lines show the 50% highest posterior density credible interval and thin lines show the 95% highest posterior density credible interval for 1967–1988 (purple, period 1), 1989–2012 (red, period 2) and 2013–2022 (yellow, period 3). Bayesian credible intervals can be interpreted as the probability a parameter falls within a given range, distributions that do not overlap can be considered time periods with distinct relationships.

Overall, this study did not find evidence that the ecological meaning of climate indices in the CCE had changed for non-salmon species (Feddern et al. 2025) based on biological datasets from Newport Hydrographic Line, Rockfish Recruitment and Ecosystem Assessment Survey, and CalCOFI. Overall, this means low trophic level species in the CCE including copepods and juvenile groundfish are responding similarly to climate variability during the most recent decade (2013 - 2023) as they did in the past. However, this work did find an overall increasing trend through time in community abundance across species sampled in the core CalCOFI area (Fig. E.5) which was not explained by variability in climate or regional upwelling phenology (Fig. E.4). This overall increasing trend may be better resolved by collectively considering the PBP index with the PDO and other indices. These results also suggest that additional research is needed to better understand how PDO-associated ocean dynamics (beyond SST) may have driven the historically observed ecological linkages (Cluett et al., 2025).

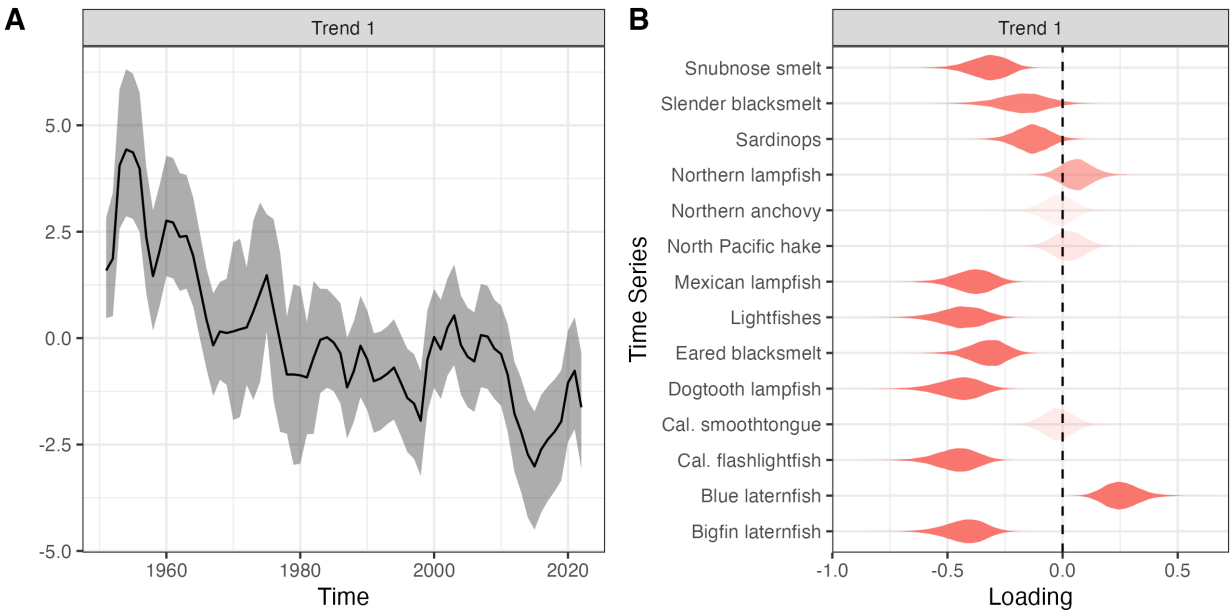


Figure E.5: DFA latent trends used as the biological indices for CalCOFI. Latent trends for the California Cooperative Oceanic Fisheries Investigations survey (A, CalCOFI) from 1951 - 2022 with 95% credible intervals of community variability. Posterior distributions for loadings on individual time series associated with the survey trend for CalCOFI (B). Loadings with darker shading indicate time series loading most strongly on the survey trends (different from 0).

E.2 New Synthesis Tools

E.2.1 Measuring and communicating projected shifts in species distributions

Data Tool Highlight: Tracking spatial shifts of important species

Previous "Developing Indices of Climate Change" Appendices have included examples of fisheries species shifting their distributions as a result of changing ocean conditions. This year, we are broadening this approach by piloting a synthesis across dozens of species, using a variety of indicators of range shifts. Looking toward the middle of the century (2050-2070), 67% of the species analyzed are expected to shift northwest, 68% of commercially targeted species will move farther from shore, and 96% of groundfish species will experience shifts of a portion of their biomass into unfishable waters exceeding 700 fathoms.

In the future, we are working to develop a dashboard that will allow Council users to interact and produce summary reports across a diverse set of species (fisheries stocks, bycatch species, and protected species), indicators of distributional shifts, and at multiple regional or jurisdictional scales. The goal is to provide an accessible, centralized dashboard

that offers direct insight into potential changes that West Coast fisheries can use to plan under projected future ocean conditions.

Community-wide Projected Shift Direction

Climate change models can be used to develop projections of spatial distributions for species-of-interest based on future ocean conditions. These projections can help inform state and federal planning processes, provide measures of historical overlap and future opportunity cost, and support regional assessment of climate-fishery-energy interactions. In previous years' reports (2024-25 Appendix, 2023-24 Appendix), we presented research on projected distributions of groundfish species (DTS complex) (Liu et al. 2023) and coastal pelagic species. Here, we collated projected distributions under the highest emissions climate change scenario for 48 species of management and ecological importance in the CCE to identify patterns in shift magnitude and direction by the middle of the century (2050-2070), which aligns with PFMC Climate and Communities Initiative time horizon interests. Additionally, we selected species' groups of commercial importance, explored shifts in distance from shore and depth on a state-by-state basis, and highlighted four species-specific, detailed, spatial shifts by quantifying projected changes in relative densities.

The 48 species distribution models include six coastal pelagic species (CPS, Muhling et al. 2025), 28 groundfish (Liu et al. 2023, 2025), nine highly migratory species (HMS) including three marine mammal species and one sea turtle species Muhling et al. (2025), and five seabird species (Gasbarro et al. 2025a). Groundfish projections were restricted to fishable waters within 700 fathoms (the bottom-trawl depth limit), while all other species were limited to the U.S. EEZ. Because groundfish were modeled using Catch Per Unit Effort (CPUE) and other species using probability of occurrence, we rescaled groundfish projections annually by their maximum CPUE to ensure comparability across distributions.

E.2.2 Community-wide projected shift direction

We analyzed broad distribution shifts by calculating annual center-of-gravity (COG), representing the mean latitude and longitude for each species. Future shifts were quantified by comparing the mean baseline COG (2011–2025) reflecting current ocean conditions to the mean projected future COG (2050–2070).

Across the projected distributions, we primarily see northwest shifts in COG (67% of species), which included all CPS, 75% of HMS, 61% of groundfish and 40% of seabird species (Fig. E.6). 21% of species are projected to shift towards the southeast, which include 32% of the groundfish species and 20% of seabird species (Fig. E.6). Highest magnitude shifts in COG are projected for groundfish, with the farthest northwestern shift projected for two flatfish (Pacific sanddab and curlfin sole) and the furthest southeastern shift for shortraker rockfish (Fig. E.6).

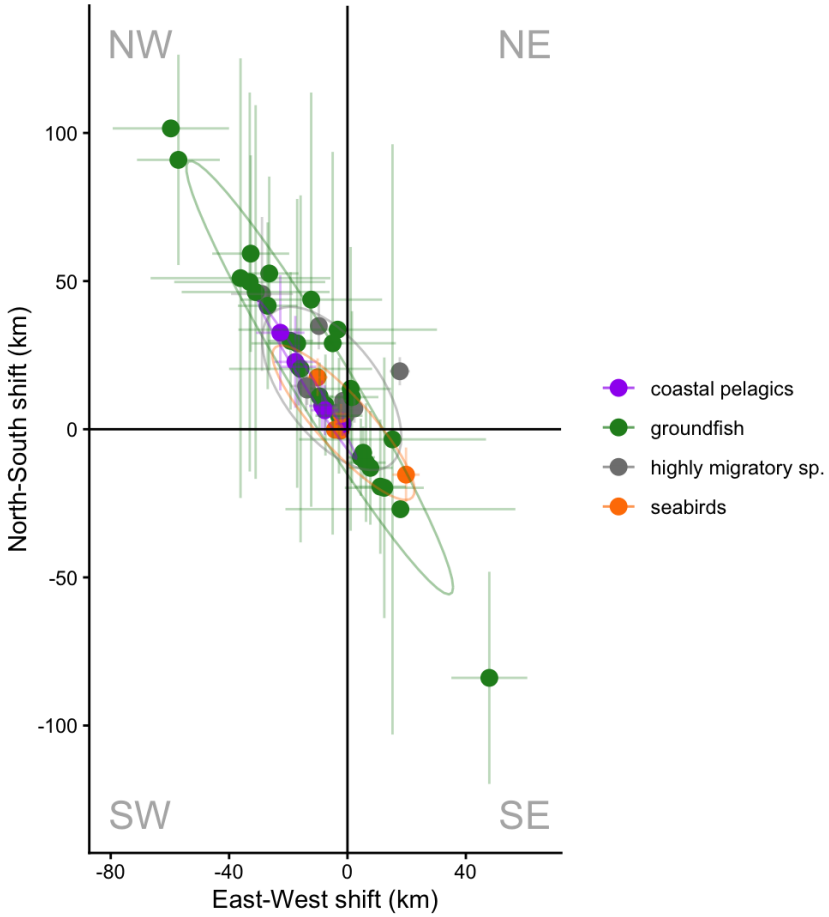


Figure E.6: Average center-of-gravity (COG) shifts between base period (2011-2025) and future (2050-2070). Each point in the plot represents an individual species and error bars represent uncertainty across Earth System Models (ESMs). Ellipses encompass 90% of data points.

E.3 Implications for Fisheries and State Jurisdictions

To assess the practical implications for fisheries, we transitioned from broad community-wide patterns to a focused analysis of commercially significant stocks. Here, we filtered the original assemblage down to 38 species, which include roundfish (2 sp.), flatfish (8 sp.), coastal pelagics (6 sp.), rockfish (18 sp.; includes thornyheads), sharks (2 sp.), billfish (1 sp.), tuna (1 sp.), and other demersal fish (1 sp.). Rockfish were further separated into groups based on size and habitat. To account for the distinct oceanographic and regulatory environments along the U.S. West Coast, we utilized state delineations, and divided California into two regions at the Point Conception latitudinal break (34.44º N) and refer to the two regions as the Southern California Bight (SCB) for waters south of Point Conception, and California (CA) to refer to the waters north of Point Conception.

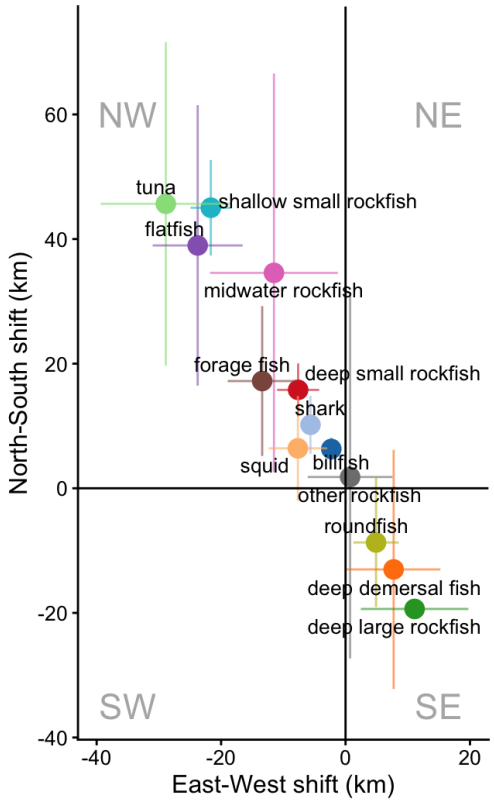


Figure E.7: Average center-of-gravity shifts between base period (2011-2025) and future (2050-2070) for 38 commercial fishery species. Each point represents various species within each functional group. Error bars represent variation in projected shifts across species and ESMs in each functional group. Data are summarized by Earth System Model, year, state region, and fish functional group.

A northwest trajectory is projected for all functional groups except for deep demersal fish (Pacific grenadier), deep large rockfish, and roundfish (Fig. E.7). Albacore, followed by flatfish and shallow small rockfish, are projected to shift the furthest north and west, and midwater rockfish are also projected to shift further north (Fig. E.7).

While center-of-gravity can show broad patterns in shift direction and is useful for comparing across various different species, it can miss nuances in projected shifts. Therefore, we calculated two fishery-relevant metrics: shifts in average distance to shore and, for groundfish, changes in the relative proportion of biomass within 700 fathoms, representing the traditional bottom-trawl limit (PFMC 2015).

The only species with a projected decrease in distance to shore across all four regions is albacore (tuna), with the strongest shifts towards shore projected to occur in California (Fig. E.8). Sharks and billfish (swordfish) are also projected to decrease in distance from shore in all regions except for Washington (Fig. E.8). In contrast, for the remaining functional groups, there is a predominant projected increase in distance from shore in all

regions except for small shoreward shifts projected for midwater rockfish in Washington and the SCB (Fig. E.8).

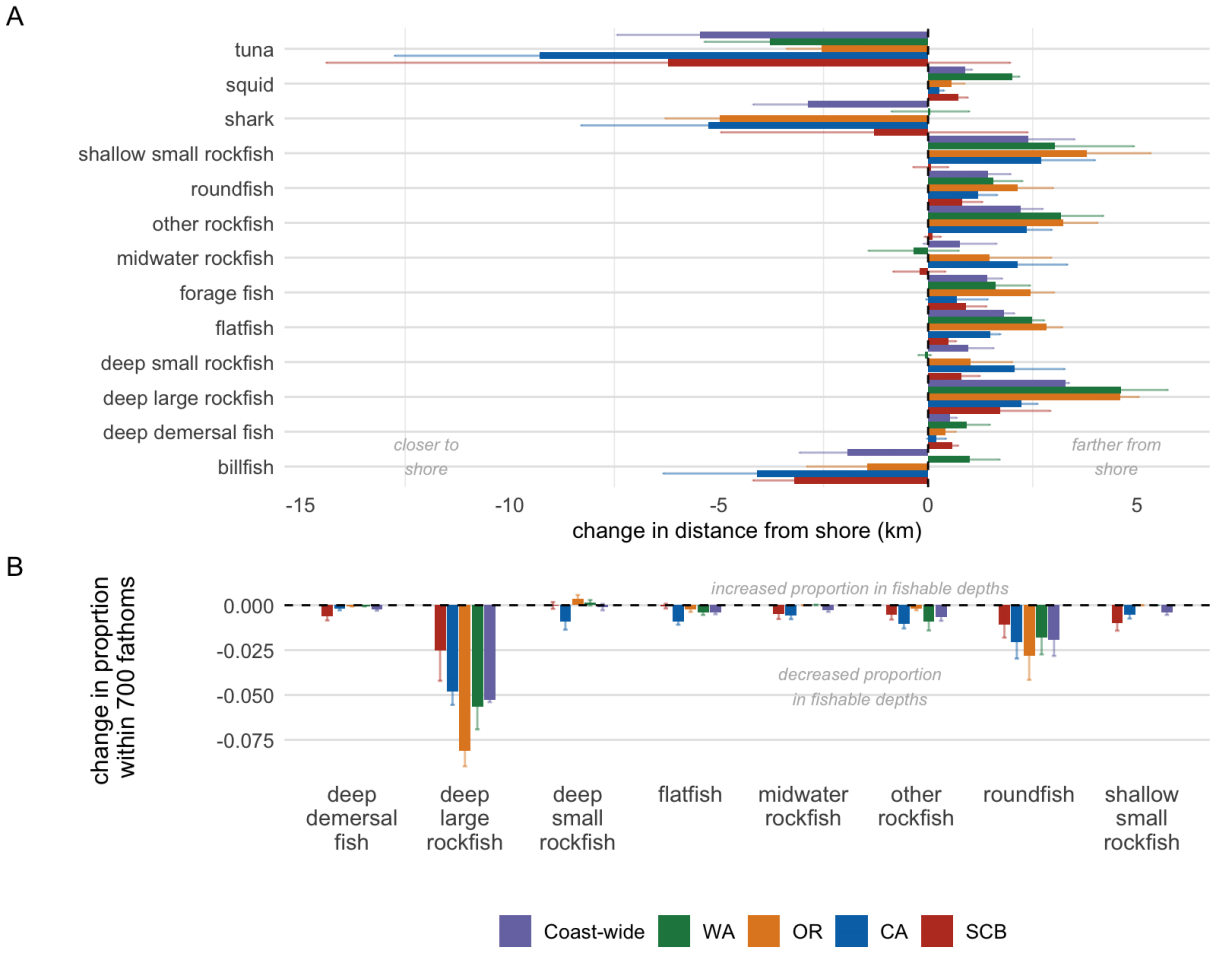


Figure E.8: Projected changes in cross-shelf distribution for 38 commercially important species between base period (2011-2025) and future (2050-2070). (A) Projected change in distance from shore (km) calculated as the biomass-weighted average distance from the coastline, (B) For groundfish species only, the projected change in the proportion of total biomass remaining within the 700-fathom depth contour, representing the traditional bottom-trawl limit. Data are summarized by Earth System Model, year, state region, and fish functional group, with variability derived from species within each functional group.

Overall, groundfish species exhibit a clear trend toward deeper waters. Specifically, 96% of the analyzed species are projected to shift further into depths exceeding 700 fathoms. The most significant declines in biomass available within the 700 fathom limit occur among deep large rockfish and roundfish (Fig. E.8). All other functional groups are projected to have relatively smaller decreases (<2.5% shift) in proportion of biomass available within

700 fathoms, except for slight increases in deep small rockfish in Washington and Oregon (Fig. E.8).

E.3.1 Species-specific spatial trends

The previous sections on center-of-gravity and cross-shelf distributions provided a broad overview of how species groups are projected to respond to climate change; however, these aggregate metrics can mask the underlying complexity and diversity of responses within these groups. To better understand these nuances, we examine four species that represent projected trajectories: sablefish, albacore, widow rockfish, and petrale sole.

We calculated projected shifts between 2011-2025 and 2050-2070 by classifying each grid cell for each time period into density thresholds (absence, low density, core density, high density) and compared changes between the two time periods. As was reported by Liu et al. (2023), projections suggest that sablefish relative density will decrease throughout the entire coast (Fig. E.9). In contrast, albacore density is expected to decrease in the SCB and increase in all other regions (Fig. E.9). Projected shifts for petrale sole and widow rockfish vary by region, with both species expected to increase in relative density in Washington (where widow rockfish are also projected to expand along the coast), decrease in central/northern California, and redistribute within Oregon and the SCB (Fig. E.9). None of these four species are projected to contract in range by the middle of the century.

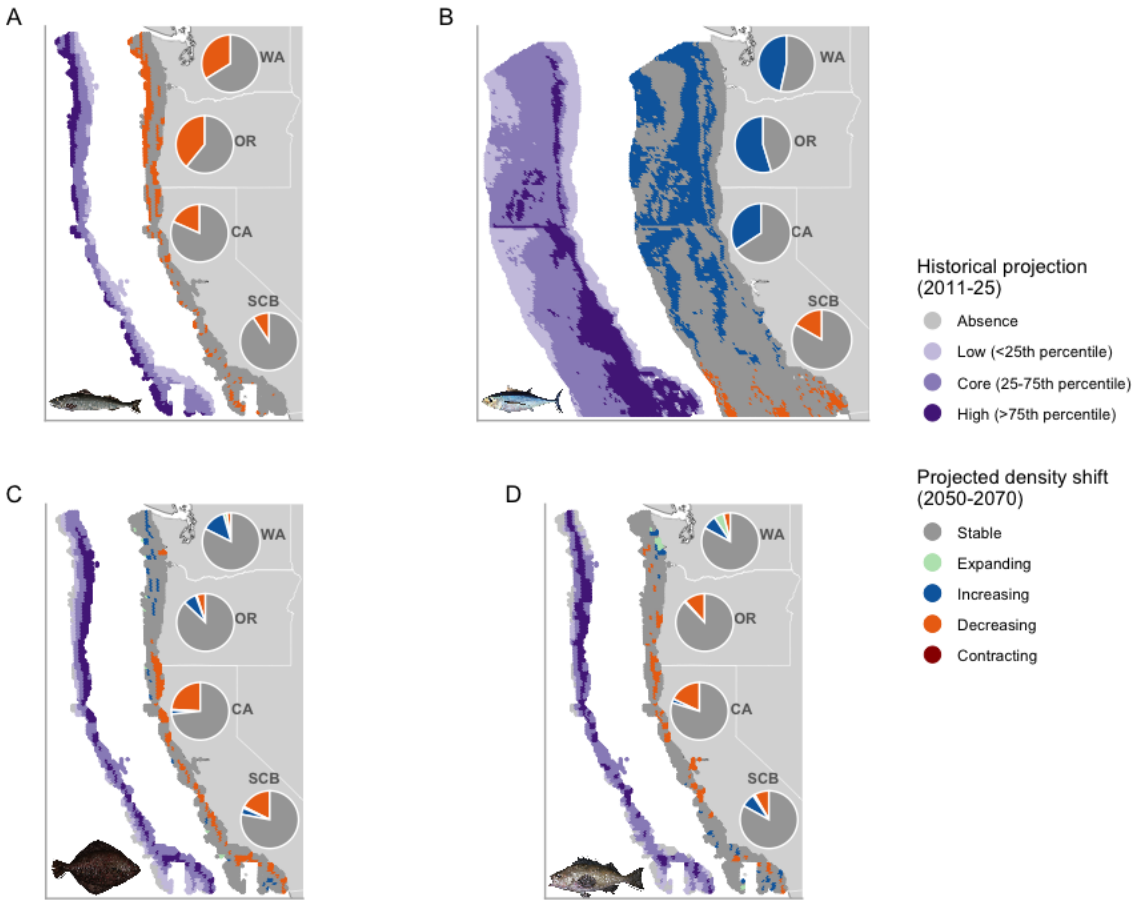


Figure E.9: Projected spatial shifts in (A) sablefish, (B) albacore, (C) petrale sole, and (D) widow rockfish distributions. For each species, the map displays the projected historical distribution (2011–2025, offset west) alongside the projected future shifts along the coastline (2050–2070). Historical distribution is classified by density thresholds: absence(light gray), low densities (<25th percentile; light purple), average densities (25th-75th percentile; medium purple), and high densities (>75th percentile; dark purple). Projected shifts represent transitions between these states: stability (no category change), expansion (absence to presence), contraction (presence to absence), and increasing or decreasing density (movement between low, core, and high density categories). Inset pie charts summarize the proportional distribution of these projected trends within waters in each region (WA, OR, CA, SCB). Groundfish species projections (sablefish, petrale sole, and widow rockfish) are limited to 700 fathoms, and the albacore projection extends to the United States EEZ.

E.4 Fishing fleets as ecosystem sentinels

Non-confidential data on fishery vessel movement and activity, combined with environmental data, can be another analytical tool that yields valuable information about species distribution changes and ecosystem variability. This information enhances our knowledge beyond what is available from scientific surveys. A recently published study (Welch et al. 2025) investigated the utility of fishing fleets as sentinels for ecological changes during climate extremes. Vessel Monitoring System (VMS) geolocation data linked to shoreside landings receipts from the U.S West Coast Pacific albacore fishery were summarized from 2010-2024 to evaluate the ability of the fleet to signal two ecological changes during marine heatwaves: 1) northward and inshore shifts of albacore and bluefin tuna (Fig. E.10), and 2) low albacore availability, particularly during the 2023 fishing season which led to a formal fisheries disaster declaration request (Fig. E.11). VMS-based metrics were compared to sea surface temperature anomalies (SSTa) to investigate whether VMS (a more complicated indicator) conferred any advantage over a simple environmental indicator. The indicators were extended through 2025 for this report.

Fig. E.10 demonstrates the co-occurrence of extreme northward shifts in both tuna species and the fishery during the 2014-2016 marine heatwave. Although sea surface temperatures were anomalously warm during this period, the warmest temperatures occurred during subsequent marine heatwave events (2019 and 2023). The most recent year of analysis (2025) did not contain extreme northward tuna/fishery shifts nor extreme positive sea surface temperatures.

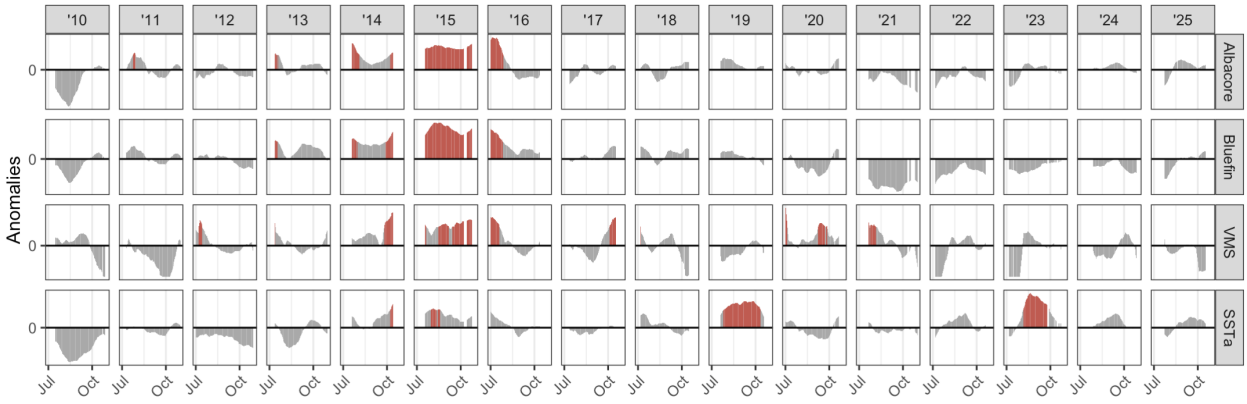


Figure E.10: Daily latitudinal anomalies for the July-October fishing season indicating the north/south movements of modeled albacore and bluefin tuna and the fishing fleet (indexed by the Vessel Monitoring System; VMS), and daily sea surface temperature anomalies; SSTa. The 90th percentile (reds) was used to define extreme northward shifts in albacore, bluefin, and VMS, and extreme positive SSTa. Anomalies and the 90th percentile are calculated relative to 2010-2024, following the methodology in Welch et al. 2025.

Fig. E.11 demonstrates relatively consistent albacore catch per unit effort (CPUE) across years except for the 2023 season. CPUE decreased by 46% during the 2023 season, indicating low albacore availability and coinciding with the federal fisheries disaster

declaration request. In contrast, SSTa was anomalously warm during the 2014, 2015, 2019, and 2023 seasons. The most recent year of analysis (2025) had relatively average CPUE and SSTa.

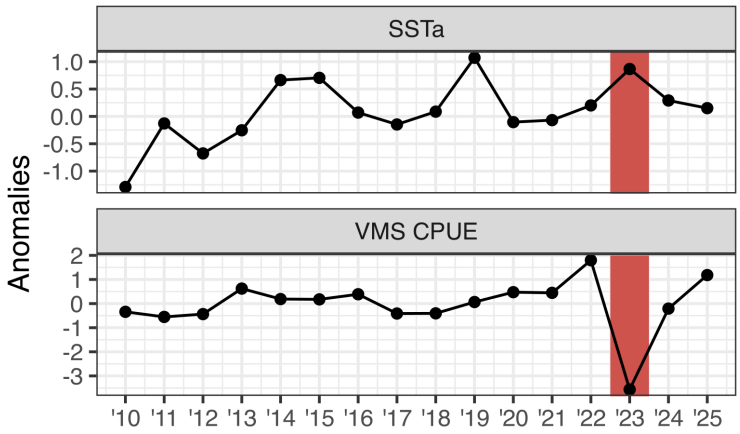


Figure E.11: Annual sea surface temperature anomalies (SSTa) and annual anomalies of catch per unit effort (CPUE in units of pounds per minute) indexed by the Vessel Monitoring System (VMS) for the July-October fishing season. Red bar for the 2023 season denotes the federal fishery disaster declaration request. Anomalies are calculated relative to 2010-2024, following the methodology in Welch et al. 2025.

These results demonstrate marine heatwaves occur frequently, but only some are accompanied by pronounced ecological changes. These ecological changes were more strongly captured by VMS than by SSTa. VMS data integrate the behavioral response of fishermen to a broad suite of environmental and ecological signals, providing a sensitive and accurate indicator of ecological change. Importantly, VMS data are available in real-time, automatically collected and disseminated, high resolution, and free to the end-user – making them suitable for operational monitoring of ecological changes that are otherwise difficult to observe.

E.5 State of knowledge on future changes in the CCE

Much of the information in this report changes year-to-year based on variability in the CCE. In contrast, many of our expectations for long-term change in the CCE remain consistent from year-to-year. Since it remains relevant, we summarize that information here for reference.

E.5.1 Ocean and biogeochemical change

Under future climate change scenarios, robust projections in the California Current Ecosystem include ocean warming (both surface and subsurface), increased stratification, reduced mixed layer depth, deoxygenation, and acidification (Pozo Buil et al. 2021). While the magnitude of these changes varies among models and scenarios, the sign of change is consistent. Under a high-emissions scenario (RCP8.5), climate change trends in many

physical and chemical trends emerge (exceed natural variability) by mid-century; mitigation scenarios delay that time of emergence (Henson et al. 2017). Lower emissions scenarios are expected to produce qualitatively similar but less pronounced effects. Changes in primary production are less certain – most but not all models suggest decreased productivity under future climate change (Jacox et al. 2024).

E.5.2 Distribution and abundance of groundfish and CPS

Focusing on the DTS complex of groundfish (Dover sole, shortspine thornyhead, longspine thornyhead, and sablefish), Liu et al. (2023) projected that the oceanographic changes summarized above would lead to declining coastwide abundance of sablefish and shortspine thornyhead, which would also shift offshore into deeper waters. Projected changes in the distributions of Dover sole and longspine thornyhead were smaller, with abundance remaining near constant or increasing.

A suite of different ecosystem models all projected a northward shift in the northern subpopulation of Pacific sardine, though there was no consensus on whether coastwide biomass would increase or decrease (Smith et al. 2023). Distribution changes for anchovy are projected to be much smaller, though an increased likelihood of "bust" periods is projected for the coastwide anchovy population (Leising et al. 2024). Wildermuth et al. (2023) found that the current sardine assessment process can effectively track changes in population status under a changing climate, and that effective management will likely depend on frequent/responsive monitoring and assessment, as well as better understanding of climate-driven recruitment changes.

E.5.3 Vulnerability and risk for groundfish and CPS fleets

Climate-driven risks to groundfish fleets are expected to be greater to the north (off Washington/Oregon) than farther south (Samhouri et al. 2024). The increased risk is because (1) current fishing grounds in the northern CCS are projected to experience higher exposure to climate change (more warming, greater shifts required to keep pace with bottom temperatures) and (2) communities in the northern CCS have greater economic dependence on these fisheries. When comparing two approaches for adapting to climate change, Samhouri et al. (2024) found that moving to follow shifting fish stocks is likely to be more effective than diversifying portfolios while remaining in place (Samhouri et al. 2024).

The projected northward distribution shift for the northern subpopulation of Pacific sardine is expected to increase landings in the Pacific Northwest while decreasing landings in California (Smith et al. 2023), though the potential effects of shifts in the southern subpopulation have not yet been modeled. Quezada et al. (2023) identified multiple segments of west coast CPS fisheries (small scale vs industrial, local vs wide-ranging, specialist vs generalist), and identified mobility and the ability to switch between target species as two qualities that will confer future adaptation potential.

Appendix F — CLIMATE AND OCEAN INDICATORS

Link to main section: Climate and Ocean Drivers

F.1 Basin-scale Climate/Ocean Indicators at Seasonal Time Scales

These plots show seasonal averages and trends of the three basin-scale climate forcing indicators shown in the main report in Fig. F.1.

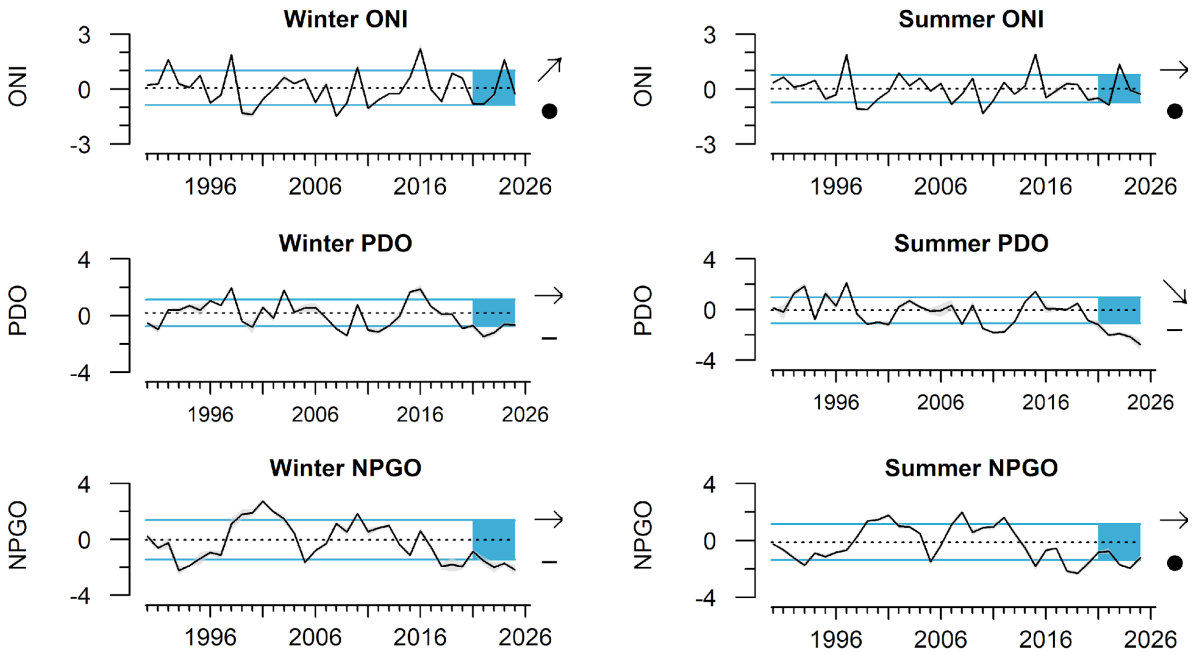


Figure F.1: Winter (Jan-Mar) and Summer (July-Sep) values for the basin-scale climate indicators: Ocean Niño Index (ONI), Pacific Decadal Oscillation (PDO), and North Pacific Gyre Oscillation (NPGO) through -2025. Mean and s.d. for 1991-2020. Lines, colors, and symbols are as in Fig. 2.1.

Satellite data, which has been collected in a similar fashion since 1982, allows for a basin-scale view of sea surface temperature (SST) at daily and sub-degree (spatial) resolution. Here we show seasonal averages of SST anomalies (the difference from climatology) across the NE Pacific (Fig. F.2). Winter saw anomalously high SST in the far offshore, with cooler-than normal conditions right at the coast. Spring and summer saw mostly cooler than normal conditions right at the coast, with continued warmer than normal waters offshore. Fall saw a shift to anomalously warm temperatures both onshore and offshore.

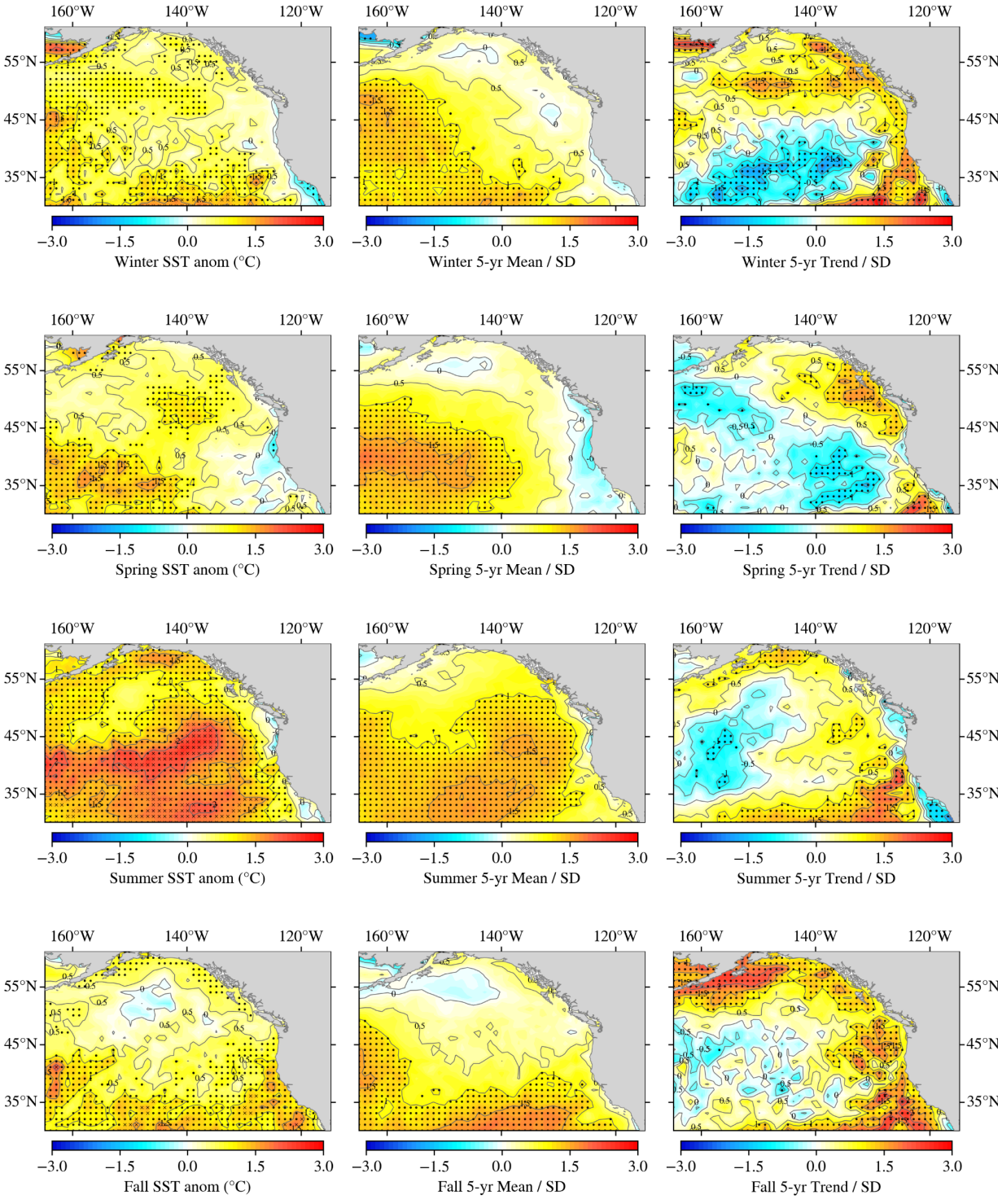


Figure F.2: Left: Sea surface temperature (SST) anomalies in 2025, based on 1982-present satellite time series in winter (Jan-Mar; top), spring (Apr-Jun), summer (July-Sept) and fall (Oct-Dec; bottom). Center: Mean SST anomalies

for 2021-2025. Right: trends in SST anomalies from 2021-2025. Black dots mark cells where the anomaly was >1 s.d. above the long-term mean (left, middle) or where the trend was significant (right). Black x's mark cells where the anomaly was the highest in the time series.

Glider data has become an increasingly useful tool for analyzing trends in subsurface water temperatures over time. The following series of plots represents data from subsurface gliders, which generally sample in cross-shore transects on a weekly to monthly basis, and have been in service long enough for the development of climatologies, which are then used to compute temperature anomalies. Examination of these subsurface anomalies over time, which are all averages from the coast out to 200 km offshore, suggests that during 2025 spatially averaged subsurface temperatures off Oregon were generally warmer than previous years, except for the beginning of the year and during the peak of the upwelling season (Fig. F.3). Off Northern California, subsurface temperatures were average, shifting to above average in the surface 100m during mid summer (Fig. F.4). Throughout California, 2025 saw warmer than normal surface and subsurface temperatures with only a slight period of average or colder than average during the spring upwelling season (Fig. F.5).

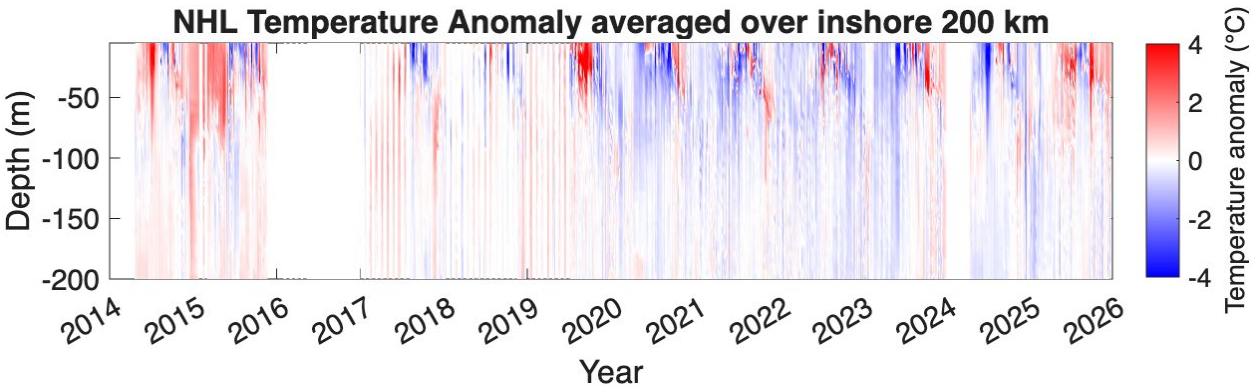


Figure F.3: Time-depth plot of average subsurface temperature anomalies from the shore to 200 km offshore along the Newport Hydrographic Line (Latitude 44.6 N), based on OSU-OOI coastal endurance array gliders (https://ceoas.oregonstate.edu/ocean-observatories-initiative-ooi). Climatology based on monthly averages created over 2014-2025

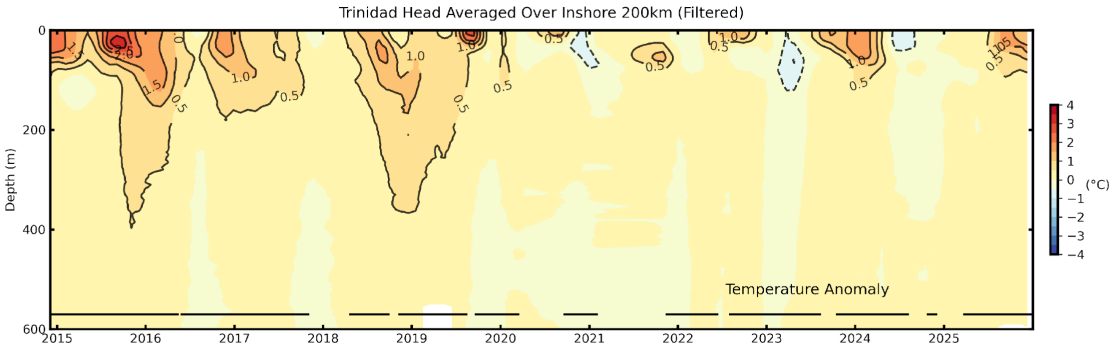


Figure F.4: Time-depth plot of average subsurface temperature anomalies from the shore to 200 km offshore along the Trinidad Head Line (Latitude 41.06 N) . Data courtesy of Oregon State University, CeNCOOS, and NANOOS.

One of the key elements driving eastern boundary currents such as the California Current system is seasonal upwelling, as it brings cool, nutrient-rich waters to the surface and is the major driver of productivity in the region. Besides examining the temporal dynamics of upwelling versus past levels (Fig. 2.4), another key indicator is the cumulative upwelling index (CUI), which allows for a summation of the total upwelling (essentially nutrient supply) received in coastal regions through the year. Here, we present the CUI for select latitudes along the west coast, as a proxy for year-to-year changes in total nutrient supply, and thus overall productivity (Fig. F.6). Except for 36° N, all latitudes saw higher than average CUI, driven mainly by earlier than normal upwelling events that occurred in late winter and early spring, as can be seen by the 2025 data being higher than the mean over the first 30-60 days of the time period.

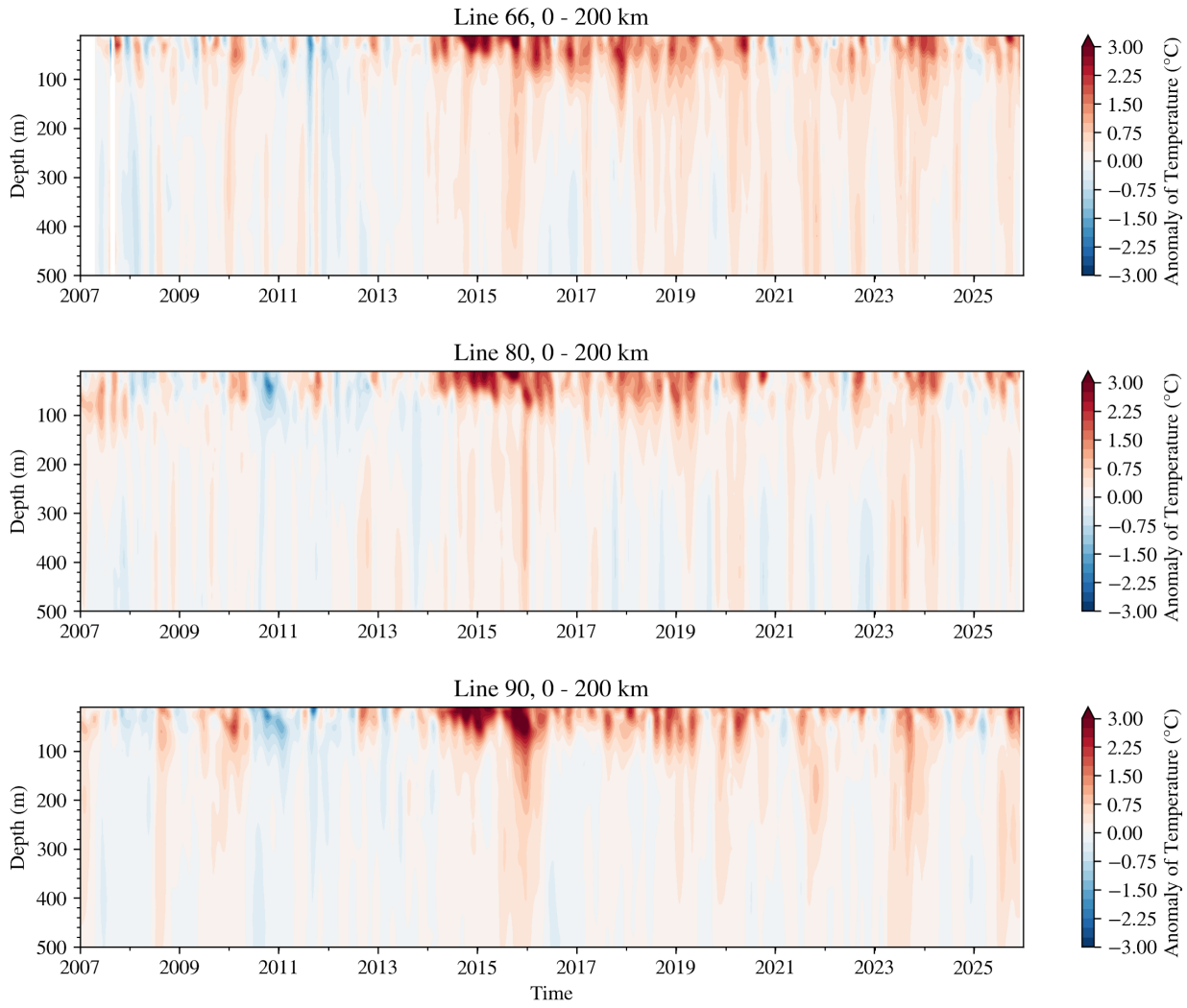


Figure F.5: Time-depth plot of average subsurface temperature anomalies from the shore to 200 km offshore along CalCOFI line 66, 80, and 90 based on SPRAY gilder data and climatology. Data from the California Underwater Glider Network are provided by Dr. Dan Rudnick, Scripps Institute of Oceanography Instrument Development Group (doi: 10.21238/S8SPRAY1618).

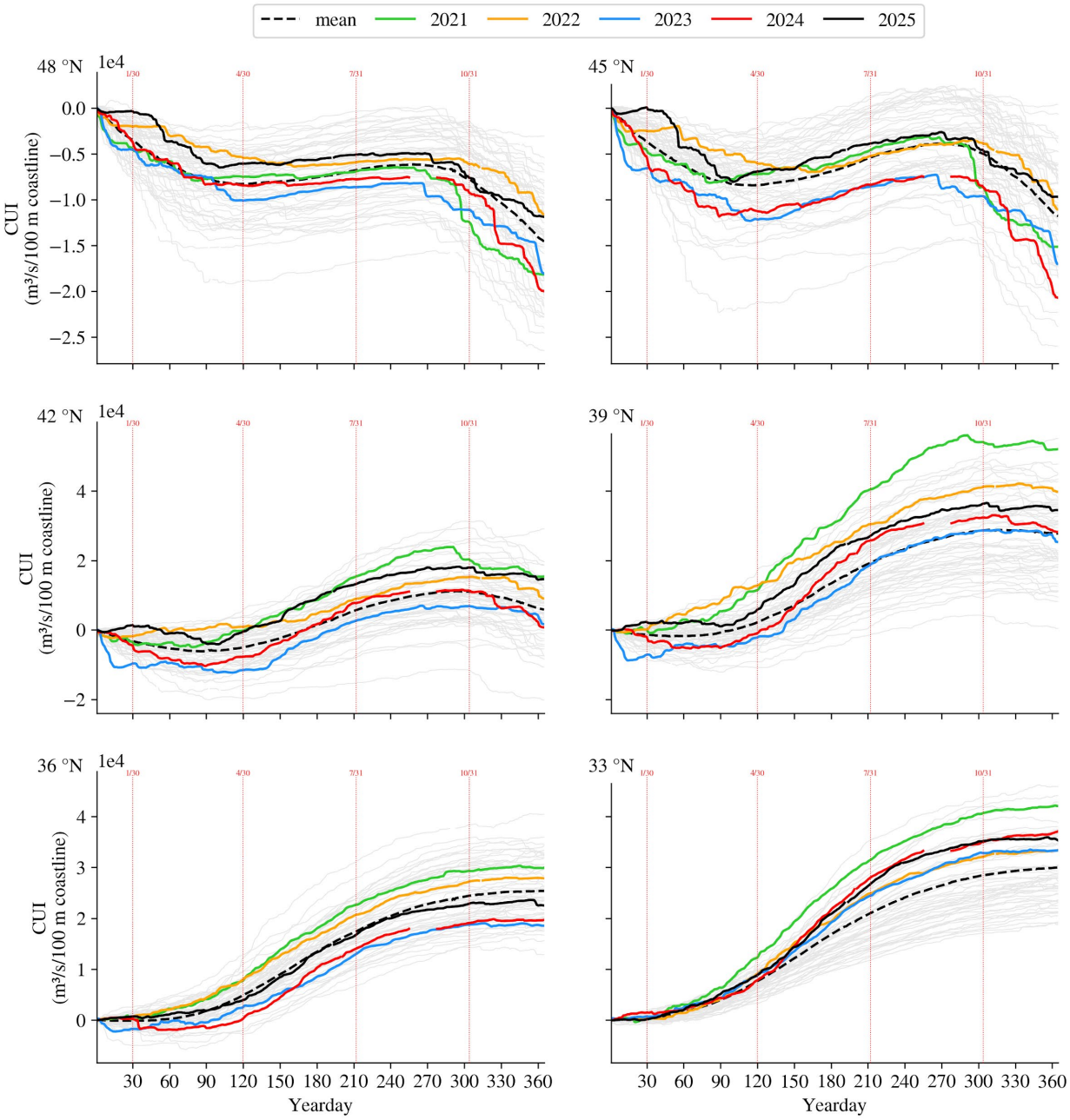


Figure F.6: Cumulative upwelling index (CUI) calculated for respective locations throughout the CCE for 2025 and the prior four years for comparison. CUI based on the Bakun upwelling index. Mean based on 1967-2025.

F.2 Assessing Marine Heatwaves in 2025

There is growing recognition that marine heatwaves can have strongly disruptive impacts on the CCE (e.g., Morgan et al. 2019). Based on an analysis of sea surface temperature anomalies (SSTa) obtained from satellite measurements (https://www.ncei.noaa.gov/erddap/griddap/ncdc_oisst_v2_avhrr_by_time_zlev_lat_lon.html), we

define marine heatwaves as: 1) times when normalized SSTa >1.29 s.d. (90th percentile) of the long-term SSTa time series at a location, and 2) lasts for >5 days; which are analogous to the thresholds suggested in Hobday et al. (2016). Here, we further report on statistics concerning large heatwaves (LHW) which were tracked through space and time, with LHW defined as those heatwaves with an area > 400,000 km^2 (these denote the top 20% of all heatwaves by area as measured since 1982 when satellite data became available for tracking; (Leising in revision). 2025 saw extensive LHW in the far offshore region beginning in May, with intrusions into the coastal region in late August through December (See red and yellow regions in Fig. F.7). This 2025 event was the largest by area (~10 million km^2), and 8th longest marine heatwave recorded since monitoring began in 1982 (Fig. F.8). Note: the underlying climatology used for SST anomaly analysis has changed from 1982-2010, to now encompass 1982-2020; hence there are small changes in the retrospective analysis of tracked heatwaves reported in Figure F.7 as compared to previous years' reports (fewer total tracked heatwaves, and a downgrading of maximum area for the 2022 event).

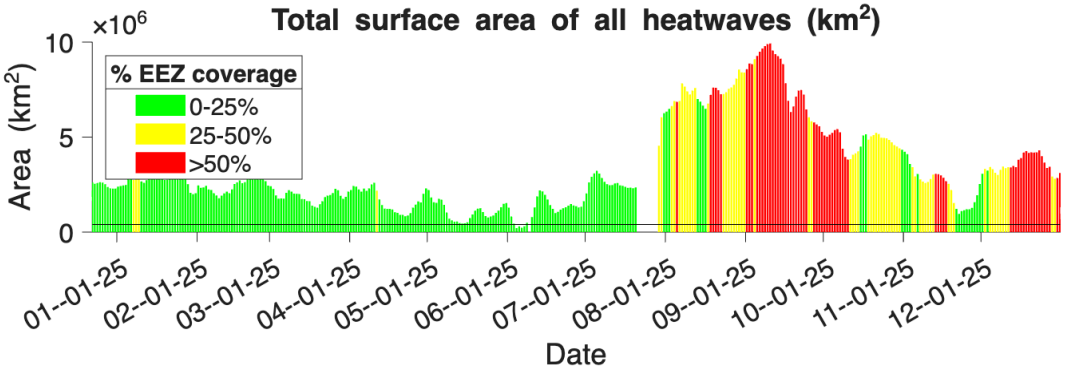


Figure F.7: Areas of North Pacific marine heatwaves during 2025. The horizontal line represents 400,000 km2, the area threshold that we use for tracking individual events over time (top 20% of heatwaves by area; Leising [in revision]). Color indicates the percentage of the U.S. West Coast EEZ that was in heatwave state.

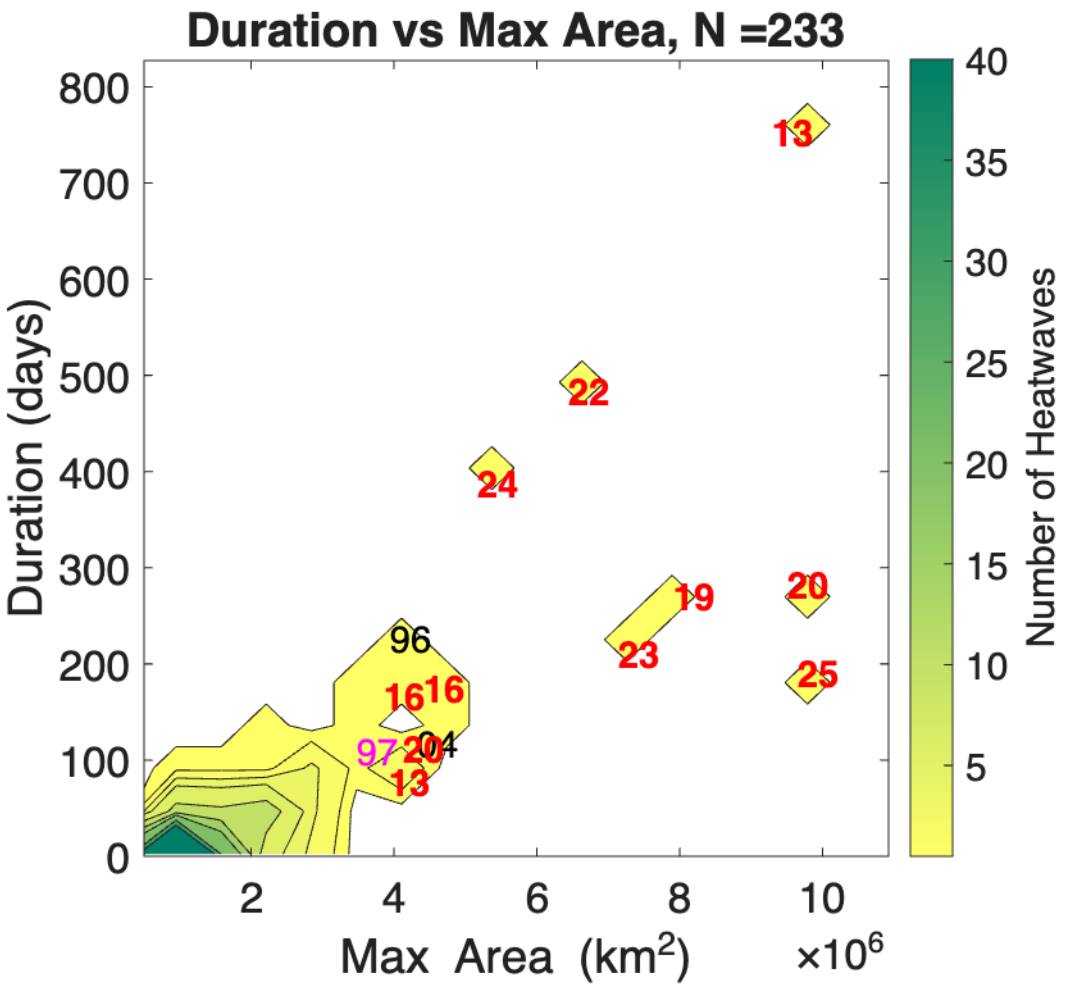


Figure F.8: Duration and maximum areas of NE Pacific large marine heatwaves, 1982-2025. Shading indicates the number of heatwaves (out of 233). Outliers are marked with numbers indicating the year the heatwave formed, with the past ten years marked in red and the 1997-1998 El Nino marked in magenta for comparison.

F.3 Habitat Compression Index

Spatial variability in patterns of upwelling, including the distribution of upwelled water and associated development of hydrographic fronts, is an important aspect of ecosystem monitoring and assessment of marine heatwaves and ecosystem shifts that can impact coastal fishing communities. Coastal upwelling creates a band of relatively cool coastal water, which is suitable habitat for a diverse and productive portion of the CCE food web. Monitoring the area and variability of upwelling habitat provides regional measures of habitat compression—an indicator to monitor the incursion of offshore warming (e.g., from heatwaves or reduced upwelling conditions) over shelf waters, which relates to shifts in the pelagic forage species community in space and time. Santora et al. (2020) applied principles of ecosystem oceanography and integration of fisheries surveys to develop the

Habitat Compression Index (HCI) to quantify how offshore warming during the 2013–2016 marine heatwave and previous warming events restricted the cool upwelling habitat to a narrower-than-normal band along the coast. This compression of habitat consequently altered prey community composition and distribution, spatial aggregation patterns of top predators, and contributed to increased rates of whale entanglements in fixed fishing gear.

HCI is derived from the CCE configuration of the Regional Ocean Modeling System (ROMS) model with data assimilation (Neveu et al. 2016), and is estimated in four biogeographic provinces within the CCE: 30°-35.5° N, 35.5°-40° N, 40°-43.5° N, and 43.5°-48° N. HCI is defined as the area of monthly averaged ROMS model temperatures at a depth of 2 m that fall below a temperature threshold. Each region/month has a unique temperature threshold, based on its distinct historic climatology. Winter and spring means for central California are shown in the main body of the report (Fig. 2.5). Winter and spring means for all four regions are shown here, in Figure F.9.

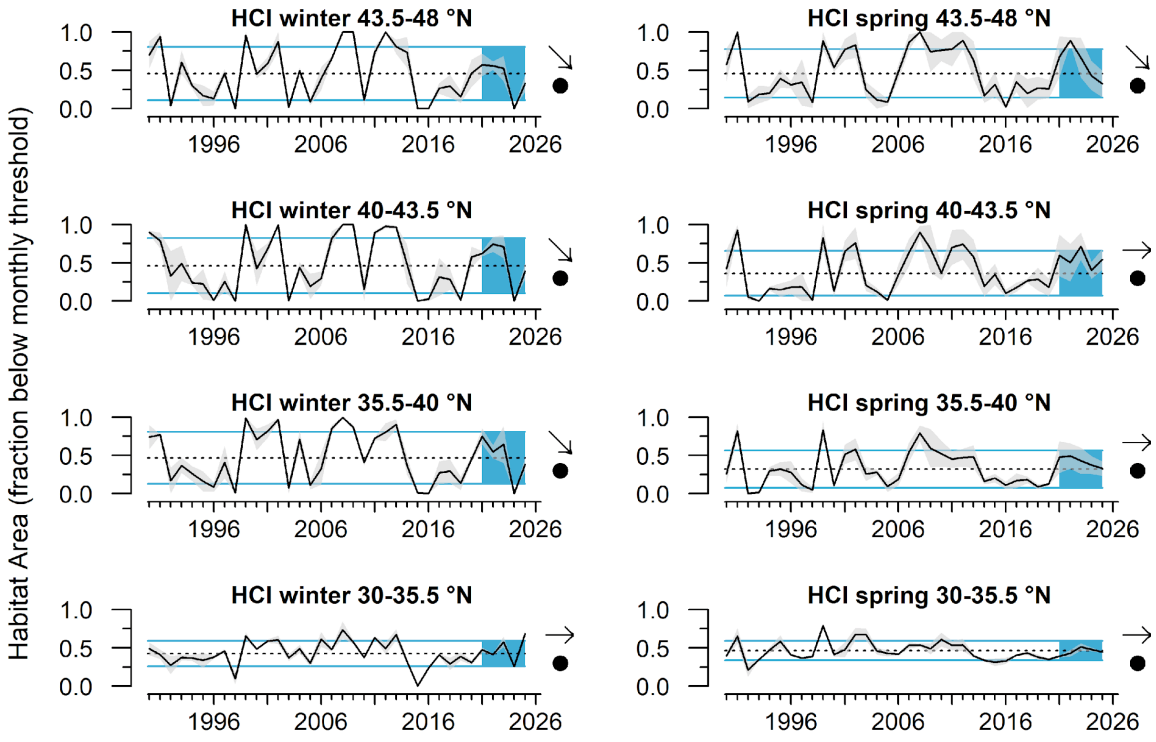


Figure F.9: Mean winter (January - March) and spring (April - June) habitat compression index by region, 1990-2025. Gray envelope indicates ±1 s.e. Data provided by J. Santora, NMFS/SWFSC, and I. Schroeder, NMFS/SWFSC, UCSC. Lines, colors, and symbols are as in Fig. 2.1.

F.4 Seasonal Dissolved Oxygen and Ocean Acidification Indicators

Nearshore dissolved oxygen (DO) depends on many processes, including currents, upwelling, air–sea exchange, and community-level production and respiration in the water column and benthos. DO is required for organismal respiration; low DO can compress

habitat and cause movement, stress or die-offs for sensitive species. Waters with DO levels <1.4 mL/L (~ 2 mg/L, note unit change) are considered to be hypoxic; such conditions may occur on the shelf following the onset of spring upwelling, and continue into the summer and early fall months until the fall transition vertically mixes shelf waters. Upwelling-driven hypoxia occurs because upwelled water from deeper ocean sources tends to be low in DO, and microbial decomposition of organic matter in the summer and fall increases overall system respiration and oxygen consumption, particularly closer to the seafloor (Chan et al. 2008).

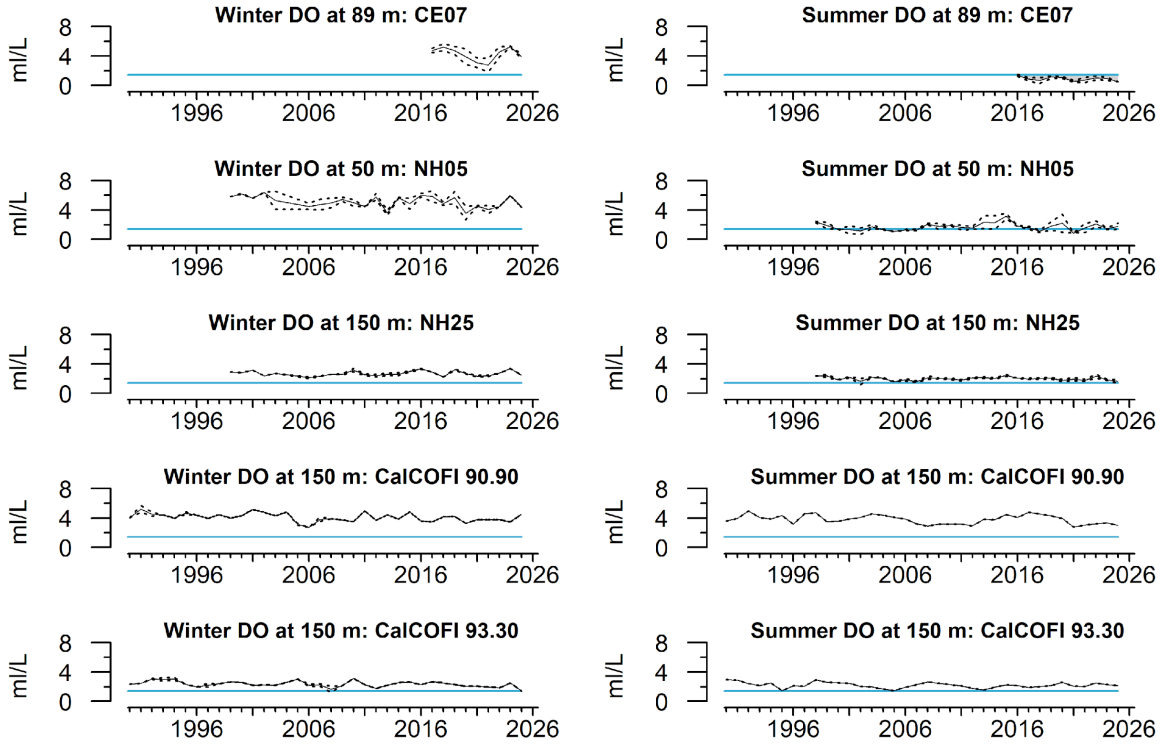


Figure F.10: Dissolved oxygen in winter (January-March) and summer (July-September) off of Washington (CEO7), Oregon (NH), and California (CalCOFI) for 1990-2025. Gray envelope indicates ±1 s.e. Blue line indicates hypoxic threshold.

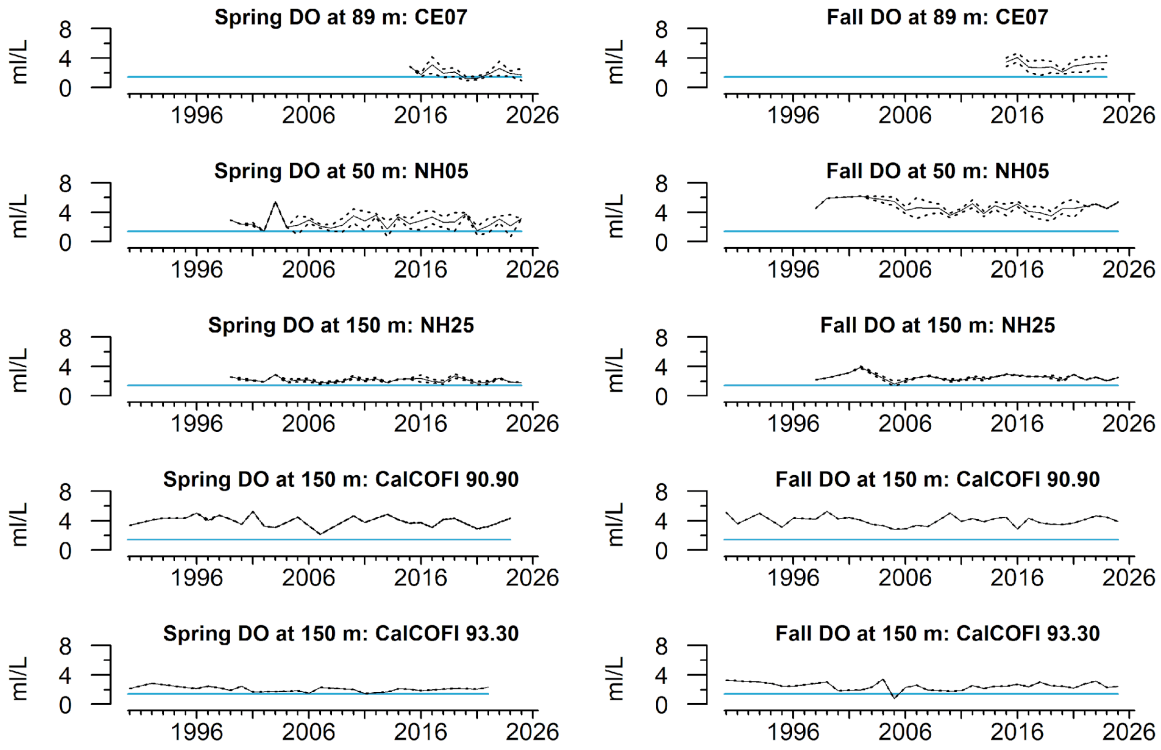


Figure F.11: Dissolved oxygen in spring (April-June) and fall (October-December) off of Washington (CEO7), Oregon (NH), and California (CalCOFI) for 1990-2025. Gray envelope indicates ±1 s.e.

Annually, on the JSOES surveys conducted mid-summer, CTD casts are taken which include measurements of oxygen levels. Figure F.12 shows the June map of oxygen compiled from this survey. This year's oxygen distribution in June supports the higher frequency measurements reported above; most waters off Washington remained above hypoxic levels during the summer, though larger regions off southern Washington and Oregon were hypoxic at the time of the survey.

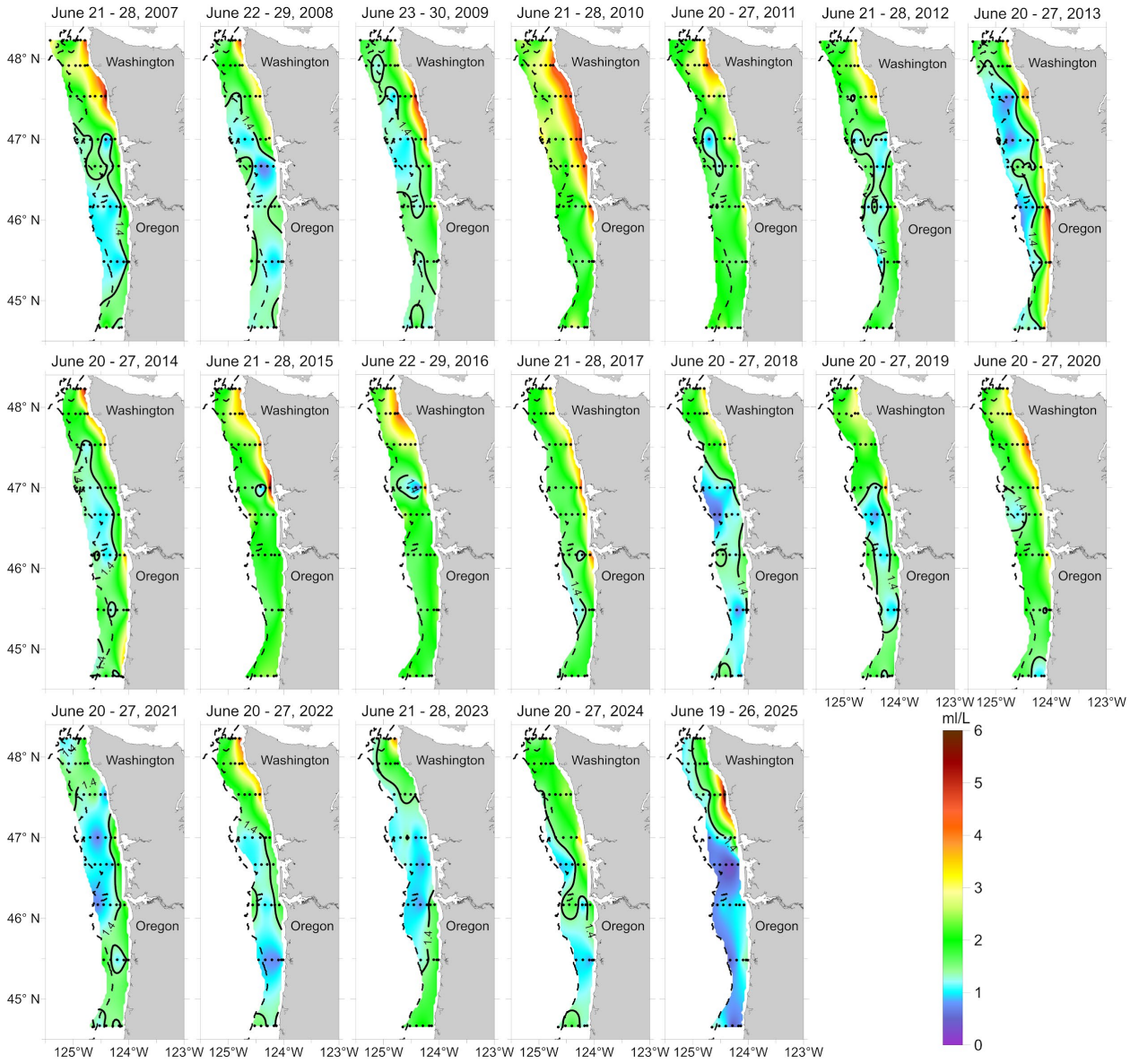


Figure F.12: Near-bottom dissolved oxygen levels (ml/L) collected from CTD casts during the June JSOES survey, 2007-2025. Solid contour represents the 1.4 mL/L hypoxia threshold; dashed contour is the 200 m isobath (shelf break); dots represent data collection locations (stations). Data provided by C. Morgan, OSU/CIMERS.

Ocean acidification (OA), which occurs when atmospheric CO_2 dissolves into seawater, which reduces seawater pH and carbonate ion levels. Upwelling transports low DO, acidified waters from deeper offshore onto the continental shelf, where increased community-level metabolic activity can further exacerbate OA (Feely et al. 2008). A key indicator of OA is aragonite saturation state, a measure related to the concentration of carbonate ions dissolved in seawater that relates to the stability of aragonite (a form of calcium carbonate). Aragonite saturation <1.0 indicates relatively acidified, corrosive

conditions that are stressful for many CCE species, particularly shell-forming invertebrates. OA impacts on these species can propagate through marine food webs and potentially affect fisheries (Marshall et al. 2017). Aragonite saturation states tend to be lowest during spring and summer upwelling, and highest in winter.

Figure F.13 shows time series of winter and summer aragonite saturation from near bottom at stations NH05 and NH25.

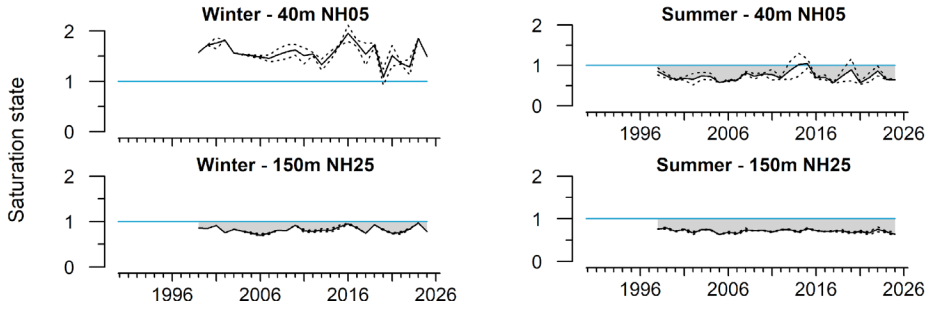


Figure F.13: Winter (Jan-Mar) and summer (Jul-Sep) mean aragonite saturation states at stations NH05 and NH25 off Newport, OR, 1998-2025. The blue line indicates aragonite saturation state = 1.0, below which are corrosive conditions for many shell-forming species. Dotted lines indicate ± 1.0 s.e. Data provided by J. Fisher, NMFS/NWFSC, OSU.

The corrosive water on the shelf at NH05 is largely driven by seasonal upwelling, where upwards of 80% of the water column becomes corrosive each summer (Fig. F.14).

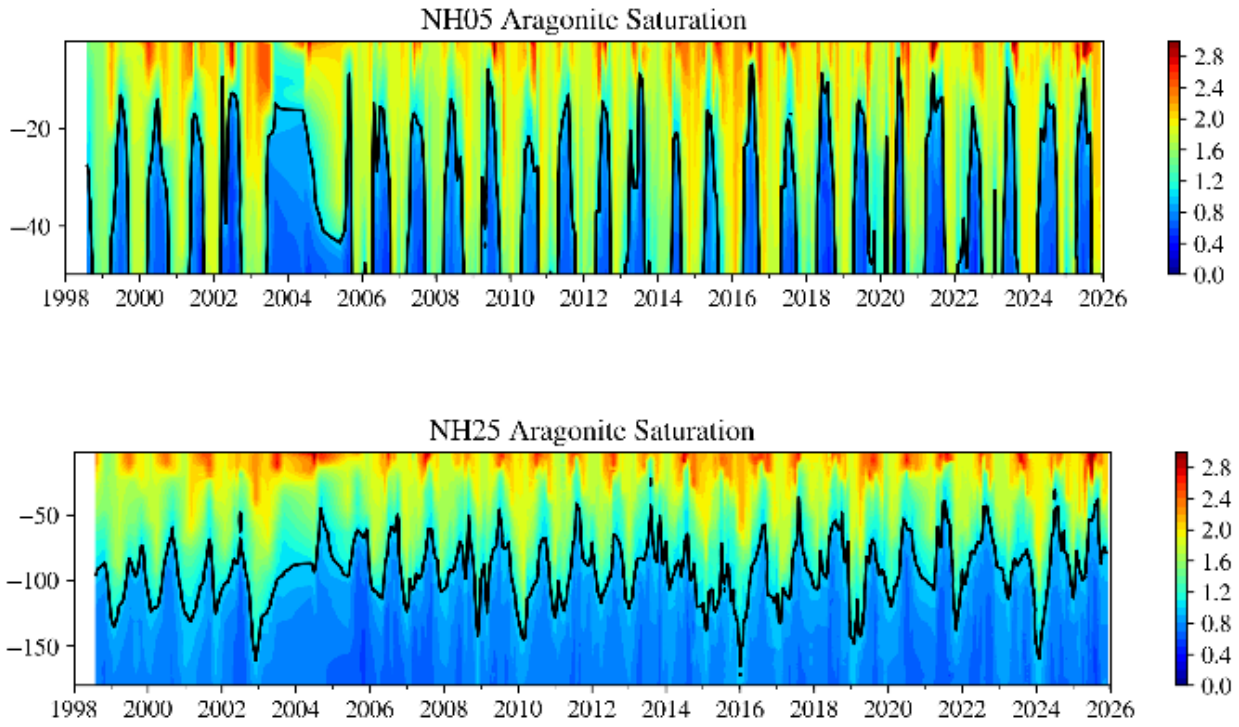


Figure F.14: Aragonite saturation state profiles for stations NH05 and NH25 off Newport, OR. Depths (y-axis) are in m. Black line indicates the depth at which aragonite saturation state = 1.0. Data provided by J. Fisher, NMFS/NWFSC, OSU.

Appendix G — SNOWPACK, STREAMFLOW, AND STREAM TEMPERATURE

Link to main section: Snowpack and Hydrology

Freshwater habitat indicators are reported based on a hierarchical spatial framework. The framework facilitates comparisons of data at the right spatial scale for particular users, whether this be the entire California Current, ecoregions within the CCE, or smaller spatial units. The framework we use divides the region encompassed by the CCE into ecoregions (Fig. 1.1), and ecoregions into smaller physiographic units. Freshwater ecoregions are based on the biogeographic delineations in Abell et al. (2008), see also www.feow.org, who define six ecoregions for watersheds entering the California Current, three of which comprise the two largest watersheds directly entering the California Current (the Columbia and the Sacramento-San Joaquin Rivers). Within ecoregions, we summarized data at scales of evolutionary significant units (ESUs) for Pacific salmonid and 8-field hydrologic unit classifications (HUC-8)(Ford et al. 2025). Years are dated in terms of water years, which occur from Oct. 1 - Sep. 30 and are indexed by the calendar year in which the water year ends. Water years are a standard method to describe annual hydrological cycles because they begin when flows are typically lowest and take place across a full, unbroken cycle of winter snow accumulation and subsequent spring runoff. Status and trends for all freshwater indicators are estimated using space-time models that account for spatial and temporal autocorrelation (Lindgren and Rue 2015)

Snow-water equivalent. Snow-water equivalent (SWE) is measured using data from the California Department of Water Resources snow survey program (California Data Exchange Center, cdec.water.ca.gov) and The Natural Resources Conservation Service's SNOTEL sites across Washington, Oregon, California and Idaho. Snow data are converted into SWEs based on the weight of samples collected at regular intervals using a standardized protocol. Measurements on April 1 are considered the best indicator of maximum extent of SWE; thereafter snow tends to melt rather than accumulate.

The outlook for snowpack in 2026 is limited to cumulative snowpack through January 31, an imperfect predictor of SWE in April. Thus far, SWE in the mountain west has been well below median levels in much of Northern California, Oregon, and parts of Washington (Fig. G.1), except the eastern side of the eastern portion of the Sierras as well as patches in Washington and Idaho. It remains too soon to say whether patterns will change by the end of this winter, although the predicted continued warm weather does not bode well for snowpack throughout the west.

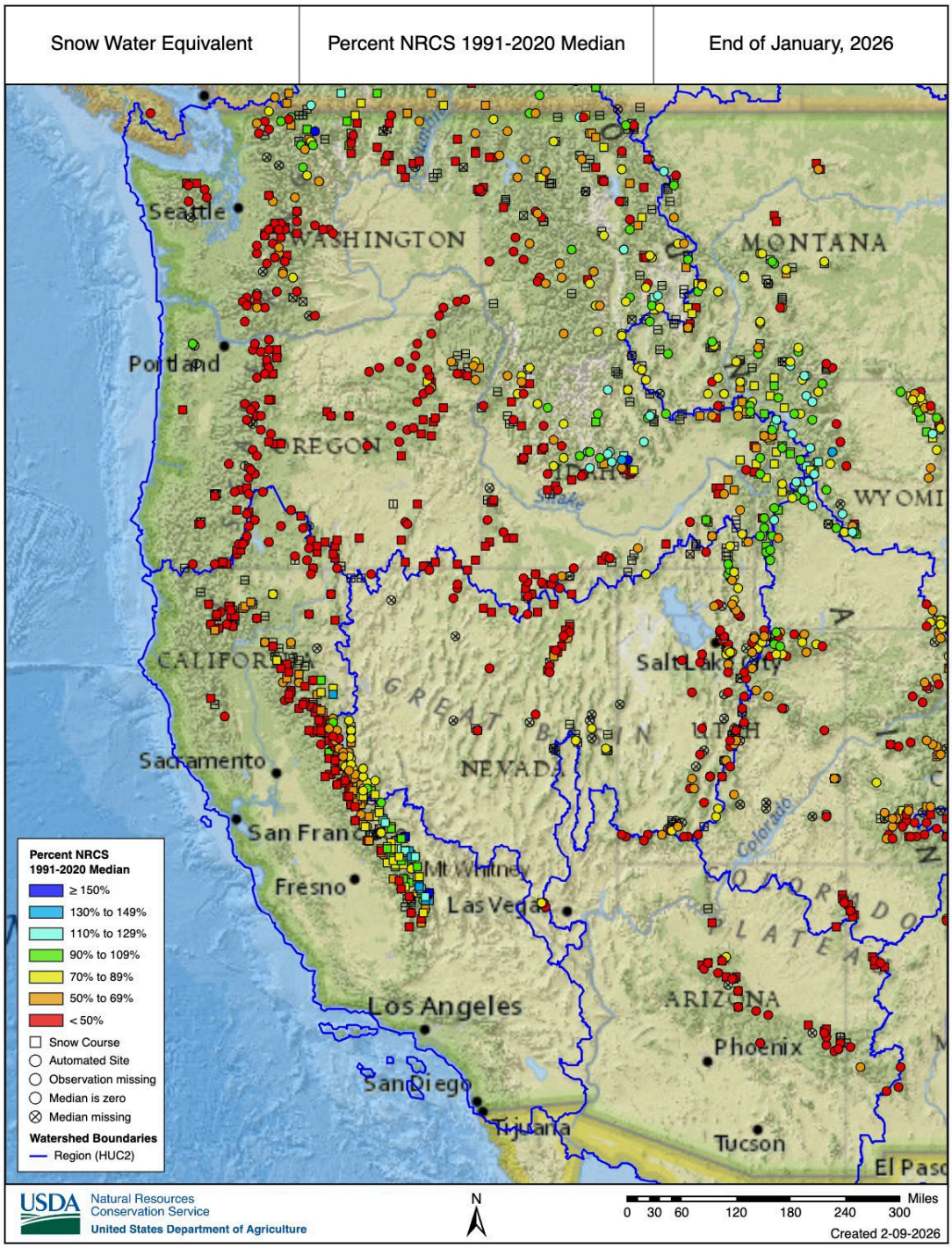


Figure G.1: Snow water equivalent as of January 31, 2026, relative to the 1991-2020 median. Data are from the California Data Exchange Center and the Natural Resource Conservation Service SNOTEL database. Open circles indicate stations that either lack current data or long-term median data.

Stream temperature. Mean maximum stream temperatures in August were determined from 446 USGS gauges with temperature monitoring capability. While these gauges did not necessarily operate simultaneously throughout the period of record, at least two gauges provided data each year in all ecoregions. Stream temperature records are limited in California, so two ecoregions (Sacramento/San Joaquin and Southern California Bight-Baja) were combined. Maximum temperatures exhibit strong ecoregional differences in absolute temperature (for example, Salish Sea and Washington Coast streams are much cooler on average than California streams).

The most recent 5 years have been marked by stream temperatures that have been above generally average across all ecoregions except the southernmost region (Fig. G.2). 2025 water stream temperatures increased from 2024, and were higher than long-term averages in all ecoregions except the southernmost region.

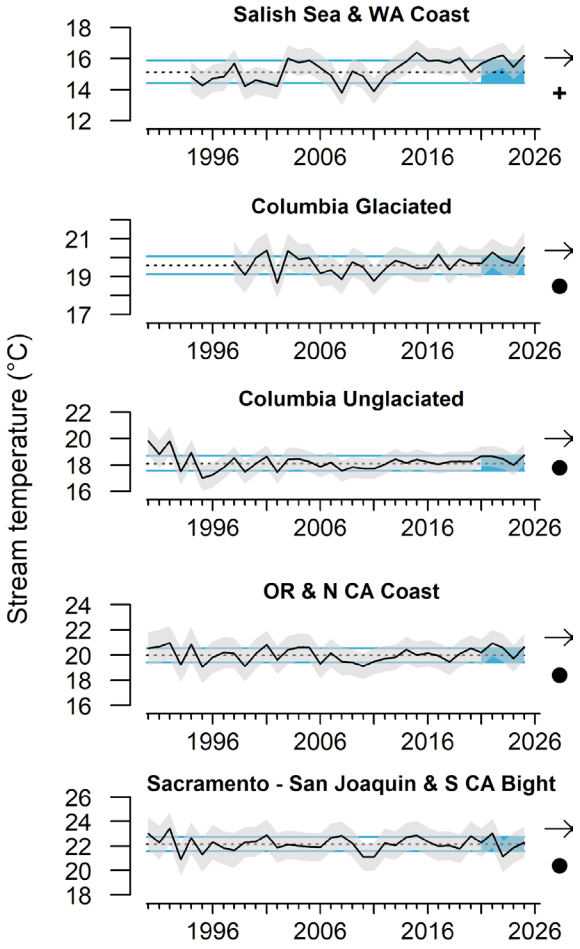


Figure G.2: Mean maximum stream temperatures in August measured at 466 USGS gauges from 1990-2025. gauges include both regulated (subject to hydropower operations) and unregulated systems, although trends are similar when these systems are examined separately. Error envelopes represent 95% credible intervals (CI). Lines, colors and symbols are as in Fig. 2.1.

Minimum and maximum streamflow. Flow is derived from active USGS gauges with records that are of at least 30 years in duration (waterdata.usgs.gov/nwis/sw). Daily means from 213 gauges were used to calculate annual 1-day maximum and 7-day minimum flows (Figs. G.3 & G.4). These indicators correspond to flow parameters to which salmon populations are most sensitive. We use standardized anomalies of streamflow time series from individual gauges.

Minimum stream flows (Fig. G.3) were mixed across ecoregions, with stream flows generally lower than average to the north, and near or slightly above average to the south, generally reflecting snowpack levels from the start of the 2025 water year. The Columbia Glaciated region continued its trend of decreasing minimum flow. Maximum stream flows (Fig. G.4) were also mixed across ecoregions, with maximum stream flows generally lower than average to the north, and near or slightly above average to the south, except for the southern California bight, which was lower than average.

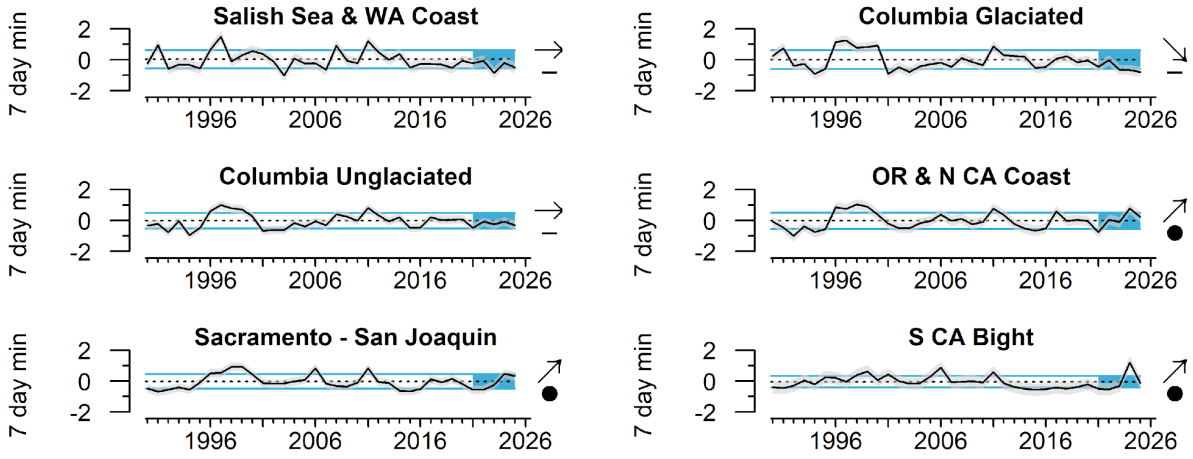


Figure G.3: Anomalies of 7-day minimum streamflow measured at 213 gauges in six ecoregions from 1990-2025. gauges include regulated (subject to hydropower operations) and unregulated systems, though trends are similar when these systems are examined separately. Gray envelopes represent 95% credible intervals. Lines, colors and symbols are as in Fig. 2.1.

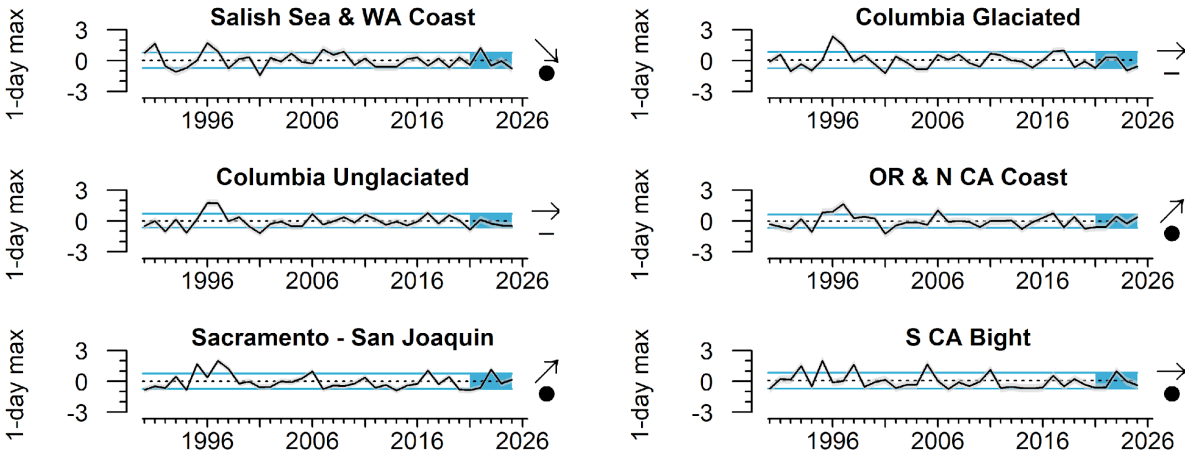


Figure G.4: Anomalies of 1-day maximum streamflow measured at 213 gauges in six ecoregions from 1990-2025. Gauges include both regulated (subject to hydropower operations) and unregulated systems, although trends are similar when these systems are examined separately. Gray envelopes represent 95% credible intervals. Lines, colors and symbols are as in Fig. 2.1.

Appendix H — COASTAL PELAGIC SPECIES DATA FROM SUMMER 2025

Link to main section: Coastal pelagic species

Acoustic-trawl method (ATM) surveys have been used by the NOAA Southwest Fisheries Science Center in most years since 2006 to map the distributions and estimate the abundances of coastal pelagic fish species (CPS) in the coastal region from Cape Flattery, Washington to San Diego, California (e.g., Demer et al. 2012; Zwolinski et al. 2014; Stierhoff et al. 2020). In some years, the surveys were expanded to include portions of Vancouver Island, Canada and Baja California, Mexico (Stierhoff et al. 2023a, b). The surveys cover waters to at least the 1,000-fathom (1829 m) isobath, or 65 km from shore. The five most abundant CPS in this domain are northern anchovy, Pacific herring, Pacific sardine, jack mackerel, and Pacific mackerel. The ATM combines data from echosounders, which record CPS echoes, and trawls, which produce information about the composition, sizes, and ages of the fishes.

The 2025 summer survey was conducted as part of the Integrated West Coast Pelagics Survey aboard NOAA Ship *Bell M. Shimada* with sampling in the core area from San Diego, California to Cape Flattery, Washington between 3 June to 14 September (Stierhoff et al. in press, pp. Fig. H.1). Additionally, two charter fishing vessels, *Lisa Marie* and *Long Beach Carnage,* sampled nearshore (within 5 NM from shore) between San Diego, and Cape Flattery, including around the northern Channel Islands (Fig. H.2).

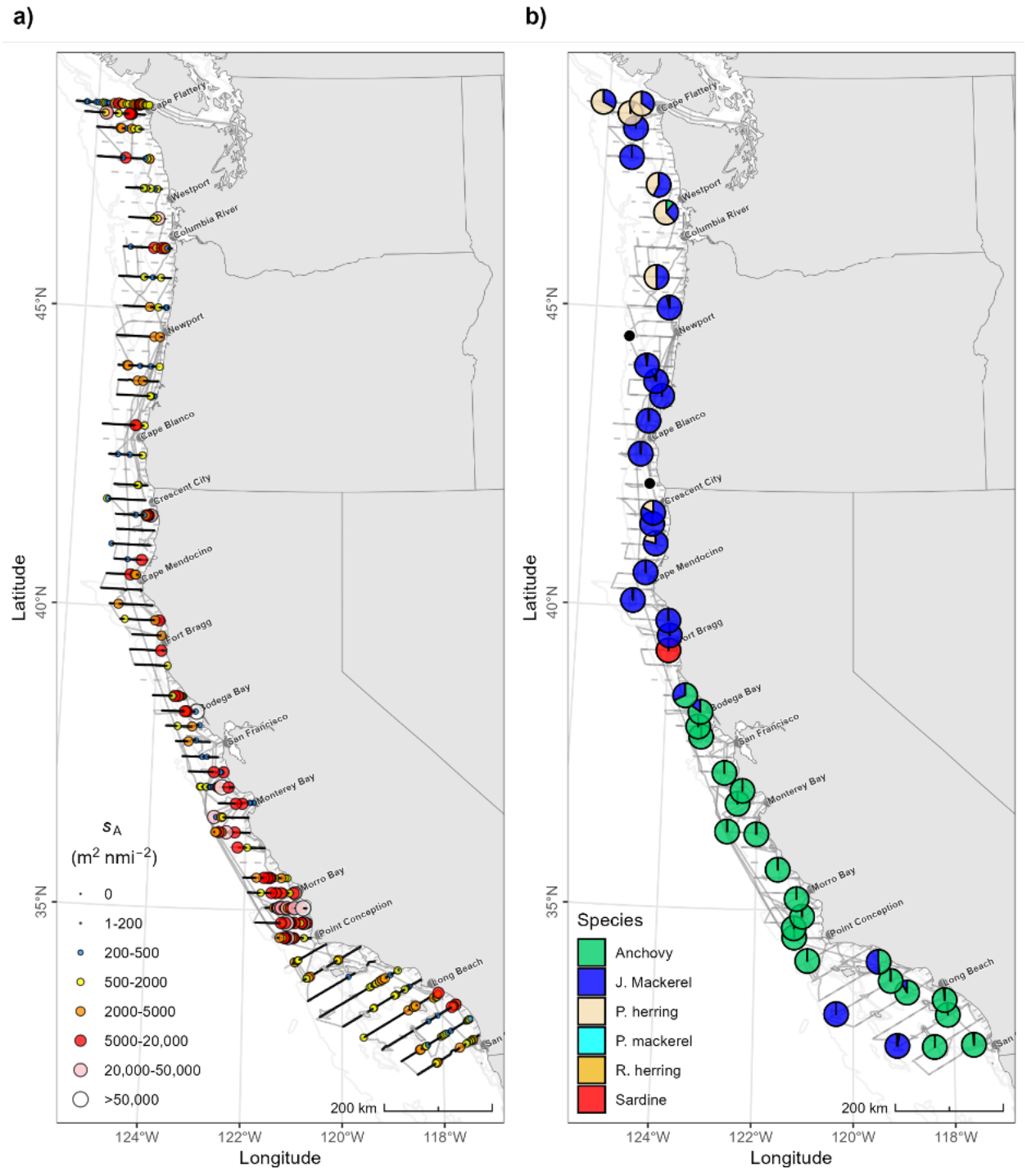


Figure H.1: Data from the 2025 summer CPS survey in the core area as sampled by FSV Shimada, including: a) 38-kHz vertically integrated backscattering coefficients attributed to CPS, and b) the proportions of CPS backscatter based on the nearest nighttime trawl cluster.

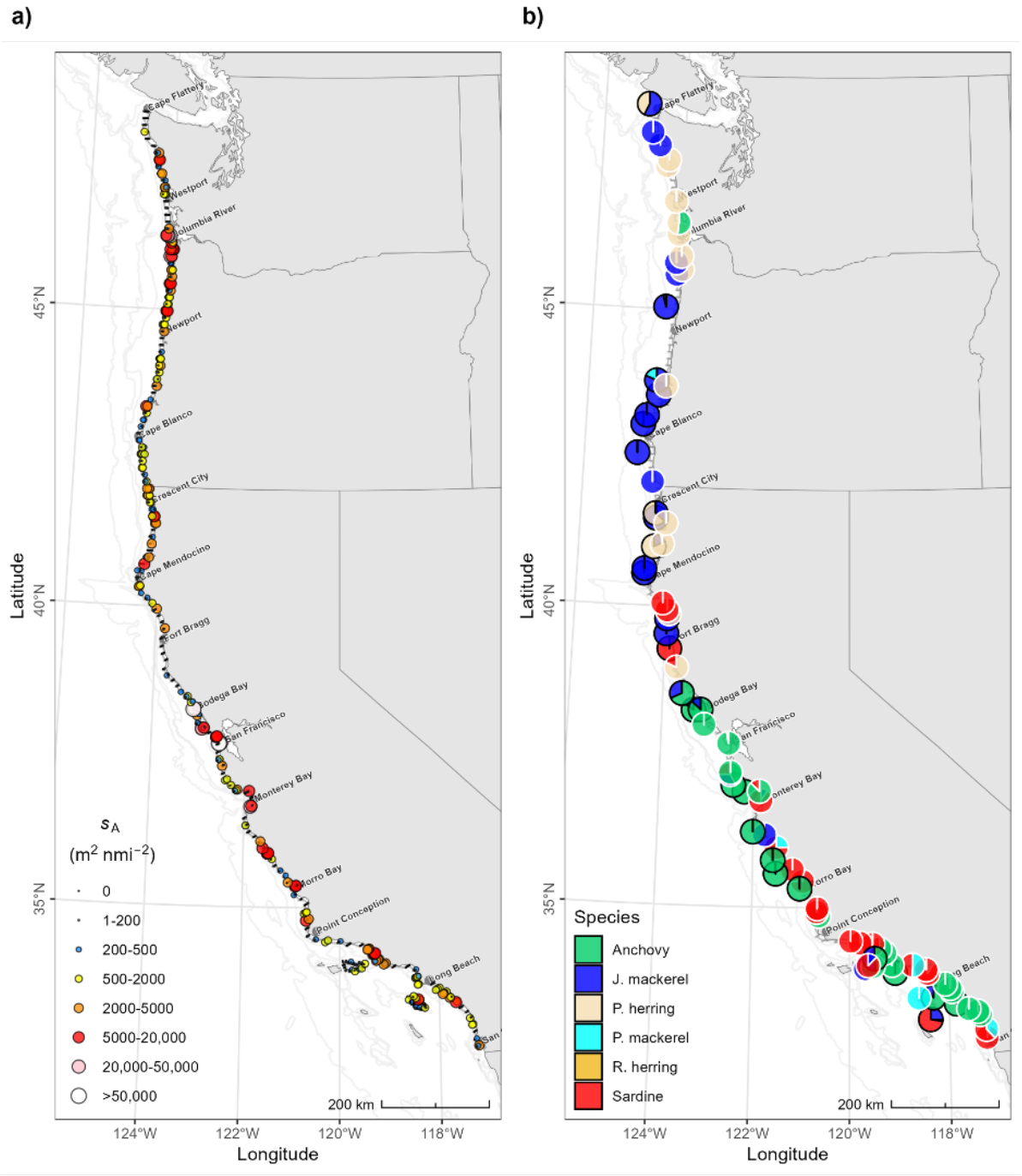


Figure H.2: Data from the 2025 summer CPS survey in the nearshore area as sampled by two fishing vessels, including: a) 38-kHz vertically integrated backscattering coefficients attributed to CPS, and b) the proportion of CPS backscatter based on the nearest purse seine catch (white border) or trawl haul (black border).

Acoustic backscatter from CPS was mapped throughout the core and nearshore survey areas. In the core region, trawl samples were mostly northern anchovy south of Fort Bragg, jack mackerel to the north, and Pacific herring off northern Oregon and Washington (Fig. H.1b). In the nearshore region, purse seine samples showed northern anchovy were prevalent south of Bodega Bay, Pacific sardine south of Monterey Bay and around Fort Bragg, and jack mackerel and Pacific herring north of Fort Bragg (Fig. H.2b).

The survey-estimated summer CPS biomasses were dominated by northern stock Pacific sardine from 2008 until 2013, jack mackerel in 2014 and 2015, and then the central stock of northern anchovy since 2015, when it began to resurge (Fig. H.3). Northern anchovy grew to ~2.75 million t by 2021 (Stierhoff et al. 2023a), but decreased by ~75% to approximately 700,000 t in 2024, similar to estimates from 2018-2019. Meanwhile, the biomass of Pacific mackerel remained the lowest in the assemblage, and the biomass of jack mackerel trended up from 2013 through 2022. Based on observations from the 2025 survey, the CPS assemblage continued to be dominated by the central stock of northern anchovy and jack mackerel, with the biomass of Pacific sardine, Pacific herring, round herring, and Pacific mackerel remaining low (Fig. H.3). Data from 2025 are preliminary (Stierhoff et al. in press) and therefore are not shown in this report.

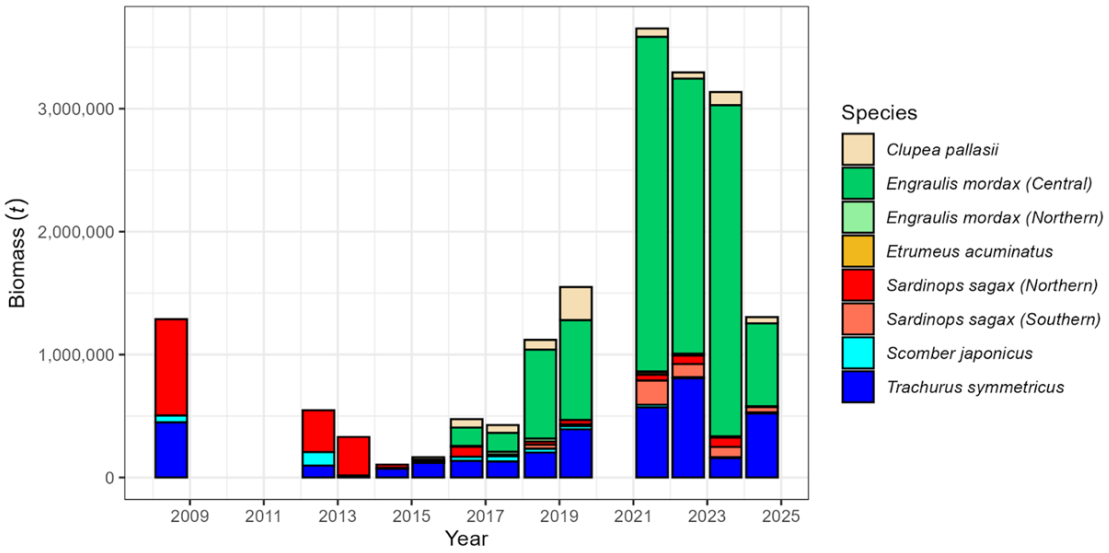


Figure H.3: Cumulative estimated biomass for Pacific herring (Clupea pallasii), northern anchovy (Engraulis mordax; central and northern stock), round herring (Etrumeus acuminatus), Pacific sardine (Sardinops sagax, northern and southern stock), Pacific mackerel (Scomber japonicus), and jack mackerel (Trachurus symmetricus) within the summer CPS survey areas, 2008-2024. Biomass estimates for the 2025 survey are still preliminary and not presented here.

Appendix I — REGIONAL FORAGE AVAILABILITY

Link to main section: Regional Forage Availability

I.1 Northern California Current Forage

The Juvenile Salmon Ocean Ecology Survey (JSOES) occurs in June and targets juvenile salmon in surface waters off Oregon and Washington (Fig. 1.1). It also collects adult and juvenile (age 1+) pelagic forage fishes, market squid, and gelatinous zooplankton with regularity. In 2025, catches of juvenile chum salmon were well over 1 s.d. above the long-term survey mean and set a record for highest catch in the 28-year time series. Juvenile chum also showed a significant five-year trend. Juvenile sockeye salmon catches were close to the long-term mean and had a non-significant five-year trend (Fig. I.1, top). Catches of subyearling Chinook salmon and yearling coho salmon were also over 1 s.d. above the long-term mean and had significant five-year trends (see Fig. 3.6) in the main body of the report).

Among non-salmonids, catches of many species have been dynamic since the values associated with the 2013-2016 marine heatwave (Fig. I.1). Catches of age-0 sablefish remained close to average in 2025, and well below the sharp peak in 2020. Pacific pompano (butterfish), a warmer-water fish whose catches peaked in 2016, were above the time series average in 2025, but only captured on a single transect. Catches of market squid in 2025 were slightly above the time series average. Several other taxa collected by the June JSOES surface trawl are noted in terms of their relative prevalence (proportion of stations where they were caught), but are not considered to be sampled quantitatively due to their behavior and mesh size of sampling gear. The prevalence of YOY rockfishes in the survey was noted as being relatively low in 2025 (data not shown, C. Morgan, pers. comm.).

Among the gelatinous zooplankton off Washington and Oregon, catches of cool-water sea nettles (*Chrysaora fuscescens*) were at their highest levels since 2004, resulting in a significant 5-year trend. Catches of offshore-oriented water jellies (*Aequorea* spp.) were also high in 2025; more than 1 s.d. above the mean for the third consecutive year (Fig. I.1). Catches of egg yolk jellies and moon jellies were slightly above and below average, respectively.

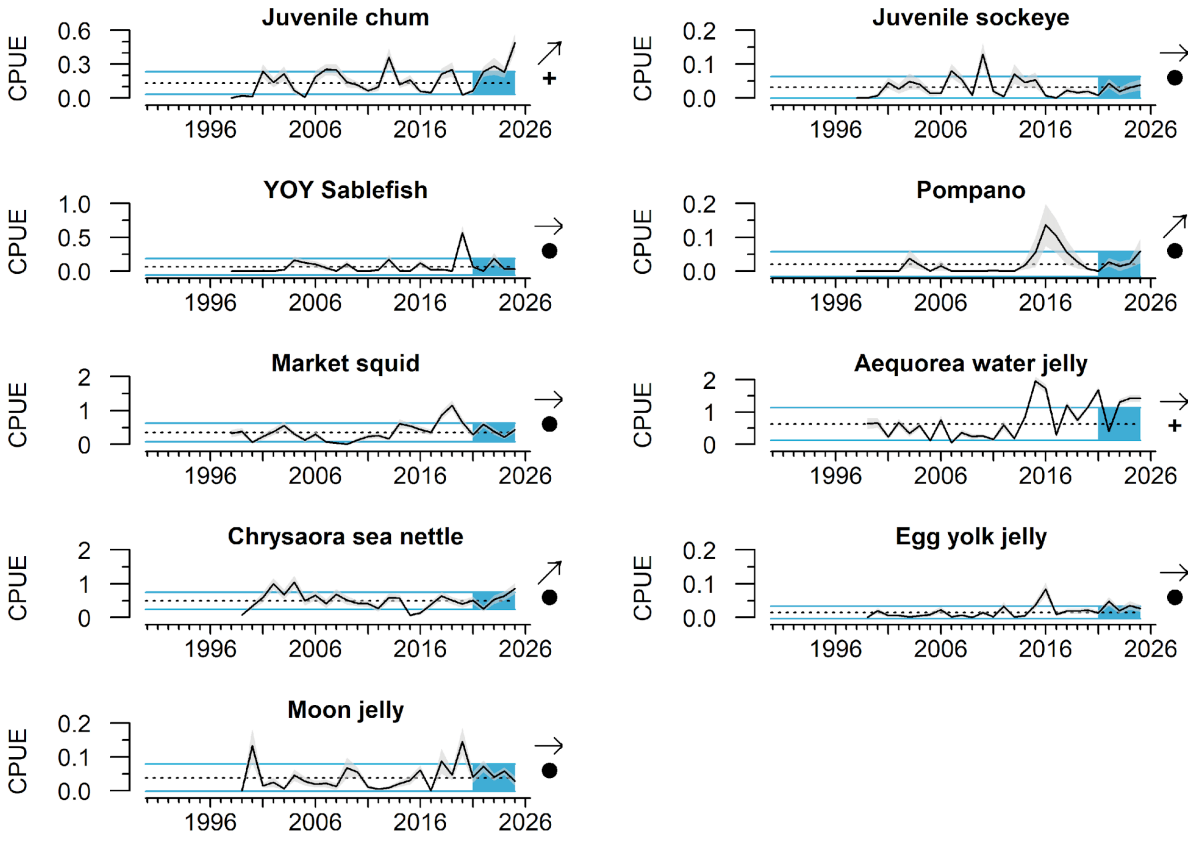


Figure I.1: CPUE (log10(number/km+1)) for pelagic species in the Northern CCE, 1998-2025. Lines, colors, and symbols are as in Fig. 2.1.

The JSOES program also samples off Oregon and southern Washington in May. During this survey a fine-mesh liner is added to the Nordic trawl to directly sample prey of juvenile salmon such as juvenile forage fishes and groundfish, krill, and crab megalopae. Notably, juvenile Pacific sardine have been present in the fine-mesh liner catches in all years from 2016-2025 (no survey in May 2020). The 2024 and 2025 catches had the highest prevalence of juvenile sardine, i.e., present at all sampling locations and high biomass (data not shown, E. Daly, pers comm).

In addition, the NCC Spring Ecosystem Survey, which samples waters north of Cape Mendocino using the same methodology as the survey for the Central CCE (midwater trawls deployed at night; see next section), observed high abundances of YOY sardine and whitebait smelt and moderate abundances of YOY rockfish, krill, and adult Pacific herring (data not shown).

I.2 Central California Current Forage

The Central CCE forage survey (known as the Rockfish Recruitment and Ecosystem Assessment Survey, RREAS) samples much of the West Coast each May to mid-June, using midwater trawls sampling between 30 and 45 m depths during nighttime hours. The survey targets young-of-the-year (YOY) rockfish species and a variety of other YOY and

adult forage species, market squid, adult krill, and gelatinous zooplankton. Juvenile rockfish, anchovy, krill, and market squid are among the most important prey for CCE predators (Szoboszlai et al. 2015). Time series presented here are from the survey area centered off Monterey Bay (Fig. 1.1). Catch data were standardized by using a delta-GLM to estimate year effects while accounting for spatial and temporal covariates to yield relative abundance indices, shown with their approximate 95% confidence limits (Santora et al. 2021). The 2025 survey effort off central California was comparable to previous years apart from 2020, when survey effort was severely constrained.

Standardized anomalies of log-transformed catch indices of key forage taxa in 2025 suggest continued above abundance of adult northern anchovies, while YOY anchovy declined from well above average in 2024 to below the time series average (Fig. I.2). Catches of adult Pacific sardine remained at low abundance levels in the central region after a modest increase in 2023.

The survey observed high abundances of YOY rockfish in 2025 resulting in an increasing five-year trend (Fig. I.2). YOY rockfish catches were at the highest level since the 2015-2016 marine heatwave. Krill abundance increased to slightly above average. Myctophids (lanternfishes) declined to below the long-term average from high levels observed the previous year. Catches of market squid were slightly more abundant in 2025 and near the long-term average, and octopus abundance increased to the highest level since 2016. Similar to the past few years, the cumulative results of these trends indicate a fairly productive ecosystem, with anchovy and juvenile rockfishes continuing to dominate the forage community, a moderate abundance of alternative forage, and very few taxa at low abundance levels.

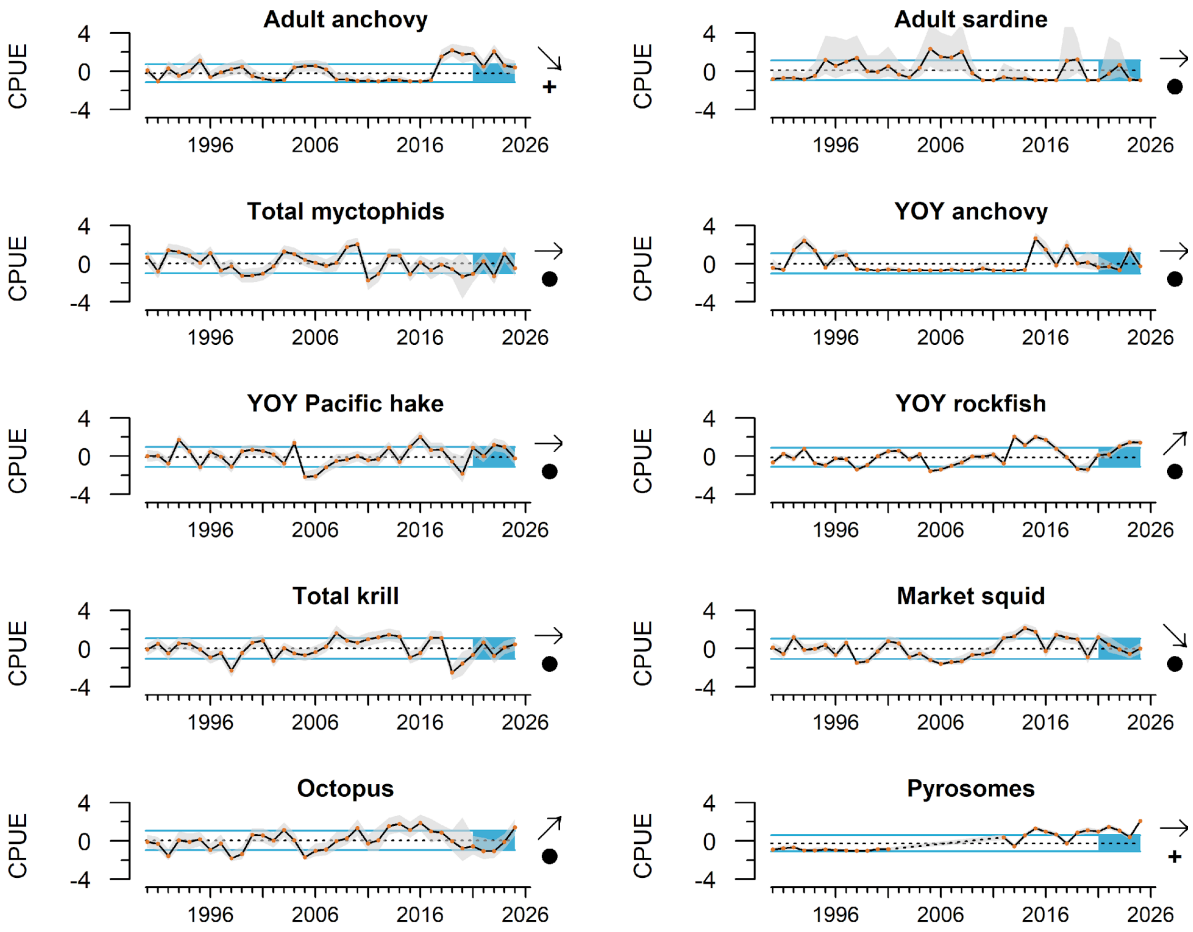


Figure I.2: CPUE (delta-GLM index and 95% CL) anomalies of a subset of key forage groups in the Core Area of the Central CCE, 1990-2025. Lines, colors, and symbols are as in Fig. 2.1.

Catches of pyrosomes (warm-water pelagic tunicates) in the RREAS survey off central California (RREAS Fig. 1.1) were the highest recorded since the start of the time series (Fig. I.2). High abundances of pyrosomes were also observed by the survey in the Southern CCE. Pyrosome catches and salps were considered low in the Northern CCE in 2025 (data not shown, B. Wells, NMFS/SWFSC)

I.3 Southern California Current Forage

Abundance indicators for forage in the Southern CCE in 2025 come from fish and squid larvae collected in the spring (May-June) CalCOFI survey (Fig. 1.1). Larval data are indicators of the relative regional abundances of adult forage fish, such as sardines and anchovy, and other species, including certain groundfish, market squid, and mesopelagic fishes. The survey samples a variety of fish and invertebrate larvae (<5 d old) from several taxonomic and functional groups, collected via oblique vertical tows of fine mesh Bongo nets to 212 m depth. In most years, CalCOFI contributes larval fish data from lines 80 and 90; however, due to staff losses and the federal government furlough in 2025, data was

limited to line 90 in this year's report. In 2020, the spring larval survey was cancelled due to COVID-19, and thus no data are available for that year.

Catches of larval anchovy in spring 2025 remained below the record level in 2022 but were still at a historically high level in 2025 (Fig. I.3). Similarly, larval California smoothtongue (a mesopelagic species) show a strong, downward, short-term trend but their abundance is still well above the time series average. Other species declined compared to the previous year to near average levels (Pacific hake, slender sole, jack mackerel, eared blacksmelt). Market squid paralarvae, which were absent in 2023 and 2024, increased significantly to the second highest abundance in the time series. Catches of larval flatfishes and southern mesopelagic were also high. In contrast, larval rockfishes were well below average in 2025, exhibiting a sharp decline relative to record high levels in recent years. Larval sardines have been low since 2012 and remained low in 2025. Recent trends for most species or species groups were significant.

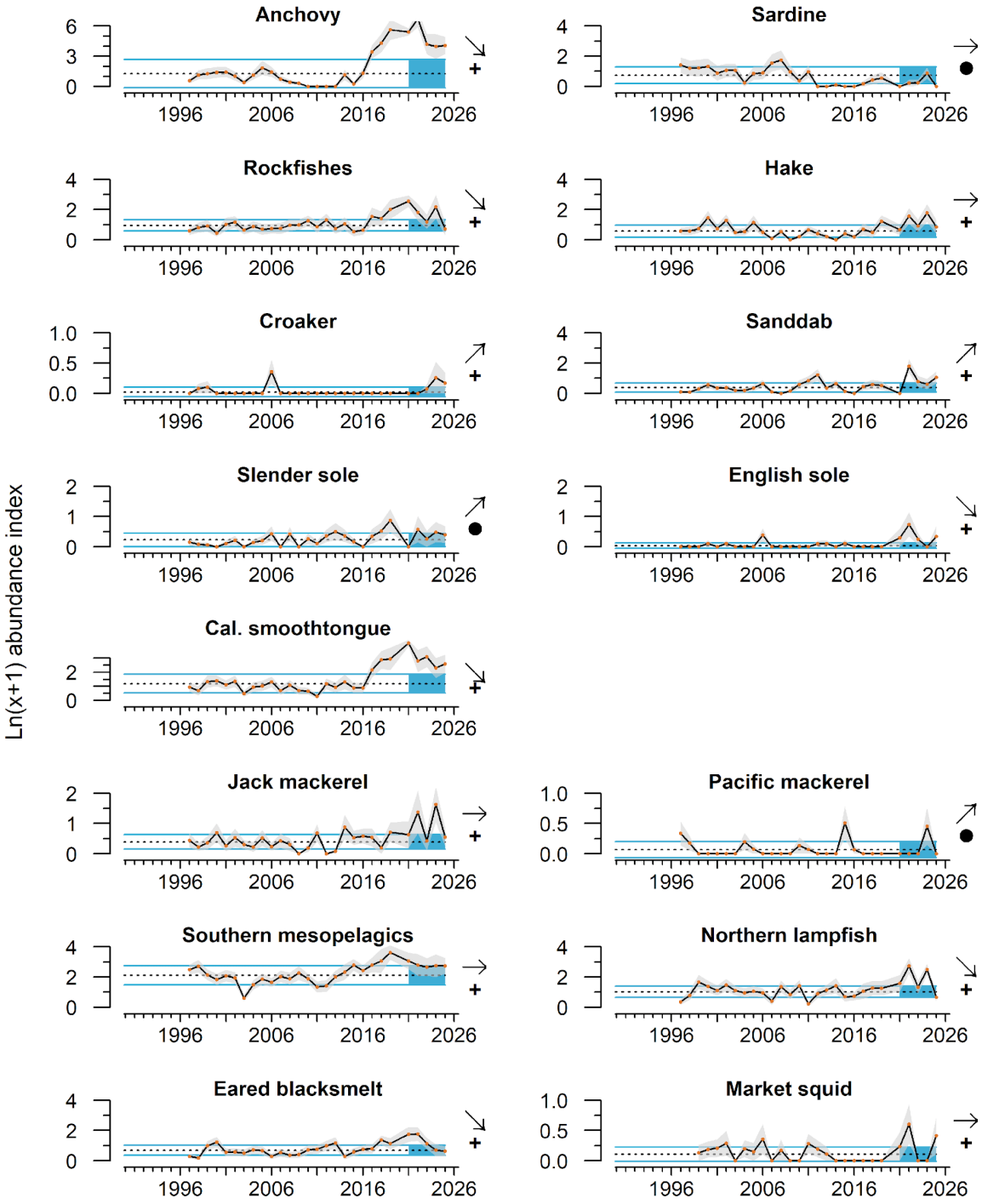


Figure I.3: Mean abundance (ln(x+1)) index of the larvae of key forage species in the Southern CCE, from spring CalCOFI surveys during 1997-2025 (no data from 2020). Lines, colors, and symbols are as in Fig. 2.1.

I.4 Coastwide krill abundance

Krill were detected acoustically during the 2025 West Coast Integrated Pelagics Survey, conducted between June-September 2023 from Point Conception, California to Dixon Entrance, British Columbia. The coastwide nautical area scattering coefficient (NASC), which represents relative krill abundance observed between 50-300 m water depth, indicated krill abundance was highest near the 200 m shelf break in waters off Oregon, Washington, and British Columbia, and lowest south of Cape Mendocino Fig. I.4. Overall krill abundance was higher this year compared to the past two survey years (2023 and 2021) (see Fig. 3.2 in main body of the report).

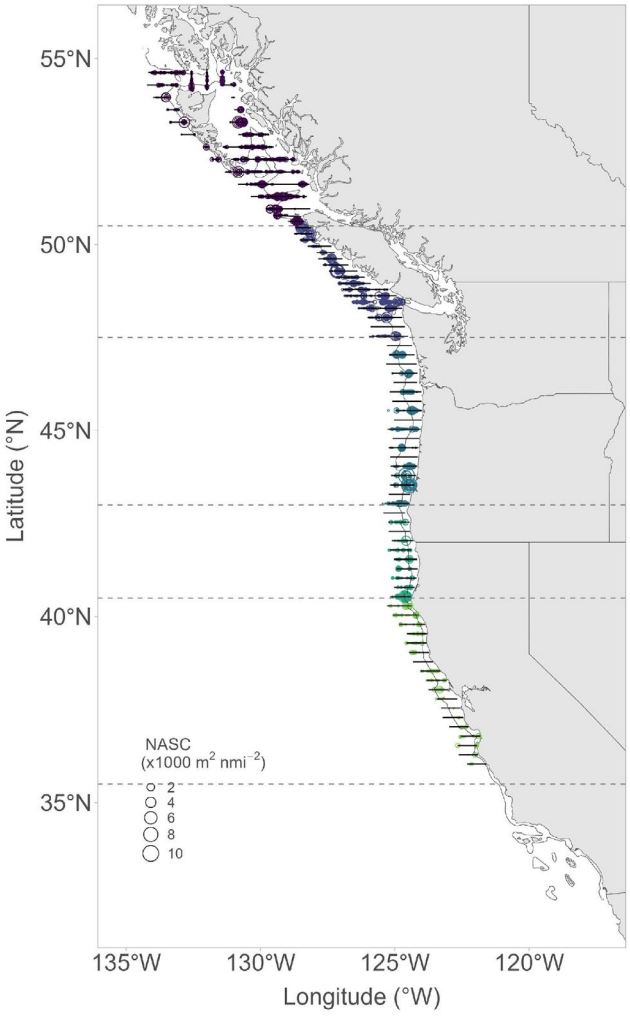


Figure I.4: The relative abundance, or NASC (scaled circles, x1000 m² nmi⁻²), of krill detected acoustically during the 2025 Integrated West Coast Pelagics Survey, conducted between June-September 2025. Black lines represent survey transects.

I.5 Dungeness crab megalopae

Dungeness crab megalopae are a lipid-rich prey source in the CCE. A 25-year time series of total annual catch of megalopae to a light trap fished in Coos Bay, Oregon shows episodic high catches every 4-5 years. Megalope abundance for 2024 and 2025 was low compared to 2023 (Fig. I.5).

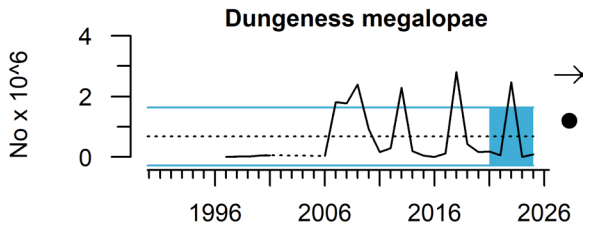


Figure I.5: Time series of total annual catch of megalopae to a light trap fished in Coos Bay, Oregon (43° 20' 41" N, 124° 19' 15" W). The trap was fished from Apr-Sept annually. Samples were collected daily and then summed for the annual catch. Strong El Niño events occurred in 1997 and 2016 when catch was lowest, 1,094 and 3,040, respectively. A gap in sampling occurred between 2001 and 2006.

Appendix J — SALMON

Link to main section: Salmon indicators

J.1 Salmon Stoplight Table Format

For the stoplight tables presented in Figure 3.7 and Figure 3.9, we use color to represent anomalous years. The statistically based format used to develop these tables produces five bins that are determined relative to a fixed baseline reference period (see Harvey et al. 2023). In this format, we assumed a normal distribution for each of the indicators, estimating a mean and standard deviation for the base period. We did this for the years within the base period, and then used the same base period mean and s.d. for the more recent years. For each cell within a given indicator, we determined how many standard deviations the values were from their respective base period mean and used a five-color set to indicate whether a value was >2 s.d. below the mean, within 1 and 2 s.d. below the mean, within 1 s.d. of the mean in either direction, 1 to 2 s.d. above the mean, or >2 s.d. above the mean.

J.2 Ecosystem Indicator-based Outlooks for Chinook Salmon Escapement in the Columbia River Basin

The main body of the report features a stoplight table (Fig. 3.7, see NWFSC salmon stoplight chart for all years) that provides a qualitative, ecosystem-based outlook of returns of adult Columbia Basin Chinook salmon in 2026 and 2027, based on indicators of conditions affecting marine growth and survival of smolts that outmigrated in 2024 and 2025. Two related quantitative analyses use a summary metric of the stoplight table, a new stock-specific metric (Burke et al. 2025), and counts of adult salmon returns to Bonneville Dam.

In these analyses, models are fit to past adult-return data and use the most recent ecosystem indicator data to predict what returns will be for cohorts that have gone to sea but not yet returned. Both models are founded on linear regressions of single ecosystem indicators versus counts of adult fish at Bonneville Dam (Fig. J.1, black points), though this approach can easily be applied to measures of salmon survival rather than adult counts. The first model uses a Dynamic Linear Model with the first principal component (PC1) from a Principal Component Analysis of the stoplight table as a covariate. The data used in this "Stoplight PC1 model" is therefore limited to years included in the stoplight table (1998-2025). The second model is a simple linear regression using a Covariance Map Index Sea Surface Temperature (CMISST, Burke et al. 2025), which is a metric derived by calculating the similarity of SST spatial patterns in the North Pacific Ocean to a stock-specific nominal pattern. Because SST data are available for a longer period, this "CMISST" model uses data starting in 1980 and continuing through 2025.

For smolts that went to sea in 2024 (which should dominate adult returns in 2026), the count estimates are mostly near averages for the past ten years (Fig. 3.8, Fig. J.1, Fig. J.2). For smolts that went to sea in 2025 (most of which will return in 2027), the Stoplight models consistently suggested higher adult returns than for those that went to sea in 2024

(Fig. 3.8, Fig. J.1). This is not too surprising as the mean rank of indicators in the stoplight table was 16.2 for 2024 and 11.5 for 2025 (NWFSC Ocean Conditions Indicators Trend; higher rank suggests poorer ocean survival). The CMISST models also indicate higher returns for spring Chinook salmon in 2027 relative to 2026, but slightly lower returns for fall Chinook salmon and steelhead in 2027 (Fig. J.2). Uncertainty in the Stoplight and CMISST model estimates (95% prediction intervals, colored vertical ribbons) is relatively high, particularly for fall Chinook salmon.

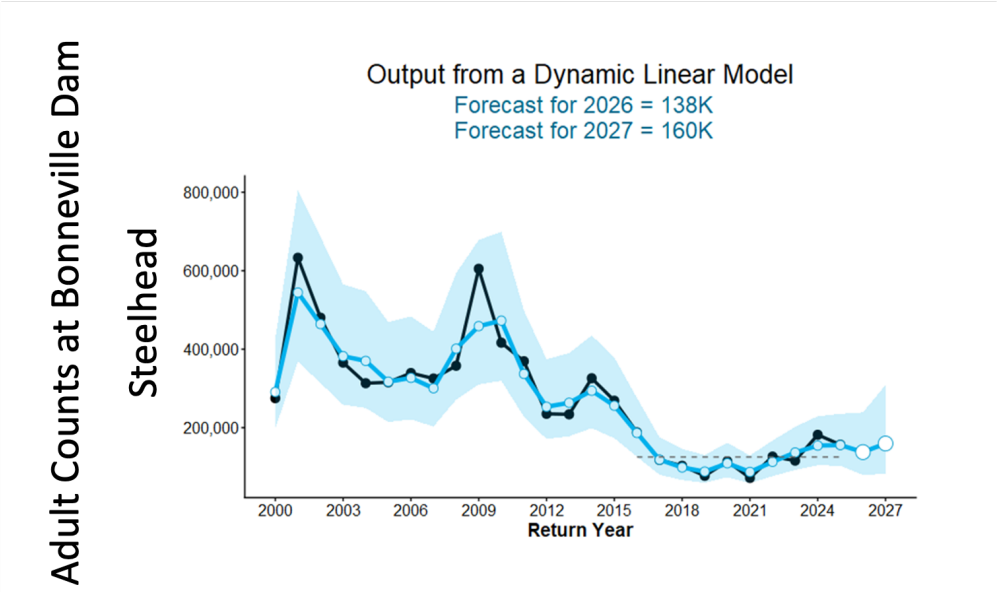


Figure J.1: Observed and modeled adult steelhead counts at Bonneville Dam. Outlooks for adult steelhead returning to the Columbia Basin in 2026 and 2027 are based on the Stoplight model. Years on the x-axes are adult return years (covariate data were lagged by 2 years before running models). Blue lines are model fits; shaded areas are 95% confidence intervals (or prediction intervals for 2026 and 2027). Gray dashed lines are the recent 10-year average.

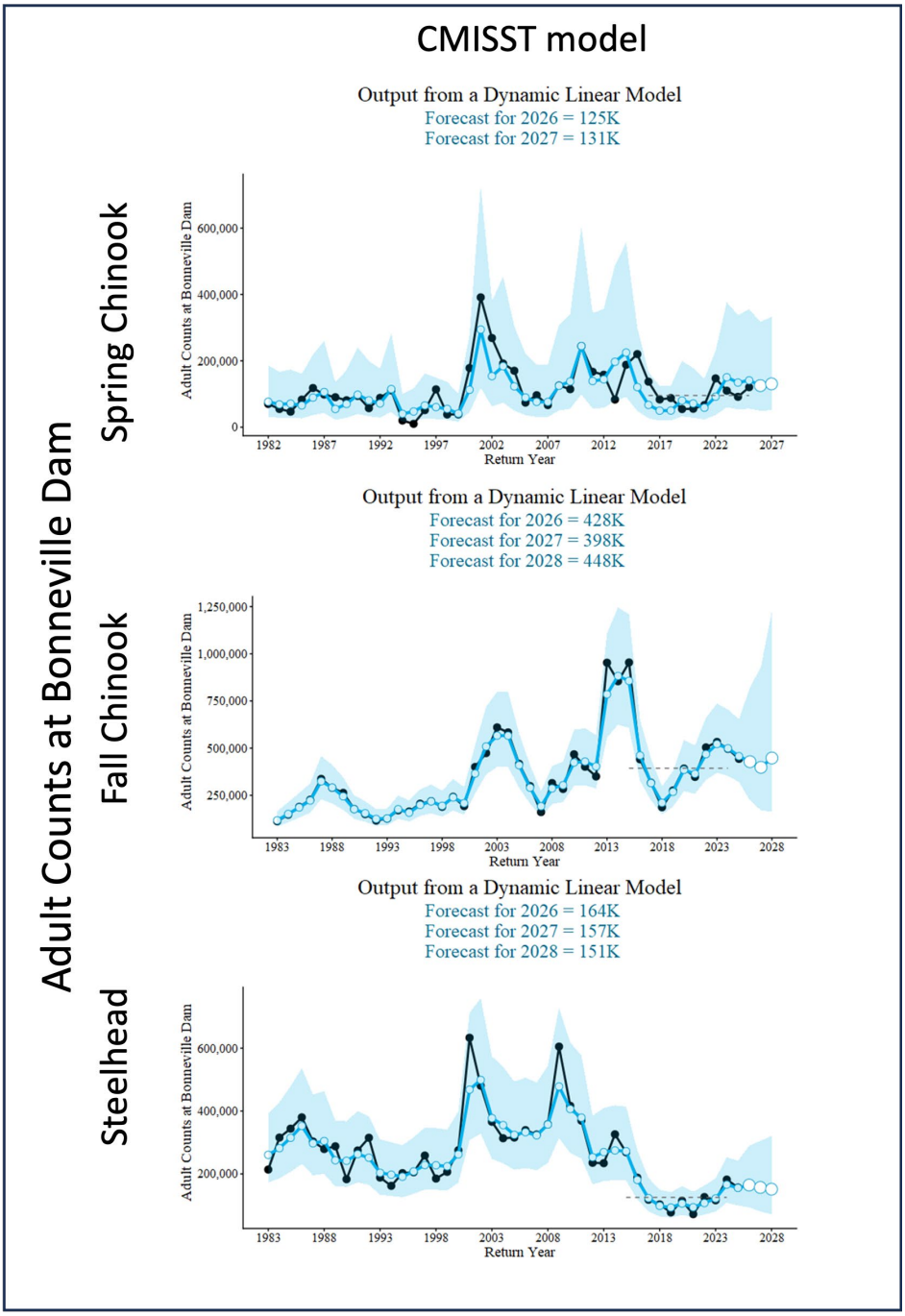


Figure J.2: Observed and modeled adult salmon counts at Bonneville Dam (black lines) for spring Chinook salmon (top row), fall Chinook salmon (middle row), and steelhead (bottom row). Outlooks for adult salmon returning to the Columbia Basin in 2026-2028 are based on the CMISST models. Years on the x-axes are adult return years (covariate data were lagged by 2 years before running models). Blue lines are model fits; shaded areas are 95% confidence intervals (or prediction intervals for 2026, 2027, and 2028). Gray dashed lines are the recent 10-year average.

Although Figure 3.7 represents a general description of ocean conditions related to multiple populations, we acknowledge that the importance of any particular indicator will vary among salmon species and runs. These analyses represent progress toward greater distinction among different Salmon Evolutionary Significant Units (ESUs) than some results shared in previous ecosystem status reports. NOAA scientists and partners continue to refine stock-specific salmon outlooks such as the CMISST approach by using both correlative and mechanistic methods that can identify and optimally weight the indicators for each response variable in which we are interested. We will continue to work with the Council and advisory bodies to identify data sets for Council-relevant stocks for which analyses like these could be possible.

J.3 Ecosystem Conditions for Chinook Salmon in California

Rebuilding plans in 2019 for Sacramento River (SRFC) and Klamath River fall Chinook salmon runs (KRFC) prompted annual updates of habitat indicators for these two stocks (see Harvey et al. 2021), which have been expanded to include Central Valley Spring-run Chinook salmon (CVSC) to inform risk assessment for this poorly assessed stock. These putative indicators ranged across the salmon life cycle and include factors relevant to adult spawning, incubation and emergence, freshwater/delta residence, and early marine residence phases, as well as hatchery influences (see Leising et al. 2024).

Overall, habitat conditions for the SRFC, CVSC, and KRFC have improved marginally in recent years (Section 3.3.1, Fig. 3.9). However, these recent improvements have happened within an overarching decline in ecosystem conditions for these salmon stocks. Since the mid-1980s, key indicator states have generally worsened over time, with some variation among years. Much of this pattern was driven by a rise in incubation, outmigration, and sea surface temperatures as well as recent droughts and a long-term decline in Sacramento River natural area spawners. Indeed, physical habitat conditions were especially poor for year classes that outmigrated in 2015 and 2016 (and returned predominantly in 2017 and 2018), and below average states have generally become more frequent thereafter. Different from other indicator patterns, marine predation during the early marine phase was especially severe for SRFC juveniles that outmigrated in 2005-2007 (and returned predominantly in 2007-2009), but has been relatively stable across other periods.

Indicators presented in Figure 3.9, along with candidate indicators considered but not presented, are described in more detail in Table J.1 below and in a forthcoming peer-reviewed publication led by Stu Munsch and colleagues (Munsch et al. In Review). The authors examined support for candidate models of recruitment across many permutations of indicator variables and time windows, then selected indicators that were persistently, increasingly, and recently important to generate recruitment outlooks.

Egg thiamine concentrations for the three stocks are not included in the stoplight chart this year. However, we note that thiamine concentrations were at low enough levels to have likely negatively impacted offspring from Central Valley Chinook salmon in brood years 2021-2024. In contrast, egg thiamine concentrations for Klamath River Fall Chinook for brood years 2021-2024 were high enough that offspring in those years were not likely

impacted by thiamine deficiency. See Mantua et al. (2025) for more information about the impacts of thiamine deficiency on California salmon stocks.

Table J.1: Definitions of candidate habitat and recruitment indicators, and data sources, for three salmon stocks: Sacramento River Fall Chinook (SRFC), Central Valley Spring-run Chinook (CVSC), and Klamath River Fall Chinook (KRFC). Bold text shows indicators with persistent importance included in Figure 3.9. Abbreviations: i: incubation, o: outmigration.

Stock	Indicator	Abbr	Definition	Source	Reference
All	North Pacific Gyre Oscillation	NPGO	Mean Mar-May value	CCIEA (2025)	Di Lorenzo et al. (2008)
	North Pacific High	NPH	Mean Jan-Mar value	CCIEA (2025)	Wells et al. (2016)
	Sea surface temperature across the NE Pacific arc	SSTarc	Mean Mar-May value	Jim Johnstone (pers com)	Wells et al. (2008), Johnstone and Mantua (2014)
SRFC	Recruitment	Recruitment	Sacramento index	PFMC (2024B)	OFarrell et al. (2013)
	Adult upriver migration flow	Flow (u)	10th percentile of 7 day mean flow from Sep-Oct at Colusa.	USGS gage 11389500 (Colusa)	Strange (2012)
	Adult upriver migration cross channel status	Cross ch (u)	Proportion of days when Delta Cross Channel was closed during Sep-Oct	USBR (2025)	PFMC (2019)
	Adult upriver migration water temp	Temp (u)	Mean max water temp from Sep-Oct at Freeport	USGS gage 11447650 (Freeport)	FitzGerald et al. (2021)
	Natural area spawners	N spawn	Adult (not jack) fall run returns to Sacramento River natural areas (not hatcheries)	PFMC (2025B) Appendix B Table B1	Friedman et al. (2019)
	Egg freshwater survival	FW surv	Egg-fry productivity	CDFW	
	Egg incubation flow	Flow (i)	Mean of z-scored 10th percentile 7 day mean flows from Oct-Dec across Oroville, Fair Oakes, Marysville, Upper Sacramento, Battle Creek, Mill Creek, Clear Creek, and Cottonwood Creek	USGS gages 11407000 (Oroville), 11446500 (Fair Oaks), 11421000 (Marysville), 11370500 (Upper Sacramento), 11376550 (Battle Creek), 11381500 (Mill Creek), 11372000 (Clear Creek), and 11376000	Jager et al. (1997)

Stock	Indicator	Abbr	Definition	Source	Reference
				(Cottonwood Creek)	
	Egg incubation temperature	Temp (i)	Mean Oct-Dec water temp at Red Bluff Diversion Dam. Until 2001, values from corrected model predictions. After 2001, values were summarized from empirical observations.	Friedman et al. (2019) until 2001, CDEC sensor RDB (Red Bluff Diversion Dam) thereafter.	Friedman et al. (2019), Martin et al. (2017)
	Juvenile outmigration flow	Flow (o)	Mean Feb-Jun flow at Colusa	USGS gage 11389500 (Colusa)	Friedman et al. (2019)
	Juvenile outmigration temperature	Temp (o)	Mean May-Jun air temp	NOAA NCEI (Sacramento Basin)	Munsch et al. (2022)
	Hatchery release number	Rel	Sum of fall run juvenile releases from Sacramento River hatcheries	Huber and Carlson (2015) & RMIS (2025)	Sturrock et al. (2019)
	Freshwater timing	FW tim	Count-weighted mean annual release day of year of fall run juveniles from Sacramento River hatcheries minus the Jan-Jun peak flow day of year on the Sacramento River at Colusa.	USGS gage 11389500 (Colusa), Huber and Carlson (2015), RMIS (2025) & CCIEA (2025)	Sykes et al. (2009), Adase et al. (2025), Burford et al. (2025)
	Marine timing	Mar tim	Count-weighted mean annual release day of year of fall run juveniles from Sacramento River hatcheries minus the spring transition day of year at 39 N	Huber and Carlson (2015), RMIS (2025) & CCIEA (2025)	Wells et al. (2008), Satterthwaite et al. (2014)
	Marine predation index	Pred	Before 2017: Total salmon biomass in diets of common murres. Thereafter: annual predicted values from a linear model that related this metric to alternative prey abundances	Murre surveys prior to 2017, then SWFSC Rockfish Survey & RMIS (2025)	Friedman et al. (2019)
KRFC	Recruitment	Recruitment	Postseason age-3 ocean abundance estimate	PFMC (2024B)	Chen et al. (2024)
	Adult upriver migration flow	Flow (u)	10th percentile of 7 day mean flow from Sep-Oct at Iron Gate	USGS gage 11516530 (Iron Gate)	Strange (2012)
	Adult upriver migration temp	Temp (u)	Mean max water temp from Sep-Oct at Seiad Valley	USFWS logger KRSV1	FitzGerald et al. (2021)
	Natural area spawners	N spawn	Adult (not jack) escapement to Klamath and Trinity River natural areas (not hatcheries)	PFMC (2025B) Appendix B Table B4	Friedman et al. (2019)
	Egg freshwater survival	FW surv	Egg-fry productivity	CDFW	

Stock	Indicator	Abbr	Definition	Source	Reference
	Egg incubation flow	Flow (i)	Mean of z-scored 10th percentile 7 day mean flows from Nov-Jan across Iron Gate, Scott, Shasta, and Trinity-Lewiston	USGS gage 11516530 (Iron Gate), 11519500 (Scott), 11517500 (Shasta), 11525500 (Trinity-Lewiston)	Jager et al. (1997)
	Egg incubation temp	Temp (i)	Mean max water temp from Nov-Jan at Klamath	USGS gage 11530500 (Klamath)	Friedman et al. (2019), Martin et al. (2017)
	Juvenile outmigration flow	Flow (o)	Mean Feb-Jun flow at Klamath	USGS gage 11530500 (Klamath)	Friedman et al. (2019)
	Juvenile outmigration temp	Temp (o)	Mean May-Jun daily max. air temp	NOAA NCEI (Medford, OR, station USW00024225)	Munsch et al. (2022)
	Krill length	Krill	Average size weighted by abundance of E. pacifica in Mar-Sep	Roxanne Robertson pers. comm.	Robertson and Bjorkstedt (2020)
CVSC	Recruitment	Recruitment	Total CVSC escapement to hatcheries and in-river areas	Azat (2025)	
	Adult upriver migration flow	Flow (u)	From hourly data, calculate mean daily flow in Butte Creek. Then, return mean daily flow in Butte Creek across Jun-Sep	CDEC sensor BCK (Butte Creek)	USFWS (1995)
	Adult upriver migration temp	Temp (u)	From hourly data, calculate mean daily temp in Butte Creek. Then, return the proportion of days above 19.4 C across Jun-Sep.	CDEC sensor BCK (Butte Creek)	USFWS (1995)
	Natural area spawners	N spawn	Spring Run returns to Central Valley natural areas (not hatcheries)	Azat (2025)	Friedman et al. (2019)
	Egg freshwater survival	FW surv	Number of outmigrants per spawner in Butte Creek	CDFW	
	Egg incubation flow	Flow (i)	From hourly data, calculate mean daily flow in Butte Creek. Then, return the 10th percentile of 7-day flow means across Sep-Dec.	CDEC sensor BCK (Butte Creek)	Jager et al. (1997)
	Egg incubation temp	Temp (i)	From hourly data, calculate mean daily temp in Butte Creek. Mean Sep-Dec water temp at Butte Creek	CDEC sensor BCK (Butte Creek)	Friedman et al. (2019), Martin et al. (2017)
	Juvenile outmigration flow	Flow (o)	Mean Feb-Jun flow at Colusa	USGS gage 11389500 (Colusa)	Friedman et al. (2019)

Stock	Indicator	Abbr	Definition	Source	Reference
	Juvenile outmigration temp	Temp (o)	Mean May-Jun air temp	NOAA NCEI (Sacramento Basin)	Munsch et al. (2022)
	Marine predation index	Pred	Before 2017: Total salmon biomass in diets of common murres. Thereafter: annual predicted values from a linear model that related this metric to alternative prey abundances	Murre surveys prior to 2017, then SWFSC Rockfish Survey & RMIS (2025)	Friedman et al. (2019)

Appendix K — GROUNDFISH

Link to main section: Groundfish

Prior groundfish appendices included analyses of trends in juvenile abundance (an indicator of recruitment for some species) and variability in the distribution of both juveniles and adults with a focus on availability to ports. U.S. West Coast Groundfish Bottom Trawl Survey (WCGBTS) data from 2025 were not available in time for this report. This year we provide additional information on groundfish stock status presented in the main report (Section 3.4.1, Section K.1) and highlight a new interactive application that serves as a coastwide synopsis for groundfish data in the northeast Pacific Ocean. We have also taken the opportunity to trial new analyses including potential indicators of recruitment of rockfishes from dive surveys on the Washington coast (Section K.2), trends in the abundance and diversity of groundfish larvae and pelagic YOY coastwide (Section K.3), and abundance trends for Ecosystem Component groundfish species from the WCGBTS (Section K.4). Sections K.2 and K.3 provide further evidence that production of YOY rockfish and other groundfish was high in the central and northern CCE in 2025.

K.1 Status of groundfish biomass and fishing pressure

Most groundfish stock biomasses are above biomass limit reference points (LRPs; Fig. 3.10, x-axis), with only one since 2021, copper rockfish in southern California, estimated to be below its LRP. The full assessment of quillback rockfish in California has updated the previously overfished stock status to being a stock above the biomass target. For management purposes, the southern California substock of copper rockfish was combined with the northern California substock, and the California substock is not considered overfished. The other new stock assessments do not indicate any new overfished or overfishing designations. Yelloweye rockfish has been declared rebuilt to its target reference point (TRP; dashed vertical line in Fig. 3.10). China rockfish in California is notably lower in biomass, but above limit levels. Despite the generally positive relative biomass measures in the new stock assessments, stock scale (e.g. unfished biomass) was reduced in yellowtail rockfish and sablefish is below the target biomass. Rougheye/blackspotted rockfish stock size (absolute number or biomass of the stock) and status (ratio of the current stock size to unfished size) have both gone up since the 2013 stock assessment. Chilipepper rockfish also shows a very high stock status that has increased even more since the last stock assessment.

"Overfishing" occurs when catches exceed overfishing limits (OFLs), but not all stocks are managed by species-specific OFLs. Species that are managed within a management complex track overfishing relative to the complex-level OFL. For summary purposes, our best alternative is to compare fishing rates to proxy rates that are based on a stock's spawner potential ratio (SPR; Fig. 3.10, x-axis). The California quillback rockfish stock is now below the fishing rate of SPR, and none of the other new stock assessments indicate fishing rates above the SPR rate. Those stocks above the SPR rate shown in Figure 3.10 are from older stock assessments and presented in the 2023 CCIEA report (Harvey et al. 2023).

K.1.1 *Pacific Survey Explorer*

Information on the biology, predicted spatial distributions, and biomass index trends for >40 groundfish species in the northeast Pacific Ocean can now be found on the Pacific Survey Explorer. This new interactive tool serves as a coastwide synopsis for groundfish, and is intended to support managers, scientists, collaborators, and others to explore available data for monitoring and management of marine ecosystems and resources. The Pacific Survey Explorer is a collaborative effort among NOAA and Fisheries and Oceans Canada (DFO) scientists. The data come from fishery-independent trawl surveys conducted by NOAA and DFO.

K.2 Recruitment of rockfishes along the Washington Coast

Strong year classes can determine age structure and set stock size for marine fishes and may also indicate favorable environmental conditions, increased future catches, and potential for impending bycatch issues. Here we present new time series of YOY rockfishes that warrant testing as an early indication of the strength of recruitment cohorts that will eventually be caught in groundfish fisheries. These time series are not included in the forage sections of the ESR (Section 3.2.2, Appendix I) because the YOY rockfishes described here are not in the water column and thus are not available as forage for many target species.

The Northwest Fisheries Science Center in collaboration with National Marine Sanctuaries has conducted annual (end of July) kelp-forest dive surveys (Tolimieri et al. 2023) at five sites within Olympic Coast National Marine Sanctuary (OCNMS) along the Washington Coast from Destruction Island to Neah Bay (Fig. K.1) since 2015. Data from this survey provide a recruitment index to the Washington black rockfish stock assessment (Cope et al. 2024) and were explored in a sensitivity run for the northern yellowtail rockfish assessment (Oken et al. 2025). The data have also contributed to a population viability analysis of the sunflower sea star (Lowry et al. 2022). The recruitment data combine several species into complexes because it is difficult to distinguish these species when they are small (< 10 cm, often ~ 5 cm in this survey).

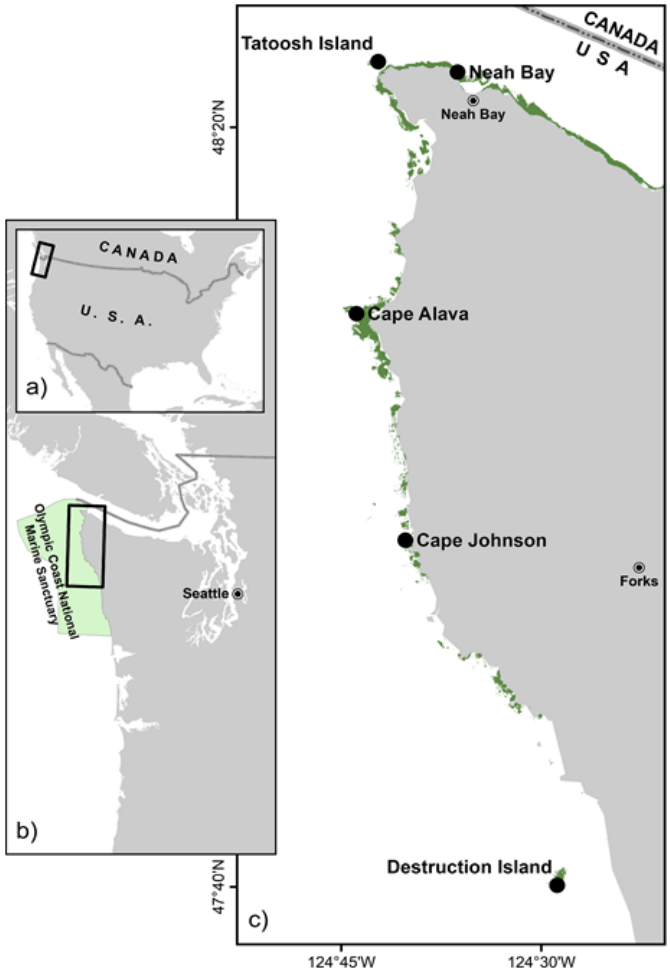


Figure K.1: Location of dive-survey sample sites within Olympic Coast National Marine Sanctuary, including areas with kelp cover (green areas in the zoomed-in pane). The abundance of adult and juvenile fishes is quantified along 30 x 2 x 2 m transects by scuba divers.

The greatest overall juvenile rockfish abundance at these sites occurred in 2016 following one of the largest marine heatwaves on record, and was primarily the yellowtail/black rockfish (YTB) complex (Fig. K.2). This 2016 event was followed by an increase in the abundance of black rockfish adults (here fish >10 cm total length from the same dive survey) in 2017 with the increase continuing through 2019 (Fig. K.3). Likewise, a smaller pulse of age-0 black rockfish in 2021 appears to have led to higher adult abundance in 2023.

In 2025, the YTB complex saw juvenile densities nearly as high as in 2016 (Fig. K.2). This high occurrence of YTB off the Washington coast is similar to observations from the RREAS survey off central California, but contrasts with lower larval rockfish abundance in the southern region of the CCE in 2025 (see Appendix I).

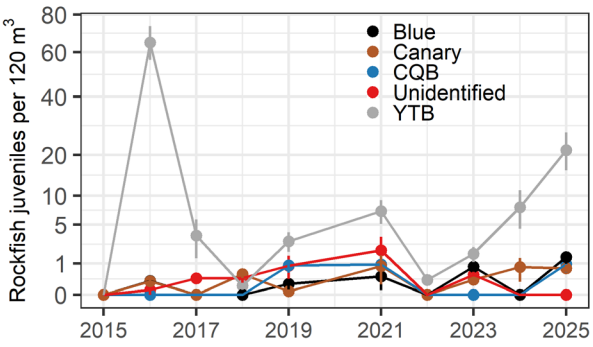


Figure K.2: Abundance of young-of-year rockfishes (< 10 cm total length) from dive surveys along the Washington Coast from 2015-2025. Blue = blue rockfish, Canary = canary rockfish, CQB = copper/quillback/brown complex, YTB = yellowtail/black complex. Data from the Olympic Coast National Marine Sanctuary kelp forest dive survey.

If further analysis of the OCNMS dive survey data indicates that YOY black rockfish abundance provides a leading indicator of changes in adult black rockfish, we might expect an increase in the abundance of black rockfish in the OCNMS in the near future. At this time, the observed patterns are best viewed as motivating hypotheses. Future indicator development could consider kelp-forest dive surveys as well as other dive surveys such as PISCO, REEF, and REEF Check as sources of information on nearshore groundfish assemblages.

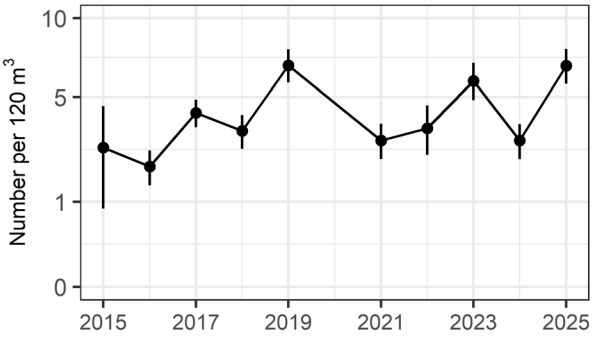


Figure K.3: Abundance of black rockfish (> 10 cm total length) from dive surveys along the Washington Coast from 2015-2025.

K.3 Pelagic juvenile groundfishes: abundance and diversity through time

Groundfish are a diverse group of fish taxa with complex life histories – including, for example, hake, rockfish, and flatfish – and play a critical role in the ecology of benthic-pelagic food webs in the CCE. Their pelagic juvenile stages are associated with coupled

oceanographic and biological dynamics within the epipelagic layer (i.e., primarily within the upper 100m), with sampling focused on a narrow temporal window in late spring through early summer when most annual production of young typically occurs. A recent study by Gasbarro et al. (2025b) collated long-term mid-water trawl data sets of pelagic YOY groundfish (n = 45 taxa) abundance from two surveys to identify distinct species assemblages and provide compositional/functional biodiversity metrics to evaluate regional biogeographic structuring throughout the CCE.

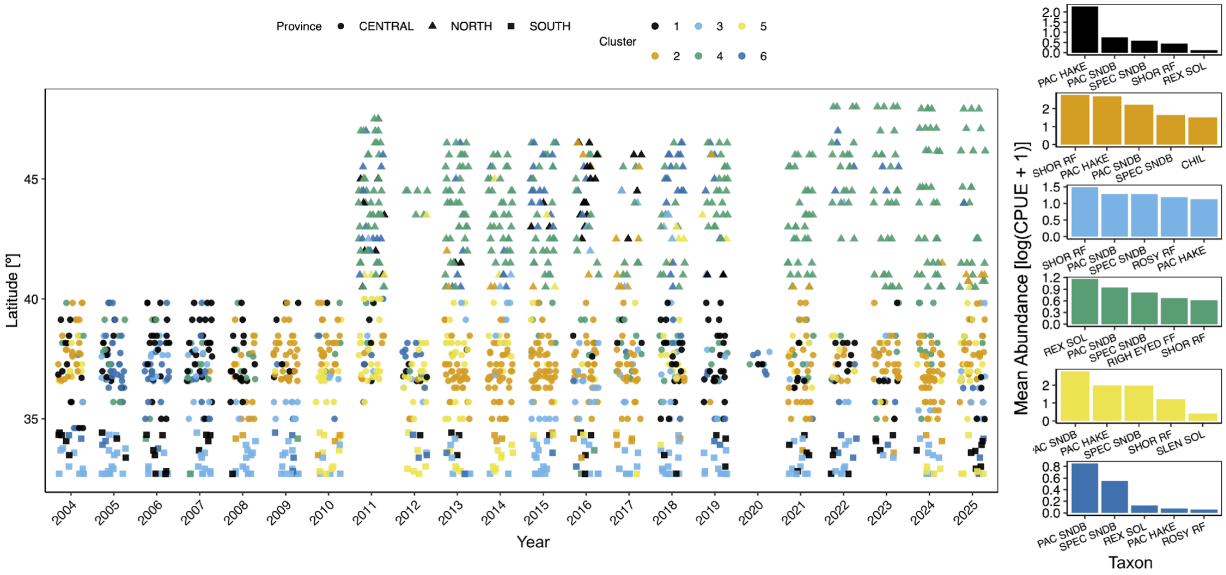


Figure K.4: Latitudinal distribution of juvenile groundfish assemblages over time (2004-2025) from cluster analyses. Points represent distinct assemblages (colors) of juvenile groundfish (n = 45) from mid-water trawl surveys revealed by cluster analysis. The average abundance [log(CPUE +1)] of the five taxa with the highest abundance in each cluster are shown at right, highlighting the main taxa associated with each assemblage. See Figure 2 in Gasbarro et al. 2025 for additional years of data.

The study found that years of high productivity were associated with both high diversity and with different pelagic YOY assemblages coastwide relative to those seen predominantly in years of low productivity (Fig. K.4). Despite the occurrence of these coastwide biodiversity events, regional biogeographic structuring was evident between the Southern (i.e., south of Point Conception), Central, and Northern (i.e., north of Cape Mendocino) CCE, with abundance and diversity metrics often correlated between regions (Gasbarro et al. 2025b). Updating the analyses through 2025 indicated that the abundance (CPUE) and diversity (species richness, Shannon Diversity index) of groundfish was higher in the Central and Northern CCE during the 2024-2025 period than it has been since the peak abundance levels of 2015 (Fig. K.5). Meanwhile, both abundance and diversity in the Southern CCE were at or approaching their lowest levels since measurement began in 2004 (Fig. K.5). Changes in biodiversity appeared primarily related to richness as changes in the

Shannon Index (which incorporates both evenness and richness) closely matched the richness trend (Fig. K.5). The results suggest strong linkages between biodiversity and regional ecosystem functioning and services (e.g., productivity of exploited species), and potential new indicators that could be broadly applicable to evaluating recruitment conditions and informing stock assessments and risk assessments in a variable and changing climate on the West Coast. For example, these biodiversity time-series were included as context in the risk table for the 2025 chilipepper rockfish stock assessment (Dick et al. 2025).

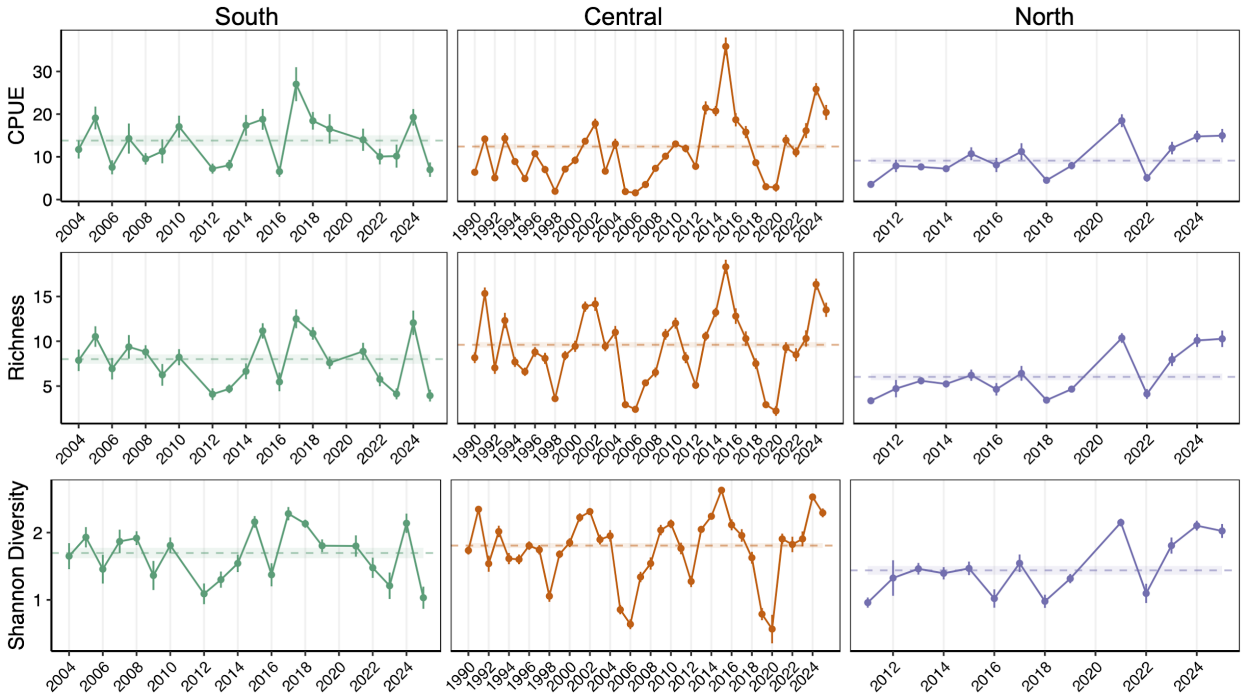


Figure K.5: Juvenile groundfish compositional biodiversity time-series by biogeographic region. Points represent annual means (± 2 SE) of biodiversity metrics from stations within each CCE bioregion. Horizontal dashed lines and shaded areas represent each region's climatological mean and standard error, respectively. Vertical grey lines are shown on even years to aid readability.

K.4 Abundance trends in Ecosystems Components species

For groundfish management, the Pacific Fishery Management Council identifies Ecosystem Component (EC) species as groundfishes that do not require conservation and management in the EEZ. However, these EC species are monitored in case new information indicates a need to evaluate changes in their status or their vulnerability to the fishery. The CCIEA ESR could potentially play a role in tracking the status of EC groundfish species for the Council. For example, here we provide abundance trends for the seven EC species that are listed in the Council's December 2025 PFMC Decision Summary Document.

Biomass of curlfin sole, greenblotched rockfish, and rocksole increased over the last five years relative to the long-term mean and s.d. (Fig. K.6). The five other EC species

(bronzespotted rockfish, Mexican rockfish, speckled rockfish, rosy rockfish, and tiger rockfish) were observed frequently and models did not converge.

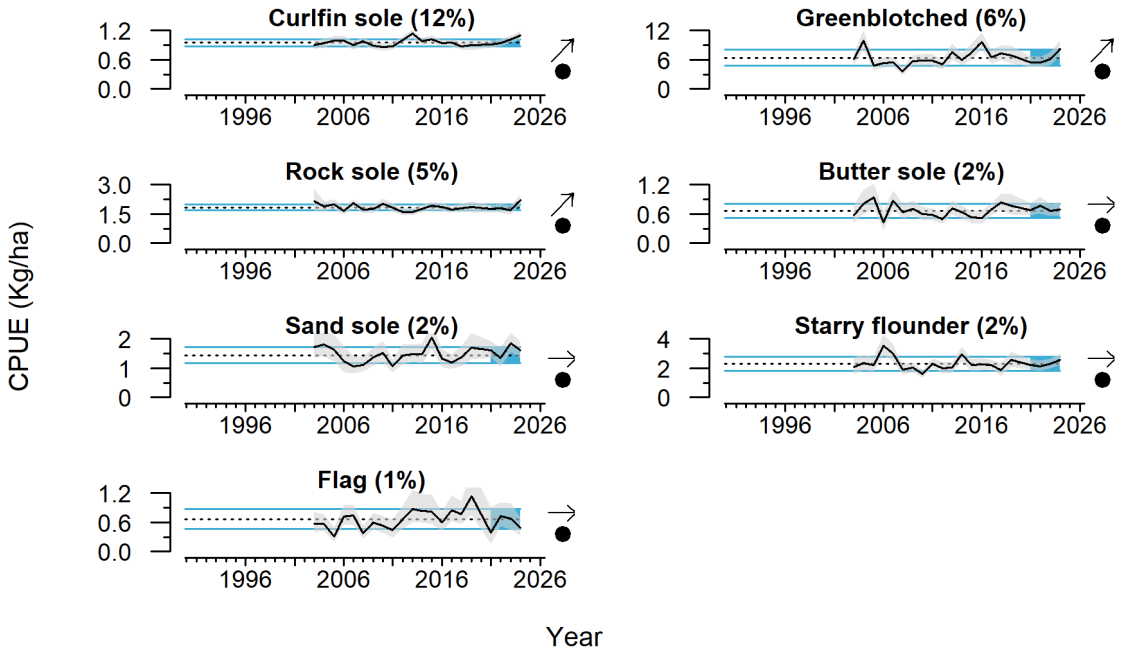


Figure K.6: Time series of CPUE (kg/ha) for seven ecosystem component groundfish species based on WCGBTS data for 2003-2024. Time series are backtransformed means and ± 1.0 s.e. from delta-lognormal models for the full coast in areas shallower than 400 m. The number in title indicates percent positive tows across all years.

Appendix L — HIGHLY MIGRATORY SPECIES (HMS)

Link to main section: Highly Migratory Species

L.1 HMS Stock Assessment Information

Recent ESRs have featured stock assessment-based biomass and recruitment estimates for several HMS stocks that occur in the CCE. Biomass and recruitment estimates for many HMS stocks that occupy the California Current are available from stock assessments conducted by collaborators under the International Scientific Committee for Tuna and Tuna-like Species in the North Pacific Ocean (ISC) or the Inter-American Tropical Tuna Commission (IATTC). The only assessment update since last year's ecosystem status report is for yellowfin tuna, where a benchmark assessment was performed by IATTC (YFT 2025 assessment).

The spatial structure for the yellowfin tuna assessment has changed substantially since last year's ecosystem status report. In the current assessment, the spatial structure is considered a substantial improvement over previous assessments and importantly for this report, now includes estimates for the North and East (NE) regions of the Eastern Pacific Ocean (EPO), which corresponds to the California Current Ecosystem. The time series shown here are the estimates for the NE region of the EPO. It should be noted that SSB estimates for yellowfin tuna are in relative units and not in mt, and the uncertainty in the recruitment estimates are very large for reasons yet undetermined. Time series of biomass and recruitment estimates for all available HMS stocks through their most recent assessments are shown in (Fig. L.1, Fig. L.2)

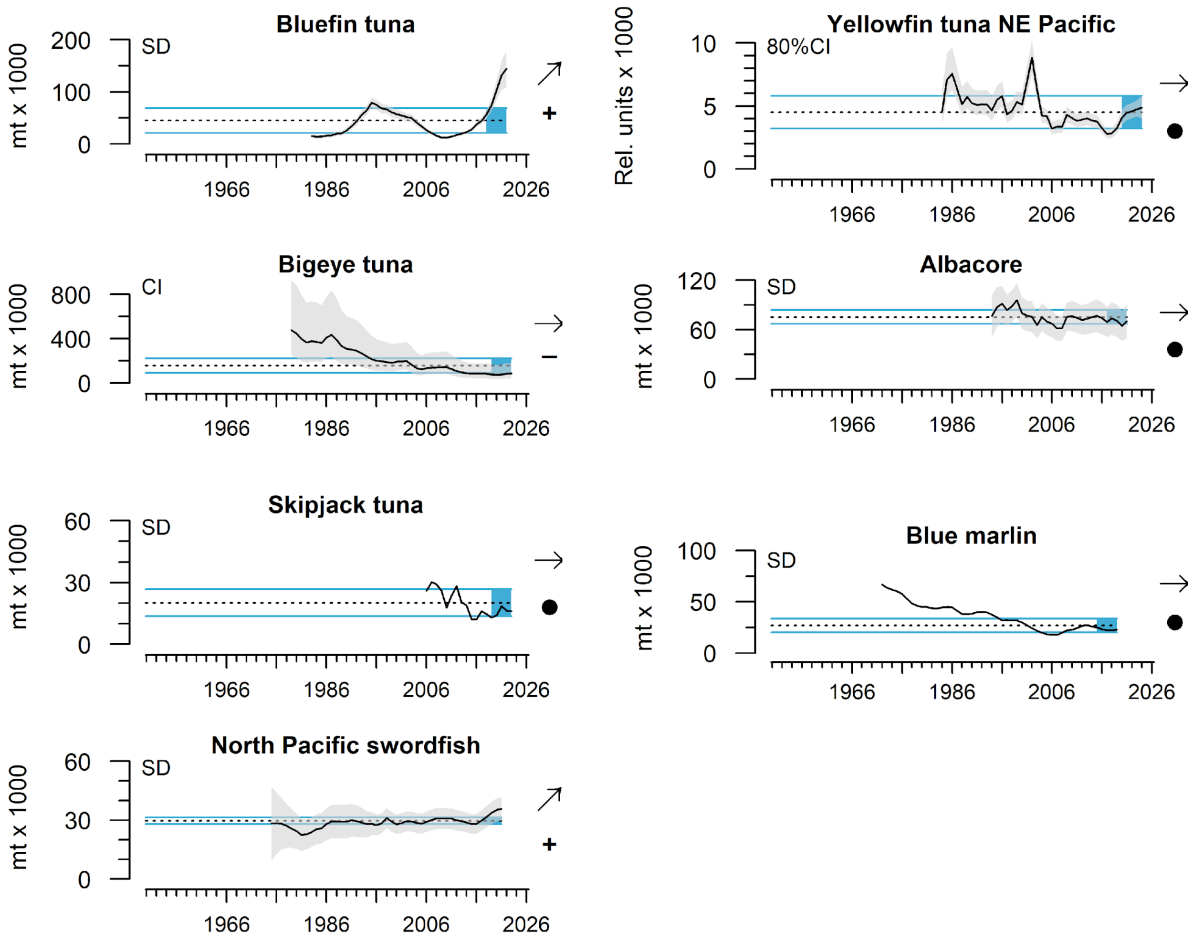


Figure L.1: Spawning biomass for highly migratory species in the north Pacific. The type of error envelope is indicated in the upper left of each panel: SD = ±1 s.d.; SE = ±1 s.e.; CL = ±95% C.L. Assessment dates were: Albacore (2023), Bigeye tuna (2024), Blue marlin (2021), Bluefin tuna (2024), Eastern Pacific swordfish (2012), Skipjack tuna (2024), North Pacific swordfish (2023), and Yellowfin tuna (2025). Lines, colors, and symbols are as in Fig. 2.1.

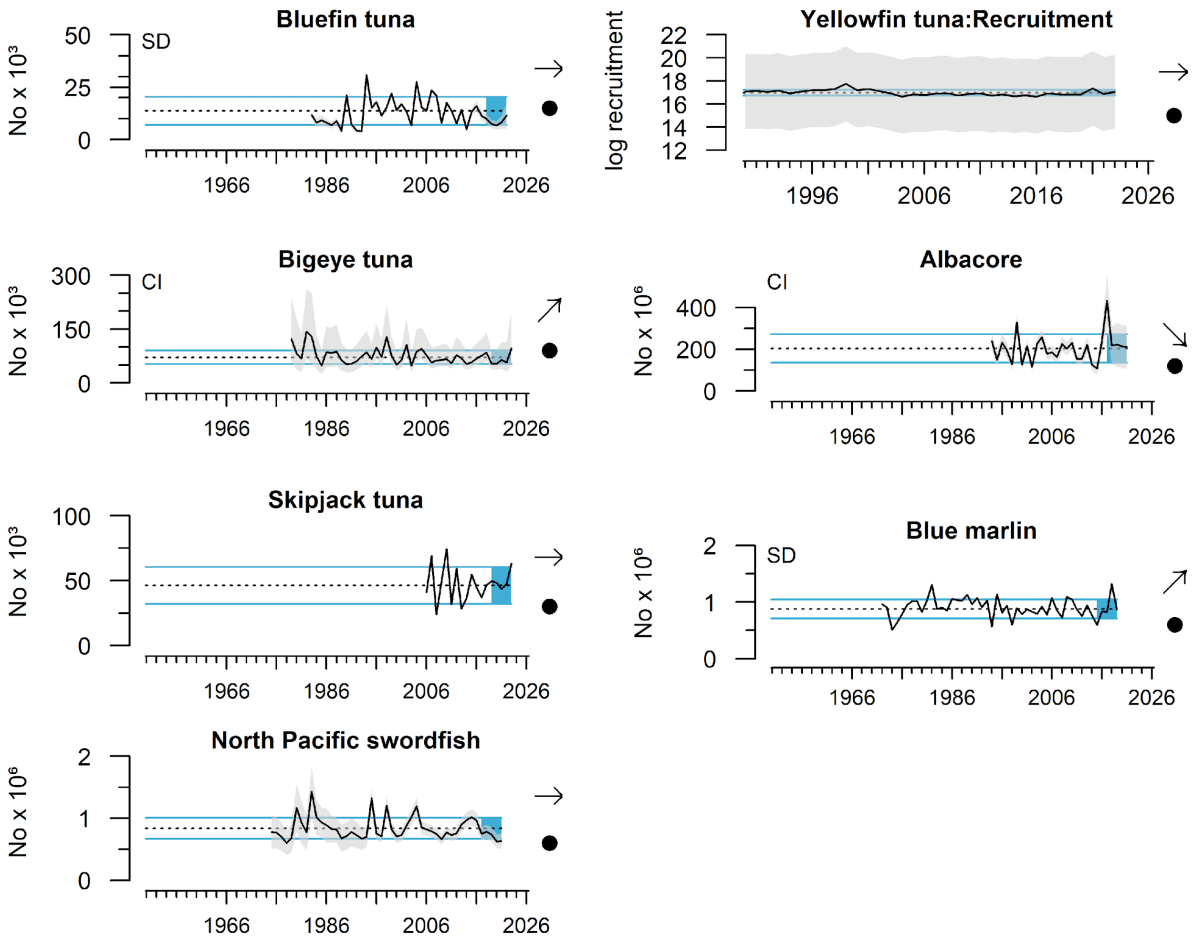


Figure L.2: Recruitment for highly migratory species in the North Pacific. The type of error envelope is indicated in the upper left of each panel: SD = ±1 s.d.; SE = ±1 s.e.; CL = ±95% C.L. Assessment dates were: Albacore (2023), Bigeye tuna (2024), Blue marlin (2021), Bluefin tuna (2024), Eastern Pacific swordfish (2012), Skipjack tuna (2024), North Pacific swordfish (2023), and Yellowfin tuna (2025). Lines, colors, and symbols are as in Fig. 2.1.

L.2 HMS Diet Information

Highly mobile predators are capable of responding rapidly to spatial shifts in oceanographic conditions and prey fields. Quantifying the diets of highly migratory fishes in the CCE can complement existing trawl-based assessments of the available forage, provide insight into how forage varies over time and space, and provide a direct metric of forage utilization. Albacore tuna, Pacific Bluefin tuna, and swordfish are opportunistic predators that consume a wide variety of prey taxa across a range of depths and habitats.

Albacore, Pacific Bluefin, and Swordfish stomachs were provided by commercial and recreational fishers, and prey were identified from whole or hard part remains and are reported as a mean proportional abundance. Diet data for four key prey groups are summarized in Figure 3.11 in the main section, and a broader subset of prey species are

presented here focusing on prey that are either themselves under a management plan, or considered ecosystem component species, to highlight their links to highly migratory species. Juvenile albacore tuna were collected off Northern California, Oregon, and Washington during the summer and fall fishing season. Pacific bluefin tuna were collected by recreational fishers in the Southern California Bight from spring until early fall. Swordfish were collected off Southern and Central California during the commercial drift gillnet season (August 15th through January 31st). Swordfish stomachs are classified by the year the fishing season began (stomachs from January are assigned to the previous year's fishing season). Data are available through 2024 for all three highly migratory species (see Fig. L.3, Fig. L.4, and Fig. L.5).

Of the focal prey species, anchovy was the most important prey of Pacific bluefin and a key prey item of swordfish, although consumption of anchovy by both predators decreased in 2024 relative to the previous year. In contrast, the consumption of Pacific hake by Pacific bluefin and swordfish was higher in 2024. Market squid was the second most important focal prey species for Pacific bluefin in 2024, continuing an upward trend observed in 2023. However, the "other" prey category represented just over 50% of bluefin diets in 2024. This category consisted primarily of myctophids along with a mix of epi- and mesopelagic fishes and squids, and tunicates. Consumption of Pacific sardine by albacore tuna decreased from record high levels in the northern region of the CCE in 2024, while Pacific Saury and "other" prey significantly increased in albacore diets (55% and 86%, respectively) (Fig. 3.11). Rockfish consumption increased for all three predators and was near to above average for swordfish and albacore in 2024.

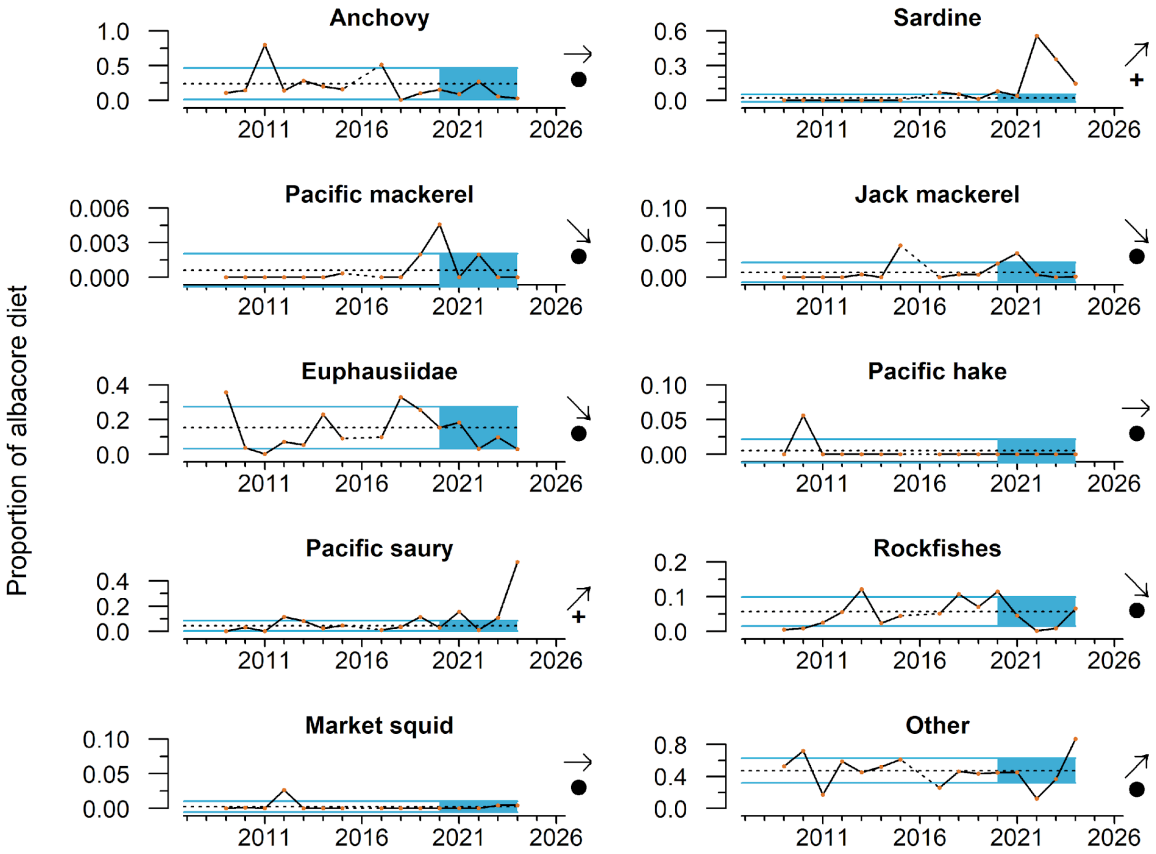


Figure L.3: The mean proportional abundance of prey items in albacore tuna diets, 2008 - 2024. Lines, colors, and symbols are as in Fig. 2.1.

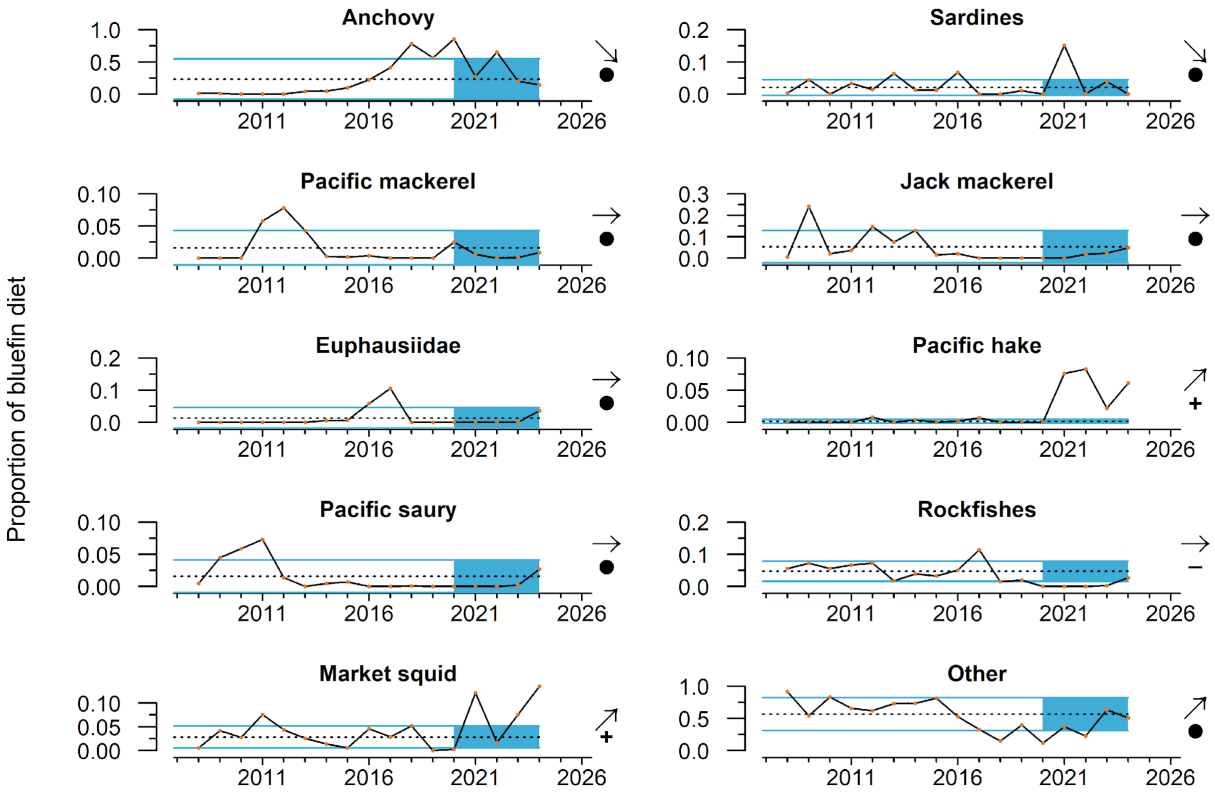


Figure L.4: The mean proportional abundance of prey items in Pacific bluefin tuna diets, 2008 - 2024. Lines, colors, and symbols are as in Fig. 2.1.

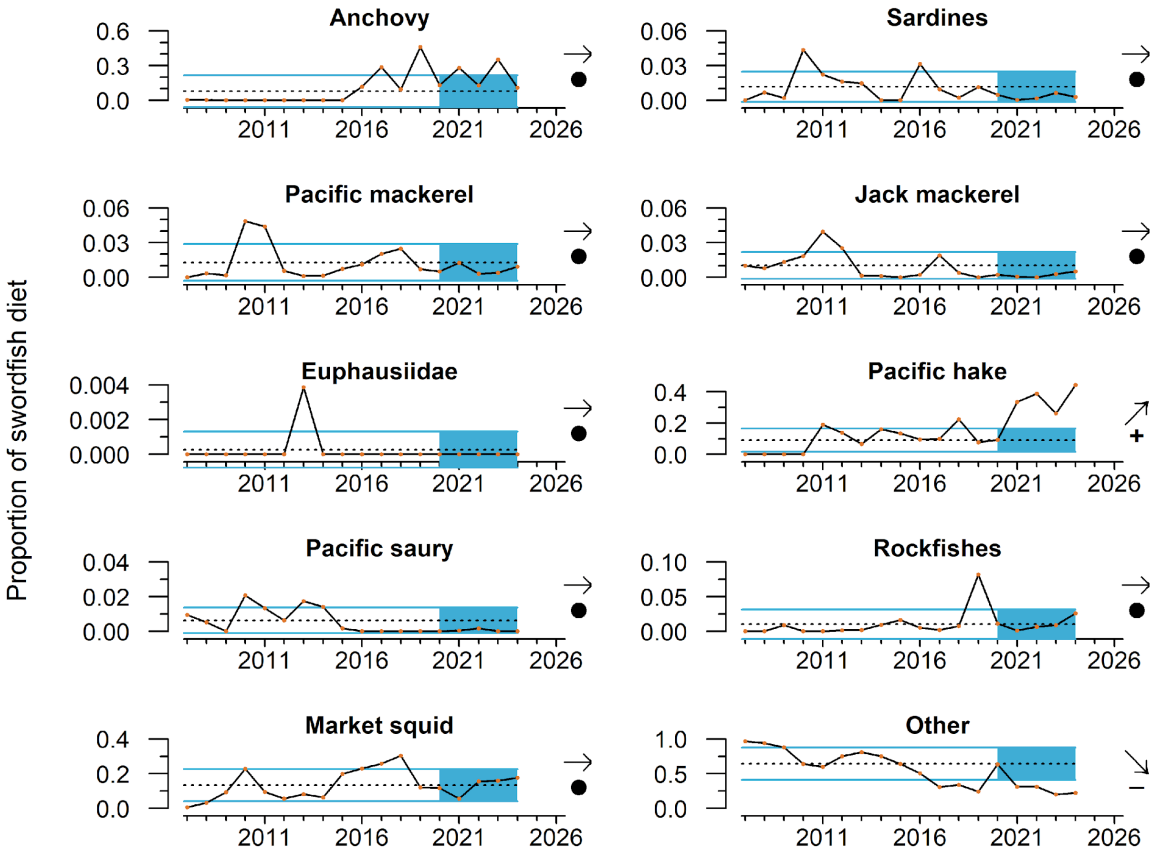


Figure L.5: The mean proportional abundance of prey items in broadbill swordfish diets, 2008 - 2024. Lines, colors, and symbols are as in Fig. 2.1.

Appendix M — SEABIRD PRODUCTIVITY, DIET, AT-SEA DENSITY, AND MORTALITY

Link to main section: Seabirds

In 2025, seabird indicators reflected generally favorable conditions for breeding in the Central and Northern CCE, with most species recovering from relatively lower productivity in 2024. Late winter upwelling may have pre-conditioned the system, through early productivity, to facilitate higher spring reproductive success. Diet indicators in the central and northern regions mirror the available forage community. In the Central CCE, anchovy re-emerged as an important prey resource after rockfish dominated diets in 2024. In the first half of the year, harmful algal blooms impacted brown pelicans in the central and southern areas of the CCE.

M.1 Seabird Productivity

Seabird population productivity, as measured through indicators of reproductive success, tracks marine environmental conditions and often reflects forage production near breeding colonies. We monitor and report on standardized anomalies of fledgling production per pair of breeding adults for multiple seabird species at Destruction Island, Washington and Yaquina Head, Oregon in the Northern CCE and Southeast Farallon Island in the Central CCE. Collectively, these focal species span a range of breeding parameters, feeding habits, and ways of provisioning their chicks, and thus provide a broad picture of the status of marine conditions.

- **Brandt's cormorants (*Urile penicillatus*)** forage primarily on pelagic and benthic fishes in waters over the shelf, generally within 20 km of breeding colonies; they return to the colony during the day to deliver regurgitated fish to their chicks.
- **Cassin's auklets (*Ptychoramphus aleuticus*)** forage primarily on zooplankton over the shelf break, generally within 30 km of colonies; they forage by day and night and return to the colony at night to feed chicks.
- **Common murres (*Uria aalge*)** forage primarily on pelagic fishes in deeper waters over the shelf and near the shelf break, generally within 80 km of colonies; they return to the colony during daylight hours to deliver single whole fish to their chicks.
- **Pelagic cormorants (*Urile pelagicus*)** forage primarily on pelagic and benthic fishes in waters over the shelf, generally within 20 km of breeding colonies; they return to the colony during the day to deliver regurgitated fish to their chicks.
- **Pigeon guillemots (*Cepphus columba*)** forage primarily on small benthic and pelagic fishes over the shelf, generally within 10 km of colonies; they return to the colony during the day to deliver single fish to chicks.
- **Rhinoceros auklets (*Cerorhinca monocerata*)** forage primarily on pelagic fishes in shallow waters over the continental shelf, generally within 50 km of colonies; they return to the colony after dusk to deliver multiple whole fish to their chicks.

Northern CCE

In the Northern CCE, productivity of rhinoceros auklets is monitored on Destruction Island, located 6 km off the outer coast of Washington. In 2025, rhinoceros auklet chick productivity was at the long-term average (Fig. M.1). Fledgling production has shown an increasing trend since 2021, when it reached the lowest level since data collection began in 2008.

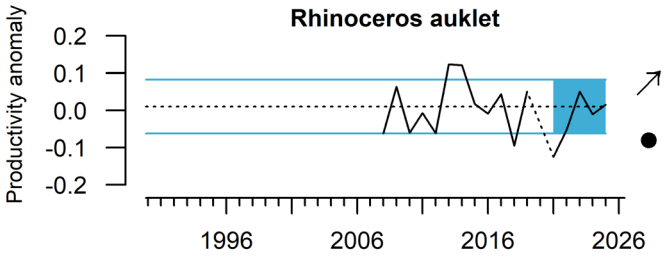


Figure M.1: Standardized productivity anomalies for rhinoceros auklet breeding at Destruction Island, WA through 2025. Data courtesy of S.F. Pearson, Washington Department of Fish and Wildlife. Lines, colors, and symbols are as in Fig. 2.1.

The productivity of common murres and Brandt's and pelagic cormorants is monitored at Yaquina Head on the central Oregon coast. Overall fledgling production in 2025 was at or above average levels for all three seabird species (Fig. M.2). Cormorant fledgling production was above average in 2025. Over the last five years, Brandt's cormorant productivity has oscillated between above average and average; while productivity has been trending down from its peak in 2021, it is still significantly greater than the long-term average. Pelagic cormorant productivity has fluctuated above and below the long-term average in recent years, and it has been trending down from its peak in 2021. Common murre fledgling production was average in 2025. Over the last seven years, murre productivity has oscillated between average and below average, and breeding failure has been attributed to bald eagle disturbance and poor ocean conditions. Observations of poor chick production in even years have alternated with successful production in odd years. The causes of this recent even-odd year pattern observed for all three species remain uncertain.

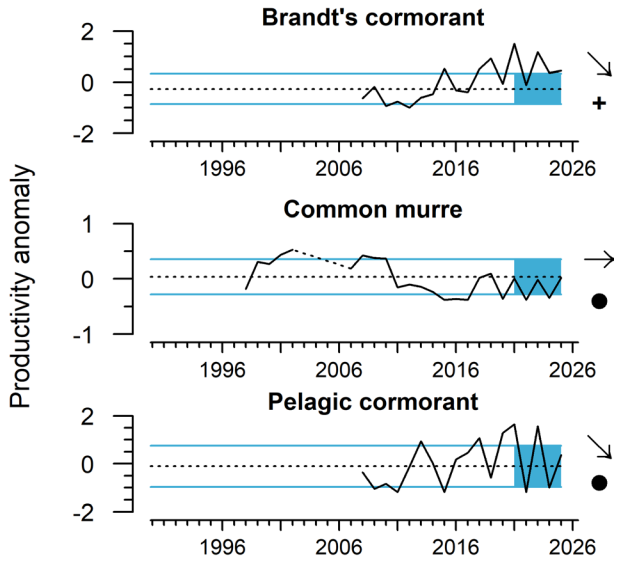


Figure M.2: Standardized productivity anomalies for three seabird species breeding at Yaquina Head, OR through 2025. Data courtesy of R. Orben, Oregon State University. Lines, colors, and symbols are as in Fig. 2.1.

Central CCE

On the central California coast, productivity of several seabird species is monitored on Southeast Farallon Island, located 48 km west of San Francisco Bay. In 2025, productivity was largely above average for the monitored species (Fig. M.3). Brandt's cormorant productivity in 2025 bounced back to an above average level from a below average level in 2024, which was an outlier from a run of largely positive productivity anomalies since 2013 (Fig. M.3). Cassin's auklet productivity was above average (Fig. M.3), with pairs initiating breeding very early and fledging chicks at a high rate. Double-brooding levels were also high in 2025; more than 80% of pairs that fledged a chick started a second brood, which is typical of years with good marine conditions (Johns et al. 2017). Common murre fledgling production was above average, while pigeon guillemot and rhinoceros auklet fledgling production was just above average (Fig. M.3).

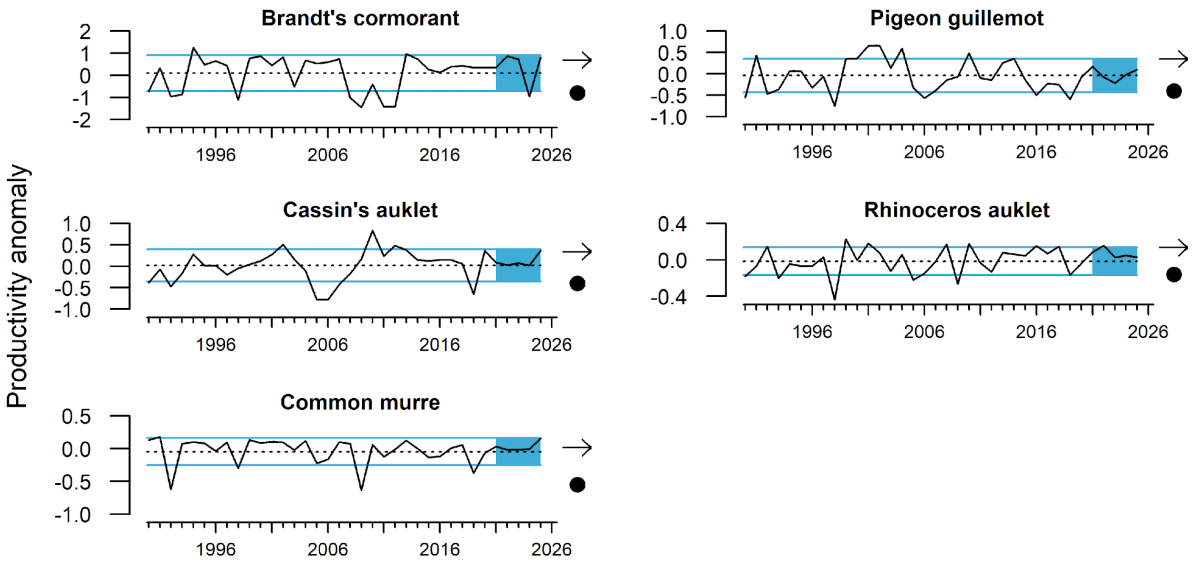


Figure M.3: Standardized productivity anomalies for five seabird species breeding at Southeast Farallon Island, CA through 2025. Data courtesy of J. Jahncke, Point Blue Conservation Science. Lines, colors, and symbols are as in Fig. 2.1.

Southern CCE

While not part of the seabird indicator portfolio, reports of brown pelicans nesting in the Channel Islands, California suggest record numbers of nesting attempts and an earlier and increasingly protracted nesting season (M. Parker, pers. comm.). For the most recent breeding season, the earliest nests appeared in November 2024, and chicks were still fledging from later nests in August. It is unknown if chick productivity tracked the number of nesting attempts.

M.2 Seabird Diets

Seabird diet composition during the breeding season reflects production and availability of forage in the vicinity of breeding colonies and often tracks regional marine environmental conditions. We monitor and report on proportions of prey taxa delivered to chicks of seabird species at Destruction Island, Washington and Yaquina Head, Oregon in the Northern CCE and Southeast Farallon Island in the Central CCE. These diet data help shed light on foraging conditions in these regions in 2025.

Northern CCE

Rhinoceros auklet chick diet data have been collected at Destruction Island, Washington since 2008. In 2025, smelts comprised 50% of the observed chick diet. This group has become increasingly important in the past several years, as anchovy have become less prevalent in the diet. The proportion of smelt in chick diet shows an increasing short-term trend as well as a significantly greater mean relative to the long-term (Fig. M.4). This is consistent with the high number of smelt collected by the NCC spring surveys off the

Oregon and Washington coasts (Appendix I). In 2025, the proportion of northern anchovy in chick diets was well below average (Fig. M.4). The recent 5-year average is significantly lower than the long-term mean, reflecting the reduced consumption of anchovy since 2018. Multiple ecosystem surveys in the CCE indicate that anchovy have been abundant in the Central and Southern CCE in recent years but less prevalent in the northern region. (Sections 3.2.1, 3.2.2, and Appendices I, H). The proportion of Pacific herring in chick diet in 2025 was just below the long-term mean and has significantly declined over the last five years. The proportion of Pacific sand lance in chick diets was above average. Since sand lance peaked (62% in 2021), there has been a short-term decline, even though the short-term mean is significantly above the long-term mean. Rockfish juveniles formed a relatively small (1%) proportion of the chick diet in 2025, below the long-term mean (note different x-axis scale). This is consistent with the low to moderate prevalence of young-of-the-year rockfish in the 2025 Northern CCE ecosystem surveys (e.g. JSOES and the NCC spring ecosystem survey) (Appendix I).

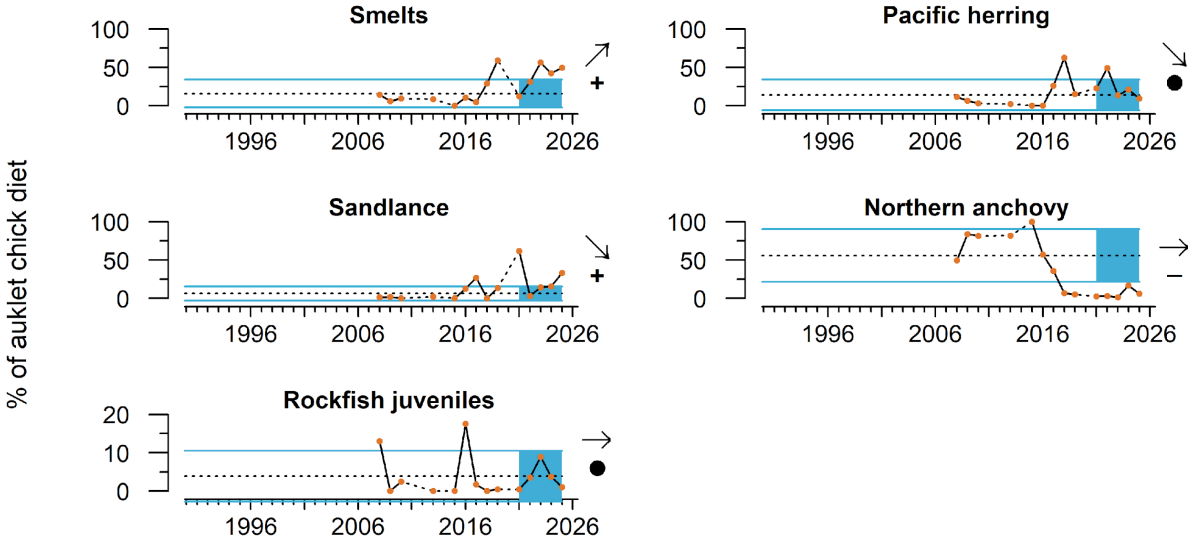


Figure M.4: Percentages of key prey items delivered to rhinoceros auklet chicks at Destruction Island, WA through 2025. Data courtesy of S.F. Pearson, Washington Department of Fish and Wildlife. Lines, colors, and symbols are as in Fig. 2.1.

Common murre chick diet data have been collected at Yaquina Head, OR since 1998. In 2025, smelts dominated their diet (82%). Murre chicks were documented consuming smelts in higher proportions than in any other year, resulting in an increasing short-term trend (Fig. M.5). Again, this is consistent with high numbers of smelt observed by ecosystem surveys off the Oregon and Washington coasts (Appendix I). Years with greater prevalence of smelts in Yaquina Head murre diet are often associated with high murre reproductive success, at least when predation pressure is not severe (Gladics et al. 2015). The proportion of herring/sardines and Pacific sand lance in chick diets were both below average in 2025, as was the proportion of flatfishes (note different y-axis scale). The proportion of rockfish juveniles in the chick diet in 2025 was average after two years of

being above average (note different y-axis scale) and is consistent with survey observations of YOY rockfishes in the Northern CCE (Appendix I). Pacific salmon juveniles were not documented in the chick diet in 2025, despite the moderate to high abundances observed on the JSOES survey (Section 3.2.2). The unusual peak of salmon in chick diets in 2021 (16%) resulted in a short-term decline even though the short-term mean is significantly greater than the long-term (note different y-axis scale).

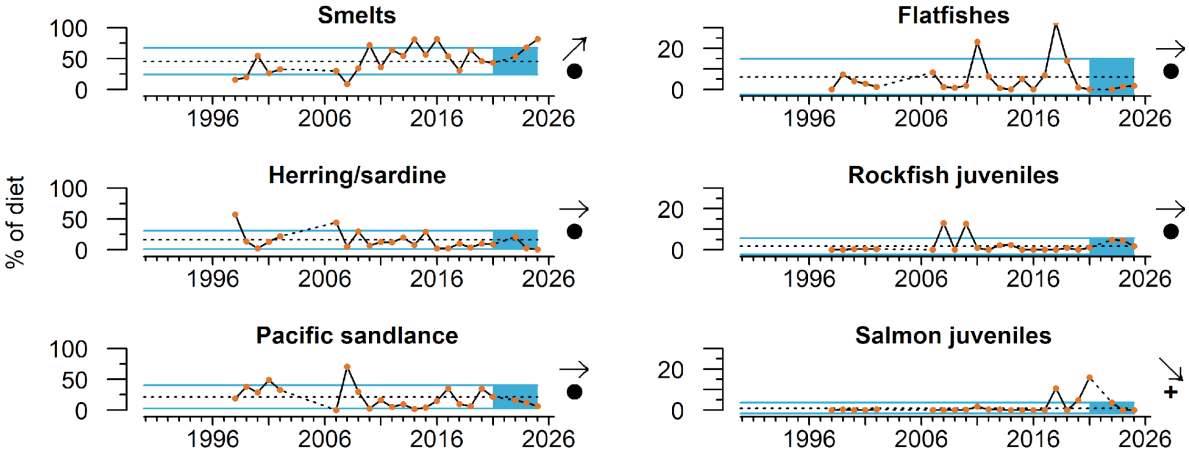


Figure M.5: Percentages of key prey items delivered to common murre chick diets at Yaquina Head, OR through 2025. Data courtesy of R. Orben, Oregon State University. Lines, colors, and symbols are as in Fig. 2.1.

Central CCE

Seabird diet data have been collected at breeding colonies on Southeast Farallon Island for more than 30 years. These colonies are close to the most intense upwelling region in the California Current and provide a uniquely valuable source of information about system productivity and prey availability to higher trophic levels. In a switch back from 2024, piscivorous birds at this colony in 2025 relied more on northern anchovy and less on juvenile rockfish. For Brandt's cormorants in 2025, the proportion of northern anchovy in chick diet was well above average, while the proportion of juvenile rockfish was below average. However, the northern anchovy proportion showed a short term decline, while the juvenile rockfish proportion showed a short-term increase (Fig. M.6). For rhinoceros auklets in 2025, the proportions of northern anchovy and rockfish juveniles in chick diet were both above average. Again, the northern anchovy proportion showed a short term decline, while the juvenile rockfish proportion showed a short-term increase (Fig. M.6). For common murre in 2025, the proportion of northern anchovy in chick diet was just below average, while the proportion of juvenile rockfish was above average. Again, the northern anchovy proportion showed a short term decline, while the juvenile rockfish proportion showed a short-term increase (Fig. M.6). These patterns reflect the above average and fluctuating abundances of juvenile rockfish and northern anchovy in the Central CCE in recent years (Fig. I.2 and Appendix I). The proportion of Pacific salmon in the diet of common murre chicks in 2025 was below average (Fig. M.6), while the proportion of juvenile rockfish in the pigeon guillemot chick diet was average (Fig. M.6). For

planktivorous Cassin's auklets, the proportion of cold-water taxa such as krill (primarily *Euphausia pacifica* and *Thysanoessa spinifera*) was above average in 2025, while the proportion of mysids, which are warm-water taxa, was below average (Fig. M.6). The general pattern of krill consumption is consistent with trends in krill abundance off central California over the same time period (Fig. I.2).

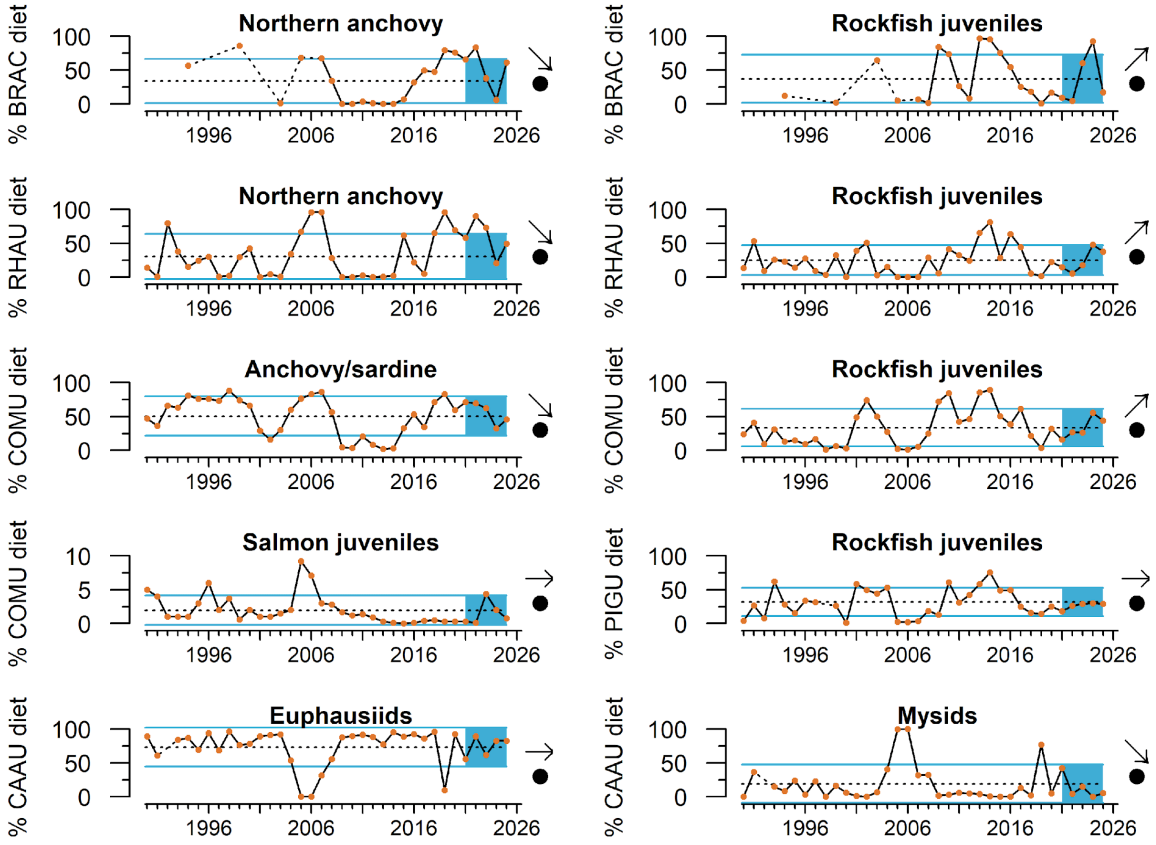


Figure M.6: Percentages of key prey items delivered to seabird chicks at Southeast Farallon Island, CA through 2025. BRAC = Brandt's cormorant; RHAU = rhinoceros auklet; COMU = common murre; PIGU = pigeon guillemot; CAAU = Cassin's auklet. Data courtesy of J. Jahncke, Point Blue Conservation Science. Lines, colors, and symbols are as in Fig. 2.1.

M.3 Seabird At-Sea Density

Seabird densities on the water during the breeding season can track marine environmental conditions and may reflect regional production and availability of forage. Data from this indicator can establish habitat use and may be used to detect and track seabird population movements or increases/declines as they relate to ecosystem change. We monitor and report on at-sea densities of three focal seabird species in the Northern, Central, and Southern CCE.

- **Sooty shearwaters** migrate to the CCE from the southern hemisphere in spring and summer to forage primarily on the outer shelf and near the shelf break on a variety of small fish, squid and zooplankton.
- **Cassin's auklets** are a resident species that feeds primarily over the continental shelf mainly on zooplankton and small fish.
- **Common murres** are a resident species that feeds primarily over the continental shelf and target a variety of pelagic fish.

Northern CCE

At-sea density patterns varied among focal species and among CCE regions in 2025. In the Northern CCE in 2025, sooty shearwater and common murre densities observed during June surveys were below average, while Cassin's auklet densities were above average (Fig. M.7, top row). The sooty shearwater density anomaly was the lowest of the time series, resulting in a short-term mean significantly below the long-term mean. The Cassin's auklet density anomaly has been above average values since 2017. The common murre density anomaly has been below average since 2022. Recent (5-year) means and trends should be interpreted with care, as no data were collected in 2020 or 2021 due to COVID-19 restrictions.

Sooty shearwaters and common murres are normally the two numerically dominant species in these surveys. In 2025, the second-most numerous species observed was the pink-footed shearwater, most of which were observed on survey tracks off La Push, Washington. Counts of this species over the time series (since 2003) have averaged ~130 birds, but the 2025 count was 524 birds (J. Zamon, unpublished data).

Central CCE

In the Central CCE in 2025, sooty shearwater and common murre densities observed during May/June surveys were above average, while Cassin's auklet densities were just below average (Fig. M.7, middle row). The sooty shearwater density anomaly was the third highest of the time series, resulting in a short-term mean significantly greater than the long-term mean. The Cassin's auklet density anomaly has been consistently below average since 2014, resulting in both a negative short-term trend and a short-term mean significantly less than the long-term mean. The common murre density anomaly has been primarily positive over recent years, resulting in a short-term mean significantly greater than the long-term mean.

Notable results from the 2025 surveys include species with high densities (at or above one standard deviation from the long-term mean). These species included brown pelican for the third straight year and Sabine's gull. Species with low densities (below one standard deviation from the long-term mean) included northern fulmar for the third straight year (Farallon Institute RREAS Report).

Southern CCE

In the Southern CCE in 2025, sooty shearwater and common murre densities observed during March/April surveys were average, while Cassin's auklet densities were well below

average (Fig. M.7, bottom row). The sooty shearwater density anomaly has largely been positive since 2013. The Cassin's auklet density anomaly was the lowest of the time series for the second straight year and has been negative since 2017, resulting in both a negative short-term trend and a short-term mean significantly less than the long-term mean. The common murre density anomaly has been neutral to positive since a negative value in 2022, resulting in a positive short-term trend. Recent means and trends should be interpreted with care, as no data were collected in 2020 or 2021 due to COVID-19 restrictions.

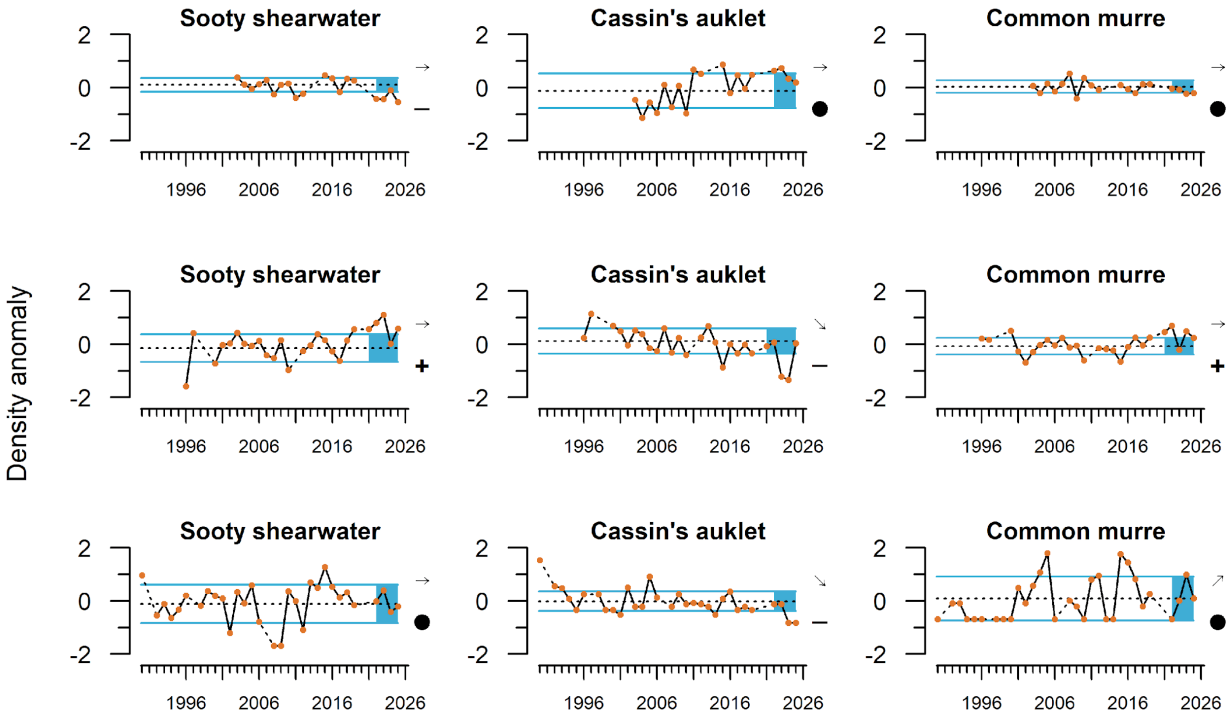


Figure M.7: Anomalies in spring/summer at-sea densities of sooty shearwaters, Cassin's auklets and common murres in the Northern (top), Central (middle), and Southern (bottom) CCE. Data are shipboard counts, transformed as ln(bird density/km2 +0.01) and expressed as an anomaly relative to the long-term mean. Data from the Northern CCE are collected on the JSOES survey and are courtesy of J. Zamon (NOAA); data from the Central and Southern CCE are collected on the SWFSC RREAS and CalCOFI surveys, respectively, and are courtesy of W. Sydeman (Farallon Institute). Lines, colors, and symbols are as in Fig. 2.1.

Notable observations from these spring surveys include species with high densities (at or above one standard deviation from the long-term mean). These included brown pelican (for the third straight year), Brandt's cormorant, Laysan albatross, and Cook's petrel. The latter two species are seasonal migrants to the CCE (Farallon Institute Report Spring).

Surveys conducted in July 2025 documented subtropical/tropical seabirds, which are becoming more common off the southern California coast. These included relatively high densities of Cook's petrel and black-footed albatross. Additional observations included one red-footed booby, one masked booby, and three red-tailed tropicbirds (Farallon Institute Report Summer).

M.4 Seabird Mortality

Monitoring of dead beached birds provides information on the health of seabird populations and ecosystem health. Over the last 30 years, seabird mortality events have been documented in the CCE in the months following prolonged marine heat waves (Jones et al. 2024). There was a die-off and strandings of brown pelicans on beaches of central and southern California in the spring and summer of 2025. Unlike 2024, when pelican mortality was largely attributed to issues of prey accessibility, in 2025 there was evidence of domoic acid poisoning in brown pelicans; domoic acid was also documented in California sea lions and other marine mammals (Section 3.8, Appendix O). In October of 2025, elevated levels of northern fulmars were noted on monitored beaches in the Central CCE; however, survey effort was reduced in October and November in some areas, as volunteers were unable to survey during the federal government shutdown. Data collected from December 2025 to early April 2026 will be used to finalize 2025 encounter rates.

Northern CCE

The COASST program monitors beaches in the California Current from Cape Flattery, Washington to Mendocino, California. The encounter rate of beachcast Cassin's auklet for 2024 (which includes January and February 2025 surveys) returned to average after an outlier year (Fig. M.8). The preliminary rate for 2025 based on October-December surveys was very low, but the final rate awaits January-February 2026 data. The encounter rate for beachcast common murre was below average in 2025 and showed a negative short-term trend (Fig. M.8). The encounter rate for beachcast northern fulmar for 2024 (which includes January through April 2025 surveys) was average (Fig. M.8). The preliminary rate for 2025 based on October-December surveys was high, but the final rate awaits January-April 2026 data. The encounter rate for beachcast sooty shearwater (note different y-axis) was below average in 2025 (Fig. M.8).

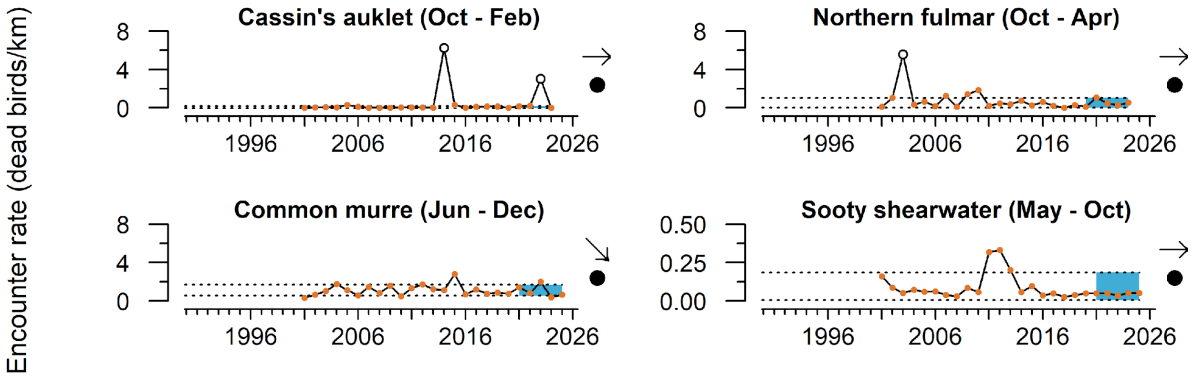


Figure M.8: Encounter rates of dead beachcast birds in Washington, Oregon and northern California. The mean and trend of the last five years (blue shaded area) are evaluated relative to the mean and s.d. of the full time series with the outliers (open circles) removed. Dotted lines indicate ±1 s.d. of the full time series with outliers removed. Data courtesy of J. Parrish, University of Washington/Coastal Observation and Seabird Survey Team (COASST). Symbols at right are as in Fig. 2.1.

Central CCE

The Beach Watch program monitors beaches in northern and central California (Point Arena to Point Año Nuevo). The encounter rate for beachcast Brandt's cormorant was above average in 2025 (Fig. M.9). The encounter rate for beachcast Cassin's auklet for 2024 (which includes January and February 2025 surveys) returned to average after two outlier years in a row, resulting in a negative short-term trend (Fig. M.9). The preliminary rate for 2025 based on October-December surveys was very low, but the final rate awaits January-February 2026 data. The encounter rate for beachcast common murre was near average in 2025 (Fig. M.9). The encounter rate for northern fulmar in 2024 (which includes January through April 2025 surveys), was below average and showed a negative short-term trend (Fig. M.9). The preliminary rate for 2025 based on October-December surveys was high, but the final rate awaits January-April 2026 data. The sooty shearwater encounter rate was above average in 2025 and shows a positive short-term trend (Fig. M.9).

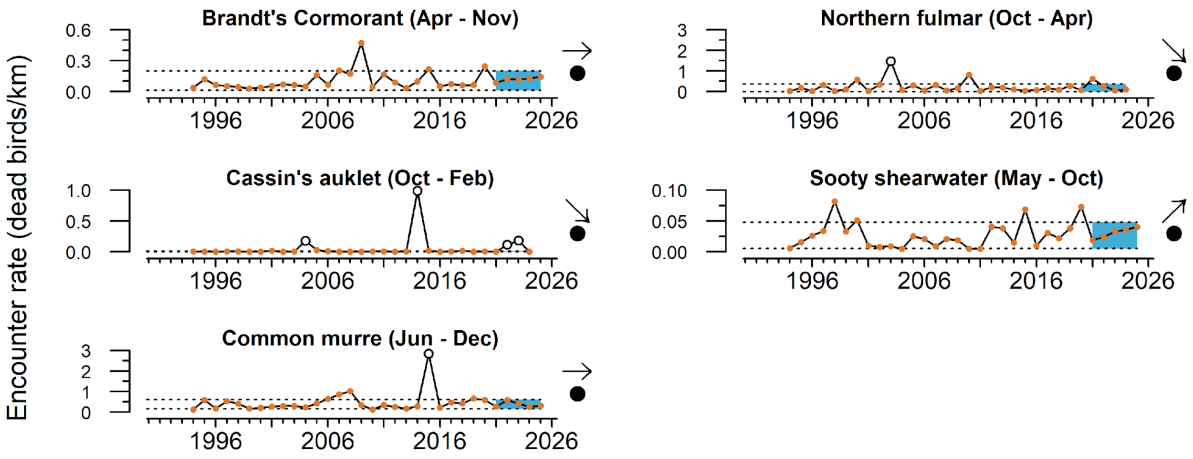


Figure M.9: Encounter rate of dead beachcast birds in north-central California through 2025. The mean and trend of the last five years (blue shaded area) are evaluated relative to the mean and s.d. of the full time series with the outliers (open circles) removed. Dotted lines indicate ±1 s.d. of the full time series with outliers removed. Note different y-axes for species. Data provided by Beach Watch. Symbols at right are as in Fig. 2.1.

The Beach Combers program monitors beaches in the CCE (North: Point Año Nuevo to Point Sur; Central: Point Sur to Point Conception, California). The encounter rate for Brandt's cormorant was below average in 2025 for both North and Central Chapter beaches (Fig. M.10). The Cassin's auklet encounter rate for 2024 (which includes January and February 2025 surveys) was below average for both North and Central Chapter beaches (Fig. M.10). The preliminary rate for 2025 based on October-December surveys was very low for both North and Central Chapter beaches, but the final rate awaits January-February 2026 data. The encounter rate for common murre was below average in 2025 for both North and Central Chapter beaches, but Central Chapter beaches show a positive short-term trend (Fig. M.10). The encounter rate for northern fulmar in 2024 (which includes January through April 2025 surveys), was below average and showed a negative short-term trend for both North and Central Chapter beaches (Fig. M.10). The preliminary rate for 2025 based on October-December surveys was high, but the final rate awaits January-April 2026 data. The encounter rate for sooty shearwater in 2025 was below average for North Chapter beaches but was above average for Central Chapter beaches, which showed a positive short-term trend (Fig. M.10).

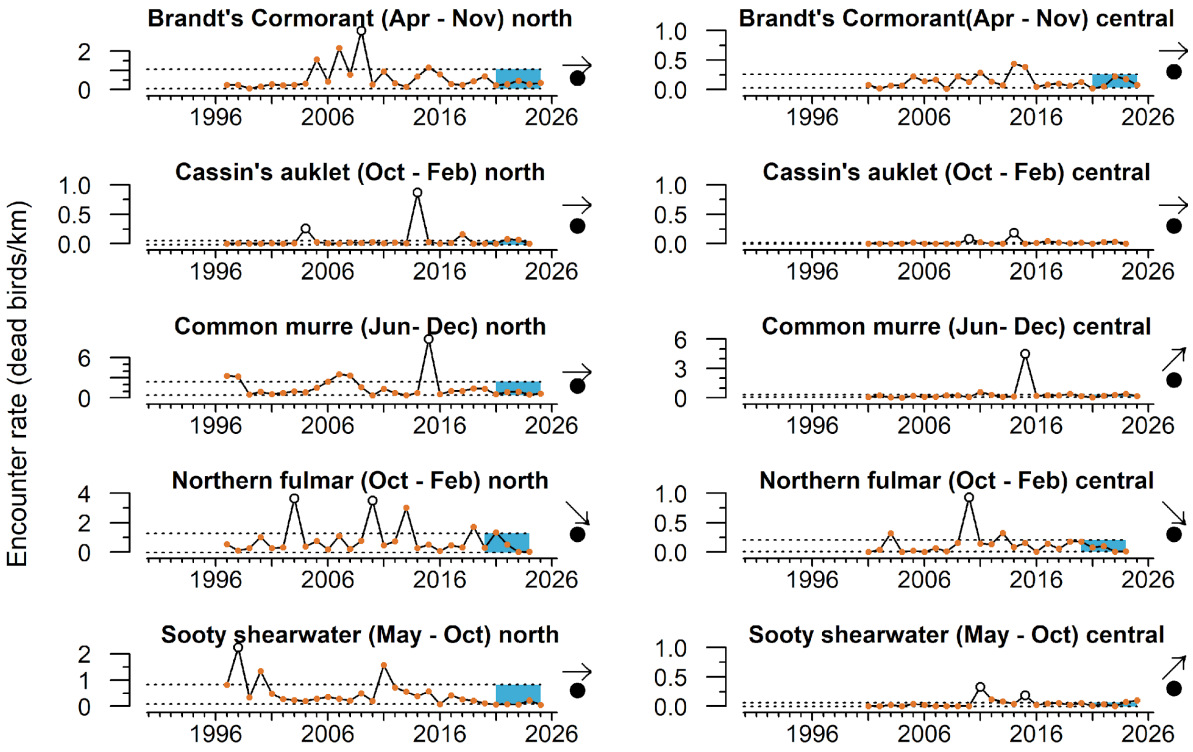


Figure M.10: Encounter rate of dead beachcast birds in central California through 2025. The mean and trend of the last five years (blue shaded area) are evaluated relative to the mean and s.d. of the full time series with the outliers (open circles) removed. Dotted lines indicate ±1 s.d. of the full time series with outliers removed. Note different y-axes for species. Data provided by BeachCombers. Symbols at right are as in Fig. 2.1.

Appendix N — MARINE MAMMALS

Link to main section: Marine Mammals

N.1 Whale Entanglements

Total confirmed entanglements have remained elevated in 2025, although still below the peak in 2015-2016 (Fig. N.1). The trend in total entanglements is driven largely by incidents with humpback whales, which are the most frequently entangled species confirmed in absolute numbers. Confirmed entanglements of all whales except humpback show decreasing or neutral trends over the past five years.

Entanglement reports in 2025 involved a range of sources, including: commercial Dungeness crab gear; commercial sablefish pot; commercial rock crab; commercial coonstripe shrimp; Canadian recreational gear; unidentified gillnet fisheries; and unidentified hook and line fishery (Table N.1). No entanglements in large mesh drift gillnet gear were confirmed in 2025. There are continued challenges with identifying the origins of entanglements, i.e. 75% of reports were identified as fishery-origin, although not all are confirmed to a specific fishery.

Table N.1: Summary of 2025 entanglement reports by species. Note: All fisheries of confirmed reports are U.S. commercial fisheries unless otherwise noted

Species	Number	Report Location of Confirmed Reports	Fisheries of Confirmed Reports
Humpback	30	18 California	7 Dungeness crab (3 CA & 4 OR)
		3 Oregon	3 unidentified gillnet
		8 Washington	2 rock crab
		1 Mexico	2 coonstripe shrimp
			1 unknown hook and line
			1 sablefish pot
			2 Canadian recreational gear
			3 monofilament line
			9 unknown
Gray	3	2 California	1 Dungeness crab (tribal)
		1 Washington	1 unidentified gillnet
			1 unidentified gillnet and rock crab

Despite actions which reduced fishing effort, confirmed humpback whale entanglement reports remained steady and above pre-2014 levels (Fig. N.1). Additional factors continue

to present obstacles to risk reduction, including derelict fishing gear and foraging by whales in nearshore waters under certain ecosystem conditions. Late-summer and early-fall increases in habitat compression Fig. 2.5 and a nearshore increase in adult anchovy (a main prey of humpback whales) may have both contributed to increased entanglement risk and possibly the likelihood of detections overall. Habitat compression levels in 2024 were similar to those in 2015-2016, when reported humpback whale entanglements peaked. More information on whale entanglements can be found on the CCIEA website.

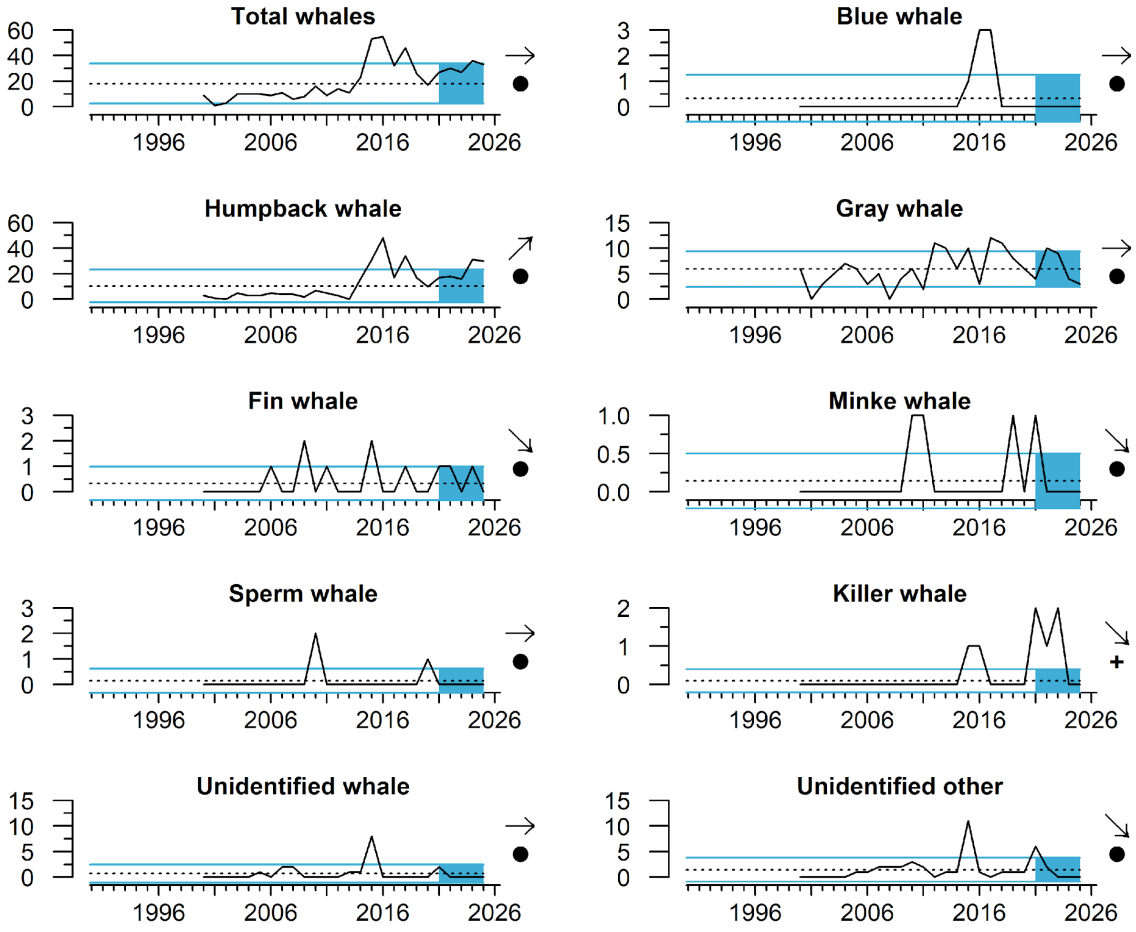


Figure N.1: Numbers of whales reported as entangled in fishing gear along the West Coast from 2000-2025.

Appendix O — HARMFUL ALGAL BLOOMS

Link to main section: HABs

Harmful algal blooms (HABs) of diatoms in the genus *Pseudo-nitzschia* have been a recurring concern along the West Coast. Certain species of *Pseudo-nitzschia* produce the toxin domoic acid, which can accumulate in filter feeders and extend through food webs to cause harmful or lethal effects on people, marine mammals, and seabirds (Lefebvre et al. 2002; McCabe et al. 2016). Because domoic acid can cause amnesic shellfish poisoning in humans, fisheries are delayed, closed, or operate under special orders or health advisories when domoic acid concentrations exceed regulatory thresholds for human consumption. Shellfish fisheries such as razor clam, Dungeness crab, rock crab, and spiny lobster are especially impacted by management actions related to domoic acid, including fishery closures or delayed openings. These measures can cost tens of millions of dollars in lost revenue and cause a range of sociocultural impacts in fishing communities (Dyson and Huppert 2010; Ritzman et al. 2018; Holland and Leonard 2020; Moore et al. 2020), including a "spillover" of fishing effort into other fisheries.

Ocean conditions associated with marine heatwaves, El Niño events or positive PDO regimes may further increase the probability of domoic acid production and fishery impacts (McCabe et al. 2016; McKibben et al. 2017). Domoic acid toxicity also tracks anomalies of southern copepod biomass (Fig. 3.1) . The largest and most toxic HAB of *Pseudo-nitzschia* on the West Coast occurred in 2015, coincident with the 2013-2016 marine heatwave, and caused the longest-lasting and most widespread HAB-related fisheries closures on record (McCabe et al. 2016; Moore et al. 2019; Trainer et al. 2020). Closures and delays in the opening of West Coast crab fisheries resulted in the appropriation of >$25M in federal disaster relief funds (McCabe et al. 2016).

According to thresholds set by the U.S. Food and Drug Administration (FDA), domoic acid levels ≥20 parts per million (ppm) trigger actions for all seafood and tissues except Dungeness crab viscera, for which the level is >30 ppm (California applies this to rock crab viscera as well) (FDA 2011). Under evisceration orders, Dungeness crab can be landed when DA levels in the viscera exceed the threshold but the leg/body meat levels remain below the appropriate threshold, provided that the crabs are eviscerated by a licensed processor. Oregon was the first West Coast state to pass legislation allowing evisceration in November 2017, followed by California in October 2021. Washington adopted an emergency evisceration rule in February 2021 and is considering legislation to grant long-term authority for issuing evisceration orders.

Other toxic HAB taxa that impact bivalve shellfish fisheries on the U.S. West Coast include dinoflagellates in the genera *Alexandrium* and *Dinophysis* (Anderson et al. 2021). *Alexandrium* species produce a suite of PSTs, the most potent being saxitoxin. *Dinophysis* species produce okadaic acid and *Dinophysis* toxins, collectively called DSTs, and/or pectenotoxins (PTXs) (Ayache et al. 2023). PSTs and DSTs can cause human illness, whereas PTXs can cause shellfish mortalities. Shellfish fisheries are closed when the action thresholds for these toxins are exceeded; 80 ug saxitoxin equivalents per 100 g shellfish tissue for PSTs and 16 ug okadaic acid equivalents per 100 g shellfish tissue for DSTs

(2011). PSTs have impacted the U.S. West Coast for centuries. Washington and California implement a seasonal mussel harvesting closure during the summer when PST risk is high, whereas Oregon relies on regular testing. DSTs were not known to be problematic on the U.S. West Coast until 2011 when illnesses were reported in Washington (Trainer et al. 2013). Washington now routinely monitors DSTs in shellfish.

Over the past six years non-HAB related management actions related to marine life entanglement risk (spatial closures, gear or depth restrictions) have overshadowed HAB related management actions in California. Note, however, that exceedances of domoic acid in Dungeness crab did sometimes occur in some regions of California prior to the eventual opening of the season in a given year, but the fishery opening was delayed during that time because of management actions regarding marine life entanglement risk and/or meat quality assessments. The toxin cleared from samples, in tandem with the resolution of the non-biotoxin factors, prior to the season opening. As such, this did not result in management action specific to domoic acid.



Figure 0.1: Paralytic Shellfish Toxin (PST) test results above the 80 ug/100 g action threshold over the last six years. Grey points indicate a test result below the action threshold. Horizontal black lines indicate state boundaries and the vertical dotted line indicates the start of 2025. Washington data compiled by the Washington Department of Health, from samples collected and analyzed by a variety of local, tribal, and state partners. Oregon data compiled and reported by Oregon Department of Fish and Wildlife from analyses conducted by the Oregon Department of Agriculture. California data compiled by the California Department of Public Health from samples collected by a variety of local, tribal, and state partners.

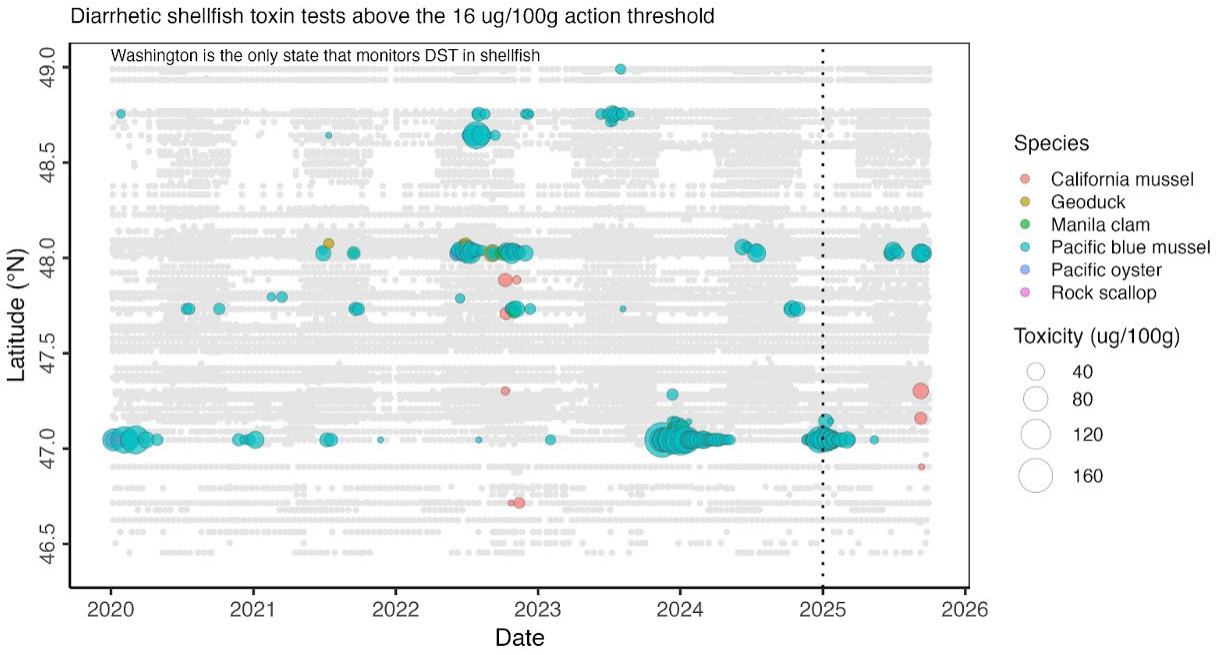


Figure O.2: Diarrhetic Shellfish Toxin (DST) test results above the 16 ug/100 g action threshold over the last six years. Grey points indicate a test result below the action threshold. Horizontal black lines indicate state boundaries and the vertical dotted line indicates the start of 2025. Note that Washington is the only state to monitor DST in shellfish. Data compiled by the Washington Department of Health from samples collected and analyzed by a variety of local, tribal, and state partners.

O.1 Domoic Acid, Paralytic Shellfish Toxins, and Diarrhetic Shellfish Toxins in Washington

Low levels of domoic acid were detectable in Washington razor clams at the start of 2025 and persisted throughout the spring, even though *Pseudo-nitzschia* species were largely absent or present only in low abundances. This is because a bloom of Pseudo-nitzschia species that occurred in August 2024 resulted in low levels of domoic acid accumulation that persisted in clams; these levels did not, however, exceed the regulatory threshold for human consumption (Fig. 3.14). *Pseudo-nitzschia* cell counts peaked in July 2025 and exceeded bloom thresholds, but razor clam tissue samples remained well below regulatory limits for human consumption, and thus, the bloom did not interfere with razor clam fisheries. Levels of domoic acid in Washington Dungeness crab viscera collected in November 2025 were low, ranging from below the detection threshold to < 3 ppm. Nevertheless, the commercial fishery start date was delayed until at least January 1, 2026, due to low meat recovery, a phenomenon unrelated to HABs.

Similar to 2024, dinoflagellates (both harmful and nonharmful) comprised a larger portion of the phytoplankton species assemblage in 2025 compared to previous years, but diatoms generally remained dominant. *Alexandrium* species were routinely observed along the

outer coast, with PSTs exceeding the action level in mussels on the north coast in late summer 2025 (Fig. O.1). Note, however, that the regular seasonal closure for recreational mussel harvesting was already in place at this time. In August, a bloom of Dinophysis species resulted in co-occurring PSTs and DSTs in shellfish tissues. In mid-December, DSTs exceeded the regulatory action level in mussels in Willapa Bay, resulting in a recreational bivalve shellfish harvest closure (Fig. O.2). Occurrences of these toxins were greatest in mussels along Washington's northern and central coast but, unlike 2024, there were no major commercial closures of bivalve shellfish associated with these blooms.

O.2 Domoic Acid and Paralytic Shellfish Toxin in Oregon

Domoic acid levels in southern Oregon coast razor clams remained above the regulatory threshold for human consumption for all of 2025 (Fig. 3.14). At the start of 2025, high levels of domoic acid persisted in clams from a bloom that occurred in September 2024 and resulted in the highest recorded level (480 ppm) of domoic acid in razor clams in Oregon. Depuration of the biotoxin was occurring at normal rates through the spring and early summer of 2025, when another toxic bloom of *Pseudo-nitzschia* species resulted in further accumulation of domoic acid in razor clams in the area. This resulted in a continued closure from Cape Blanco to the Oregon/California border.

Paralytic Shellfish Toxins continued to curtail mussel harvesting in Oregon for 2025, but not nearly to the extent of 2024 (Fig. O.1). The area from Tillamook Head to the Siuslaw River was closed for 28 days from June 27 to July 25, 2025. This was followed by another closure from July 25 to October 24, 2025 in the area from Cape Blanco to the Oregon/California border. In the same period, PST levels were above the threshold from the Oregon/Washington Border to the Siuslaw River from August 26 to October 24, 2025. A portion of the central coast was opened but the area from the Oregon/Washington Border to Cascade Head remained closed until November 7, at which time the entire coast was open to mussel harvesting. On November 21, PST levels exceeded the closure threshold and the area from Cape Blanco to the Oregon/California border was closed through much of December. An individual contracted paralytic shellfish poisoning from consuming mussels harvested during the August closure from Cape Blanco to the Oregon/California border. This is the second year in a row that mussel harvesting during a closure has resulted in illness.

Levels of domoic acid in Oregon Dungeness crab viscera remained below the regulatory threshold throughout 2025. The opening of the 2025-26 commercial crab season was delayed on the southern Oregon coast (Cape Falcon to the OR/CA border) to December 16, 2025 and on the northern Oregon coast until December 31, 2025 (Fig. 3.15). Both delays were due to low meat recovery in tests off southern Washington.

O.3 Domoic Acid and Paralytic Shellfish Toxins in California

Domoic acid closures persisted in 2025 for the recreational razor clam fishery in northern California (Fig. 3.14). The razor clam fishery closure in Del Norte County issued on November 9, 2023 lasted until July 30, 2025, and the razor clam fishery in Humboldt County issued on May 2, 2024 remained in effect through 2025 . The northern rock crab

fishery remained closed in one area due to domoic acid concerns since the November 2015 closure (see https://wildlife.ca.gov/fishing/ocean/health-advisories). Another 2015 rock crab closure area in the far north of California was able to finally open on April 24, 2025.

A major domoic acid and PST event in the Southern California Bight developed in early spring of 2025 and lasted more than 3 months (Fig. 3.14, Fig. O.1). The marine HAB event resulted in the strandings of thousands of marine mammals, particularly California sea lions and common dolphins. A PST-related health advisory warning against the consumption of sport-harvested bivalve shellfish from Santa Barbara County was instituted on March 20, 2025. A domoic acid bivalve advisory for Santa Barbara and Los Angeles counties was issued March 28, 2025. Additional counties along the Southern California Bight, Ventura, Orange and San Diego, had sport-harvested bivalve shellfish advisories issued in April 2025, due to both domoic acid and PST. The commercial shellfish harvester located in the Santa Barbara Channel was closed due to PST from March 18 to May 28, 2025. The sport harvest bivalve shellfish advisories were lifted June 5 for San Diego County, July 10 for Santa Barbara, Ventura and Los Angeles counties, and August 11 for Orange County. Additionally, a commercial and recreational fishery restriction was declared by the California Department of Fish and Wildlife on Pacific sardine in the southern California Bight (Pt Conception south to the CA/MX border) to the use as bait only from May 9, 2025 until June 13, 2025 based on samples that exceeded ≥ 20 ppm for domoic acid in the viscera and whole bodies. In May 2025, CDPH warned distributors and retailers of domoic acid toxicity from certain lots of frozen anchovies distributed from California and tied to landings from September 2024 in Monterey Bay.

During the fall of 2025, there were several sites that tested above domoic acid alert levels in the viscera (also known as guts) and meat of Dungeness crab. Domoic acid exceedances in the viscera (> 30 ppm) and meat (≥ 20 ppm) were detected at Manchester Beach in Mendocino County, Trinidad Head and Lagoons in Humboldt County, and George Reef in Del Norte County with exceedances of just the viscera (> 30 ppm) occurring at Klamath River, Del Norte County and northern Eureka, Humboldt County. The recreational Dungeness crab fishery was delayed in northern California from the CA/OR border (42° 0.00’ N) to the Sonoma/Mendocino County line (38° 46.125’ N). A partial opening of the entire closure area occurred on December 12, 2025 about six weeks after the recreational season start date of November 1, 2025 with some of these areas under health advisory. CDFW opened the recreational Dungeness crab fishery on 12/30/2025 in the remaining Humboldt County closed area [from the southern boundary of the Reading Rock State Marine Protected Areas (41° 17.6’ N) to Cape Mendocino (40° 10.0’ N). The CDPH health advisory for northern California to not eat crab viscera and to clean crab prior to cooking remains in effect. The commercial Dungeness crab fishery was delayed due to entanglement risk and meat quality testing (Fig. 3.15). The meat quality test was unable to be completed this year during the domoic acid event in northern California. The commercial fishery in central California was delayed due to the presence of high numbers of whales, particularly humpbacks. This is the seventh consecutive year that the commercial Dungeness crab fishery has been delayed in California because of marine mammal entanglement risk concerns. In one area of northern California, state health agencies determined that Dungeness crab have unhealthy levels of domoic acid and

recommended delaying the opening of the commercial fishery in that area. After 22 days from the delayed start date, the area between the southern boundary of the Reading Rock State Marine Protected Areas (41° 17.6' N) to Cape Mendocino (40° 10.0' N) was opened.

Appendix P — PORT-LEVEL REVENUE CONCENTRATION

The Theil index is an annual measure of how unevenly fishery revenue is distributed among ports (Theil 1967). It provides one approach to assessing whether access to fishing opportunities and associated revenues is becoming more concentrated in a smaller number of locations over time. Higher values of the index indicate greater concentration of revenue in fewer port groups.

Each year, we calculate the Theil index for total commercial fishing revenue and across FMPs at the scale of the 21 IO-PAC port groups (Leonard and Watson 2011). The resulting time series of Theil index values for total revenue and major management groups is shown in Fig. P.1 for the period 1981–2024. Across the full time series, the index for total commercial fishing revenue remains relatively low and stable, indicating that, in aggregate, commercial fishing revenues have not become substantially more geographically concentrated over the past four decades.

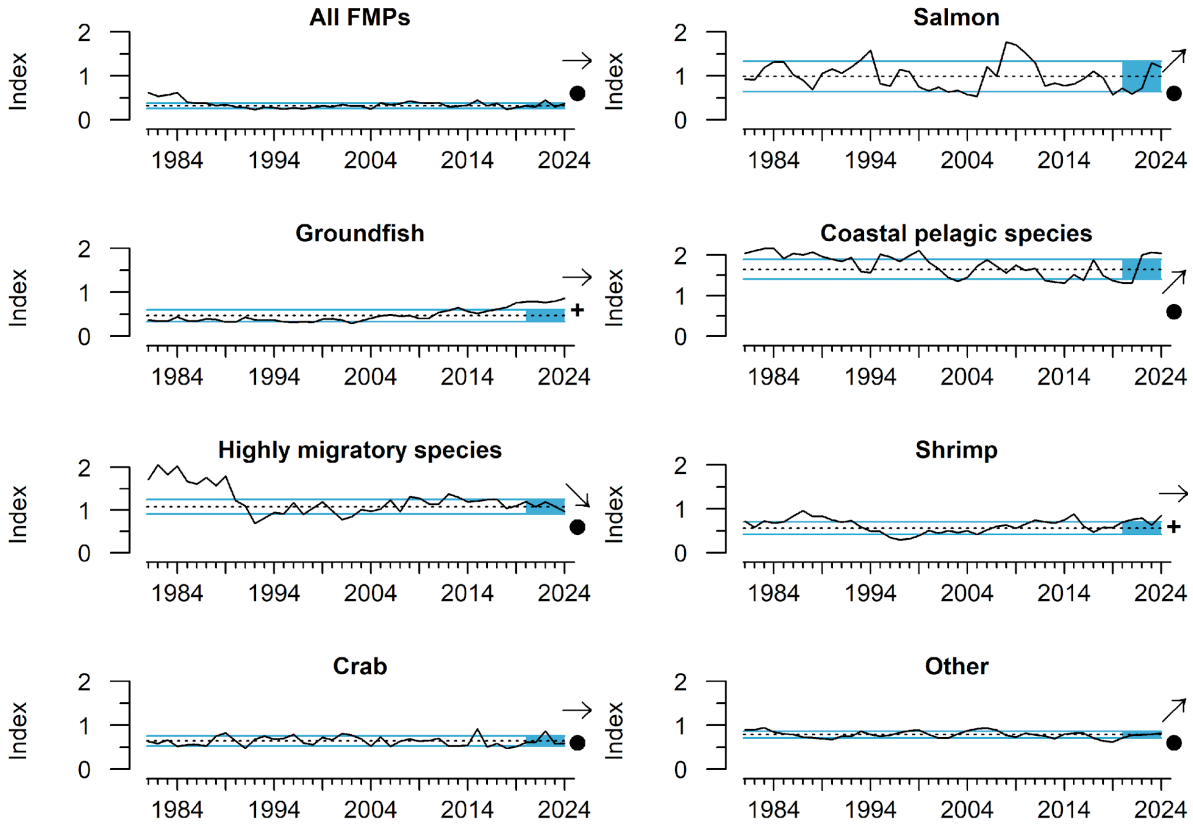


Figure P.1: Theil index estimation of commercial fishery revenue concentration in West Coast IO-PAC port groups, 1990 - 2024. Increasing values indicate greater concentration of revenue in a smaller number of port groups

When examined by management group, several management groups show notable revenue consolidation over time, while others remain relatively stable. Coastal pelagic species have

high interannual fluctuations reflecting variability in landings, market conditions, and management measures, however Theil index values have remained steadily high since 2022, suggesting revenues have stabilized in a smaller subset of port groups. Salmon fisheries continue to be impacted by geographic closures in California in 2023-2025, driving increases in the Theil index value. Groundfish revenue concentration shows a gradual increase over time; 2024 represents the highest level of groundfish revenue concentration in the time series. HMS fisheries, which have historically exhibited among the highest levels of concentration, show lower Theil index values in recent years relative to much of the past decade.

Appendix Q — SOCIAL VULNERABILITY OF COMMERCIAL and RECREATIONAL FISHING-DEPENDENT COMMUNITIES

Link to main section: Social Vulnerability

Community Social Vulnerability Index (CSVI) as an indicator of social vulnerability in coastal communities that depend upon commercial fishing was presented in Section 4.1 of the main report. To gain further insight into community vulnerability in relation to commercial fishing, fishing engagement per capita is presented below. Fishing engagement per capita should be interpreted alongside total fishing engagement when evaluating the role of fishing and social vulnerability in coastal communities. Engagement per capita highlights small communities where fishing activity represents a relatively large share of local activity, whereas total engagement reflects the absolute scale of fishing activity and infrastructure present in larger population centers. To provide this complementary perspective, Figure 4.1 presents commercial and recreational fishing engagement without standardizing by population, illustrating where fishing activity is concentrated across the California Current region. Together, Figure 4.1 and Figure Q.1 allow for consideration of both highly exposed small communities and major fishing hubs when assessing patterns of fishing dependence. Of note are the groupings of communities above and to the right of the dashed lines, which mark at least 1 standard deviation above the mean of both indices as averaged across all fishing communities.

Several communities appeared among the most highly engaged within their respective regions for either commercial or recreational fishing on a per capita basis in 2023 (Fig. Q.1). As in prior years, communities differed in their relative position along the engagement axis due in part to year-to-year variation in landings and participation. Communities may shift left or right on the x-axis in years with reduced fishing activity, which can give the appearance of lower engagement per capita even when underlying fishing infrastructure remains in place. These results therefore reflect relative positioning among communities rather than absolute levels of fishing activity and should be interpreted with care when making comparisons across years.

In 2023, communities in northern California continued to exhibit relatively high social vulnerability compared to other regions, with Crescent City, Fort Bragg, and Klamath among those combining elevated social vulnerability with moderate to high levels of commercial fishing engagement per capita (Fig. Q.1, left). In Washington, Westport remained among the most highly engaged communities on a per capita basis for commercial fishing, while other coastal communities clustered closer to regional means for social vulnerability. In Oregon, Port Orford continued to stand out for commercial fishing engagement per capita relative to other communities, whereas several communities with relatively high recreational fishing engagement per capita exhibited moderate social vulnerability (Fig. Q.1, right). Across regions, recreational fishing engagement per capita was generally higher in Washington and Oregon communities than in those in California.

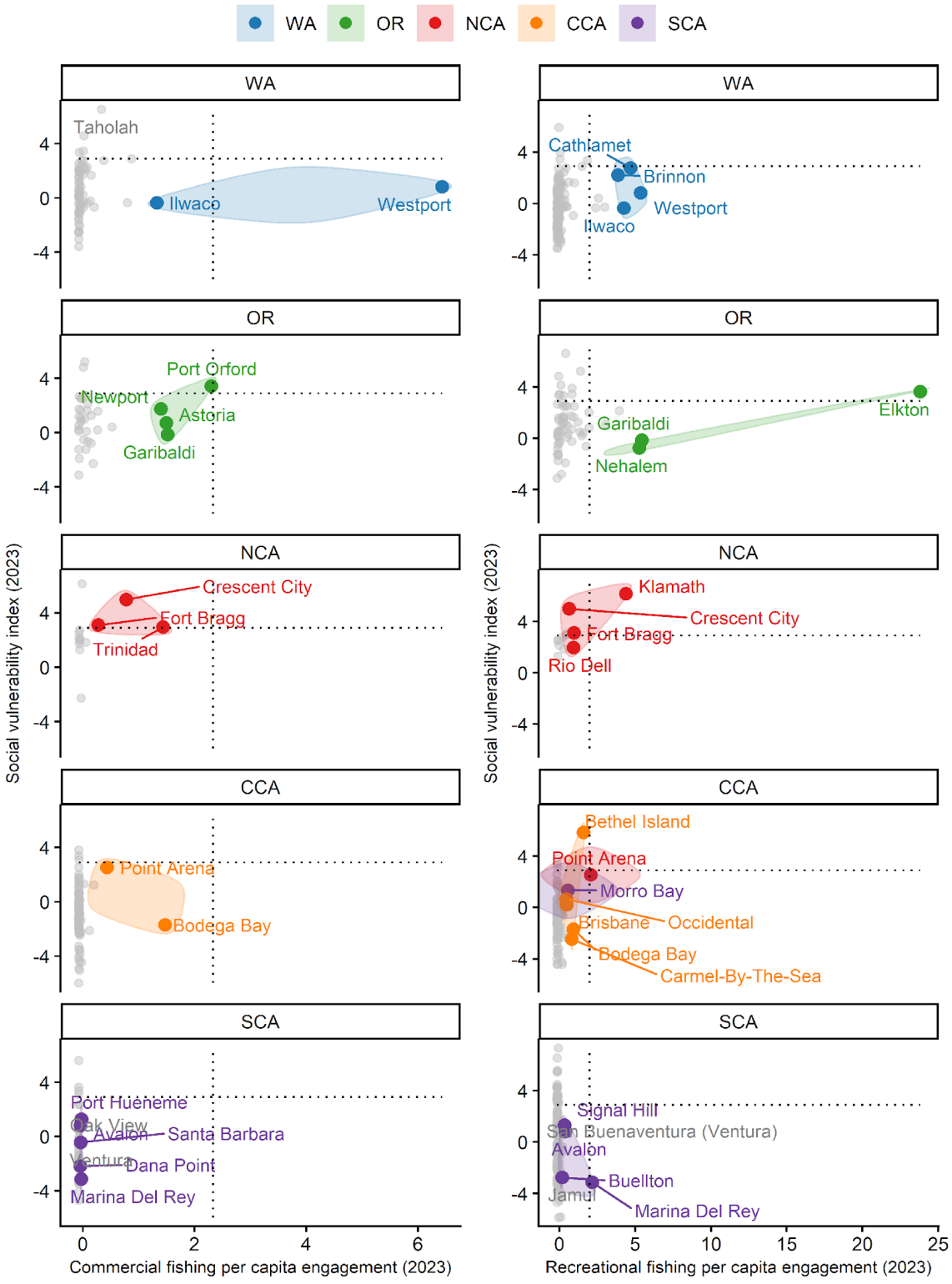


Figure Q.1: Commercial (left) and recreational (right) fishing reliance with social vulnerability scores in 2023 for communities in Washington, Oregon, and northern, central, and southern California. The five highest-scoring communities for fishing reliance are shown for each region. Dotted lines indicate 1 s.d. above the means for all communities.

Interpretation of Figure Q.1 should also consider limitations associated with calculating the Community Social Vulnerability Index (CSVI) at fine spatial scales. The CSVI requires complete sets of census-based indicators, and for very small census designated places (CDPs), one or more ACS variables, particularly housing characteristics and disruption, may be unavailable or suppressed. These data gaps occur most frequently in communities with very small populations, which are also the communities that can exhibit the highest fishing engagement per capita because of small population denominators. As a result, several highly fishing-engaged communities (e.g., Moss Landing, CA [population 34]; Tokeland, WA [99]; Winchester Bay, OR [184]; Jenner, CA [17]) are excluded from Figure Q.1 despite ranking among the most engaged communities coastwide on a per-capita basis. This limitation reflects constraints of census-based social indicators at small spatial scales rather than an absence of fishing dependence, and Figure Q.1 should therefore be interpreted as a screening of communities with available social vulnerability data rather than a comprehensive representation of all highly fishing-dependent communities.

The Community Social Vulnerability Index (CSVI) and fishing engagement indices are constructed independently for each year using Principal Component Analysis (PCA), following the approach of Jepson and Colburn (2013) and subsequent applications. Because PCA loadings are recalculated annually, index values are relative within each year and are not directly comparable across years. For this reason, the analyses in this report emphasize within-year spatial patterns rather than temporal trends.

Calculation of CSVI at fine spatial scales requires complete sets of census-based indicators. For very small census designated places (CDPs), one or more American Community Survey variables, particularly housing characteristics, and disruption, may be unavailable or suppressed. These data limitations most frequently affect very small communities that can exhibit high fishing engagement per capita because of small population denominators. As a result, some highly fishing-engaged communities are not represented in figures that combine engagement per capita with CSVI, reflecting constraints of census-based social indicators at small spatial scales rather than an absence of fishing dependence.

A national inter-regional working group is currently reviewing the construction and application of community vulnerability and fishing dependence indicators, including approaches for improving temporal comparability of index values across years. Ongoing work by this group is exploring alternative methods for addressing the time-series limitations inherent in annually re-estimated PCA-based indices and for improving coverage of small communities in census-based social vulnerability measures.

Appendix R — FLEET DIVERSIFICATION INDICATORS FOR MAJOR WEST COAST PORTS

Link to main section: Diversification of Fisheries Revenue

Catches and prices from many fisheries exhibit high interannual variability, leading to high variability in fisher's revenue, but variability can be reduced by diversifying activities across multiple fisheries or regions (Kasperski and Holland 2013). Individuals may have good reasons to specialize, including reduced costs or greater efficiency; thus while diversification may reduce income variation, it does not necessarily promote higher average profitability.

We use the Effective Shannon Index (ESI) to examine diversification of fishing revenue for more than 28,000 vessels fishing off the West Coast and Alaska over the last 40 years. In the main body of the report (Fig. 4.2), ESI increases as revenues are spread across more fisheries; ESI = 1 when a vessel's revenues are from a single species group and region; ESI = 2 if revenues are spread evenly across 2 fisheries; ESI = 3 if revenues are spread evenly across 3 fisheries; and so on. If revenue is not evenly distributed across fisheries, then the ESI value is lower than the number of fisheries a vessel enters.

There has been a moderate decline in average fishery diversification since the mid-1990s or earlier for most vessel classifications (see main report, Fig. 4.2). Changes in diversification are due both to entry and exit of vessels and changes for individual vessels. Although vessels remaining in the fishery have become less diverse on average over time, less diversified vessels have been more likely to exit and newer entrants have generally been more diversified than those who left (Abbott et al. 2023). Within the average trend there are wide ranges of diversification levels and strategies, and some vessels remain highly diversified.

As is true with individual vessels, the variability of landed value at the port level is reduced with greater diversification of landings. Revenue diversification scores are highly variable year-to-year for some ports, making it difficult to discern trends. Some major ports have seen long-term declines in fishery diversification. Changes in diversification of ports in 2024 relative to 2023 varied from negative to positive but diversification generally remained lower than levels prior to 2000. (Fig. R.1).

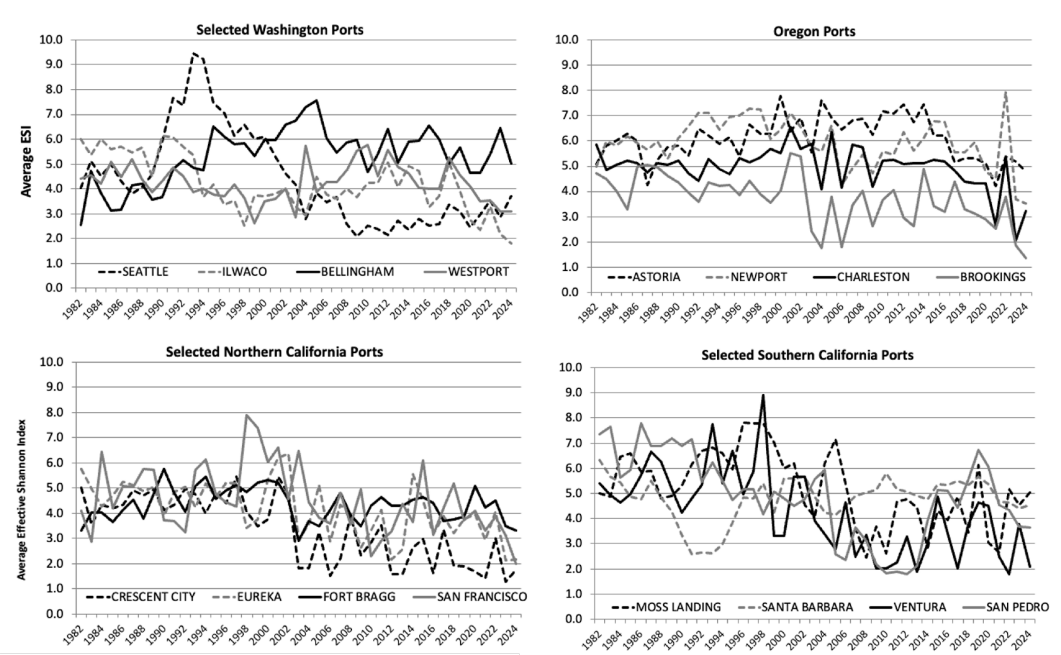


Figure R.1: Trends in fishery revenue diversification in major U.S. West Coast ports, grouped by state. Data from D. Holland (NMFS/NWFSC) and S. Kasperski (NMFS/AFSC).

Appendix S — FISHERIES PARTICIPATION NETWORKS

Link to main section: Fishery participation networks

Fisheries participation networks add levels of detail or context to other analyses in this report, such as those related to community vulnerability, fishery diversification, and port-level revenue concentration. As such, fisheries participation networks offer one way to respond to requests from the EAS and EWG for deeper characterization of social and economic conditions in West Coast fishing communities, information relevant to meeting NS-8 under the Magnuson–Stevens Act, and may be informative for PFMC Special Project 2.

We developed vessel-level fisheries participation networks, which provide a visual representation of the portfolio of fisheries that are economically-important to individual vessels within a port group (Fuller et al. 2017; Fisher et al. 2021). The networks are derived from landings receipts and summarized annually from week 46 in one year through week 45 in the following year (e.g., week 46 of November 2020 to week 45 of November 2021) to capture the beginning of the Dungeness crab fishing season. Fisheries landings data were retrieved from the Pacific Fisheries Information Network (PacFIN; http://pacfin.psmfc.org) database. We note that in Washington, fish tickets include a port assigned based on the actual port of landing or derived from the license database; prior to 2018, most port data were derived (Table S.1).

To focus the analysis on vessels that derive a substantial amount of income from commercial fishing, we include only vessels that generate at least $5,000 annually (adjusted for inflation from 2005 USD) in total fisheries revenue. In addition, vessels must generate at least $500 (adjusted for inflation from 2005 USD) of revenue from a given fishery (node) to be included as participants in that fishery. We assume that economically-important fisheries are those that contribute to at least a median of 10% of the annual revenue of associated vessels. Vessels are represented in all port groups for which their landings meet these conditions. To maintain confidentiality, we include only fisheries with at least three vessels participating in a port group.

Tracking changes in networks over time may support Council activities by providing insight into how fishing communities are changing and potentially adapting to external forces such as changing stock availabilities, environmental conditions, regulations (such as rebuilding plans), and economic and social systems. To that end, we present time series for each port group of the number of fisheries (Fig. S.1) and of a network metric called Edge Density within the participation networks from 2004-2025 (Fig. S.2). The number of fisheries indicates how varied the types of economically-important, commercial fishing opportunities are within a port group (the nodes in the networks in figures S.3-S.6). Edge Density, which we refer to below as connectivity, represents the extent to which nodes within a network are connected (the lines in the networks in figures S.3-S.6) by vessels that participate in multiple fisheries. Declines in Edge Density imply less well-connected fisheries and a simplification of network structure, which can in turn reduce resilience to environmental or regulatory shocks (e.g., Fisher et al. 2021). In contrast, networks with high edge density suggest that fishers have greater ability to move effort between fisheries and thus substitute for lost revenue from a fishery that is closed or has a poor year.

Table S.1: Summary of WDFW landings receipts (fish tickets), indicating the percentage of receipts, landings, and revenue that included port information that was not derived, derived, or unknown. Note that if a landing port is derived from the license database, it does not always mean it is an error. Most of the time, the address on the license reflects their home port, the port they use most often (T. Tsou, personal communication). Years refer to crab years, as in the Fisheries Participation Networks (e.g., 2023 reflects November 2022 (week 46) - November 2023 (week 45)).

	Not Port Derived			Port Derived			Unknown if Port Derived		
Year	% of tickets	% of landings	% of revenue	% of tickets	% of landings	% of revenue	% of tickets	% of landings	% of revenue
2004	0.00	0.00	0.00	88.80	81.70	56.90	11.20	18.30	43.10
2005	0.00	0.00	0.00	98.10	89.90	69.00	1.90	10.10	31.00
2006	0.00	0.00	0.00	98.20	90.60	67.00	1.80	9.40	33.00
2007	0.00	0.00	0.00	98.10	88.70	65.70	1.90	11.30	34.30
2008	0.00	0.00	0.00	98.10	87.70	68.80	1.90	12.30	31.20
2009	0.00	0.00	0.00	98.20	88.20	66.80	1.80	11.80	33.20
2010	0.00	0.00	0.00	98.40	89.10	71.20	1.60	10.90	28.80
2011	0.00	0.20	0.00	98.60	90.00	74.70	1.30	9.90	25.30
2012	0.20	0.40	0.00	98.40	89.80	73.80	1.40	9.80	26.10
2013	0.00	0.00	0.00	98.40	91.50	72.00	1.60	8.50	28.00
2014	0.00	0.00	0.00	98.50	88.50	72.70	1.50	11.50	27.30
2015	0.10	0.00	0.10	98.00	86.00	71.60	1.90	13.90	28.30
2016	0.70	3.90	0.30	96.60	83.30	71.00	2.70	12.80	28.70
2017	17.90	50.60	4.30	74.50	38.70	66.20	7.60	10.80	29.40
2018	19.10	50.30	4.30	45.90	25.50	35.30	35.10	24.20	60.30
2019	25.50	63.00	18.20	38.20	13.20	20.50	36.30	23.80	61.40
2020	23.50	72.80	26.10	33.10	6.20	17.50	43.50	21.00	56.40
2021	25.30	71.70	26.10	33.00	10.00	19.30	41.80	18.30	54.50
2022	20.20	66.60	36.20	37.10	10.00	15.90	42.70	23.40	47.90
2023	24.50	71.20	35.20	33.60	7.50	14.40	41.90	21.30	50.50
2024	25.30	67.60	44.80	25.40	6.60	12.70	49.40	25.80	42.50
2025	28.60	76.20	58.00	19.20	4.20	9.20	52.20	19.70	32.90

Temporal patterns for the number of fisheries in a network vary widely across port groups, and the range of variability spans from roughly ±1 fishery (e.g., Puget Sound) to 5 or 6 fisheries for several port groups (Fig. S.1). While all port groups show year-to-year variation, most have not experienced significant increases or decreases over the most recent five years; two port groups show significant short-term increases (Astoria, Bodega Bay), and six port groups saw short-term decreases (Puget Sound, Tillamook, Coos Bay,

Eureka, Fort Bragg, Morro Bay). Relative to the full two-decade time series, the WA Coast, Astoria and San Francisco port groups have had fewer fisheries on average over the past five years, while San Diego has participated in more fisheries on average.

Edge Densities also varied through time and by port group (Fig. S.2). Four port groups experienced increased Edge Density over the last five years (WA Coast, Astoria, Morro Bay, Santa Barbara), while eight port groups experienced decreases in the same time period (Puget Sound, Newport, Brookings, Crescent City, Eureka, Bodega Bay, Monterey, Los Angeles).

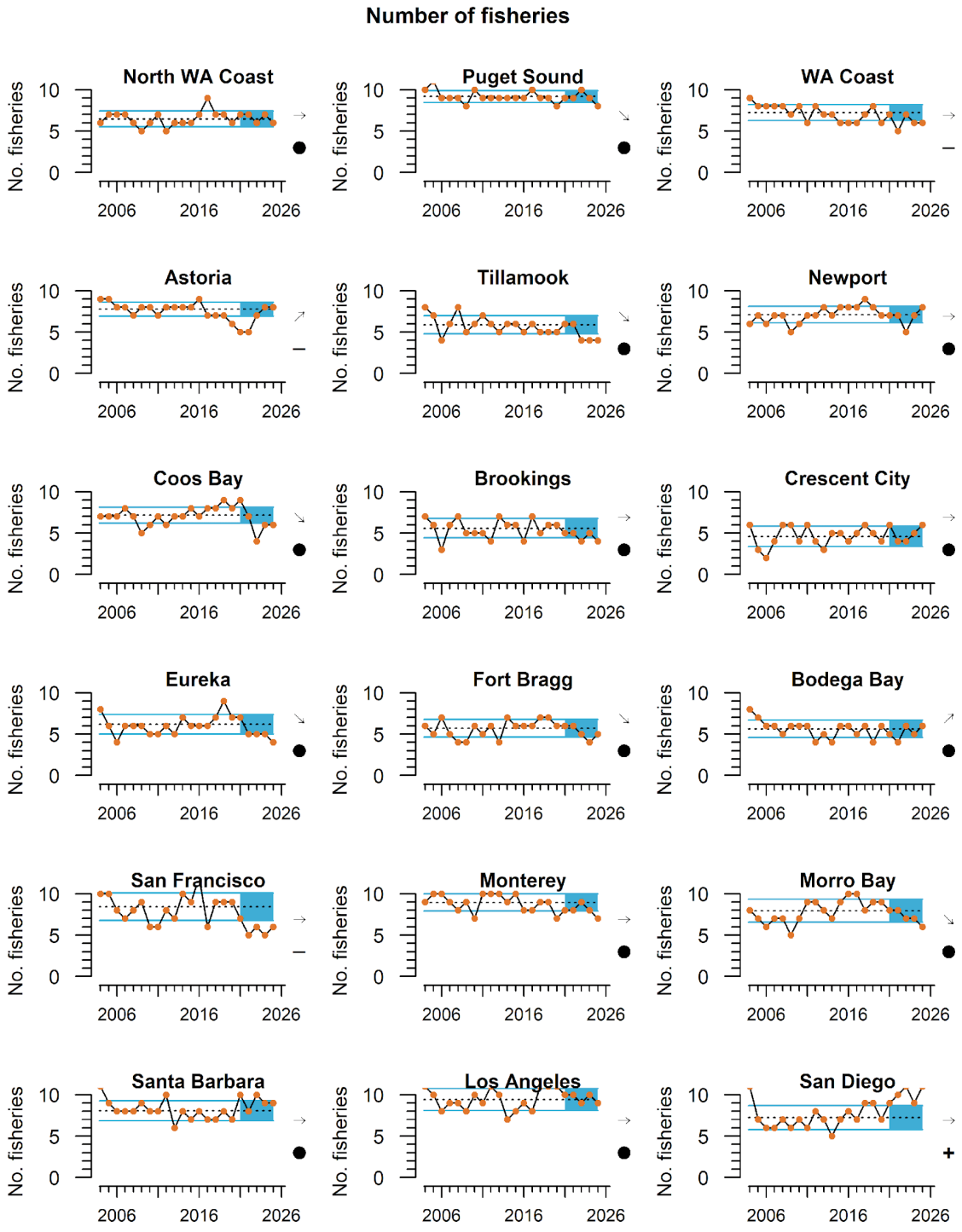


Figure S.1: The number of fisheries (nodes) represented in fisheries participation networks for IO-PAC port groups from November 2004-November 2025. More fisheries indicate greater variation in the types of commercial fishing opportunities within a port group. Each year represents landings from November of the previous year through November of the labeled year (i.e., the 2025 crab year runs from November 2024-November 2025). The following port groups are not shown: Other Coastal Washington, Columbia River, and Unknown Ports. Data and analyses provided by J. Samhouri (NMFS/NWFSC), with data derived from PacFIN (http://pacfin.psmfc.org)

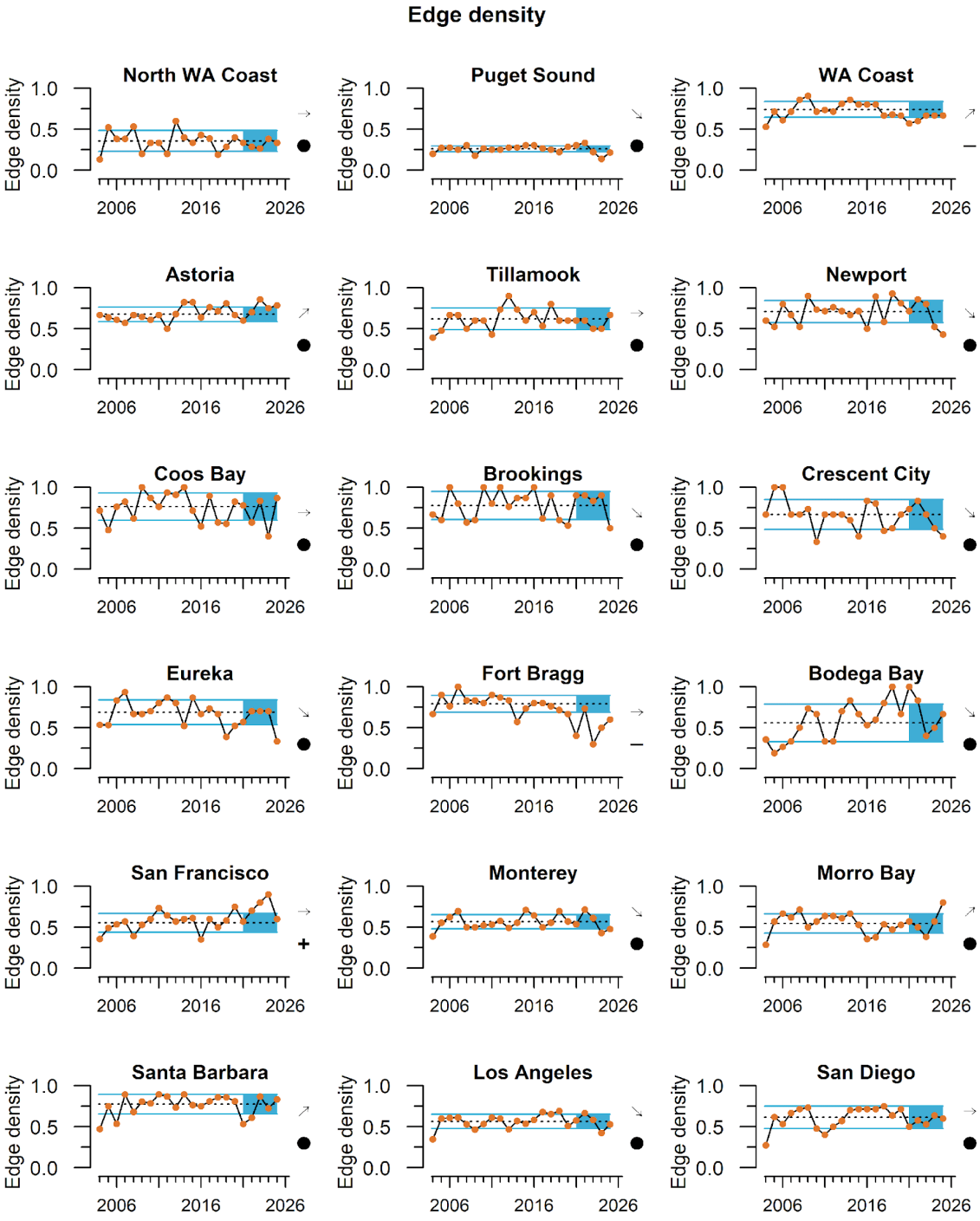


Figure S.2: Edge Density in fisheries participation networks for IO-PAC port groups from November 2004-November 2025. Higher edge densities correspond to greater connectivity in fishery participation among all vessels represented in the network. Note that edge density scales with network size (it is easier to achieve a high density in a low complexity network), so comparisons across networks of different sizes should be interpreted carefully.

In network graphs, node size represents the median proportional contribution of a fishery to annual vessel-level revenue; it is scaled relative to the fishery with the maximum median proportional contribution to annual vessel-level revenue in each network, summarized by port group. Therefore, node sizes are not comparable across port groups, only within them. The edges connecting pairs of nodes indicate that vessels participate in both fisheries. The widths of the edges between nodes increase with more vessels participating in a pair of fisheries, the amount of revenue those fisheries generate, and the more equally revenue is split between the fisheries (Fuller et al. 2017). As with node sizes, edge widths are not comparable across port groups, only within them.

Fisheries participation networks representing IO-PAC port groups in the past year (November 2024 to November 2025) consisted of one to nine fisheries nodes, with 0–21 links between the fisheries within each network (Figs. S.3-S.6); all IO-PAC port groups are illustrated in these figures except for Other Coastal WA and Unknown Ports. Section 4.3 of the main report describes how networks for several port groups changed relative to prior years.



Figure S.3: Fisheries participation networks for IO-PAC port groups in Washington, based on November 2024-November 2025 (a Dungeness crab year) landings receipts. Node size is proportional to the median contribution of a given fishery to annual vessel-level revenue; values in parentheses are the number of vessels participating in the fishery. Thickness of lines ("edges") is proportional to the number of vessels participating in both of the fisheries connected by the lines, and the evenness of revenue generated by each fishery in the pair. Data and analyses provided by J. Samhouri (NMFS/NWFSC), with data derived from PacFIN (http://pacfin.psmfc.org).

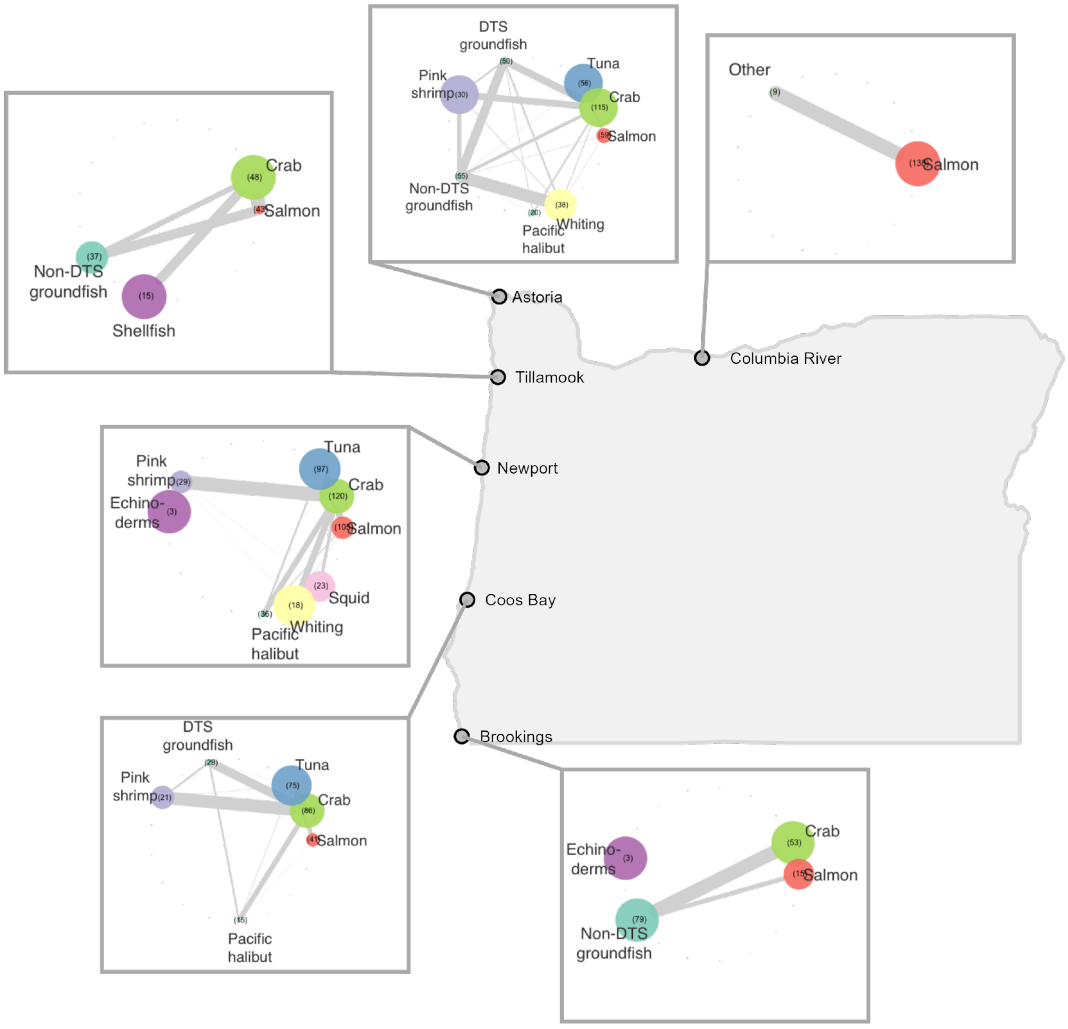


Figure S.4: Fisheries participation networks for IO-PAC port groups in Oregon, based on November 2024-November 2025 (a Dungeness crab year) landings receipts. Node size is proportional to the median contribution of a given fishery to annual vessel-level revenue; values in parentheses are the number of vessels participating in the fishery. Thickness of lines ("edges") is proportional to the number of vessels participating in both of the fisheries connected by the lines, and the evenness of revenue generated by each fishery in the pair. Data and analyses provided by J. Samhouri (NMFS/NWFSC), with data derived from PacFIN (http://pacfin.psmfc.org).

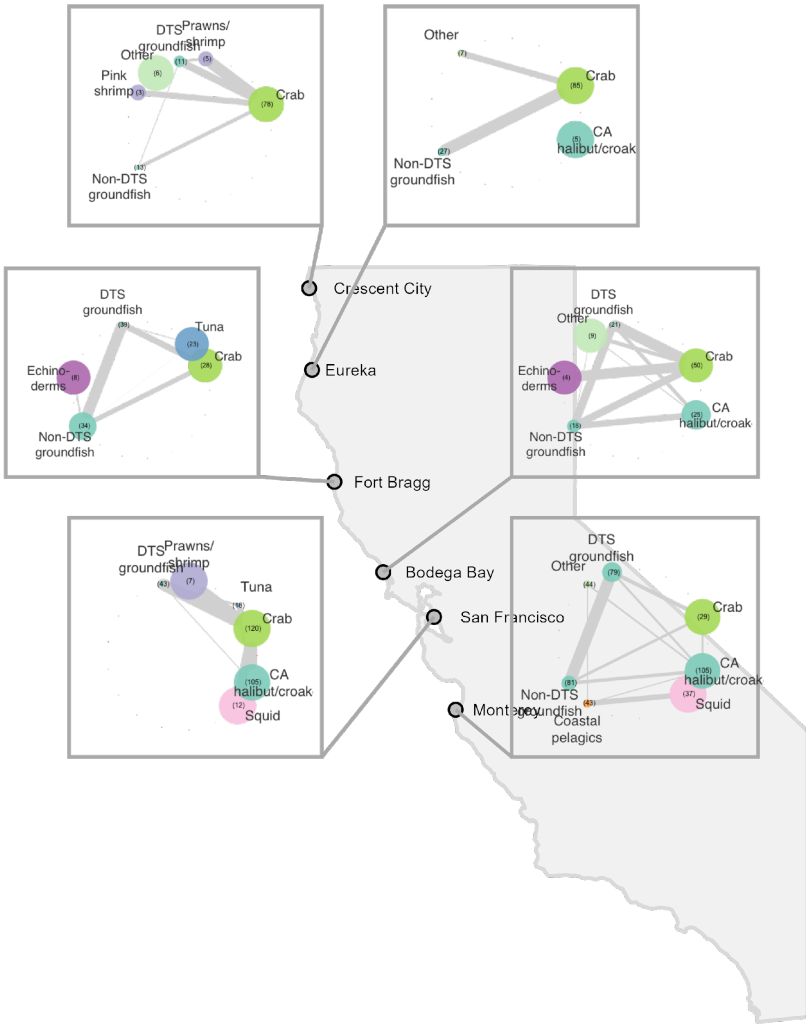


Figure S.5: Fisheries participation networks for IO-PAC port groups in Northern California, based on November 2024-November 2025 (a Dungeness crab year) landings receipts. Node size is proportional to the median contribution of a given fishery to annual vessel-level revenue; values in parentheses are the number of vessels participating in the fishery. Thickness of lines ("edges") is proportional to the number of vessels participating in both of the fisheries connected by the lines, and the evenness of revenue generated by each fishery in the pair. Data and analyses provided by J. Samhouri (NMFS/NWFSC), with data derived from PacFIN (http://pacfin.psmfc.org).

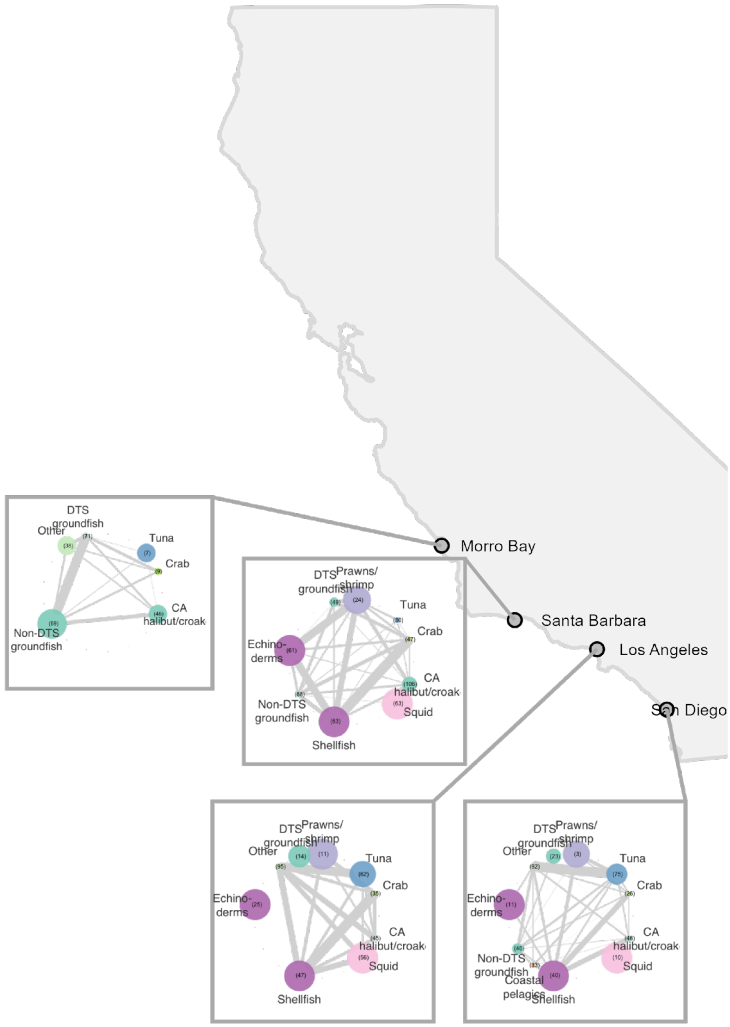


Figure S.6: Fisheries participation networks for IO-PAC port groups in Southern California, based on November 2024-November 2025 (a Dungeness crab year) landings receipts. Node size is proportional to the median contribution of a given fishery to annual vessel-level revenue; values in parentheses are the number of vessels participating in the fishery. Thickness of lines ("edges") is proportional to the number of vessels participating in both of the fisheries connected by the lines, and the evenness of revenue generated by each fishery in the pair. Data and analyses provided by J. Samhouri (NMFS/NWFSC), with data derived from PacFIN (http://pacfin.psmfc.org).

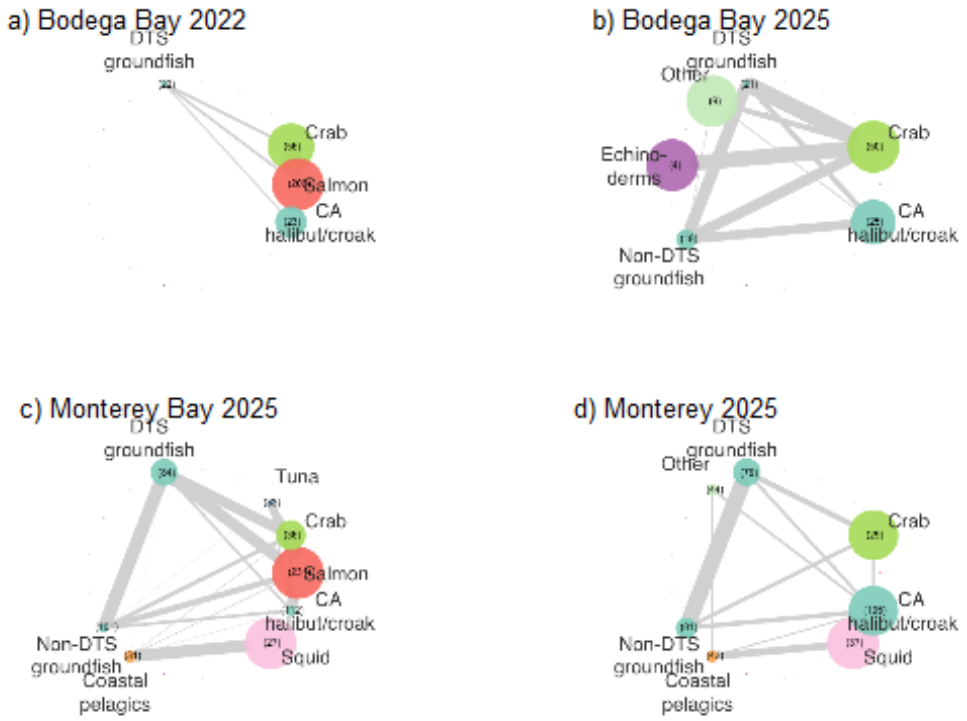


Figure S.7: Fisheries participation networks for IO-PAC port groups in Bodega Bay and Monterey Bay, California, based on November 2021-November 2022 and November 2024-November 2025 landings receipts. Node size is proportional to the median contribution of a given fishery to annual vessel-level revenue; values in parentheses are the number of vessels participating in the fishery. Thickness of lines ("edges") is proportional to the number of vessels participating in both of the fisheries connected by the lines, and the evenness of revenue generated by each fishery in the pair. Data and analyses provided by J. Samhouri (NMFS/NWFSC), with data derived from PacFIN (http://pacfin.psmfc.org).

Appendix T — STATE-BY-STATE FISHERY LANDINGS AND REVENUES

Link to main section: Coastwide Landings by Major Fisheries

The Council and EWG have requested information on state-by-state fisheries landings and revenues; these values are presented here. Commercial landings and revenue data are best summarized by the Pacific Fisheries Information Network (PacFIN; pacfin.psmfc.org), and recreational landings are best summarized by the Recreational Fisheries Information Network (RecFIN; www.recfin.org). Data from 1981 to 2025 were downloaded from PacFIN and RecFIN on January 1, 2026. Landings provide the best long-term indicator of fisheries removals. Revenues are calculated based on consumer price indices in 2025 dollars. Status and trends are estimated relative to a frame of reference of 1991-2020.

T.1 State-by-State Landings

Total fisheries landings in Washington increased 2% in 2025 from 2024, but showed no overall trend and were >1 s.d. below the long-term average over the last five years, with the three lowest values in the time series observed in 2023, 2024 and 2025 (Fig. T.1). These fisheries-wide patterns were driven primarily by landings of Pacific whiting over the last five years and across the entire time series. Commercial shrimp landings were >1 s.d. above the long-term average, while salmon and Pacific whiting landings were >1 s.d. below the long-term average. All other major commercial fisheries showed no trends and were within 1 s.d. of the long-term average from 2021 to 2025.

Total landings of recreational catch data (excluding salmon and halibut) in Washington were complete through October 2025 and varied within 1 s.d. of the long-term average from 2021 to 2025 (Fig. T.1). Recreational landings of Chinook and coho salmon were within 1 s.d. of the long-term average from 2020 to 2024 (2025 data were not available at time of report).

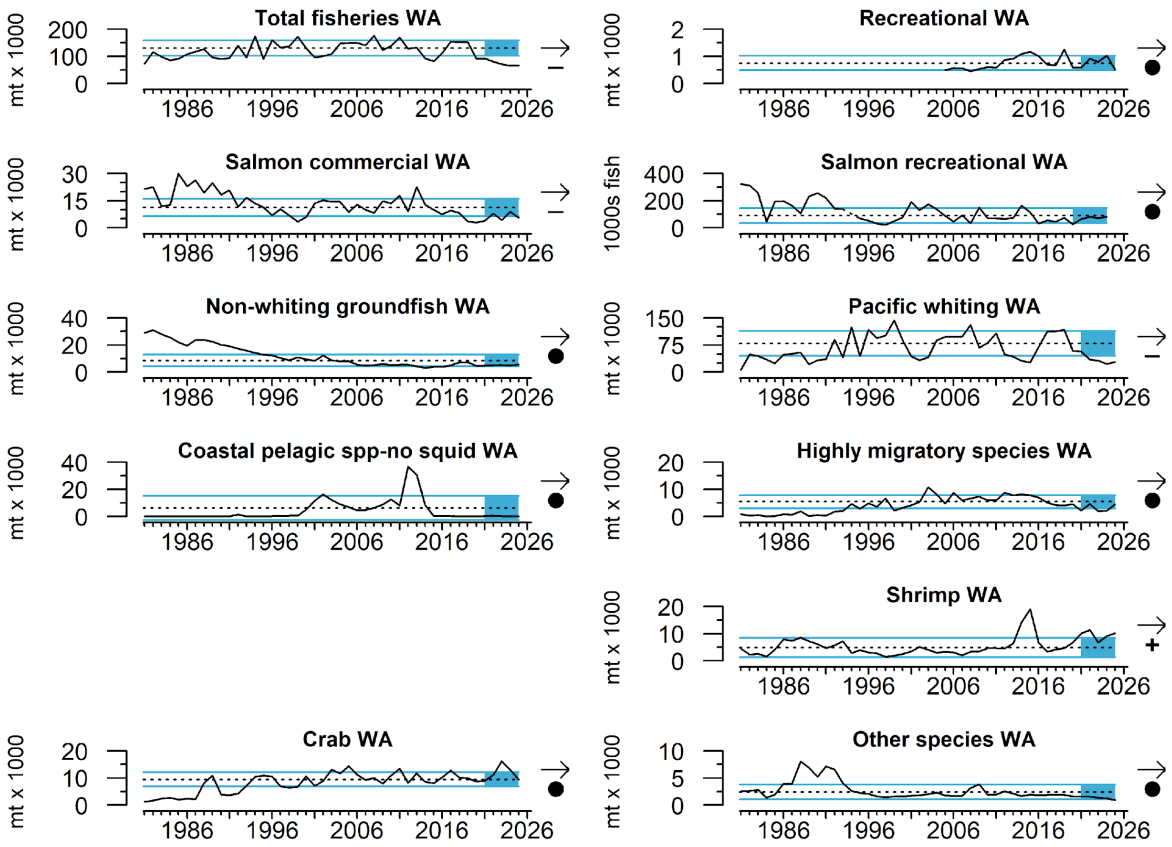


Figure T.1: Annual Washington landings from West Coast commercial (data from PacFIN) and recreational (data from RecFin) fisheries, including total landings across all fisheries from 1981 - 2025. Lines, colors, and symbols are as in Fig. 2.1.

Total fisheries landings in Oregon increased 36% in 2025 from 2024, and were >1 s.d. above the long-term average from 2021 to 2025 (Fig. T.2). Similar to Washington, these patterns were driven primarily by landings of Pacific whiting. Commercial landings of highly migratory species increased, while landings of market squid decreased by >1 s.d. of the long-term average from 2021 to 2025. Landings of shrimp and Pacific whiting were >1 s.d. above the long-term average. Landings of market squid in Oregon ports have increased slightly since 2023, but remain well below landings that occurred between 2016 and 2022. Landings of all other commercial fisheries showed no significant recent trends and had short-term averages within 1 s.d. of long-term averages.

Recreational fisheries landings data (excluding salmon and Pacific halibut) in Oregon were complete through October 2025, showed no significant trend, and varied within 1 s.d. of the long-term average from 2021 to 2025 (Fig. T.2). Recreational landings of Chinook and coho salmon showed no significant recent trend, and were within 1 s.d. of the long-term average since 2020 (2025 data were not available at time of report).

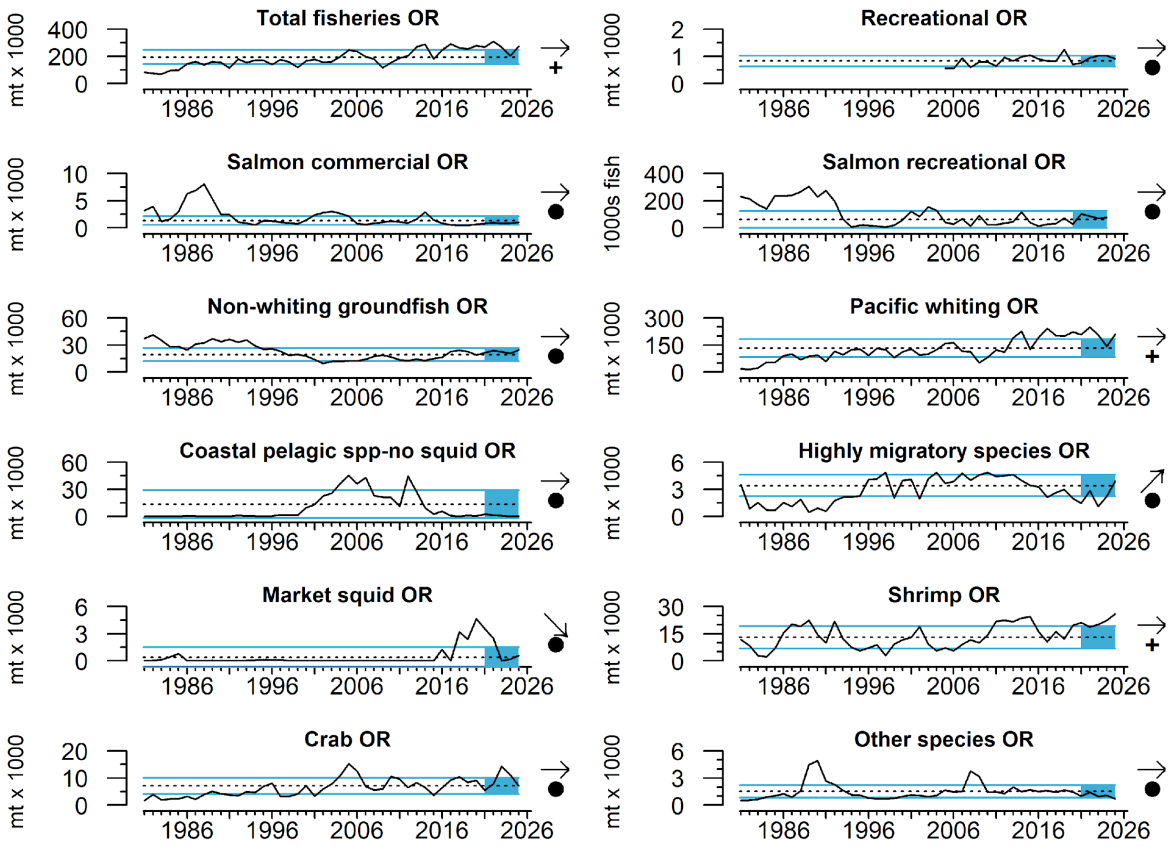


Figure T.2: Annual Oregon landings from West Coast commercial (data from PacFIN) and recreational (data from RecFin) fisheries, including total landings across all fisheries from 1981 - 2025. Lines, colors, and symbols are as in Fig. 2.1.

Total fisheries landings in California increased 21% in 2025 from 2024, but were >1 s.d. below the long-term average from 2021 to 2025 (Fig. T.3). Landings for CPS finfish, shrimp and Other species were >1 s.d below the long-term average over the last five years. Commercial salmon landings decreased by >1 s.d. of the long-term average because the fishery was closed in 2023-2025. All other major fisheries showed no significant trends and were within 1 s.d. of long-term averages over the last five years.

Recreational landings data (excluding salmon, Pacific halibut and HMS) in California were complete through October 2025. Recreational landings decreased by >1 s.d. of the long-term average and were >1 s.d. below the long-term average over the past five years (Fig. T.3). The low status level was largely due to relatively low levels of landings for lingcod and vermilion rockfish over the last five years. Similar to commercial fisheries, the recreational salmon fishery in California was closed in 2023 and 2024, but was opened for very limited recreational fishing opportunities in 2025 (2025 data were not available at time of report).

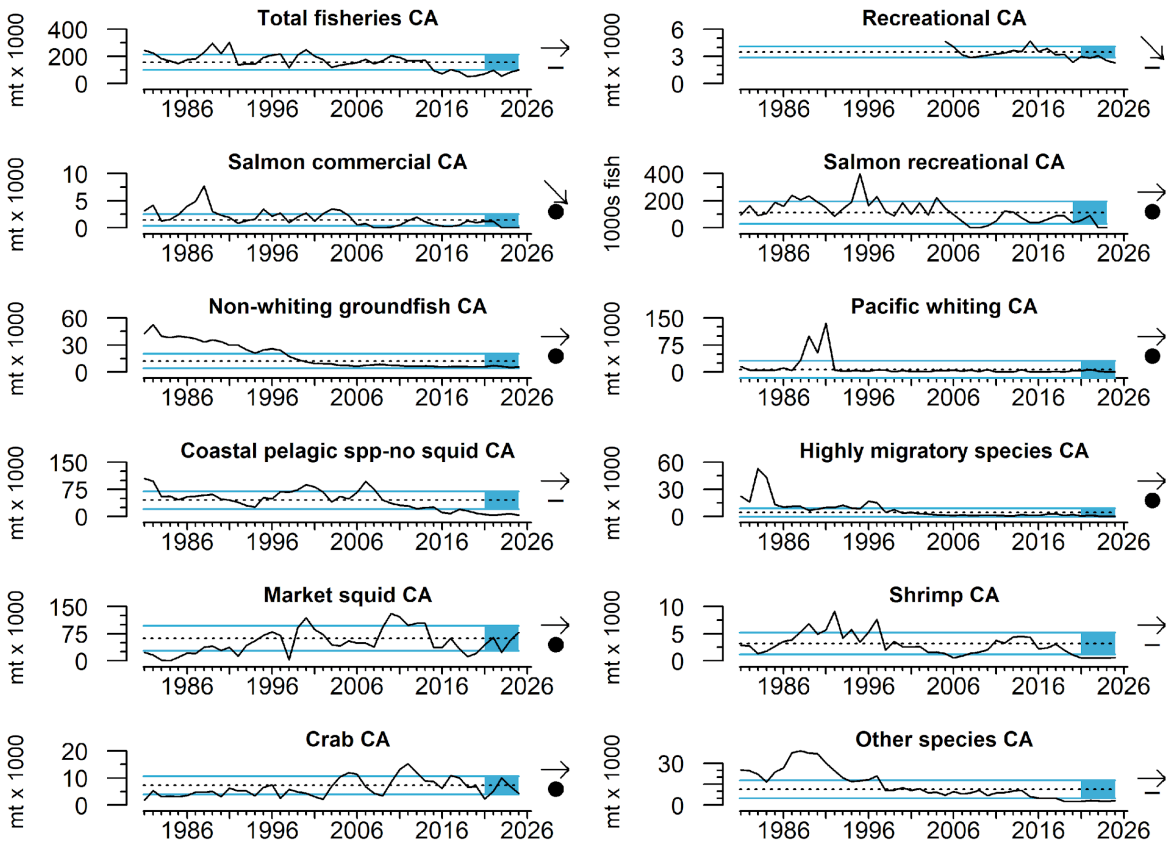


Figure T.3: Annual California landings from West Coast commercial (data from PacFIN) and recreational (data from RecFin) fisheries, including total landings across all fisheries from 1981 - 2025. Lines, colors, and symbols are as in Fig. 2.1.

T.2 Commercial Fisheries Revenue

Total revenue across U.S. West Coast commercial fisheries in 2025 increased by 6% from 2024, based on data currently available (Fig. T.4). Over the most recent five years, total revenue was highly variable, but remained within 1 s.d. of the long-term average. Recent revenue patterns have been driven by large variation in market squid and Pacific whiting revenues and smaller one- or two-year changes in crab and HMS revenues since 2021. Revenue for 5 of 9 commercial fisheries increased from 2024 to 2025 (ordered by 2025 revenue): market squid (20%), Pacific whiting (53%), non-whiting groundfish (36%), shrimp (3%), and HMS (118%). In contrast, Other species (-13%) and CPS finfish (-19%) fisheries generated less revenue in 2025 than in 2024, while crab (0%) and salmon (0%) fisheries revenue in 2025 were the same as 2024. Commercial revenue for salmon and CPS finfish fisheries decreased by >1 s.d. of their long-term average from 2021 to 2025. Revenue from crab fisheries was >1 s.d. above long-term averages, while salmon, non-whiting groundfish, CPS finfish, and HMS revenue was >1 s.d. below long-term averages over the last five years. All other fisheries' revenues showed no trends and were within 1 s.d. of long-term averages.

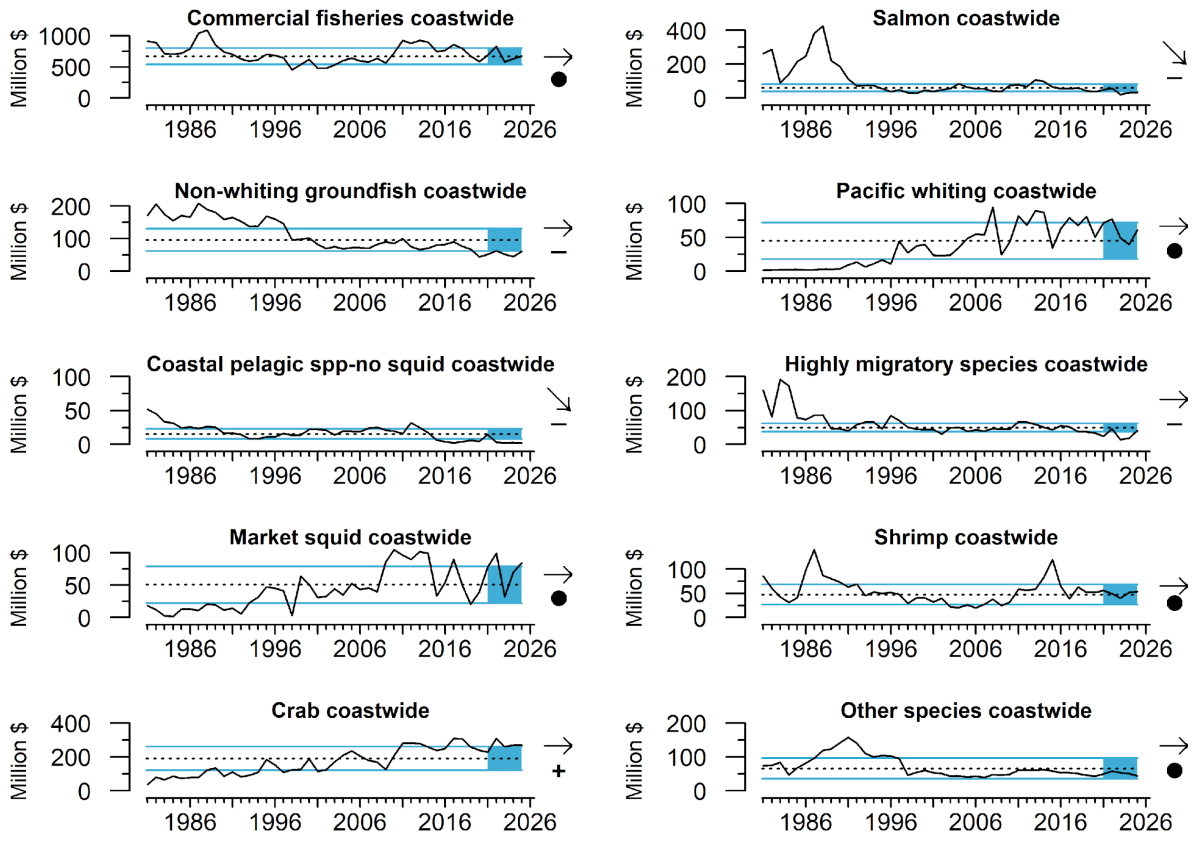


Figure T.4: Annual coastwide revenue (ex-vessel value in 2025 dollars) from West Coast commercial fisheries (data from PacFin) from 1981 - 2025. Whiting revenue includes shoreside and at-sea values from PacFIN, NORPAC (North Pacific Groundfish Observer Program) and NMFS Office of Science & Technology. Lines, colors, and symbols are as in Fig. 2.1.

Total revenue across commercial fisheries in Washington decreased from 2021 to 2025, with a 9% decrease in 2025 from 2024 (Fig. T.5). These patterns were largely driven by variability in revenue from crab, shrimp and HMS landings over the last five years. Overall, 4 of 8 major fisheries increased in revenue in 2025 from 2024 levels (in order of 2025 revenue): HMS (171%), non-whiting groundfish (78%), Pacific whiting (77%), and CPS finfish (1%). In contrast, revenue from crab (-6%), salmon (-13%), shrimp (-10%), and Other species (-1%) fisheries was lower in 2025 compared to 2024. Crab fisheries' revenue was >1 s.d. above long-term averages, while non-whiting groundfish revenue was >1 s.d. below long-term averages. All other fisheries showed no trends and were within long-term averages over the last five years.

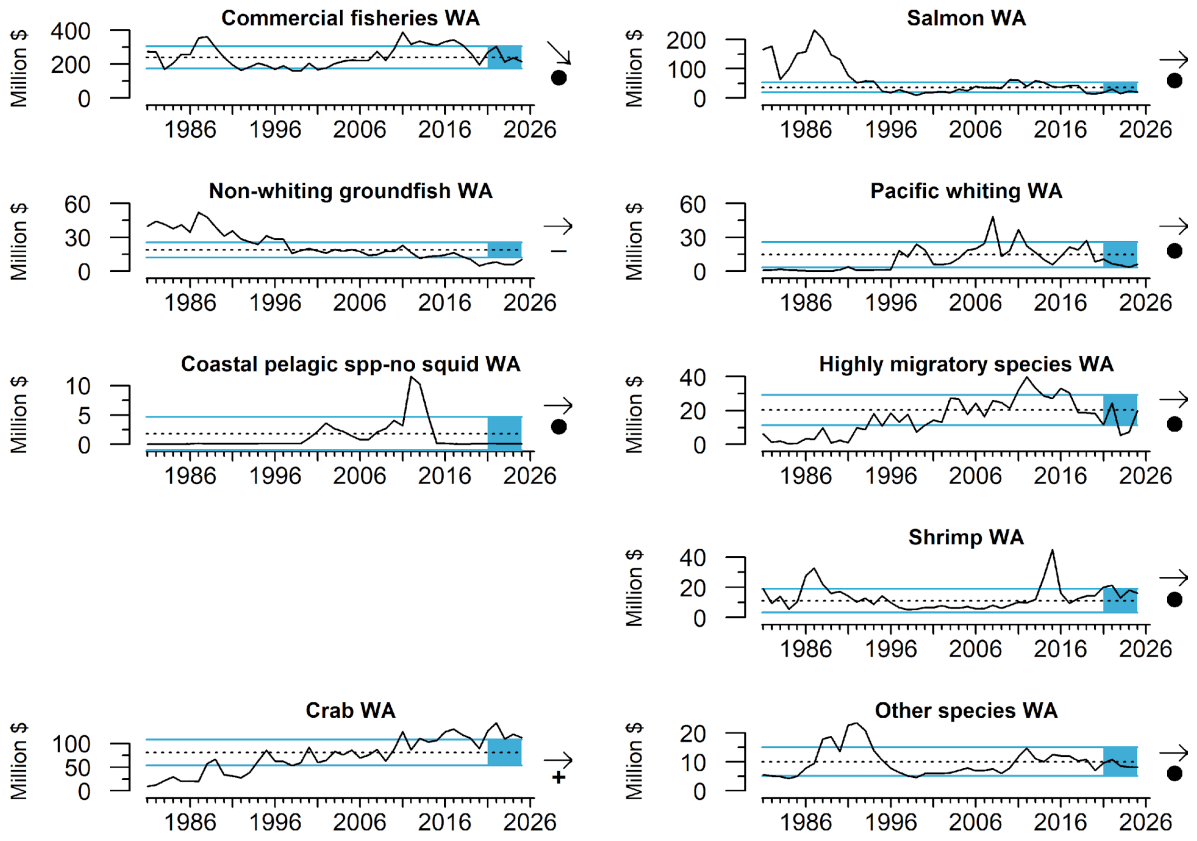


Figure T.5: Annual Washington revenue (ex-vessel value in 2025 dollars) from West Coast commercial fisheries (data from PacFin) from 1981 - 2025. Whiting revenue includes shoreside and at-sea values from PacFIN, NORPAC (North Pacific Groundfish Observer Program) and NMFS Office of Science & Technology. Lines, colors, and symbols are as in Fig. 2.1.

Total revenue across commercial fisheries in Oregon increased by 22% in 2025 from 2024 levels, but showed no overall trend and was within 1 s.d. of the long-term average over the last five years (Fig. T.6). These patterns were largely driven by changes in revenue from crab and Pacific whiting fisheries over the last five years. Overall, all 9 major fisheries increased in revenue in 2025 from 2024 levels (in order of 2025 revenue): crab (1%), Pacific whiting (50%), non-whiting groundfish (39%), shrimp (7%), HMS (109%), salmon (38%), Other species (17%), market squid (192%), CPS finfish (568%). Even though there was a relatively large year-to-year increase in revenue observed in the CPS finfish, revenue levels have been consistently at very low values over the last decade. Pacific whiting and crab fisheries' revenue were >1 s.d. above long-term averages, while non-whiting groundfish was >1 s.d. below its long-term average. Revenue from market squid and Other species fisheries decreased by >1 s.d. of its long-term average, while all other fisheries showed no trends over the last five years.

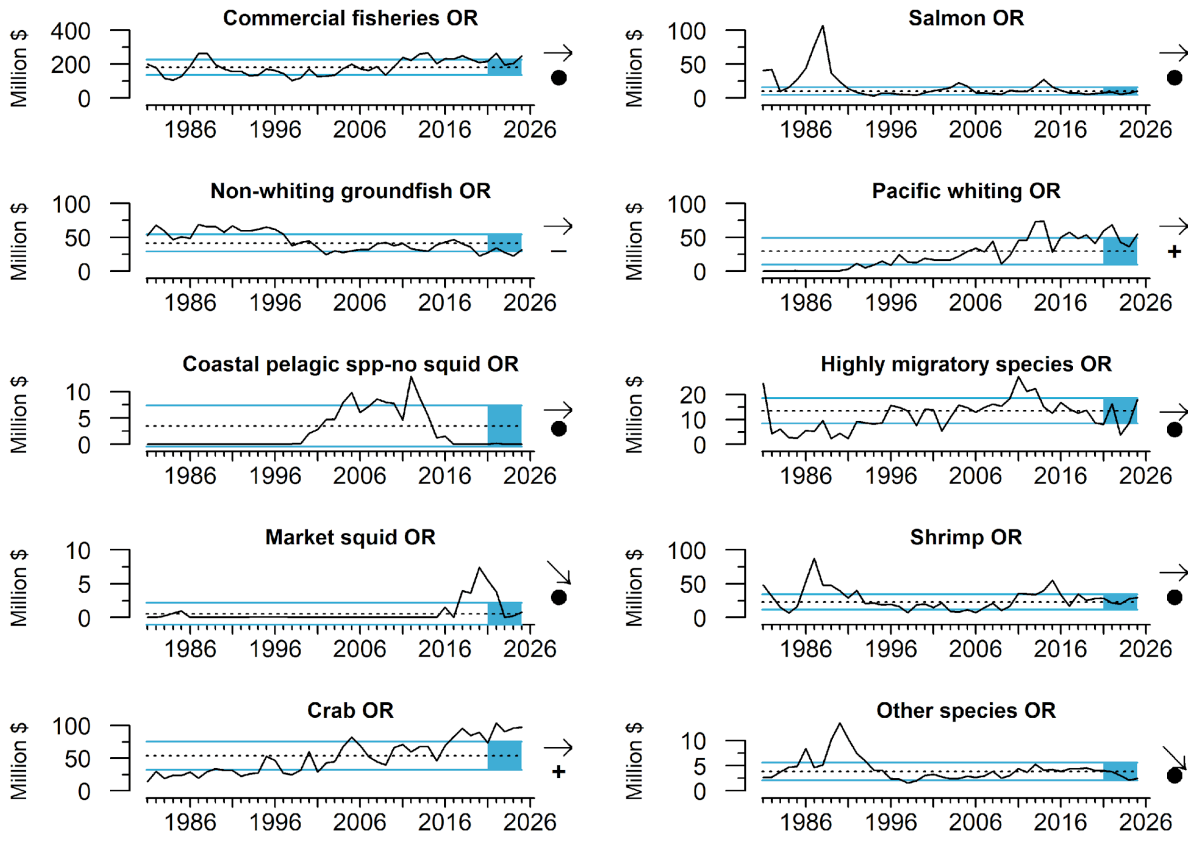


Figure T.6: Annual Oregon revenue (ex-vessel value in 2025 dollars) from West Coast commercial fisheries (data from PacFin) from 1981 - 2025. Whiting revenue includes shoreside and at-sea values from PacFIN, NORPAC (North Pacific Groundfish Observer Program) and NMFS Office of Science & Technology. Lines, colors, and symbols are as in Fig. 2.1.

Total revenue across commercial fisheries in California increased 8% from 2024 to 2025, but is near the lower range of its long-term average (Fig. T.7). This timeseries is largely driven by annual variation in revenue from market squid and an overall decline in crab revenue since 2012. Overall, 6 of 9 major fisheries increased in revenue in 2025 from 2024 levels (in order of 2025 revenue): market squid (19%), crab (11%), non-whiting groundfish (17%), shrimp (22%), HMS (13%), and Pacific whiting (268%). In contrast, revenue from Other species (-17%) and CPS finfish (-22%) fisheries was lower in 2025 compared to 2024. Even though there was a relatively large increase in revenue observed in the Pacific whiting fishery in 2025, revenue levels are at very low values, and this revenue comes from fishing events that occur in CA waters but processed at sea and landed outside of California. Revenue from salmon (closed in 2023, 2024 & 2025), CPS finfish, and Pacific whiting fisheries decreased by >1 s.d. of long-term averages, while all other fisheries showed no trends. Revenue from non-whiting groundfish, CPS finfish, and shrimp fisheries were >1 s.d. below their long-term average, while all other fisheries were within 1 s.d. of their long-term average over the last five years in California.

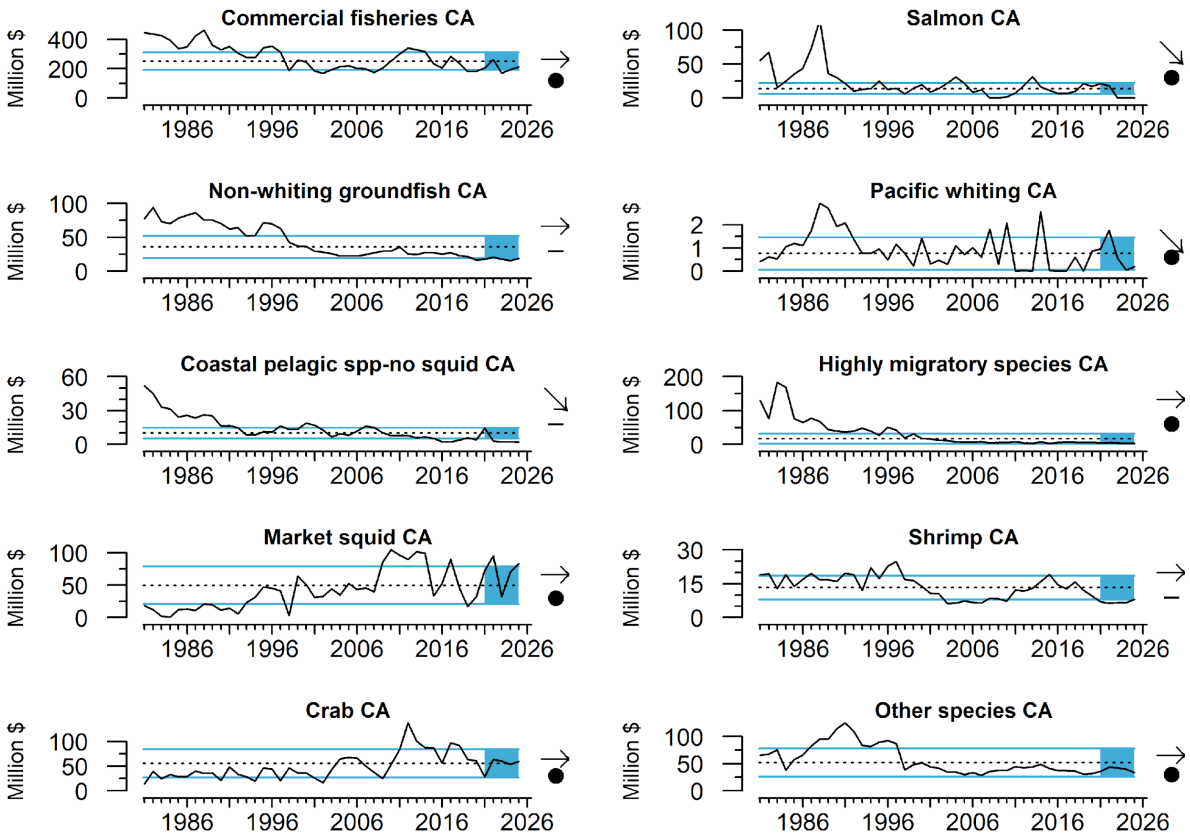


Figure T.7: Annual California revenue (ex-vessel value in 2025 dollars) from West Coast commercial fisheries (data from PacFin) from 1981 - 2025. Whiting revenue includes shoreside and at-sea values from PacFIN, NORPAC (North Pacific Groundfish Observer Program) and NMFS Office of Science & Technology. Lines, colors, and symbols are as in Fig. 2.1.

Appendix U — IDENTIFYING INTERACTIONS AMONG ECOSYSTEM INDICATORS & NEW OCEAN-USE SECTORS

Link to main section: Ecosystem Interactions with New Ocean-use Sectors

Federal and state processes to pursue the development of new projects and completely new ocean-use sectors in the CCE have been underway in recent years. These new sectors include offshore aquaculture; oil, gas, and renewable energy extraction; and critical minerals mining. Development of new economic sectors in the CCE suggests the need for a portfolio of indicators that can inform planning, siting, monitoring, and mitigating for potential interactions with important ecosystem components. Understanding how oceanic and atmospheric processes, protected species and their habitats, fisheries and fisheries stocks' habitat, fishing communities, and NMFS scientific surveys will be affected by new ocean-use sectors is needed to ensure effective marine spatial planning and adaptive management, and to minimize conflicts across the West Coast into the future.

Here, we outline the IEA framework relevant to understanding potential ecosystem interactions with new ocean-use sectors. This outline describes a long-term vision of the science process to identify and use portfolios of ecosystem indicators to measure baseline conditions, tradeoffs across ecosystem components, and detect changes in physical, biological, and ecological processes that may result from these new ocean-use sectors with a case study using previous research related to offshore wind energy (OSW) development to walk through the steps of the overall approach.

U.1 IEA Approach to Understanding Interactions with New Ocean-use Sectors

We propose using the general IEA approach (Levin et al. 2009) to help inform State and Federal planning and permitting and relevant PFMC marine planning processes in the CCE. Imperative to this approach will be engaging experts, managers, and stakeholders and including key components of these new sectors in order to identify tradeoffs across the social-ecological system (SES). This approach iterates across each of the primary steps identified in the NOAA IEA loop:

1. *Define Ecosystem Management Goals & Targets* – engage experts, stakeholders, and managers of fisheries, the greater CCE, and new ocean uses to identify ecosystem components likely to respond to activities associated with new ocean uses.
2. *Develop Ecosystem Indicators* – evaluate and select indicators capable of measuring baseline conditions and detecting changes in status and trends of key ecosystem components.
3. *Assess Ecosystem* – identify ocean areas important to individual SES components and the overall structure and function of the CCE.
4. *Analyze & Evaluate Uncertainty & Risk* – identify appropriate spatial and temporal scales of overlap with and calculation of vulnerability from impact factors of new ocean activities.

5. *Management Strategy Evaluation* – deploy indicator data into planning, siting, monitoring, and mitigation analyses in cooperation with lead State and Federal agencies.

A conceptualized product resulting from Steps 1 and 2 above is illustrated in Figure U.1. This framework shows the hierarchy of SES and relevant ecosystem components, and the indicators selected to represent those components. The x's in the table are hypothetical, but illustrate how this portfolio could identify ecosystem components (and indicators) important to specific, and across, new ocean-use sectors. In the following section, we describe work to-date to develop a portfolio of ecosystem indicators and how these indicators could be applied to planning, assessment, and management actions using OSW as a case study.

SES Components	Climate & Ocean Drivers				Habitat				Ecological Integrity				Human Activities				Human Wellbeing				Local Social Systems				Social Drivers			
	Ecosystem Component 1		Ecosystem Component *n*		Ecosystem Component 1		Ecosystem Component *n*		Ecosystem Component 1		Ecosystem Component *n*		Ecosystem Component 1		Ecosystem Component *n*		Ecosystem Component 1		Ecosystem Component *n*		Ecosystem Component 1		Ecosystem Component *n*		Ecosystem Component 1		Ecosystem Component *n*	
Non-fishing Ocean-use Sectors	Indicator 1	Indicator *n*	Indicator 1	Indicator *n*	Indicator 1	Indicator *n*	Indicator 1	Indicator *n*	Indicator 1	Indicator *n*	Indicator 1	Indicator *n*	Indicator 1	Indicator *n*	Indicator 1	Indicator *n*	Indicator 1	Indicator *n*	Indicator 1	Indicator *n*	Indicator 1	Indicator *n*	Indicator 1	Indicator *n*	Indicator 1	Indicator *n*	Indicator 1	Indicator *n*
Offshore Aquaculture	x				x	x	x	x	x		x		x		x		x				x		x		x	x	x	
Oil and Gas	x				x		x	x		x	x		x						x				x				x	
Offshore wind	x	x			x				x	x	x	x	x	x			x				x				x			
Wave energy	x		x		x						x		x		x				x				x				x	
Tidal energy			x	x			x				x		x				x	x					x		x	x		
Critical minerals mining			x		x		x	x	x		x		x		x		x	x	x			x			x		x	

Figure U.1: Conceptual illustration of a portfolio of indicators across six new ocean-use sectors.

U.2 Ecological and Fisheries Indicators relevant to Offshore Wind Planning and Development

Planning for OSW has paused at the federal level on the West Coast, but California continues to plan and develop entities and priorities to identify, monitor, and mitigate potential effects of OSW on the CCE. The first step (*Define Ecosystem Management Goals & Targets)* we took in the development of ecosystem indicators relevant to OSW development was to create a working conceptual model of the key ecosystem components likely to respond to the activities associated with OSW. During the creation of the NMFS West Coast Offshore Wind Energy Strategic Science Plan, we solicited input from scientists and managers across the West Coast to inform this model. Figure U.2 identifies a broad-scale set of ecosystem components and potential interactions with OSW across the CCE. The interactions are derived from two main pathways of potential impacts from (i) associated

OSW infrastructure and (ii) the specific locations identified for development (blue background components in Fig. U.2).

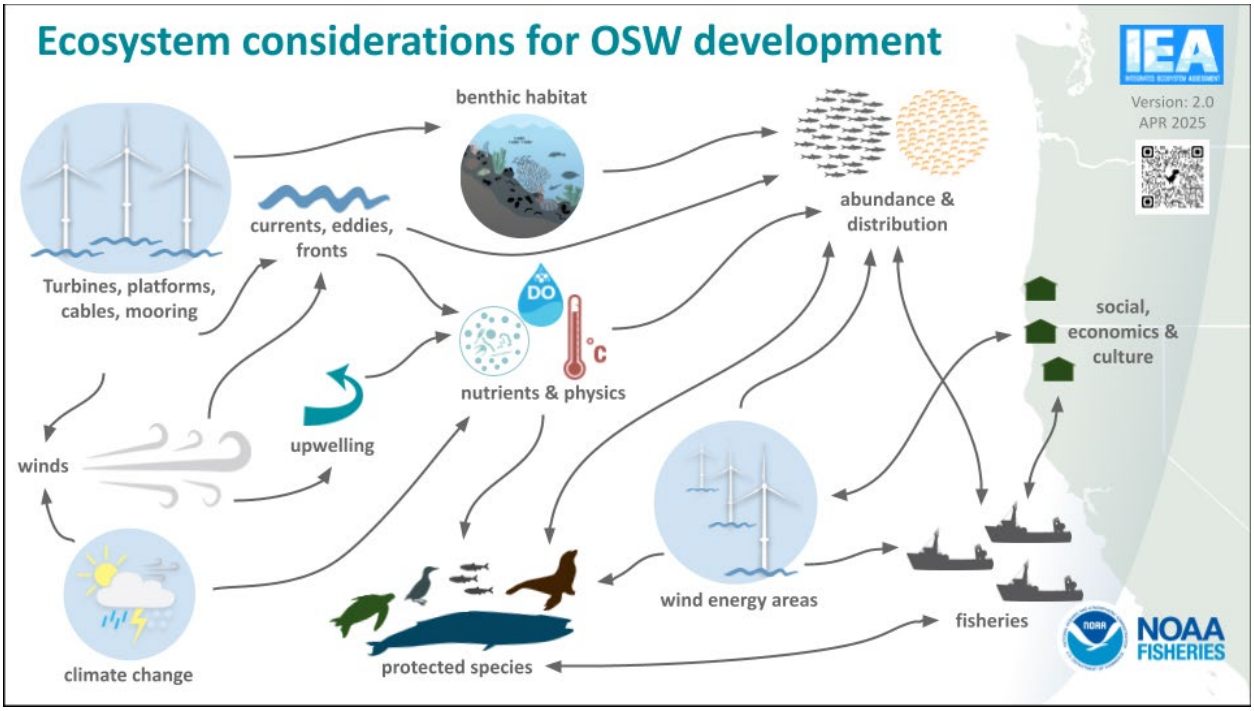


Figure U.2: Conceptual model of key ecosystem components and interactions of interest for evaluating potential effects of offshore wind (OSW) energy development in the CCE. Figure created by K. Andrews & Su Kim, NMFS/NWFSC

Using the conceptual model, we focused initial indicator development efforts on ecosystem components that were likely to provide broad-scale context across the CCE or early warning of potential changes in the underlying structure and function of the ecosystem, and/or be immediately affected. This narrowed our focus to atmospheric and oceanographic drivers, measures of productivity, lower trophic-level or early life-history components, and fisheries activity of the CCE. With the exception of fisheries activity, these are typically components of the ecosystem not strictly accounted for in specific planning and permitting actions (e.g., protected species and essential fish habitat).

U.2.1 Ecological Components

For the ecological components of the SES, we evaluated, selected, and calculated indicators (Step 2: *Develop Ecosystem Indicators*) capable of capturing long-term, spatial variation in oceanographic processes and lower-trophic level productivity and identifying important areas of the CCE (Step 3: *Assess Ecosystem*). The ecosystem indicators selected include:

1. Average wind-driven upwelling during March-July (Fig. U.3a), calculated at 40m depth from 1988-2012 using the Regional Ocean Modeling System (Raghukumar et al. 2023).

2. Proportion of days that a front was identified during March-July, based on edge-detection analysis applied to satellite SST data from 2000-2023 (Fig. U.3b; GHRSST 2024).
3. Long-term, spatial variability and hotspots in primary productivity (Fig. U.3c), calculated from a biogeochemistry model as the average concentration of surface phytoplankton in May-July, 1995-2020 (Fiechter et al. 2018).
4. Long-term, spatial variability and hotspots in secondary productivity from May-August (Fig. U.3d), calculated as an ensemble of four different estimates of krill abundance/biomass across the West Coast (Cimino et al. 2020; Fiechter et al. 2020; Messié et al. 2022; Phillips et al. 2022).
5. Long-term, spatial variability and hotspots for young-of-year (YOY) rockfishes during their pelagic juvenile life stage in May-June from 2001-2022 (Fig. U.3e; Field et al. 2021).
6. Long-term, spatial variability and hotspots for YOY Pacific hake in May-June from 2001-2022 (Fig. U.3f; Field et al. 2021).
7. Long-term, spatial variability and hotspots of groundfish nursery habitat on the seafloor (Fig. U.3g), based on summed average densities of juveniles from 13 groundfish species in May-October from 2003-2018 (Tolimieri et al. 2020).

In order to inform marine spatial planning analyses being considered for OSW development in 2024 (Step 4: *Analyze & Evaluate Uncertainty & Risk* and Step 5: *Management Strategy Evaluation*), we then calculated an index of suitability that integrated across all seven indicators, ranging from 0 (least suitable for OSW) to 1 (most suitable for OSW; see methods in KL et al. 2021). A hotspot of overall ecosystem importance has been identified offshore from Humboldt Bay, CA, which may signify this area is less suitable for OSW than areas further to the north or south as a function of the seven ecosystem indicators (Fig. U.3h). In addition to being applicable to siting of new areas, the individual indicators could help establish baseline conditions that could be used to measure changes in status and trends resulting from OSW development.

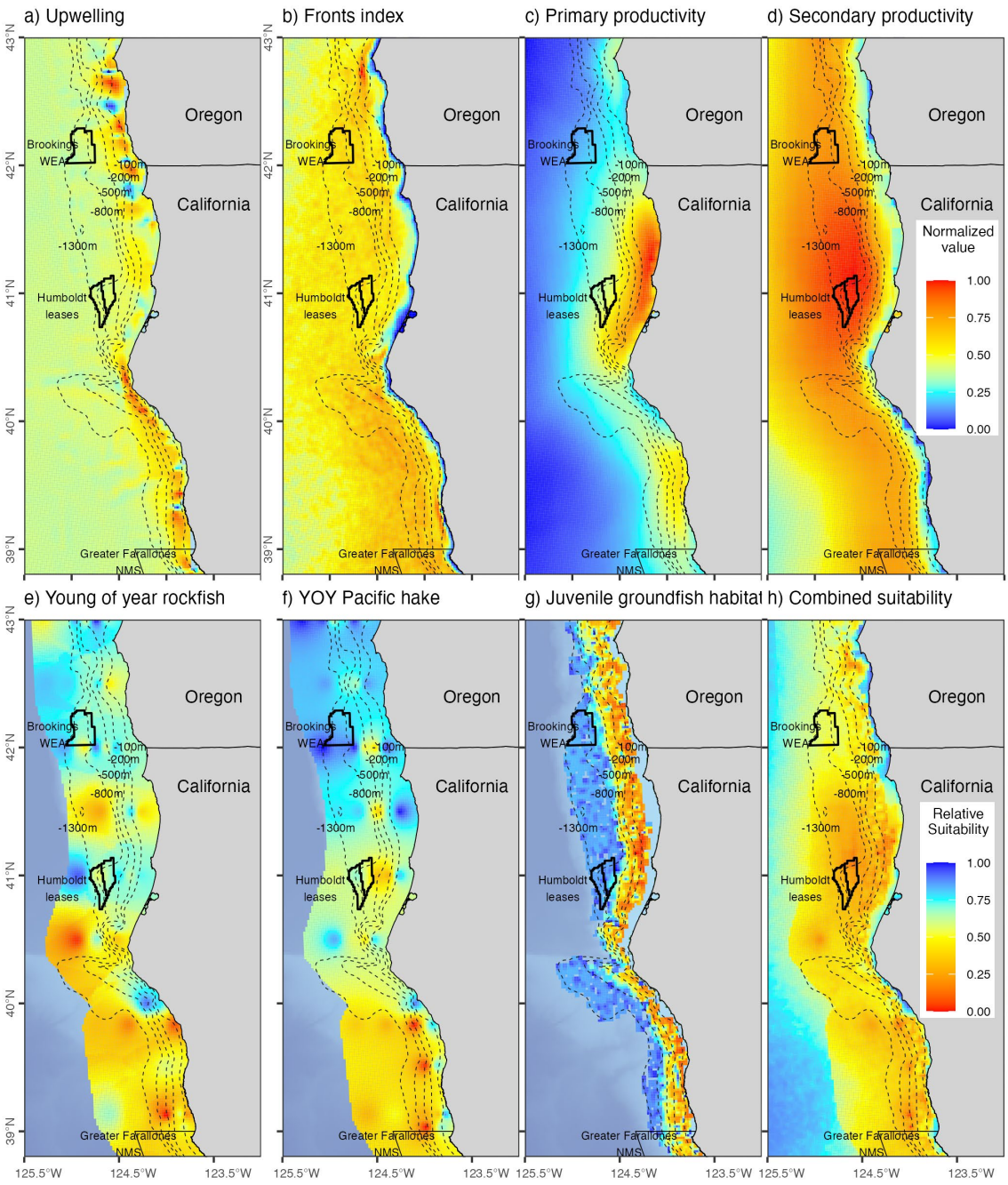


Figure U.3: Ecosystem indicators developed for offshore wind energy development planning. Values for each indicator have been cropped and normalized across the area of interest and represent long-term, spatial variation during peak seasonal production. Panel h is an integrated suitability index across the seven indicators and highlights how these indicators could be used to identify important areas of the ocean relative to sites being considered for new development. The black outlines show a previously identified Wind Energy Area (WEA) off the coast of Brookings, OR and two current lease areas off the coast of Humboldt Bay, CA. Leasing of the Brookings WEA was postponed in 2024. Panels a-g use the "Normalized value" legend shown in panel d. Data compiled by NMFS/NWFSC from sources summarized in report text. Boundaries of proposed Wind Energy and Lease Areas from BOEM (https://www.boem.gov/renewable-energy/state-activities/Oregon; https://www.boem.gov/renewable-energy/state-activities/California). Figure created by K. Andrews, NMFS/NWFSC

U.2.2 Fisheries Components

For the human activity component of the SES, we evaluated, selected, and calculated indicators (Step 2: *Develop Ecosystem Indicators*) capable of capturing recent and long-term, spatial variation in fishing activity across the CCE. Here, we show seven indicators selected to describe fishing activity using the groundfish bottom trawl fleet from 2002-2023 as a case study (logbook data for 2024-2025 was not available at the time of this report) and we evaluate regions of the CCE that have been considered for OSW development off the coast of northern California and southern Oregon (Fig. U.4).

We used logbook set and retrieval coordinates from the limited-entry/catch shares groundfish bottom trawl fisheries to estimate duration trawled annually on a 2x2-km grid. These durations were then used to calculate (1) total duration trawled in the most recent year (2023), (2) the anomaly of the most recent year relative to the entire time series, (3) the most recent 5-year mean (2019-2023), (4) the most recent 5-year trend (2019-2023), (5) the sum of duration trawled across all years, (6) the proportion of years trawled, and (7) the number of years since trawling occurred within each grid cell. To maintain confidentiality, grid cells with <3 vessels operating within the grid cell across the years associated with the indicator have been removed.

The first four indicators are consistent with measuring the 'status' and 'trends' of other ecosystem indicators presented in this report, while the last three have been developed as indicators to use within risk analyses and management strategy evaluations. In recent years, we have used the sum of duration indicator (Fig. U.4e) to help identify important areas of the ocean for fisheries (Step 3: *Assess Ecosystem*). This indicator has helped inform siting analyses for OSW off the coast of southern Oregon (Step 4: *Analyze & Evaluate Uncertainty & Risk* and Step 5: *Management Strategy Evaluation*). Briefly, we integrated fishing activity indicators across nine commercial and recreational fisheries to calculate a relative suitability index within two OSW Call Areas (thin black outlines, Fig. U.4h). This suitability index (and spatial data from other ecosystem components) was used by the Bureau of Ocean Energy Management (BOEM) to identify regions of the Call Areas that were most suitable for OSW development. The fishing activity indicators identified areas of potential overlap and conflict with commercial and recreational fisheries, and BOEM's final siting analysis found that Wind Energy Areas were most suitable in areas that avoided many of the most important fishing grounds for these nine fisheries Fig. U.4h). Full methods can be found in Carlton et al. (2024).

Indicators such as these for fisheries activity and the broad-scale ecosystem indicators presented above will continue to be used in multi-sector, integrative marine spatial planning analyses. It will be important to engage early and often with lead state and federal agencies to ensure key ecosystem components of the CCE are included in planning, siting, monitoring, and mitigation processes to avoid and/or minimize potential conflicts across California Current's social-ecological system.

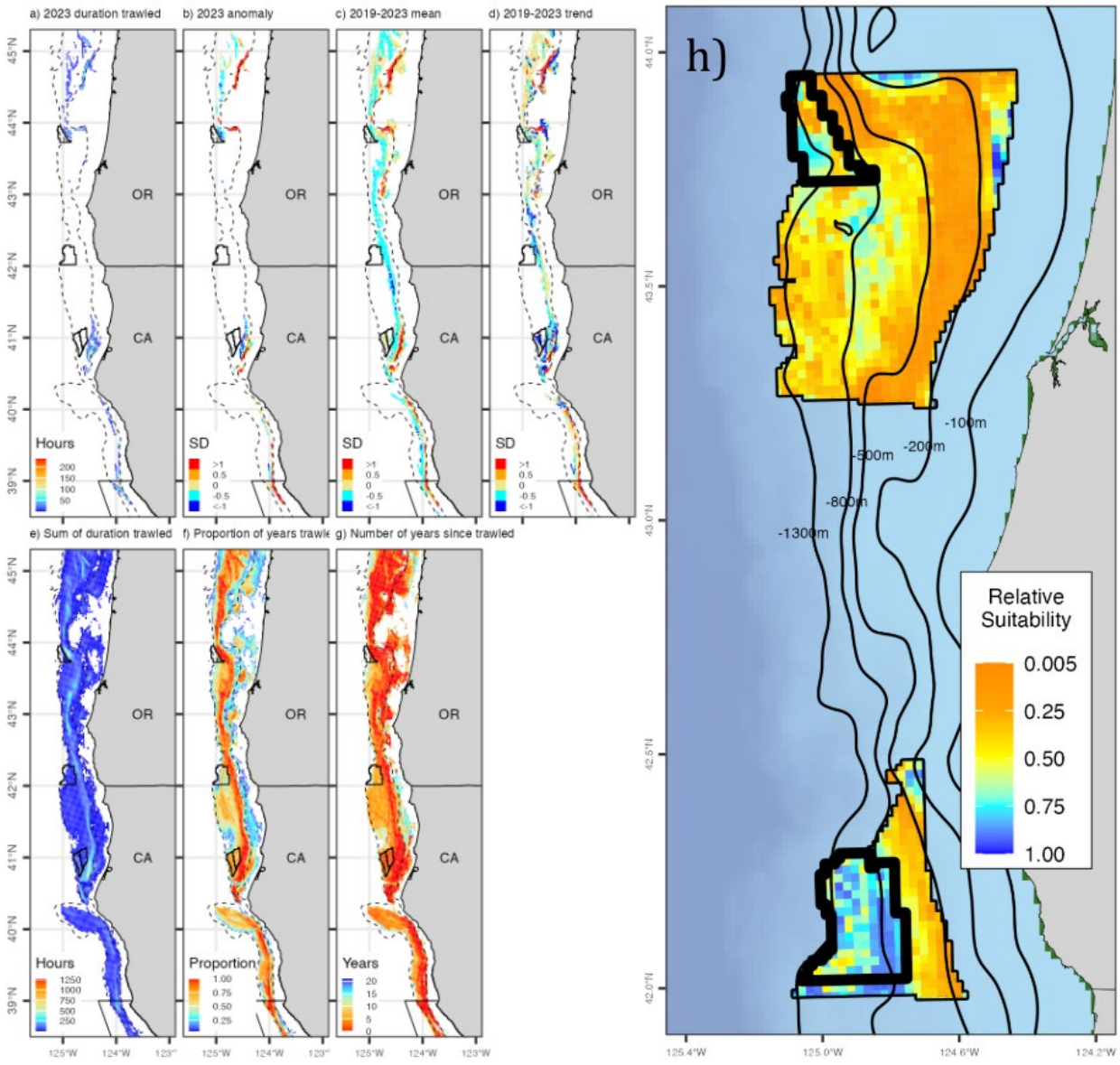


Figure U.4: Indicators of groundfish bottom trawl fisheries activity in areas once considered for new offshore wind energy development Panels show (a) total duration trawled in 2023, (b) anomaly of distance trawled relative to the entire time series, (c) the most recent 5-year mean, (d) the most recent 5-year trend, (e) the sum of duration trawled across all years, (f) the proportion of years trawled (2002-2023), (g) the number of years since trawling last occurred within each 2x2-km grid cell, and (h) relative suitability index for OSW development within two Call Areas (thin black outlines) using indicator data from nine commercial and recreational fisheries. Coos Bay and Brookings Wind Energy Areas (rescinded in 2025) and the Humboldt lease areas shown in heavy black lines from north to south, respectively (a-h). Grid cell values in (b-d) > 1 (red) or < -1 (blue) represent a cell in which the annual anomaly or 5-year mean was at least 1 s.d. from the long-term mean or where the 5-year trend increased or decreased by >1 s.d. of the long-term mean of that cell. The dashed lines in (a-g) are the 200-m and 1300-m depth contours, while more detailed depth contours are shown in (h).

Appendix V — Methodological Overviews

Link to methods overviews: Methods overview

https://cciea-esr.github.io/ESR-Technical-Documentation-FY2026/

For more detail on methods for information presented in this report, see the online documentation linked above.

Appendix W — Changes In This Year's Report

Below we summarize major changes in the 2025-2026 Ecosystem Status Report (Table W.1). As in past reports, many of these changes are in response to requests and suggestions received from the Council and advisory bodies (including those related to FEP Initiative 2, "Coordinated Ecosystem Indicator Review" (March 2015, Agenda Item E.2.b), or in response to annual reviews of indicators and analyses by the SSC-Ecosystem Subcommittee (SSC-ES). We also note items we have added and information gaps we filled since last year's report (Leising et al. 2025). Further, in this year's report we include a table documenting indicators that were delayed or lost as a result of the temporary government furlough and changes in funding (Table W.2).

Table W.1: Major changes in the FY 2026 report.

Request/Need/Issue	Response/Location in Document
The ESR is labor-intensive to produce, and efficiencies such as automation are needed to sustain the report and build it out to meet evolving needs of the Council and other partners. (March 2022, Agenda Item H.2.b, Supplemental EWG Report 1)	In 2025, the ESR team continued to improve automation of the report and create a more efficient and user-friendly process for updating the report annually. Advances to this year's report include: The CCIEA data "uploader" (https://cciea-esr.github.io/CCIEA-uploader/, the system by which the data providers submit their yearly data to the ESR) was completely rewritten and transitioned from a webpage to a GitHub application, improving reproducibility, accessibility, and succession planning. The online Technical Documentation https://cciea-esr.github.io/ESR-Technical-Documentation-FY2026/, was also updated to accommodate new or changing methods and clarify some information. The Technical documentation is another resource maintained in GitHub to sustain repeatable reporting and

	enable broad access for report writers and readers. Initial steps were taken to integrate the Targets package into our Quarto report generation process. Targets is a pipeline tool for statistics and data science in R; the package skips runtime for tasks that are already up to date, orchestrates the necessary computation with implicit parallel computing, and abstracts files as R objects.
Added Figure 3.2 "Regional abundance of krill in the California Current…" *(need for additional data on krill relative abundance)*	After review by PFMC-SSC it was determined that reporting of krill relative abundance from the coastwide hydroacoustic survey was an acceptable measure of prey in the CCE for inclusion in the report. This data is especially valuable this year given the gap left by no data on krill biomass from the Trinidad Head Line during 2025 for the current report.
Added Figure 3.8 "Observed and modeled adult salmon counts at Bonneville Dam…"	This figure has been included in the salmon appendix in past reports. We chose to highlight the outlooks for spring and fall Chinook salmon returning to the Columbia Basin in the main section of the report this year.
Section 3.4 "Groundfish" includes Fig. 3.10 "Stock status of CCE groundfish." Instead of previous year's figures "Coastwide abundance of juveniles of Dover sole, sablefish, and thornyhead…" and "Distribution of juvenile sablefish…"	In previous ESRs, we have included trends in juvenile groundfish biomass indices. However, U.S. West Coast Groundfish Bottom Trawl Survey (WCGBTS) data from 2025 were not available in time for us to generate those indices for this year's report.
Added Figure 3.14 "Domoic acid test results above the 20 ppm action threshold…." to the harmful algal bloom section. *(better synthesis of coastwide domoic acid occurrence)*	Based on interest, we now include this additional analysis showing domoic acid data versus latitude as a clearer way to document temporal sequence of possibly impactful harmful algal bloom events.

Added Figure B.1. "Regional survey highlights assembled mid-year by the IEA team" to Appendix B. *(increase responsiveness of ESR to mid-cycle council needs)*	New for 2025 the CCIEA team has been developing an approach for producing , more-frequent and more-focused ecosystem status report updates,which can eventually be targeted towards specific matters discussed at the PFMC beyond the March Council Meeting. This year, the CCIEA team produced a mid-year report covering initial highlights from the surveys conducted from the start of the year to September, based mainly on the "at-sea" observations of the scientists conducting those surveys.
Added Figure I.4 "The relative abundance of krill detected acoustically…" to Appendix I. (need for increased coverage of Krill relative distribution)	After review by SSC-ES it was determined that reporting of krill relative abundance from the coastwide hydroacoustic survey was an acceptable measure of prey in the CCE for inclusion in the report. This data is especially valuable this year given the gap left by no data on krill biomass from the Trinidad Head Line during 2025 for the current report.
Added Figure I.5 "Time series of total annual catch of Dungeness megalope…" to appendix I. (need for additional measures of prey in the northern CCE)	After review by the SSC-ES it was determined that reporting of Dungeness crab megalope was an acceptable addition to the ESR for use as an additional index of meroplankton prey for fisheries species in the NCC region.

Many changes to Appendix E. "Developing indicators of climate variability and change."	As usual, this appendix is always evolving and changing as per needs of the PFMC and in response to comments from previous years' reports. This year the appendix contains many new items, including a discussion of the PDO and the pan-basin-warming pattern, and two new synthesis tools: a new analysis of projected species shifts, and the utility of the HMS fishing fleet as a sentinel of ecosystem change.
Multiple figure changes in Appendix K. "Groundfish"	The 2025 WCGBTS survey data were not available in time to update previously included indicators in the Groundfish appendix. Instead, we provide new analyses, which may be of interest to the Council. New indicators include (1) time series of rockfish abundance along the WA coast, from scuba surveys, (2) time series of pelagic groundfish recruits diversity metrics from pelagic surveys, and (3) biomass time series Ecosystem Component groundfish species from the WCGBTS.
Multiple Changes to Appendix P. "Port-level revenue concentration"	Due to time limitations in report production, case studies for key management groups were not included.
Multiple changes to Q "Social Vulnerability of commercial…"	Engagement per capita was included in the appendix instead of the main report, and several communities were omitted to avoid confusion based on the previous year's report. Figure P.3, categorical social vulnerability scores were omitted as index scores over time were found to be not comparable.
Multiple changes to R "Fleet diversification indicators…"	Due to personnel loss, temporal diversification was not able to be produced.

Minor changes to Figures/Data/Text	Description
Subsurface glider data figures in the climate-oceans appendix differ in color scheme	Due to time limitations in report production these figures were not able to be adapted to the same color scheme as in previous reports.
The BEUTI and CUTI indices typically used in the report to monitor upwelling during the year have been replaced by the BAKUN transport index	The model output used to calculate these indices was not available for the entire year due to model downtime issues. The BAKUN transport index serves as a reliable and known replacement indicator for the CUTI index; the two indices are highly correlated for the majority of locations and time spans examined in the report.
Removed wind and atmospheric pressure at sea level data from Fig. 2.2	Removed data layers to simplify figure so the main message could be more clearly amplified
Changes to Figure 3.9 "stoplight charts of indicators key to the recruitment of Sacramento River Fall Chinook…"	Last year, CCIEA scientists, in collaboration with members from the Council's Habitat Committee and Salmon Technical Team presented a comprehensive stoplight table for Central Valley Spring Chinook salmon, Sacramento River Fall Chinook salmon, and Klamath River Fall Chinook salmon, featuring indicators from throughout the stocks' life histories spanning the 1983-2024 brood years. In 2025 the extensive table was refined to a subset of these indicators based on their utility generating recruitment outlooks; this work is more thoroughly described in a peer-reviewed manuscript (Munsch et al. In Review).
Figure H.3. "Cumulative estimated biomass for Pacific herring…" was added to appendix H.	Figure was added to better illustrate the relative abundance of CPS stocks over time.
Added Table N.1. "Summary of 2025 entanglement reports…" to Appendix N.	Added to better summarize data on confirmed whale entanglements by species.

Added new Figures O.1 and O.2. as replacements for previous harmful algal toxin figures.	New figures better illustrate both the latitudinal differences in harmful algal toxin observations and the temporal sequence of events in a more readily digestible format.
Added new table S.1 “Summary of WDFW landing…” to Appendix S	New table was added to illustrate what proportion of port data was derived.
Added new figure S.7 “Fisheries participation networks…” in Appendix S.	New figure was added to highlight changes in two Californian ports that underwent significant change in 2024.
Changed figured 4.1 in Human Wellbeing	Figure 4.1 highlights Engagement rather than per capita Engagement to avoid port selection confusion.

Table W.2: Data availability for the FY 2026 report.

2025 ESR Data Availability Stoplight Table

	Climate / Ocean / Habitat	Biology	Human Well-being / Activities
Lost or Unlikely The CCIEA Team lost 11 FTEs, not including contractors and others who contributed data.	• Upwelling: BEUTI / CUTI	• HMS diets • Sea lion pup weight / growth / diet (57-y history) • Trinidad Krill size and number	• Theil Index
Delayed*, Abbreviated, or otherwise Impacted	• Habitat Compression Index • Snowpack / SWE • Gliders • CalCOFI Hydro	• Krill biomass (acoustic) • CA salmon stoplight • SCC forage (CalCOFI) • HMS stock assessments • Sea lion pup count • CPS survey biomass • Groundfish survey	• Fishery revenue diversification • Multisector Interactions • Social vulnerability and reliance (CSVI) • Newport fishermen roundtable
On track or Good	• Satellite data • Stream flow/temperature • NHL / JSOES hydrographic data	• NHL Copepods • NCC forage / juv salmon (JSOES) • CCC forage (RREAS) • PNW salmon stoplight • HABS • Whale Entanglement • Seabirds	• Fishery landings and revenue • Fishery participation networks (FPN) • Ocean Uses

*Some time series may be included in the presentation to the PFMC at the March Council meeting